# Soviet Physics

## Acoustics

[illegible]

A Translation

of the

Journal of Acoustics

of the

Academy of Sciences of the USSR

*Published by the*

AMERICAN INSTITUTE OF PHYSICS

INCORPORATED

Translation of the "Journal of Acoustics" of the USSR.

American Institute of Physics Advisory Board on Russian Translations

ELMER HUTCHISSON, Chairman

DWIGHT GRAY, MORTON HAMERMESH, VLADIMIR ROJANSKY, VICTOR WEISSKOPF

"Soviet Physics–Acoustics" is published by the American Institute of Physics for the purpose of making available in English reports of current Soviet research in acoustics as contained in the "Journal of Acoustics" of the Academy of Sciences of the USSR, and will regularly consist of four issues annually.

Transliteration of the names of Russian authors follows the system employed by the Library of Congress.

This translation and publication project was undertaken by the Institute in the conviction that dissemination of the results of research everywhere in the world is invaluable to the advancement of science. The National Science Foundation of the United States and the Office of Naval Research encouraged the project initially and are supporting it in large part by a grant. Translation and printing are being handled by Consultants Bureau, Inc.

The American Institute of Physics and its translators propose to translate faithfully all the scientific material in the "Journal of Acoustics" of the Academy of Sciences of the USSR appearing after January 1, 1955, the first year of its publication. The views expressed in the translated material, therefore, are intended to be those expressed by the original authors, and not those of the translators nor of the American Institute of Physics.

One volume is published annually. Volume 1 will contain all of the scientific material published in the original Russian journal during the calendar year 1955, and Volume 2 will contain all of the scientific material published in the original Russian journal during the calendar year 1956.

---

### Subscription Prices

| | |
|---|---|
| Per year, beginning with Volume 2 (4 issues) | |
| *United States and Canada* | $20.00 |
| *Elsewhere* | 22.00 |
| *Back Numbers (beginning with Volume 2) | |
| *Single copies* | $ 6.00 |

*Volume 1, consisting of two issues, is available only as a set at the yearly rates quoted above.

Subscriptions should be addressed to the American Institute of Physics, 335 East 45th Street, New York 17, New York.

Officers and Staff

[illegible]
*Chairman, Governing Board*
ELMER HUTCHISSON
*Director*
HENRY A. BARTON
*Associate Director*
WALLACE WATERFALL
*[illegible] Secretary*
[illegible]
*Treasurer*
THEODORE VORBURGER
*Advertising Manager*
RUTH F. BRYANS
*Publication Manager*
KATHRYN SETZE
*Assistant Treasurer*
[illegible]
*Circulation Manager*
EUGENE H. KONE
*Director of Public Relations*

*Copyright by American Institute of Physics 1957*

# SOVIET PHYSICS

# Acoustics

SOVIET PHYSICS – ACOUSTICS VOLUME 1, NUMBERS 1 AND 2

## FROM THE EDITOR

**In view of the rapid development of scientific and engineering acoustics in the USSR and of the need for widely publicizing scientific-research and engineering work on acoustics, the Presidium of the USSR Academy of Sciences has deemed it necessary to publish the "Acoustic Journal" of the USSR Academy of Sciences, starting with 1955.**

**The principal task of the journal is to publish regularly the results of research in the field of theoretical and experimental acoustics and to deal with improvement and manufacture of acoustic measuring equipment, improvement of the quality of acoustic apparatus, improvement of the quality of sound-reproducing and sound-transmitting systems, improvement of the acoustic properties of public and residential buildings, combatting noise and vibration, and also with developments in practical and scientific application of ultrasonics.**

**In addition to publishing original works, the journal will publish reviews on basic problems in scientific and applied acoustics, and also letters to the editor, reviews of newly-published books, and news of the acoustic activities in the USSR and abroad.**

**"Journal of Acoustics" will be published four times a year.**

**The editor of "Journal of Acoustics" asks that readers address remarks and requests to: Moscow B-64, Podsosenskii Per. 41, editor of "Journal of Acoustics."**

# CONCERNING CERTAIN SECOND-ORDER QUANTITIES IN ACOUSTICS

N. N. Andreev

This investigation concerns the density and flux of sound energy and the momentum and pressure of sound radiation. The analysis is based primarily on the method of first-order and second-order successive approximations, with allowances being made for the need of clearly distinguishing between the Lagrange and Euler points of view.

The fact that there is a certain contradiction between the conventional views on the density and flux of sound energy and the point of view presented in this work is explained. It is shown that allowances must be made for the boundary conditions if the problem is to be fully solved. The article concludes with a specific example that illustrates the statements contained in this work.

Scientific journals, particularly in recent times, continue to publish discussions of the density and flux of sound energy, of the momentum and pressure of sound radiation, etc. Yet, in our opinion, these topics are not very clearly treated in the articles, and particularly in textbooks.

I attempted to present a clear exposition of these topics in Reference [1], starting with the following points of view.

1. It is necessary to distinguish clearly whether the Lagrange (L) or Euler (Eu) point of view is used; failure to do so leads to errors in all second-order approximations.

2. In acoustics, the system of hydrodynamic equations is replaced by first-order and second-order approximation equations; these equations contain, naturally, all the properties of the acoustic mediums, but the general relationships obtained from these equations cannot by themselves yield a solution that is satisfactory for practical applications unless the boundary and initial conditions that are characteristic of the case under consideration are taken into account. Naturally, although this circumstance imposes a limitation on these general theorems, it does detract from their significance; the physical picture of the phenomenon is indeed presented by these equations.

The analysis that follows is made from the same points of view. This circumstance, as well as the fact that my previously referred-to article was not printed in Russian, call for a more detailed exposition than is customary in publications; I am including in the exposition the suitable corrections and improvements, as well as a discussion of recent investigations that are continuations of my work.

We consider a non-viscous non-heat-conducting liquid medium, in equilibrium prior to the disturbance, having an equation of state

$$p = p(\rho)$$

which we put in the particular form:

$$\frac{p}{p_0} = \left(\frac{\rho}{\rho_0}\right)^{\gamma}.$$

We assume that our medium is free of eddies, a customary boundary condition in acoustic problems.

We use the same definition of potential energy as Lamb: the potential energy stored per unit mass is the work that can be extracted from this mass by expanding its volume from a pressure $p$ to $p = 0$.

This yields

$$A_p = \frac{p_0}{\rho_0}\frac{1}{\gamma-1}\left(\frac{\rho}{\rho_0}\right)^{\gamma-1} = \frac{p}{\rho(\gamma-1)}.$$

The energy density is, therefore,

$$E_p = \frac{p}{\gamma-1}.$$

The sound energy per unit mass is taken to mean

$$A_p - A_{p_0} = \frac{p_0}{\rho_0(\gamma-1)}\left[\left(\frac{\rho}{\rho_0}\right)^{\gamma-1} - 1\right].$$

The density of sound energy is defined as

$$W_p = \rho(A_p - A_{p_0}) = \rho\frac{p_0}{\rho_0(\gamma-1)}\left[\left(\frac{\rho}{\rho_0}\right)^{\gamma-1} - 1\right] = \frac{p_0}{\gamma-1}\left(\frac{p}{p_0} - \frac{\rho}{\rho_0}\right).$$

These are commonly accepted definitions. We mention this because they are in contradiction with other definitions, which we usually see in texts on acoustics and which, as will be shown below, are not adequately founded.

The fact that $W_p$ can be expressed as a function of $p$ alone, shows that $p - p_0$, which is the sound-radiation pressure, is fully determined by $W_p$.

Let us agree to restrict ourselves hereinafter to first and second-order approximations of the equations given above, i.e., let us put

$$\begin{aligned} p &= p_0 + p' + p'' + \dots \\ \rho &= \rho_0 + \rho' + \rho'' + \dots \\ v &= v' + v'' + \dots \end{aligned}$$

and let us require hereinafter that p', v', and $\rho'$ satisfy the usual equations of acoustics, and p'', v'', and $\rho''$ are calculated as second-order corrections to the hydrodynamic equations.

The equation of state and the definitions of the potential and kinetic energy lead to the following relationships:

$$c_0^2 = \frac{\gamma p_0}{\rho_0}; \qquad p' = c_0^2\rho'; \qquad p'' = \frac{\gamma-1}{2\rho_0}c_0^2\rho'^2 + c_0^2\rho'',$$

$$W_p = \frac{p'}{\gamma} + \frac{p''}{\gamma} + \frac{p'^2}{2\rho_0 c_0^2}; \qquad W_k = \frac{\rho_0 v'^2}{2}.$$

Putting $p = p_0 + c_0^2(\rho - \rho_0)$ we obtain a linear equation of state applicable to liquids:

$$p' = c_0^2\rho'; \qquad p'' = c_0^2\rho'',$$

$$W_p = \frac{p_0 p'}{\rho_0 c_0^2} + \frac{p_0 p''}{\rho_0 c_0^2} + \frac{p'^2}{2\rho_0 c_0^2} = qp' + qp'' + \frac{p'^2}{2q}.$$

Let us denote the energy per unit mass by $E_L$ and the energy flux by $\vec{I}_L = p\vec{v}$.

The integral form of the law of conservation of energy is:

$$\frac{d}{dt}\int_\tau E_L\rho\, d\tau - \int_S p\,\vec{v}\,\vec{n}\, dS = 0, \qquad \textbf{(1) L}$$

where $\underline{\vec{n}}$ is the inward normal.

Using the known method, we obtain from this

$$\frac{d}{dt}E_L = -\frac{1}{\rho}\frac{\partial}{\partial a_i}I_{L,i}\,^*, \qquad \textbf{(2) L}$$

where $a_i$ are the coordinates of the particles of the unperturbed medium.

Introducing $W = \rho E_L$ and using the usual transformations, we get

$$\frac{\partial W}{\partial t} = -\frac{\partial}{\partial x_i}\left[v_i(p + W)\right] = -\frac{\partial}{\partial x_i}I_{Eu,i} \qquad \textbf{(3) Eu}$$

This equation tells us that the energy flux, expressed in Euler's coordinates, consists of two parts: the work performed by the inner part of the medium on the outer one, and the energy transferred with the medium across the boundary.

---

* Here and hereinafter, summation is implied when an index is repeated.

Expressing the quantities in (2) and (3) in terms of their first and second-order approximations, we get

$$\vec{I} = \rho_0\vec{v}' + \rho_0\vec{v}'' + p'\vec{v}', \tag{4) L}$$

$$\vec{I} = \rho_0\vec{v}' + \frac{p'\vec{v}'}{\gamma}(\gamma + 1) + \rho_0\vec{v}''. \tag{5) Eu}$$

We obtained for $W_p$

$$W_p = \frac{p'}{\gamma} + \frac{p''}{\gamma} + \frac{p'^2}{2\rho_0 c_0^2}. \tag{6}$$

For liquid

$$W_p = qp' + qp'' + \frac{p'^2}{2q}. \tag{6'}$$

Using $W_k$, we get

$$W = \frac{p'}{\gamma} + \frac{p'^2}{2\rho_0 c_0^2} + \frac{\rho_0 v'^2}{2} + \frac{p''}{\gamma}. \tag{7}$$

$$W = qp' + \frac{p'^2}{2q} + \frac{\rho_0 v'^2}{2} + qp''. \tag{7'}$$

Both these expressions contain the usual expression for the energy density, represented by the two central terms; even if averaged over the time, when we can put $\overline{p'} = 0$, there still remains the last term, which in general does not vanish on the average, as will be shown below; the same applies to $v''$. Naturally, there exist particular cases, when second-order quantities vanish. For example, the radiation pressure against the free surface of a liquid is identically zero: $p' + p'' = 0$, from which $\overline{p''} = 0$ for usual acoustic phenomena. A second example is the radiation produced in a pipe by a sinusoidally-oscillating piston, when it is readily seen that $\overline{v''}$ vanishes.

To investigate the matter further we must turn to the first and second-order approximation equations.

Using the Euler symbols, we can assume the existence of a velocity potential, for the initial and boundary conditions that are usually used in acoustics do not give raise to eddies.

Omitting the detailed calculations, let us write down the results.

First approximation

$$\frac{\partial^2\varphi'}{\partial t^2} = c_0^2\frac{\partial^2\varphi'}{\partial x_k\partial x_k},$$

$$v_i' = -\frac{\partial\varphi'}{\partial x_i},$$

$$p' = c_0^2\rho' = \rho_0\frac{\partial\varphi'}{\partial t}. \tag{8) Eu}$$

**Second approximation**

$$\frac{\partial^2\varphi''}{\partial t^2} = c_0^2\frac{\partial^2\varphi''}{\partial x_i\partial x_i} + (\gamma-1)\ \frac{\partial\varphi'}{\partial t}\frac{\partial^2\varphi'}{\partial x_i\partial x_i} + 2\ \frac{\partial\varphi'}{\partial x_i}\frac{\partial^2\varphi'}{\partial x_i dt}. \tag{9) Eu}$$

Putting $\gamma = 1$ makes this equation applicable to liquid;

$$p'' = \rho_0\left(\frac{\partial\varphi''}{\partial t} - \frac{1}{2}\frac{\partial\varphi'}{\partial x_i}\frac{\partial\varphi'}{\partial x_i}\right) - \frac{\rho_0}{c_0^2}\left(\frac{\partial\varphi'}{\partial t}\right)^2. \tag{9') Eu}$$

The three-dimensional set of Lagrange's equations is too complicated to use here; we have for one measurement

$$\begin{aligned}\frac{\partial^2\xi'}{\partial t^2} &= c_0^2\,\frac{\partial^2\xi'}{\partial a^2},\\ \frac{\rho'}{\rho_0} &= -\frac{\partial\xi'}{\partial a},\\ \frac{p'}{p_0} &= -\gamma\,\frac{\partial\xi'}{\partial a},\end{aligned} \tag{8) L}$$

and for the second approximation

$$\frac{\partial^2\xi''}{\partial t^2} = c_0^2\frac{\partial^2\xi''}{\partial a^2} - c_0^2(\gamma+1)\cdot\frac{\partial^2\xi'}{\partial a^2}\cdot\frac{\partial\xi'}{\partial a}, \tag{9) L}$$

$$\frac{\rho''}{\rho_0} = -\,\frac{\partial\xi''}{\partial a} + \left(\frac{\partial\xi'}{\partial a}\right)^2, \tag{10) L}$$

$$\frac{p''}{p_0} = -\gamma\,\frac{\partial\xi''}{\partial a} + \frac{\gamma(\gamma+1)}{2}\cdot\left(\frac{\partial\xi'}{\partial a}\right)^2. \tag{11) L}$$

In addition, let us remark that we can readily derive from the three-dimensional first-approximation equation the following equations, which will prove to be of value later,

$$\frac{\partial}{\partial t}\left[\frac{p'^2}{2\rho_0 c_0^2} + \frac{\rho_0 v'^2}{2}\right] = -\,\frac{\partial}{\partial x_i}(p'v_i'), \tag{12) Eu}$$

$$\frac{\partial}{\partial t}\left[\frac{p'^2}{2\rho_0 c_0^2} + \frac{\rho_0 v'^2}{2}\right] = -\,\frac{\partial}{\partial a_i}(p'v_i');\qquad v_i' = \frac{\partial\xi_i}{\partial t}. \tag{12) L}$$

The principal question raised by an examination of equations (4) – (12) is how to explain the contradiction between these equations and the usual equations for the energy density and flux. Only in recent years were attempts made to explain these contradictions, in References [2], [3], [4], and [5]. The basic work here is that by Schoch [2] whose ideas agree with those contained in Markham's papers [3], [4], which were published before Schoch's. Schoch showed that our equations for the flux and density, which in his opinion correctly describe the phenomena, can be divided into two parts, one essential and in agreement with the usual equations, and the second inessential. Schoch, too, bases his works on Lamb's definition of energy, but does not specify the equation of state and carries out his argument with an expression for the energy per unit mass;

$$u = -\int_{1/\rho_0}^{1/\rho} p\,d\left(\frac{1}{\rho}\right) = u_{\rm I} + u_{\rm II}.$$

The "inessential" and "essential" parts are:

$$u_{\rm I} = -p_0\left(\frac{1}{\rho_0} - \frac{1}{\rho}\right),$$

$$u_{\rm II} = -\int_{1/\rho}^{1/\rho_0} (p - p_0)\,d\frac{1}{\rho}.$$

Using our notation

$$u_{\rm I} = -\frac{p_0}{\rho_0}\left(\frac{\rho'}{\rho_0} + \frac{\rho''}{\rho_0} - \frac{\rho'^2}{\rho_0^2}\right),$$

$$u_{\rm II} = \frac{1}{\rho_0}\,\frac{p'^2}{2\rho_0 c_0}.$$

We discard here third-order terms: for the energy flux we have

$$\vec{I}_{\rm I} = p_0\vec{u},$$

$$\vec{I}_{\rm II} = (p - p_0)\vec{u},$$

and in our approximation

$$\vec{I}_{\rm I} = p_0(\vec{u}' + \vec{u}''),$$

$$\vec{I}_{\rm II} = p'\vec{u}'.$$

Using a simple argument, Schoch shows that

$$\rho\frac{du_{\rm I}}{dt} + \operatorname{div}\vec{I}_{\rm I} = 0,$$

$$\rho\frac{du_{\rm II}}{dt} + \operatorname{div}\vec{I}_{\rm II} = 0.$$

He notes correctly in his subsequent argument that "in principle, first-approximation solutions are inadequate for calculation of the acoustic energy. It seems, however, that the increments $u_{\rm I}$, $\vec{I}_{\rm I}$ are considerably less essential in acoustics than $u_{\rm II}$, $\vec{I}_{\rm II}$."

Similarly, inconclusive results are obtained also by Markham [3], [4], who leans on Schoch's work, but who considers the particular case of one-dimensional radiation.

Schock's ideas on the inessential nature of $u_{\rm I}$ reduce to the following:

1. Since $\int \rho u_I d\tau = -p_0(V - V_0)$ (where d$_\tau$ is the volume element and V and V$_0$ are the instantaneous and equilibrium volumes of the mass under consideration), the energy corresponding to the subscript "I" vanishes if the phenomenon occurs in a solid body, "a case which, however, cannot be considered strictly realizable."

2. Consider a transmitter radiating within a limited time interval. If the radiating mechanism of the transmitter returns to its initial position upon completing the radiation (there is no increase in volume), the energy radiated through a surface S is

$$\oint_S p_0(\vec{u}d\vec{\sigma}) = p_0 \frac{dV}{dt};$$

the time average (in the Lagrangian sense) is zero, since it was assumed periodic.

One cannot deny that these considerations favor the conclusion that $u_I$ is inessential; however, they do not constitute the desired proof, and apparently, the author himself felt the same way; one cannot, therefore, consider the problem settled.

As we emphasized in the start of our discussion, one must not forget in problems of this type that the boundary conditions must be used; the idea of subdividing the energy into two terms, suggested by Schoch, must be supplemented by formulation of those boundary and initial conditions, which would determine the aggregate of acoustic experimental conditions of interest to us. Let us, therefore, consider the case of radiation from a transmitter (one or several) into a medium having boundaries of practical interest (receiver, screen, solid or absorbing body, etc.); let us assume in equation (1) L, which describes the energy state of the medium, that the surface S comprises the surface of the radiator, the reflecting surfaces, and an infinitely-remote surface that encloses the sound field. One can state in this case that the average sound energy entering into the medium whenever the transmitter is in operation is determined by the energy flux p'v', where v' is the specified velocity of the points on the radiator surface, and p' the first-order pressure resulting from the structure of the field boundaries.

In fact, it follows from (4) L that

$$\overline{I_i} = p_0\overline{v_i'} + p_0\overline{v_i''} + \overline{p'v_i'} = \overline{p'v_i'}, \qquad \text{L}$$

so that for cases of interest in acoustics the first term vanishes on the average, and under ordinary transmitter operating conditions, the second is zero even prior to averaging. Subtracting equation (12) L from the general expression (2) L, written with allowances for the approximations made, i.e., from the expression

$$\frac{dW}{dt} = \frac{d}{dt}\left(p' + \frac{p'^2}{2\rho_0 c_0^2} + \frac{\rho_0 v'^2}{2} + c_0^2 \rho''\right),$$

we obtain

$$\frac{d}{dt}(p' + c_0^2\rho'') = 0,$$

i.e., the instantaneous rate at which energy is delivered to the medium is determined from the usual expression;

$$\frac{p'^2}{2\rho_0 c_0^2} + \frac{\rho_0 v'^2}{2}, \tag{13}$$

which Schoch calls the second energy. The first energy $p' + c_0^2\rho''$ does not vanish, but does not enter into the medium from the radiator boundaries. This, naturally, does not mean that the energy density of the medium is given by equation (13) for all points of the medium; to the contrary, the example below will show that it does enter into the medium and will be drawn from the total energy arriving into the medium. On this basis, one can call $p' + c_0^2\rho''$ the "storable" energy; this indeed is done by Markham [4], although this term does not fully characterize the nature of the matter.

The process of storing the second energy can be elaborated on somewhat. According to acoustic practice, only a weak discontinuity can exist at the boundary of the front that results from the radiator wave acting only at distances not too great from the radiator, for in this case the radiator starts operating with zero velocity. The waves traveling from the reflector separate the sound field into layers moving with a velocity $c_0$; there is no transfer of energy through the boundaries of these layers ($v' = v'' = 0$), and therefore, each layer contains the same amount of energy that it receives at the instant it was formed on the radiator. But this does not exclude the possibility of conversion of the potential energy in each element into kinetic energy and vice versa; this will also be shown in the example below.

This explains, therefore, why in many cases the generally-accepted equations can be used but only subject to certain limitations on their validity.

From the equations given above one derives useful results concerning radiation pressure. The pressure is determined by the potential energy, but in actual cases the value of the pressure can be obtained only by taking into account boundary and initial conditions. The pressure cannot be determined from the total energy, as is commonly stated; as shown in [1] and confirmed by Schoch [5], the average density of the potential energy is not equal to the average density of the kinetic energy. In fact, the average potential energy differs from the average kinetic energy by $\frac{\overline{p''}}{\gamma}$, which in general is not equal to zero.

4. The conclusions given above become quite evident if we consider the well-known particular example, pertaining to one-dimensional propagation [1, 5, 6]. Let us examine the solution to the system (8) – (11) for the following boundary and initial conditions:

1) At $t \leq 0$; $\xi = 0$ everywhere;

2) at $t > 0$; $\xi = A(1 - \cos\omega t)$;

3) no reflecting structures at $a > 0$.

Under these conditions there will propagate in the medium a train of traveling waves, bounded on the forward end by a weak discontinuity. Let us consider a region in which a strong discontinuity has not yet built up. The solution of this problem is of the form:

$$\xi' = A\left[1 - \cos\omega\left(t - \frac{a}{c_0}\right)\right],$$

$$\xi'' = A^2\omega^2 a\,\frac{\gamma + 1}{8c_0^2}\left[1 - \cos 2\omega\left(t - \frac{a}{c_0}\right)\right],$$

$$\begin{cases} \dfrac{\partial \xi'}{\partial t} = v' = \omega A \sin \omega \left(t - \dfrac{a}{c_0}\right), \\ \dfrac{\partial \xi''}{\partial t} = v'' = \omega^3 A^2 a \,\dfrac{\gamma + 1}{4c_0^2} \sin 2\omega \left(t - \dfrac{a}{c_0}\right), \\ \dfrac{\rho'}{\rho_0} = \dfrac{A\omega}{c_0} \sin \omega \left(t - \dfrac{a}{c_0}\right), \\ \dfrac{\rho''}{\rho_0} = \dfrac{A^2\omega^2}{4c_0^2}\left[(3 - \gamma) \sin^2 \omega \left(t - \dfrac{a}{c_0}\right) + \dfrac{a(\gamma+1)\,\omega}{c_0} \sin 2\omega \left(t - \dfrac{a}{c_0}\right)\right], \\ \dfrac{p'}{p_0} = \gamma \dfrac{A\omega}{c_0} \sin \omega \left(t - \dfrac{a}{c_0}\right), \\ \dfrac{p''}{p_0} = \dfrac{A^2\omega^2}{4c_0^2} \gamma (\gamma + 1) \left[\sin^2 \omega \left(t - \dfrac{a}{c_0}\right) + a \dfrac{\omega}{c_0} \sin 2\omega \left(t - \dfrac{a}{c_0}\right)\right]. \end{cases}$$

This leads to the following conclusions, first formulated with sufficient completeness by Fubini-Giron [6] and supplemented by many workers [1, 2, 4, 5, 7].

1. According to our approximation, the phenomenon propagates with a velocity $c_0$, but the waveform of the oscillation varies from place to place (old result, already derived by Airy).

As the wave propagates, its amplitude increases at double the initial frequency. This process can be compared with the known statistical process of energy equalization as the system strives to equilibrium; we are dealing with the initial stage of this process; what is important is such an equalization process can occur only in the presence of non-linearities in the system. In our case this non-linearity has two sources: the non-linearity of the equations themselves, and the non-linearity of the equation of state. At $\gamma = 1$ (liquid) the second cause is eliminated, but the first remains.

2. In the region touched by the sound wave, there exists an average displacement of the medium $A_0$, but $\overline{v''} = 0$ over the entire space. This means that there is no "sonic wind". The question whether a sonic wind that is not due to the viscosity of the medium is possible at all, still remains unresolved. In our example, the boundary conditions are such (non-porous piston: $\overline{v''}_{a=0} = 0$) are such that the wind is impossible.

I. G. Rusakov [8] considered the case of an oscillating sphere and came to the conclusion that the sought for sonic wind exists. It would be desireable to check his results.

3. The sound-radiation pressure, which we define as $\overline{p - p_0}$ for a point under consideration in the medium, is

$$\overline{p - p_0} = \overline{p''} = \rho_0 \frac{A^2\omega^2}{8}(\gamma + 1).$$

4. The average kinetic-energy density in the vicinity of the point of the medium is independent of the point of observation

$$\overline{W_k} = \frac{\rho_0 A^2 \omega^2}{4},$$

and the average potential-energy density is

$$\overline{W_p} = \frac{\rho_0 A^2 \omega^2}{8}(\gamma + 3)$$

and does not equal the average kinetic-energy density. This result is confirmed also by Schoch for any equation of state. The ratio of the two quantities is

$$\frac{\overline{W}_p}{\overline{W}_k} = \frac{\gamma + 3}{2}\,.$$

In the case of a liquid, the potential energy is twice the kinetic one.

5. It was shown in Reference [1] that the time average and the average over the length are different, and therefore, the known argument that leads to the equation $\overline{I} - c_0\overline{W}$ is not valid [5].

In fact, since the quantities of interest to us depend not only on $t - \frac{a}{c_0}$, but also on a, the averages can in general not equal each other. However, the equation written above can be used in our particular case. In fact, as shown above, the amount of energy inside each segment of the wave contained between two zero values of the velocity, carries an amount of energy that is numerically equal to that calculated from the ordinary equation. Therefore, the equation written above remains valid if it is applied to discrete trains.

6. The next quantity of interest is the momentum per unit mass, carried by the soundwave. The time average of its value is evidently zero, for this average is $v' + v''$. This result is understandable: in the Lagrangian system the velocity v pertains to a particle of the medium, and we have seen that there is no sonic wind (according to the boundary conditions of the problem). This makes it clear that the radiation pressure cannot be related to the time average of the momentum. This circumstance was first noticed in 1912 by Ehrenfest during a discussion with Brillouin [9].

If, however, we calculate the momentum contained in a section equal to the length of the wave train, we obtain the correct result: the momentum equals the product of the radiation pressure by the time duration of the wave train [5, 9].

What is important for further treatment of problems in non-linear acoustics is in our opinion the remark that the usual arguments apply essentially only to phenomena with certain particular types of boundary and initial conditions. At the same time one must note, that unless viscosity and heat conductivity are considered, second-approximation acoustics cannot account for many interesting and important phenomena.

## LITERATURE CITED

[1] N. Andrejew, "Uber die energieausdrucke in der akustic," J. Phys. USSR 2, 305-312 (1940).

[2] A. Schoch, "Remarks on the concept of acoustic energy," Acustica 3, 181-184 (1953).

[3] I. Markham, "Second-order acoustic fields: energy relations," Phys. Rev. 86, 712 (1952).

[4] I. Markham, "Second-order acoustic fields: relations between energy and intensity," Phys. Rev. 89, 972 (1953).

[5] A. Schoch, "Zur Frage nach dem Impuls einer Schallwelle," Z. Naturforschung 72, 273-279 (1952).

[6] Fubini-Giron, "Pressione di radiatione acustica e onde di grande ampiezza," Alta frequenza, 4, 530-581 (1935); 4, 650-653 (1937).

[7] P. I. Westerwelt, "Mean pressure and velocity in a plane acoustical wave in gas," J. Acoust. Soc. Am. 22, 319-327 (1950).

[8] I. G. Rusakov, "Concerning sonic wind," J. Appl. Phys. (USSR) 7, 67-106.

[9] L. Brillouin, "Sur les tensions de radiation," Ann. phys. 4, 528-586 (1925).

Acoustics Institute of the USSR Academy of Sciences,
Moscow.

Received December 21, 1954.

# MEASUREMENT OF NONLINEAR DISTORTION IN LOUDSPEAKERS BY USING INFRASONIC MODULATION

**B. G. Belkin**

The fact that loudspeakers do not have uniform frequency characteristics makes it difficult to measure their nonlinear distortion by ordinary methods. It is therefore proposed to determine the nonlinear distortion in loudspeakers by applying to them signals at sonic and infrasonic frequency and measuring the sound pressure due to the displacement of the moving system at infrasonic frequency.

At present nonlinear distortion in electro-acoustic apparatus is measured by various methods and correspondingly various criteria are used to estimate the nonlinear distortion. Thus, for example, the composition and relative level of higher harmonics, produced by the tested apparatus when reproducing a sinusoidal signal (the harmonic method), is widely used to estimate the distortion. Another group of methods call for applying to the apparatus two sinusoidal signals at different frequencies; the nonlinear distortion is estimated from the relative level of the resulting combination tones (intermodulation method, difference-tone method, etc.). All these methods have one common shortcoming, that the measurement results depend to a considerable extent not only on the nonlinear properties themselves, but also on the frequency response of the apparatus under test. This shortcoming manifests itself particularly strongly when measuring nonlinear distortion in loudspeakers, which in the majority of cases have a very uneven frequency characteristic.

It is therefore of interest to develop a method for measuring non-linear distortion specifically suitable for the investigation of loudspeakers, and therefore as free as possible from the above shortcoming. Such a method may be the measurement of non-linear distortion in loudspeakers described in this article, called arbitrarily the "infrasonic-modulation method" and representing a special modification of the intermodulation method.

Consider the block diagram shown in Fig. 1. It contains an audio frequency signal generator with an amplifier, an infrasonic generator producing a frequency on the order of one cycle, and a mixing device to combine linearly the audio and infrasonic signals; the receiving portion contains a sound-pressure meter with a microphone, detector, and indicator. Let the key K be open. Then the loudspeaker receives only the audio frequency signal, and if the latter is constant in time, the voltage measured by the indicator is also constant. Let us now close key K; then, the loudspeaker receives not only the audio frequency signal but also an infrasonic voltage. Were the loudspeaker linear, the infrasonic vibrations of the moving system would not affect at all the radiated audio frequency signal, and the indicator readings would remain unchanged. Actually, however, the loudspeaker introduces nonlinear distortion and the radiated audio frequency signal varies in synchronism with the infrasonic displacement moving system. If the time constant of the detector in the receiver is small compared with the period of the infrasonic signal, the detector output contains in addition to a dc component, also an ac component at infrasonic frequency. The relative magnitude of this component can serve as a measure of the combination-type nonlinear distortion, introduced by the loudspeaker.

Let the loudspeaker, energized as shown in Fig. 1, produce at a certain fixed point of the field a sound pressure of effective value $\overline{p(t)}$. If the sound signal applied to the loudspeaker is constant and there is no nonlinear distortion, $\overline{p(t)}$ = const. If nonlinear distortion is produced in the loudspeaker, $\overline{p(t)}$ varies periodically with a period T, equal to the period of the infrasonic-frequency voltage. Expanding $\overline{p(t)}$ in a series with respect to the period T, we can write

$$\overline{p(t)} = \overline{p_0} + \sum_{n=1}^{\infty} \overline{p_n} \cos (n\Omega t + \varphi_n),$$

**where $\Omega = \frac{2\pi}{T}$. We define the coefficient of infrasonic modulation as the ratio**

$$k = \frac{\sqrt{\sum_{n=1}^{\infty} \overline{p_n^2}}}{\overline{p_0}}. \qquad (1)$$

**It is easy to see that if the audio frequency signal is a pure tone, the definition of the infrasonic-modulation coefficient agrees with the usual definition of the intermodulation coefficient. However, in general, the infrasonic-modulation coefficient has a wider meaning, for its definition imposes no limitations whatever on the type of the modulated sound signal.**

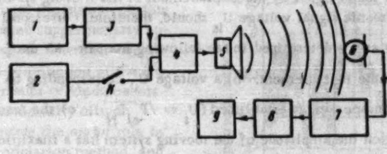

**Fig. 1. Block diagram for measuring nonlinear distortion in loudspeaker using the infrasonic-modulation method.**
**1) audio frequency signal source, 2) infrasonic-frequency generator, 3) amplifier, 4) mixing device, 5) loudspeaker under test, 6) measuring microphone, 7) sound-pressure meter, 8) detector, 9) indicator.**

**In addition to introducing the infrasonic-modulation coefficient k, let us also introduce the concept of the infrasonic-inhomogeneity coefficient m, which will be defined by the following expression**

$$m = \frac{P_{max} - P_{min}}{P_{max} + P_{min}}, \qquad (2)$$

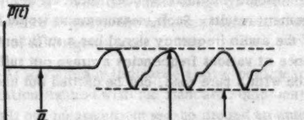

**Fig. 2. Concerning the determination of distortion coefficients.**

**where $\overline{p}_{max}$ and $\overline{p}_{min}$ are the maximum and minimum values of the effective value of the sound pressure respectively (Fig. 2). If the audio frequency signal is a pure tone, the definition of the infrasonic-inhomogeneity coefficient agrees with the generally accepted definition of the amplitude-modulation coefficient. In general, however, the coefficient of infrasonic inhomogeneity, like the coefficient of infrasonic modulation, has a wider meaning, for here, too, the definition imposes no limitations on the type of the modulated signal.**

It is important to emphasize that the definition of the infrasonic-modulation coefficient is based on an estimate of the energy spectrum of the sound pressure developed by the loudspeaker, while the definition of the infrasonic-inhomogeneity coefficient is based on an estimate of the time properties of the sound pressure. There can be, therefore, no one-to-one correspondence between these two coefficients.

The principal criterion of nonlinear distortion as measured with the infrasonic-modulation method is naturally the infrasonic-modulation coefficient, since it is defined on the basis of the spectral properties of the signal under investigation just as the generally accepted nonlinear distortion coefficients, namely the harmonic coefficient, the intermodulation coefficient, etc., are defined. In certain cases, however, as will be shown below, the measurement of the infrasonic-inhomogeneity coefficient is significant in itself.

The waveform of the infrasonic signal used in measurements by this method does not play a substantial role. However, the most convenient is a sinusoidal signal having a frequency on the order of one cycle, for it is barely radiated by the loudspeaker and makes it possible to record the measurement results automatically. No particular requirements are made with respect to the accuracy of the frequency and its constancy.

Let us consider the problem of the required magnitude of the infrasonic signal. Nonlinear distortion is usually estimated in a loudspeaker for a specified value of the electric power $P_{el}$ delivered to the speaker. The infrasonic-modulation method obtains a measure of the combination distortion of the intermodulation-type, introduced into the transmitted sound signal by the displacement of the moving system of the loudspeaker at the infrasonic frequency. The infrasonic-signal voltage $U_{is}$ should, therefore, correspond to the power $P_{el}$ called for by the measurement conditions and is determined in the following manner: a) the power $P_{el}$ is established in accordance with the purpose of the measurement; b) a voltage $U_s$, corresponding to this power $P_{el}$ and to the nominal resistance $R_N$ of the loudspeaker, is established ($U_s = \sqrt{P_{el} R_N}$); c) the frequency $f_s$ within the reproducible frequency range, at which the amplitude of the moving system has a maximum, is determined; d) the displacement X is measured at the frequency $f_s$ and at the voltage $U_s$; e) the infrasonic-signal voltage $U_{is}$, at which the moving system has a displacement X, is established. This voltage $U_{is}$ is used in measurements of the nonlinear distortion.

The audio frequency signal can be either a pure tone of any frequency, a multiple tone, white noise, sections of arbitrary width from the white-noise spectrum, etc. The audio frequency signal power $P_s$ should be so chosen as to make the displacement of the moving system under the influence of this signal small compared to the displacement produced by the infrasonic signal. A suitable ratio is $P_s = (0.05\text{-}0.10)\ P_{is}$.

As is known, the electro-acoustic parameters of loudspeakers should usually be measured either in open air or in soundproof chambers. Matters are different if nonlinear distortion is measured using the infrasonic-modulation method. If the audio frequency signal employed is a pure tone, the measurement process does not involve comparison of levels of components of different frequency, and interference phenomena do not affect the results of the measurements. These measurements can, therefore, be performed under all acoustic conditions. If the audio frequency signal has a more complicated spectral composition, interference may affect the relative roles of the individual spectral components. The dependence of the infrasonic-modulation coefficient on the frequency of the audio signal may correspondingly change also the measurement results. Such measurements would have, therefore, to be made in a special acoustic set-up. However, if the audio frequency signal has a sufficiently rich spectrum, such as white noise, the errors introduced by interference at various frequencies average out sufficiently well and in practice such measurements, like measurements made with a pure tone, can be carried out under all acoustic conditions.

Let us consider several variants of measurements of greatest interest.

Measurement of the frequency characteristic of the infrasonic-modulation coefficient. In this measurement the audio frequency source is an audio signal generator. The value of the infrasonic-modulation coefficient is read with an infrasonic "modulometer", connected at the output of the sound-pressure meter. The measurement consists of finding the infrasonic-modulation coefficient at various frequencies of the audio frequency tone, and plotting the frequency variation of the infrasonic-modulation coefficients from the obtained values.

The measurement of the frequency characteristic of the infrasonic-inhomogeneity coefficient differs from the preceding measurement only in that the infrasonic modulometer is replaced here by an ordinary effective-value voltmeter. The nonlinear distortion causes corresponding changes in the voltmeter readings, which are recorded. Equation (2) is then used to calculate the corresponding infrasonic-inhomogeneity coefficient. Such measurements are very easy to automatize: it is enough to replace the voltmeter with a corresponding automatic-recording instrument and to vary the setting of the audio frequency generator in synchronism with the motion of the chart. Fig. 3 shows a typical sensitivity vs. frequency curve, plotted under ordinary conditions, and the same plot obtained in the presence of an infrasonic signal. It is easy to see that the latter characteristic presents a clear idea of the infrasonic-inhomogeneity coefficient and of its dependence on the audio frequency signal.

It is not without interest to note that the set-up used for such measurements differs from the one usually employed to measure loudspeaker frequency-sensitivity characteristics only in that the latter contains an additional infrasonic-frequency generator and a mixing device. These measurements thus do not require any complicated supplementary apparatus and can be readily made wherever equipment is available for the determination of the frequency-sensitivity characteristics of loudspeakers. By virtue of the exceeding simplicity of such measurements, they can assume the major role in the use of the infrasonic-modulation method, and the infrasonic-modulation coefficients can be measured if more detailed investigations are needed.[*]

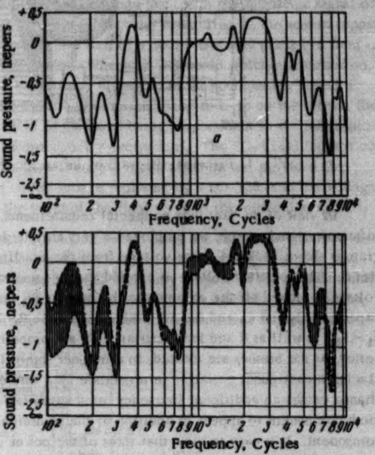

Fig. 3. Typical frequency characteristic of a loudspeaker.
a – recorded under ordinary conditions, b – the same characteristic, recorded in the presence of an infrasonic signal.

Measurement of average infrasonic-modulation and inhomogeneity coefficients. The average nonlinear-distortion coefficient is a rough criterion of the quality of a loudspeaker. In certain cases, however, it may be of interest in itself. It is appropriate here to make an analogy between nonlinear distortion and the sensitivity. As is known, the average sensitivity of a loudspeaker has little to do with its quality. Nevertheless, in many cases when a comparative estimate or sampling of regular production runs is required, measurement of the average sensitivity is of some interest. The average nonlinear-distortion coefficients can be obtained by measuring the areas of the corresponding frequency characteristics with a planimeter, but such a procedure is quite laborious. It is, therefore, advantageous to measure the average distortion coefficients directly. To perform such measurements it is enough to obtain the audio frequency signal from a white noise-generator, which covers the entire range of the audio frequencies. By passing the white noise through suitable filters, it is possible to gauge the nonlinear distortion with allowances for the properties of the ear, for the spectral properties of real signals, etc.

As was already indicated above, nonlinear distortion of loudspeakers can be measured with the infrasonic-modulation method with the standard equipment used to investigate the frequency characteristics of loudspeakers. We built our measurement set-up around an automatic "characterograph" (level recorder) and an ordinary sound-pressure meter. The set-up was supplemented only with an infrasonic-signal source, mixer, and modulation meters.

---

[*] Let us further remark that experience with the measurements already performed shows that in practice the ratio of the infrasonic-inhomogeneity and modulation coefficients does not vary over a very wide range (from 1 to 2).

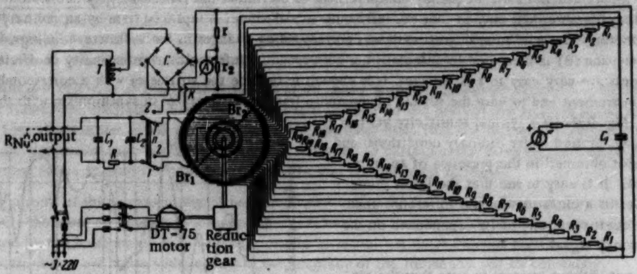

Fig. 4. Principal diagram of infrasonic-frequency generator.

In view of the fact that no special requirements, except for sufficient power, have been imposed on the infrasonic signal source, we employed a very simple device, a rheostatic dc to ac inverter; its principal diagram is shown in Fig. 4. The voltage from the ac line is applied to auto-transformer T and from there to rectifier C. The rectified voltage is applied through resistances $R_1 - R_{19}$ to the segments of a commutator K. The voltage is picked off the commutator by brushes $Br_1$ and $Br_2$ and is fed to the load through a filter, containing capacitors $C_2$ and $C_3$ and the adjustable resistance R. If the commutator is properly constructed and if resistances $R_1 - R_{19}$, as well as R and load resistance $R_1$ are properly selected, the load current varies during one-fourth of a period, as the brushes are rotated, in a manner shown in Fig. 5, i.e., the current varies nearly sinusoidally. Replacing a continuous variation in resistance by a discrete change causes an additional frequency-modulated sawtooth component to appear in addition to the sinusoidal component. It is easy to show that most of the power of this interfering signal is concentrated in the audio frequency range. It is eliminated by means of a filter, consisting of resistance R and capacitances $C_2$ and $C_3$. If the filter is used, the load current hardly differs from a sinusoidal one. A voltage divider, consisting of resistances $r_1$ and $r_2$, and an ammeter A are used to calibrate the setup, the calibration being reduced to measuring the load resistance by the voltmeter-ammeter method.

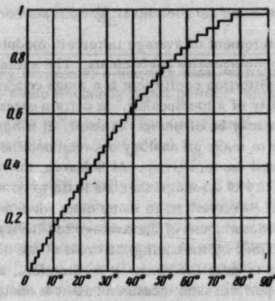

Fig. 5. Curve showing current in infrasonic-frequency generator.

The modulation meters employed were essentially effective-value and peak-value voltmeters to measure the corresponding parameters of the infrasonic component of the signal at the output of the sound-pressure meter.

A diagram of a modulation meter for the infrasonic-modulation coefficient is shown in Fig. 6. The rectified voltage from the sound-pressure meter is fed to potentiometer R and from it to the zero-center meter M. Equalizing battery B is also connected to the meter. With the infrasonic-frequency generator disconnected, the potentiometer R is adjusted until the pointer of indicating meter IM is at zero, after which switch $S_1$ is placed in position 2. This substitutes a large-time-constant thermocouple meter TM in the circuit for meter M. If necessary, potentiometer R is readjusted to obtain no reading on the TM instrument. The infrasonic voltage is then applied to the loudspeaker under test and the TM meter is read, its reading being proportional to the modulation coefficient. The scale of the TM instrument is graduated directly in infrasonic-modulation coefficient units. Switch $S_2$ and resistances $R_2$, $R_3$, and $R_4$ serve to vary the sensitivity of the instrument.

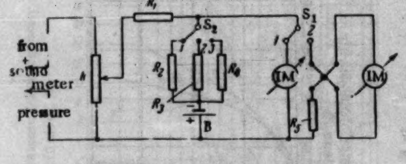

Fig. 6. Principal diagram of modulation meter to measure infrasonic-modulation coefficients. Resistances: R – 600 ohms; $R_1$ – 300 ohms; $R_2$ – 250 ohms; $R_3$ – 750 ohms; $R_4$ – 4,750 ohms; $R_5$ – 250 ohms; B – battery.

Fig. 7 shows a modulation-meter circuit for the infrasonic-inhomogeneity coefficient. Rectified voltage from the output of the sound-pressure meter is applied through potentiometer R to the grid of tube V-1 and next to the vertical deflecting plate of cathode-ray tube V-2, which has a long-persistence screen. The line voltage is applied to the horizontal plates of the tube. By adjusting potentiometer R with the infrasonic signal off it is possible to set the sweep line on the screen opposite the abscissa axis of a coordinate grid placed in front of the screen. When the infrasonic voltage is turned on, the nonlinear distortion in the loudspeaker causes a horizontal illuminated band to form on the screen, the width of the band being proportional to the infrasonic-inhomogeneity coefficient. The EO-4 oscillograph can be used as such a modulation meter, provided the LO-737 tube is replaced by a LO-736, and the voltage from the output of the sound-pressure meter is applied to the input of the final stage of the vertical amplifier.

The detailed systematic study of the nonlinear distortion in loudspeakers using the infrasonic-modulation method, the disclosure of the causes of distortion, the development of means for reducing this distortion, and similar problems could all serve as a subject for a special investigation. The only purpose of the experimental data cited below is to illustrate the practical application of the infrasonic-modulation method. Nevertheless, these data furnish some information concerning the magnitude and character of the nonlinear distortion in a loudspeaker.

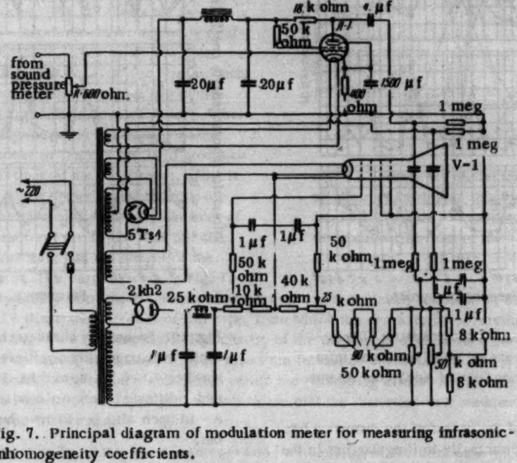

Fig. 7. Principal diagram of modulation meter for measuring infrasonic-inhomogeneity coefficients.

Fig. 8 shows graphs of average infrasonic-inhomogeneity coefficients for several industrial types of motion-picture cone speakers as functions of the power delivered to the loudspeaker. White noise was used in these measurements as the audio frequency signal. The audio-frequency voltage was normalized with respect to that particular sound frequency, at which the displacement of the moving system of the loudspeakers was a maximum for a constant applied voltage.* The best of the measured speakers was the 2A-8, which has an average distortion coefficient not exceeding 3 percent at the nominal power rating. Loudspeakers 1A-10 and 4D-6 have comparable nonlinear properties. The 1A-10 speaker is somewhat worse at high power, at which the distortion of the 4D-6 speaker is somewhat lower.

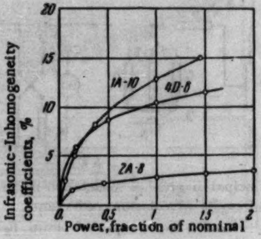

Fig. 8. Plots of average infrasonic-inhomogeneity coefficients.

Fig. 9 shows the frequency characteristics of the infrasonic-modulation and infrasonic-inhomogeneity coefficients of the above loudspeakers. These curves are obtained by "point-by-point" measurements in which the nominal audio frequency voltage was applied to the loudspeakers. The graphs show that in these speakers the ratio of the infrasonic-inhomogeneity to the infrasonic modulation coefficient ranges from 1 to 2. The curves in Fig. 10 were measured under different acoustic conditions and show that the measurement results are independent of the acoustic environment.

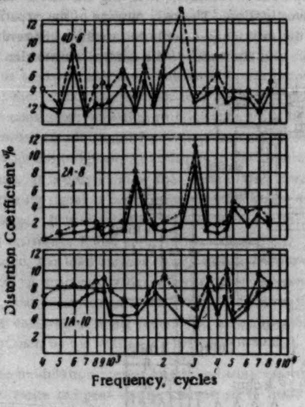

Fig. 9. Frequency characteristics of infrasonic-inhomogeneity (solid line) and infrasonic-modulation (dotted line) coefficients.

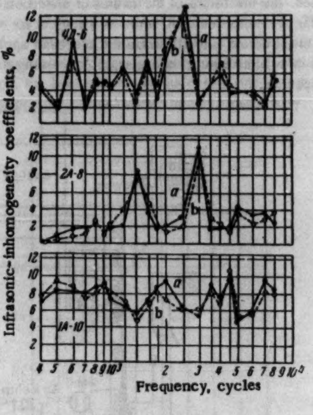

Fig. 10. Frequency characteristics of infrasonic-inhomogeneity coefficients of loudspeakers 4D-6, 2A-8, and 1A-10, measured under different acoustic conditions:
a – in open air, b – in reverberation chamber.

Investigation of the causes of the distortion has shown that it is due principally to irregularities in the magnetic field in the operating gap and that it depends greatly on the position of the moving system. Fig. 11 shows infrasonic-inhomogeneity coefficient curves, obtained with the moving system in its normal position and with the system artificially displaced by 1.5 and 3 mm.

---

* The displacement amplitudes were measured in this investigation either optically, or by using a capacitive probe.

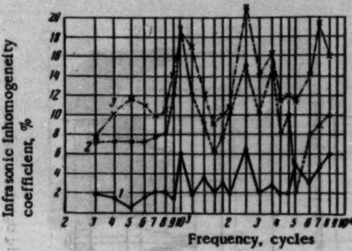

Fig. 11. Frequency characteristics of coefficient of infrasonic inhomogeneity of 2A-8 speaker at various positions of the voice coil.
1 – normal position; 2 – displaced by 1.5 mm;
3 – displaced 3 mm.

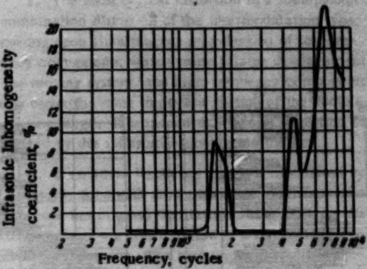

Fig. 12. Frequency characteristic of infrasonic-inhomogeneity coefficient of loudspeaker 1A-13.

The distortion increases sharply when the moving system is incorrectly placed. The horn speaker chosen for investigation was the 1A-13, which is used as the high-frequency element in the 30A-1, -2, -3 motion picture speaker systems. Fig. 12 shows the frequency characteristic of the infrasonic-inhomogeneity coefficient of this loudspeaker. This curve was plotted at an infrasonic displacement equal to the displacement produced by nominal applied power at 500 cycles (5 va). Investigation of the causes of distortion has shown that it is due principally to changes in the volume of the chamber in front of the horn produced by infrasonic oscillations of the diaphragm. This is proven by Fig. 13, which shows characteristics obtained for various heights of the chamber in front of the horn.* It is seen from the figure that the distortion decreases noticeably as the height of the chamber is increased. The curves shown in Fig. 13 were obtained analytically from the frequency characteristics automatically recorded in the presence of an infrasonic signal. Fig. 14 illustrates a record of this type, from which the characteristics serving as a basis for calculating the graphs of Fig. 13 were obtained. The quality of the diaphragm also exerts a not insignificant influence on the formation of nonlinear distortion. Fig. 15 shows the frequency characteristic of the 1A-13 loudspeaker, having a diaphragm with a deficiency commonly called the "crackling effect" in practice. This curve corresponds to the nominal power at 500 cycles; it is easy to see that the distortion in a loudspeaker with a defective diaphragm of this type is very high.

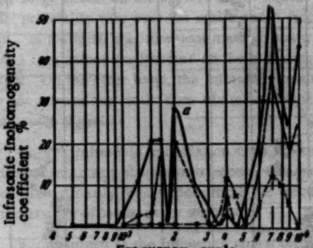

Fig. 13. Frequency characteristics of coefficient of infrasonic inhomogeneity of 1A-13 loudspeaker at varying heights of the chamber in front of the horn:
a – 0.7 mm, b – 1 mm, c – 2 mm.

In conclusion let us formulate the advantages and shortcomings of the infrasonic-modulation method. The advantages of the method can be summarized as follows:

---

* These curves were plotted with an infrasonic displacement corresponding to four times the nominal displacement at 500 cycles.

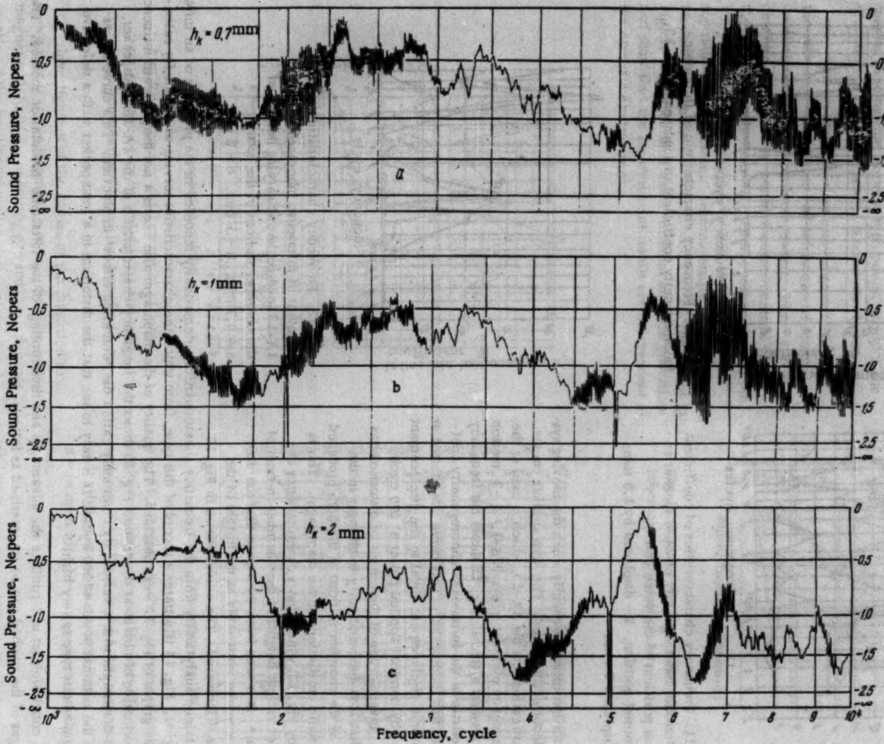

Fig. 14. Frequency characteristics of 1A-13 loudspeaker, plotted in the presence of an infrasonic signal, at various heights of the chamber in front of the horn: a) 0.7 mm, b) 1 mm, c) 2 mm.

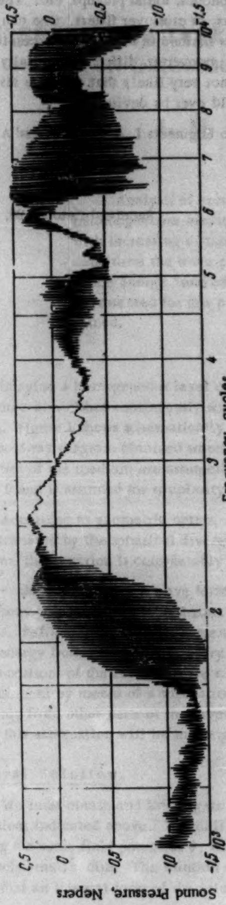

Fig. 15. Frequency characteristics of 1A-13 loudspeaker with defective moving system; the characteristic is plotted in the presence of an infrasonic signal.

1. The most typical distortion in a loudspeaker is combination distortion of the intermodulation type, occurring upon simultaneous reproduction of low-frequency components, which cause a large displacement of the moving system, and high-frequency components, which cover the most important portion of the audible-frequency range. It is indeed this type of distortion that is gauged by the infrasonic-modulation method.

2. If an audio frequency signal is modulated by an infrasonic tone with an approximate frequency of one cycle, both the original oscillations, as well as the distortion products are concentrated in a rather narrow section of the spectrum. The measurement results are, therefore, practically independent of the frequency characteristics of the loudspeakers.

3. The magnitude and character of the intermodulation distortion occurring in the loudspeaker depend to a very large extent on the applied high frequency which should preferably vary over the entire audio frequency range. In the usual measurement method, many substantial limitations are imposed on the high frequency applied. On the other hand, the infrasonic modulation does not impose any limitations whatever on the frequency of the audio signal.

4. The infrasonic modulation calls for a small number of relatively simple instruments, the majority of which are ordinarily used to determine the frequency characteristics of loudspeaker sensitivity.

5. Inasmuch as the frequency characteristics of the nonlinearity distortion coefficients of loudspeakers are very uneven, it is extremely desirable to be able to record this distortion automatically. The infrasonic-modulation method affords such an opportunity.

6. Measurements made with the infrasonic-modulation method require no special acoustic environments and can be performed practically under all conditions.

Along with the above advantages, the infrasonic-modulation method has the following shortcomings.

1. No wave process is produced in the horn if the moving system of a horn loudspeaker is made to vibrate at a frequency of approximately one cycle. The infrasonic-modulation method, therefore, does not permit measurement of the nonlinear distortion occurring in the horn.

2. When nonlinear distortion is measured with the infrasonic-modulation method it is first necessary to normalize the amplitudes of the infrasonic displacements of the moving-system displacements relative to the displacement produced at a certain suitably-selected audio frequency. Such normalization can be readily effected with the aid of rather simple instruments; it does involve supplementary measurements, however, and is, therefore, a shortcoming of the method.

3. The infrasonic-modulation method is applicable only to loudspeakers and other electro-acoustic apparatus responsive to the action of an infrasonic signal, such as microphones, sound pickups, etc. The method cannot be used to measure distortion produced in amplifiers, transformers, or crossover filters. One can readily understand, however, that this shortcoming cannot seriously discredit this method in any manner when it comes to loudspeakers. The loudspeaker, being a complicated electro-acoustic converter, differs substantially in its properties from all other electro-acoustic apparatus, and it is therefore not very likely that a simple distortion measurement procedure, common for all electro-acoustic apparatus could ever be devised.

The author takes advantage of this occasion to express gratitude to Engineers I. A. Khraban and A. G. Smirnov for help in performing this work.

Scientific-Research Motion Picture Photography Institute,
Moscow.

Received October 20, 1954

# CONCERNING ONE TYPE OF ATTENUATION OF WAVES PROPAGATING IN INHOMOGENEOUSLY-STRATIFIED MEDIA

**L. M. Brekhovskikh and I. D. Ivanov**

Analysis of propagation of waves in a layer, bounded on one end by an inhomogeneous medium, in which the velocity of wave propagation diminishes with increasing distance from the layer boundary. It is shown that under these conditions the wave propagation is subject to supplementary attenuation, due to the energy "soaked up" by the inhomogeneous medium. A complete theory is presented for this problem and the magnitude of the attenuation is determined.

Imagine a homogeneous layer of thickness h, directly under a medium in which the velocity of wave propagation c diminishes continuously with increasing distance from the layer; in the homogeneous layer we have $c = c_0$. Figure 1 shows schematically the dependence of the velocity of wave propagation on the coordinate z, and also a ray diagram obtained when a wave source is located at point O inside the homogeneous layer. The properties of the medium are assumed to be constant at the planes z = const. The lower boundary of the layer is z = 0 and is assumed for simplicity to be perfectly reflecting.

According to geometric optics, a ray leaving O propagates horizontally as far as can be imagined, becoming attenuated by the spherical divergence of the wave and by the absorption of energy by the medium. Actually, however, the situation is considerably more complicated. Diffraction will cause the ray to become blurred. At $r \sim \frac{h^2}{\lambda}$ the ray becomes a wave formation occupying the entire thickness of the layer. Starting with this instant, the inhomogeneous medium will start "soaking up" the energy from the ray. This soaking can be visualized as follows. Refraction by the inhomogeneous medium causes the rays to be deflected away from the layer, and the wave energy from the upper boundary of the layer is rapidly consumed in the inhomogeneous medium. This causes portions of the layer that are close to the upper boundary to become poorer in the energy sense. This impoverishment by means of a mechanism, frequently called "transverse diffusion," is compensated by the influx of energy from other parts of the layer, causing additional attenuation of the waves propagating through the layer; this attenuation will be investigated below.

## General Solution.

We must obtain and investigate a rigorous solution to the problem of the propagation of waves under the conditions indicated above. We shall restrict ourselves to the scalar problem and to be specific we shall speak of finding the sonic field potential $\psi$, while the radiator O will be represented in the form of a pulsating sphere of infinitely small radius. The solution of such a problem was given in general form in Reference [1]. It was shown there that an integral form of the solution can be written down as follows.

a) The potential of the field in the homogeneous layer (z < h) is

$$\psi_0(r, z) = \int_\Gamma \Phi_0(z, \alpha)\, H_0^{(1)}(k_0 r \cos\alpha) \cos\alpha\, d\alpha, \tag{1}$$

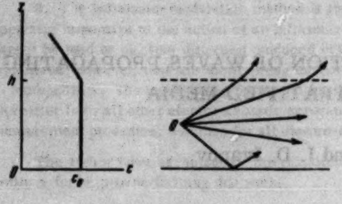

Fig. 1

where $\alpha$ is the complement of the angle of incidence of the plane wave, $k_0$, the wave number for the homogeneous layer, and $H_0^{(1)}$ is the Hankel function of the first kind and of zero order.

Furthermore,

$$\Phi_0(z, \alpha) = -\frac{ik_0}{2}\frac{\Phi_{01}(z, \alpha)}{\Phi_{02}(\alpha)}, \tag{2}$$

whereby

$$\Phi_{01}(z, \alpha) = [\exp\{-ik_0 z \sin\alpha\} + V_1 \exp\{ik_0 z \sin\alpha\}]\,[\exp\{ik_0 z_0 \sin\alpha\} + + V \exp\{ik_0(2h - z_0)\sin\alpha\}], \tag{3}$$

$$\Phi_{02}(\alpha) = 1 - V_1 V \exp\{2ik_0 h \sin\alpha\}. \tag{4}$$

Here $z_0$ is the coordinate of the radiator, and $V_1$ and $V$ are the reflection coefficients for the plane wave from the lower and upper boundaries of the layer respectively.

Expression (3) for the function $\Phi_{01}$ is valid for the case $z < z_0$. If $z > z_0$, $\Phi_{01}$ is obtained from (3) by interchanging $z$ and $z_0$. $\Gamma$ denotes the integration contour in the complex $\alpha$-plane, going from $\pi - i\infty$ along a straight line to $\pi$, then along the real axis to zero, and from there along the positive imaginary axis to $i\infty$.

b) The potential of the field in the inhomogeneous medium ($z > h$) is

$$\psi(r, z) = \int_\Gamma \Phi(\alpha)\,\varphi(z, \alpha)\,H_0^{(1)}(k_0 r \cos\alpha)\cos\alpha\, d\alpha, \tag{5}$$

where $\varphi(z, \alpha)$ is the potential of the field in the inhomogeneous region, corresponding to a plane wave of unit amplitude, incident from the homogeneous layer into the inhomogeneous layer. Furthermore,

$$\Phi(\alpha) = -\frac{ik_0}{2}\frac{\Phi_1(\alpha)}{\Phi_2(\alpha)}, \tag{6}$$

where

$$\Phi_1(\alpha) = \exp\{ik_0(h - z_0)\sin\alpha\} + V_1 \exp\{ik_0(h + z)\sin\alpha\}, \tag{7}$$

$$\Phi_2(\alpha) = 1 - V_1 V \exp\{2ik_0 h \sin\alpha\} = \Phi_{02}. \tag{8}$$

---

The factor $e^{-i\omega t}$ is omitted from all equations for the sake of brevity.

## Reflection Coefficient for Plane Wave Reflected from Inhomogeneous Medium.

To make the problem more specific, we must specify the velocity distribution in the inhomogeneous medium (at $z > h$) and to obtain the reflection coefficient of a plane wave $V = V(\alpha)$.

Assume that the velocity $c$ depends on the coordinate $z$ in the following manner:

$$\left.\begin{aligned} c &= c_0, && \text{at} \quad 0 \leqslant z \leqslant h, \\ c &= \frac{c_0}{\sqrt{1+2a(z-h)}}, && \text{at} \quad z \geqslant h. \end{aligned}\right\} \tag{9}$$

Since the quantity $a$ can be considered sufficiently small in practical cases, the chosen variation of $c$ with $z$ is essentially equivalent to a linear relationship

$$c = c_0[1 - a(z-h)]. \tag{10}$$

Let a plane wave be incident on an inhomogeneously-stratified medium of this type, making an angle $\alpha$ with its surface. It is convenient to introduce a new variable $z_1 = z - h$, and to drop the index everywhere from now on. Then the field in the homogeneous medium, consisting of an incident and reflected wave, can be written in the following manner:

$$\varphi_0(z, \alpha) = [\exp\{ik_0 z \sin\alpha\} + V \exp\{-ik_0 z \sin\alpha\}] \exp\{ikx \cos\alpha\}. \tag{11}$$

The corresponding field in the inhomogeneous medium $\varphi(z, \alpha)$, which is the solution of the wave equation, shown in Reference [1], is of the form

$$\varphi = C w^{1/3} H^{(1)}_{1/3}(w), \tag{12}$$

where C is an arbitrary constant, $H^{(1)}_{1/3}$ is the Hankel function, and

$$w = \frac{k_0}{3a}(\sin^2\alpha + 2az)^{3/2}. \tag{13}$$

For the function $H^{(1)}_{1/3}(w)$ to represent an outgoing wave at large values of w, the positive square root $\sqrt{\sin^2\alpha + 2az}$ must be taken, so that we have $\arg w = 0$ at real values of $\alpha$.

The continuity conditions for the sound pressure and for the normal component of velocity at the boundary $z = 0$ are written as

$$\left.\begin{aligned} \varphi_0 &= \varphi \\ \frac{\partial\varphi_0}{\partial z} &= \frac{\partial\varphi}{\partial z} \end{aligned}\right\} z = 0.$$

This yields V and C. Substituting the resultant value of C into (12) we get

$$\varphi = 2\left(\frac{w}{w_0}\right)^{1/3} \frac{H^{(1)}_{1/3}(w)}{H^{(1)}_{1/3}(w_0) - iH^{(1)}_{-2/3}(w_0)}, \tag{14}$$

where

$$w_0 = w_{z=0} = \frac{k_0}{3a}\sin^3\alpha. \tag{15}$$

The corresponding expression for V is of the form:

$$V = -e^{i\eta}, \tag{16}$$

where

$$\eta = -2\arctan\frac{H^{(1)}_{1/3}(w_0)}{H^{(1)}_{-2/3}(w_0)}. \tag{17}$$

We assume the reflection coefficient from the lower boundary to be $V_1 = -1$, corresponding in the case of radio waves to the reflection of horizontally-polarized waves from a perfectly conducting boundary. The case $V_1 = -1$ occurs in acoustics when sound waves are reflected from a water-air boundary.

## Solution in Series.

As shown in [2], it is possible, by deforming the contour of integration $\Gamma$, to represent integrals (1) and (5) in the region $\operatorname{Im}\alpha \leq 0$; $0 < \operatorname{Re}\alpha < \frac{\pi}{2}$, in the form of sums of residues about the poles to which are added the integrals at the edges of the cuts, should it become necessary to pass around a branch point when deforming the contour $\Gamma$. In our case the branch points $\pm\sinh^{-1}\sqrt{2az}$ are not touched when the integration path is deformed. Consequently, the potential of the field is represented only by a sum of residues, or using P. E. Krasnushkin's terminology, by a sum of "normal waves":

$$\psi_0 = 2\pi i\sum_l \operatorname{Res}\left[\Phi_0(z,\alpha)\, H_0^{(1)}(k_0 r\cos\alpha)\cos\alpha\right]_{\alpha=\alpha_l}, \tag{18}$$

$$\psi = 2\pi i\sum_l \operatorname{Res}\left[\Phi(\alpha)\,\varphi(z,\alpha)\, H_0^{(1)}(k_0 r\cos\alpha)\cos\alpha\right]_{\alpha=\alpha_l}, \tag{19}$$

where $\alpha_l$ are the zeros of function (8). Since $V = -e^{i\eta}$ and $V_1 = -1$, the equation for the poles $\alpha_l$ can be written as

$$\eta(\alpha) + 2k_0 h\sin\alpha = 2\pi l, \tag{20}$$

where $l$ is an integer.

Let us calculate the values of the residues in expressions (18) and (19). For this purpose it is necessary, as is known, to replace the denominator of the integrands in (1) and (5), i.e., the function $\Phi_2(\alpha)$, by $\frac{d\Phi_2}{d\alpha}$ and then substitute $\alpha_l$ everywhere for $\alpha$. Assuming $k_0 r\cos\alpha_l \gg 1$, the function $H_0^{(1)}(k_0 r\cos\alpha)$ can be replaced by its asymptotic expression. As a result we obtain

$$\psi_0 = \sqrt{\frac{2\pi k_0}{r}} \exp\left\{-i\frac{\pi}{4}\right\} \sum_l A_0(z, \alpha_l) \exp\{ik_0 r \cos\alpha_l\}, \tag{21}$$

where

$$A_0(z, \alpha) = \frac{\sqrt{\cos\alpha}}{\eta' + 2k_0 h \cos\alpha} [\exp\{-ik_0 z \sin\alpha\} - \exp\{ik_0 z \sin\alpha\}] \times$$

$$\times [\exp\{ik_0 z_0 \sin\alpha\} - \exp\{i\eta + ik_0(2h - z_0)\sin\alpha\}], \tag{22}$$

$$\eta' \equiv \frac{d\eta}{d\alpha};$$

$$\psi = \sqrt{\frac{2\pi k_0}{r}} \exp\left\{-i\frac{\pi}{4}\right\} \sum_l A(z, \alpha_l) \exp\{ik_0 r \cos\alpha_l\}, \tag{23}$$

where

$$A(z, \alpha) = \frac{\sqrt{\cos\alpha}}{\eta' + 2k_0 h \cos\alpha} [\exp\{ik_0(h - z_0)\} - \exp\{ik_0(h + z_0)\sin\alpha\}]\,\varphi(z, \alpha). \tag{24}$$

Let us make the following remark concerning the Hankel function contained in $\varphi(z, \alpha)$ and $\eta(\alpha)$. The functions $\varphi$ and $\eta$ in equations (21) and (23) are taken at values $\alpha = \alpha_l$. The poles $\alpha_l$ are located in the fourth quadrant, i.e., $-\frac{\pi}{2} \leq \arg \alpha_l \leq 0$; consequently, according to (13) we have $-\frac{3\pi}{2} \leq \arg w \leq 0$. The Hankel functions $H_\nu^{(1)}(w)$ and $H_\nu^{(2)}(w)$ are determined for $|\arg w| > \pi$ with the aid of the imaginary-argument equations. In this case, for the functions $H_{1/3}^{(1)}(w)$ and $H_{-2/3}^{(1)}(w)$, entering into $\varphi$ and $\eta$, these equations are written as

$$H_{1/3}^{(1)}(w) = H_{1/3}^{(1)}(we^{i\pi}) + e^{-i\frac{\pi}{3}} H_{1/3}^{(2)}(we^{i\pi}), \tag{25}$$

$$H_{-2/3}^{(1)}(w) = -H_{-2/3}^{(1)}(we^{i\pi}) - e^{-i\frac{\pi}{3}} H_{-2/3}^{(2)}(we^{i\pi}), \tag{26}$$

where

$$-\pi < \arg(we^{i\pi}) \leqslant \pi. \tag{27}$$

As a result, equations (14) and (17) are written as

$$\varphi = 2\left(\frac{w}{w_0}\right)^{1/2} \frac{H_{1/3}^{(1)}(w_0 e^{i\pi}) + e^{-i\pi/3} H_{1/3}^{(2)}(we^{i\pi})}{\left[H_{1/3}^{(1)}(w_0 e^{i\pi}) + e^{-i\pi/3} H_{1/3}^{(2)}(w_0)\right] + i\left[H_{-2/3}^{(1)}(w_0 e^{i\pi}) + e^{-i\pi/3} H_{-2/3}^{(2)}(we^{i\pi})\right]}, \tag{28}$$

$$\eta = 2 \operatorname{arc\,tan} \frac{H_{1/3}^{(1)}(w_0 e^{i\pi}) + e^{-i\pi/3} H_{1/3}^{(2)}(w_0 e^{i\pi})}{H_{-2/3}^{(1)}(w_0 e^{i\pi}) + e^{-i\pi/3} H_{-2/3}^{(2)}(w_0 e^{i\pi})}. \tag{29}$$

Hereinafter, we shall use the approximate expressions for the functions $\varphi$ and $\eta$, obtained as a result of the series expansion.

At small values of $w_0$ and $w$, expressing the Hankel function in terms of the Bessel functions, and expressing the latter in series form and discarding higher-order terms, we obtain

$$\varphi = \frac{2e^{-i\pi/6}\gamma w_0^{1/3}}{1 + e^{-i\pi/6}\gamma w_0^{2/3}}\left[1 - \frac{3}{2\gamma}e^{-i\pi/3}w^{2/3}\right], \tag{30}$$

$$\left.\begin{aligned} \eta &= i\sqrt{3}\,\gamma w_0^{1/3} + (\gamma w_0^{2/3} - 2\gamma_1 w_0) \\ \gamma &= \frac{1}{2^{1/3}}\frac{\Gamma\left(\frac{1}{3}\right)}{\Gamma\left(\frac{2}{3}\right)} \\ \gamma_1 &= \frac{3}{2} - \frac{1}{3}\gamma^3 \end{aligned}\right\}; \tag{31}$$

At large values of $w_0$ and $w$ we employ the asymptotic expansion of the Hankel function

$$H_\nu^{(1)}(u) = \sqrt{\frac{2}{\pi u}}\exp\left\{i\left(u - \frac{\nu\pi}{2} - \frac{\pi}{4}\right)\right\}\left[1 + \frac{4\nu^2 - 1}{-8iu} + \cdots\right], \tag{32}$$

$$-\pi < \arg u < 2\pi$$

$$H_\nu^{(2)}(u) = \sqrt{\frac{2}{\pi u}}\exp\left\{-i\left(u - \frac{\nu\pi}{2} - \frac{\pi}{4}\right)\right\}\left[1 + \frac{4\nu^2 - 1}{8iu} + \cdots\right]. \tag{33}$$

$$-2\pi < \arg u < \pi.$$

Using (32) and (33) we obtain from (28) and (29)

$$\varphi = \exp\{i(w - w_0)\} + \exp\left\{-i(w + w_0) - i\frac{\pi}{2}\right\}, \tag{34}$$

$$\eta = -2\left(w_0 - \frac{\pi}{4}\right). \tag{35}$$

Inasmuch as according to (33) the second-kind Hankel function of argument $we^{i\pi}$ is valid for $\arg(we^{i\pi}) < \pi$, expressions (34) and (35) are also valid only under this condition, i.e., at $\arg w < 0$. If $\arg w = 0$ (corresponding at $\operatorname{Im} k_0 = 0$ to a real angle $\alpha$), it is necessary to start out with expressions (14) and (17).

In that case we have

$$\varphi = \exp\{i(w - w_0)\}. \tag{36}$$

$$V = 0 \tag{37}$$

At large values of $w_0 = \frac{k_0}{3a}\sin^3\alpha$, i.e., at sufficiently large values of $\alpha$, the reflection coefficient of a plane wave from an inhomogeneous medium of the type under consideration is thus equal to zero in first approximation. If, however, we take into account the second terms of expansions (32) and (33), we get

$$\eta = i\ln(12w_0) - \frac{\pi}{2}. \tag{38}$$

For small $w_0$ but large $w$, a case possible if the angle $\alpha$ is small and the distance from the homogeneous layer is great ($\underline{az}$ is sufficiently large), the Hankel function of the argument $w_0$ must be expanded into a series in the vicinity of zero, and the function of the argument w must be represented in the asymptotic form. As a result we obtained the following expression for $\varphi$:

$$\varphi = 2^{-1/3}\sqrt{\frac{3}{\pi}}\,\Gamma\left(\frac{1}{3}\right)\frac{(w_0^2/w)^{1/3}}{1+\exp\{-i\pi/6\}\gamma w_0^{1/3}}\exp\left\{i\left(w-\frac{5}{12}\pi\right)\right\}. \tag{39}$$

The function $\eta$ is given in this case by (31).

## Poles of Integrands.

The poles of the integrands in (1) and (5) are determined by the roots of equation (20). It is difficult to obtain accurate solutions of this equation. We shall employ the approximate expressions for $\eta$ ($\alpha$), obtained above. The function $\eta$ depends on $\alpha$ only through $w_0$. Let us examine (20) for large values of $w_0$.

Inserting (35) into (20) we obtain the following equation for the poles at large values of $w_0$:

$$x^3 - 3Sx + \left(l - \frac{1}{4}\right)\pi = 0, \tag{40}$$

where

$$x = \left(\frac{k_0}{3a}\right)^{2/3}\sin\alpha, \tag{41}$$

$$S = \frac{1}{3}k_0 h\left(\frac{3a}{k_0}\right)^{1/3}. \tag{42}$$

Since (35) is valid for arg $w_0 < 0$, i.e., since x cannot be positive real, it is necessary to put $l > 0$ in equation (40). In addition, the smallest value of $l$ must be so chosen as to keep the pole corresponding to this value of $l$ away from the real axis. To determine the poles located near the real axis it is necessary to employ the approximate equation (38). Inserting (38) into (20), we get

$$\frac{3i}{2}\ln x + 3Sx + \frac{i}{2}\ln 12 - \left(l - \frac{1}{2}\right)\pi = 0. \tag{43}$$

At large values of S this equation can be solved by successive approximations.

Inserting (31) into (20) we obtain an equation for the poles at small values of $w_0$

$$x^3 - \frac{1}{\gamma_1}\left(3S + \frac{1}{2}\gamma + i\frac{\sqrt{3}}{2}\gamma\right)x + \frac{\pi}{\gamma_1}l = 0. \tag{44}$$

The location of the poles depends on the value of S. If S < 1, the poles are obtained from equation (40) and are located in the region corresponding to $|w_0| > 1$ away from the real axis. At large values of S the first poles are obtained from equation (44); these poles are located in the region corresponding to $|w_0| < 1$, near the real axis. For large values of S equation (44) can be written approximately as $-3Sx + \pi l \approx 0$, hence $x \sim \frac{l}{S}$. Since x must not exceed unity, the number of poles determined from equation (44) is of the order of magnitude of S. Higher-number poles are obtained from equations (43) and (40).

**Estimating the Sum of the Residues.**

Knowing the poles $\alpha_l$, it is possible to estimate the sums in expressions (21) and (23). The factor $\exp\{-k_0 r \operatorname{Im} \cos \alpha_l\}$ causes each term of these sums to diminish with increasing r; the higher the number of the normal wave, the faster the rate of decrease. However, at sufficiently close distances this diminishing factor varies little from one normal wave to the neighboring one. Of importance in this case is a sufficiently large number of normal waves. Within the homogeneous layer, the excitation amplitudes of the first series of normal waves differ little from each other. The distance at which a large number of normal waves still plays an important role is therefore determined from the condition

$$k_0 r \operatorname{Im} \cos \alpha \ll 1. \qquad (45)$$

If this inequality is applied to $\alpha_{l=1}$ and if equation (44) is used to determine $x_1$, (45) can be written as

$$r \ll \frac{h^2}{\lambda} S. \qquad (46)$$

For values of r satisfying condition (46), the sum of normal waves can be replaced by an integral. The latter gives us the value of the field as approximated by the ray theory. We shall take the liberty of omitting the proof of this statement and of not calculating the field by ray methods.

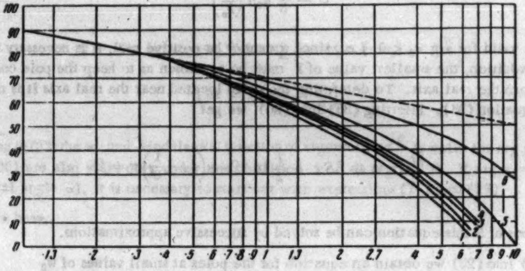

Fig. 2. Variation of Sound intensity with the dimensionless quantity

$$qr = k_0 r \left(\frac{3a}{k_0}\right)^{1/3};$$

1) n = 0.2, m = 0.2, S = 0.2; 2) n = 1, m = 0.2, S = 0.2; 3) n = 0.2, m = 0.4, S = 0.4; 4) n = 1, m = 0.4, S = 0.5; 5) n = 0.4, m = 0.2, S = 0.8; 6) n = 0.4, m = 0.2, S = 1. Dotted line shows the inverse-square law decrease.

Of real interest to us is the region of relatively large distances, when condition (46) is not satisfied. There the field must be calculated by summing over the normal waves. This calculation does not involve great difficulties, for the series converge rapidly for large r.

Figure 2 shows graphically the decrease in the sound intensity with distance in the homogeneous layer for values of S equal to 0.2, 0.4, 0.8, and 1. The ordinates are calibrated in 10 log $|\psi_0|^2$, i.e., essentially in decibels of sound intensity. The zero decibel reference was chosen arbitrarily, corresponding to a definition of $\psi_0$ with an accuracy to within a constant factor.

The parameters $\underline{m}$ and $\underline{n}$ define the respective depth of the radiator and of the receiver: $m = z_0/h$ and $n = z/h$.

It is evident from Fig. 2 that the placement of the receiver within the confines of the homogeneous layer does not affect substantially the rate at which the sound intensity diminishes, and that the smaller S the faster the sound intensity diminishes with distance. At small distance the intensity diminishes approximately as $1/r^2$, marked on the figure by a dotted line. The greater the value of S, the greater the distance for which the inverse-square law holds.

## LITERATURE CITED

[1] L. M. Brekhovskikh, "On the field of a point radiator in an inhomogeneously-stratified medium," Bull. Acad. Sci. USSR, Phys. Ser. 8, 5 (1949).

[2] L. M. Brekhovskikh, "Concerning one case of propagation of sound in an inhomogeneous medium," Doklady Akad. Nauk SSSR 87, 5 (1952).

Acoustics Institute of the USSR Academy of Sciences,
Moscow.

Received November 15, 1954.

# CONCERNING THE GENERAL RELATIONSHIP BETWEEN ABSORPTION AND DISPERSION OF SOUND WAVES

**V. L. Ginzberg**

The general relationship between dispersion and absorption of sound waves is discussed. The problem is first attacked as applied to propagation of electromagnetic waves, and previously-known results are derived. Analogous equations are then obtained to relate the velocity and absorption coefficient of sound. The features that distinguish the acoustic case from the electromagnetic one are discussed.

When the problem of absorption and dispersion of electric and sound waves in various media is analyzed by means of certain model representations, it always turns out that absorption and dispersion are interrelated. This is not accidental, but shows a common relationship to exist between absorption and dispersion, regardless of the particular model chosen. This connection has been known for quite a while, although not extensively for the electrodynamic case [1, 2]. As far as we have been able to find out, the problem of a universal relationship between absorption and dispersion of sound has never been brought up. This too may not be accidental, for from certain considerations there is some doubt whether corresponding relationships from electrodynamics can be extended to acoustics. Actually, however, certain predictions concerning a relationship between absorption and dispersion can be made also for the case of sound waves. This article is devoted to this problem. Yet, for the sake of convenience and for the sake of maximum clarity, it seems advisable, before we go on to acoustics, to dwell on the known connection between absorption and dispersion of electromagnetic waves.

As is known, an electromagnetic wave propagating in a homogeneous medium has the form;

$$E = E_0 \exp\left\{i\omega t - i\frac{\omega}{c} nz - \frac{\omega}{c}\varkappa z\right\},$$

where the refraction and absorption indices n and $\kappa$ are determined from a complex dielectric constant $\varepsilon'$;

$$\varepsilon' \equiv \varepsilon - i\frac{4\pi\sigma}{\omega} \equiv \varepsilon_1 - i\varepsilon_2 = (n - i\varkappa)^2. \tag{1}$$

It is therefore evident that a connection between absorption and dispersion, i.e., between the functions $\kappa(\omega)$ and $n(\omega)$ is equivalent[*] to a connection between the dielectric constant $\epsilon(\omega) \equiv \epsilon_1(\omega)$ and the conductivity $\sigma(\omega) \equiv \frac{\omega\epsilon_2(\omega)}{4\pi}$. Relative to these quantities, the universal connection mentioned above is of the form

---

[*] Here, as is already clear from equation (1), the medium was assumed to be nonmagnetic ($\mu = 1$). In addition, it is possible to introduce the quantities n and $\kappa$ also under those conditions, when the use of the quantity $\epsilon'$ is not valid in the ordinary electrodynamic sense. However, the above limitations, related with the use of equation (1), are quite insignificant in our case.

$$\left.\begin{aligned} \varepsilon(\omega)-1&=\frac{2}{\pi}\int_0^\infty \frac{\omega'\varepsilon_2(\omega')}{\omega'^2-\omega^2}\,d\omega' \equiv 8\int_0^\infty \frac{\sigma(\omega')\,d\omega'}{\omega'^2-\omega^2} \\ \frac{4\pi\left[\sigma(\omega)-\sigma(0)\right]}{\omega}&=-\frac{2}{\pi}\,\omega\int_0^\infty \frac{\varepsilon(\omega')-1}{\omega'^2-\omega^2}\,d\omega' \end{aligned}\right\}, \qquad (2)$$

**where the integrals are taken in the sense of their principal values, i.e.,**

$$\int_a^b \frac{f(\omega')\,d\omega'}{\omega'-\omega}=\lim_{\delta\to 0}\left\{\int_a^{\omega-\delta}\frac{f(\omega')\,d\omega'}{\omega'-\omega}+\int_{\omega+\delta}^{b}\frac{f(\omega')\,d\omega'}{\omega'-\omega}\right\},$$

**where $f(\omega')$ is the function that has no singularities at the point $\omega'=\omega$. Knowing the relationship $\varepsilon(\omega)$, it is possible to determine $\sigma(\omega)$ with the aid of equations (2) and vice versa, but since the integration is over all the frequencies, equations (2) can be used only for different estimates. Knowing, for example, the absorption for a certain number of frequencies, it is possible to obtain the upper limit of the dispersion, i.e., the variation of the velocity of the electromagnetic waves in a certain frequency interval, etc. [1]. Such estimates, let alone the possibility in principle of performing more accurate calculations, are sometimes very useful, for they make it possible, for instance, to neglect with assurance the dispersion, without making any special measurements.**

**The proof of equation (2) is divided into two stages. The first consists of establishing the fact that the quantity $\varepsilon'(\omega)$, considered as a function of the complex variable $\omega$, has no poles in the lower half-plane. This statement can be proven by various methods [1, 2]. We shall cite here only one such proof, due as far as the author knows to L. D. Landau, which can be most readily carried over directly to the acoustic case. In a linear and isotropic medium, the total current**

$$\vec{j}+\frac{1}{4\pi}\frac{\partial\vec{D}}{dt},$$

**entering into Maxwell's equations ($\vec{j}$ is the conduction current and $\vec{D}$ the electric induction) can be most generally related to the electric field $\vec{E}$ by the equation**

$$j(t)+\frac{1}{4\pi}\frac{\partial D(t)}{\partial t}=\frac{1}{4\pi}\int_{-\infty}^{t}K(t-\tau)\frac{\partial E(\tau)}{\partial\tau}\,d\tau, \qquad (3)$$

**where K is a certain unknown function, and where, by virtue of the fact that $\vec{j}$, $\vec{D}$, and $\vec{E}$ are parallel, we shall no longer pay attention to their vector character (incidentally, it is not difficult to generalize all these relationships to the anisotropic case). That the function K can be assumed to depend only on the difference $t-\tau$ is due to the evident homogeneity of the problem with respect to time. The circumstance that $\frac{\partial E}{\partial\tau}$ is found under the integral sign and not, say, $E(\tau)$, is strictly for convenience and has no particular significance. Finally, the choice of t as the upper time limit in expression (3) takes into account the requirements of the causality principle (the value of $j(t)+\frac{1}{4\pi}\frac{\partial D(t)}{\partial t}$ should be determined by the values of $\frac{\partial E(\tau)}{\partial\tau}$ or $E(\tau)$ at $\tau\le t$). Let us further make two very general and natural assumptions relative to the function $K(t-\tau)$. We shall assume**

that $K(t-\tau)$ approaches zero as $|t-\tau|$ approaches infinity, and that the function $K(t-\tau)$ has no non-integrable singularities for any values $\xi = t-\tau$.

Let us now consider the particular case of a harmonic field, i.e., let us assume $E(t) = E_0 e^{i\omega t}$. Then $D = D_0 e^{i\omega t}$, $j = j_0 e^{i\omega t}$, and from the definition of the quantity $\epsilon'(\omega)$ and from (3) we get

$$j + \frac{1}{4\pi}\frac{\partial D}{\partial t} = \frac{i\omega}{4\pi}\left(D - i\frac{4\pi}{\omega}j\right) = \frac{i\omega}{4\pi}\left(\varepsilon - i\frac{4\pi\sigma}{\omega}\right)E_0 e^{i\omega t} =$$
$$= \frac{i\omega}{4\pi}\varepsilon'(\omega)E_0 e^{i\omega t} = \frac{i\omega}{2\pi}\int_{-\infty}^{t} K(t-\tau)E_0 e^{i\omega\tau}\,d\tau = \frac{i\omega}{4\pi}\left[\int_0^{\infty} K(\xi)e^{-i\omega\xi}d\xi\right]E_0 e^{i\omega t},$$

hence

$$\varepsilon'(\omega) = \int_0^{\infty} K(\xi)e^{-i\omega\xi}\,d\xi. \tag{4}$$

Let us remark that it is very important for what follows to carry out the integration in expression (4) from zero, and not from $-\infty$. This follows from the principle of causality.

At $\omega = 0$, i.e., in a static field, the quantity $\epsilon'(0) = \int_0^{\infty} K(\xi)\,d\xi$ may become infinitely large under the assumptions made. This indeed occurs in the presence of conductance in a static field, for in this case we have $\omega\epsilon'(\omega) \approx -i\,\dfrac{4\pi\sigma}{\omega}$ for small values of $\omega$ (it is assumed that the substance is not superconducting; see [4] concerning that case). But if $\omega \neq 0$, the value of $\epsilon'(\omega)$ must already become finite by virtue of the assumed properties of the function K. Let us now consider the frequency $\omega$ to be a complex quantity, meaning that along with harmonic processes we must consider also processes that rise and decay exponentially with time. Putting $\omega = a + ib$ one readily sees that when $b < 0$, i.e., in the lower half of the complex $\omega$-plane, the quantity

$$\varepsilon'(\omega) = \int_0^{\infty} K(\xi)e^{-ia\xi}e^{b\xi}\,d\xi \quad (b<0)$$

is everywhere finite. This also proves that the function $\epsilon'(\omega)$ has no poles either in the lower half-plane or on the real axis, with the possible exception of the point $\omega = 0$.*

Proceeding to the second part of the derivations of equations (2), let us take into consideration the equality

$$\int_L \frac{\varepsilon'(\omega) - \varepsilon'(\infty)}{\omega' - \omega}\,d\omega' = 0, \tag{5}$$

where the integration is carried out over any contour L, located in the lower half-plane and parallel to the real axis. Equation (5) follows from the fact that $\oint \dfrac{\varepsilon'(\omega') - \varepsilon'(\infty)}{\omega' - \omega}d\omega'$, taken along contour L and an infinite semicircle closing this contour in the lower half-plane, vanishes simply because, as proven above, there are no poles of the function $\epsilon'(\omega')$ within the contour selected. Furthermore, the integral of the function

---

* Let us remark that the above statements do not hold for the functions $\epsilon(\omega)$ and $\sigma(\omega)$ individually. This is explained by the fact that the quantities $\epsilon$ and $\sigma$ do not have a direct physical meaning for complex $\omega$, and a proof of the type used for $\epsilon'$, employing definite physical assumptions, cannot be applied to these quantities.

$\frac{\epsilon'(\omega') - \epsilon'(\infty)}{\omega' - \omega}$ over the infinite half-circle vanishes, leading therefore to (5).

Let us now choose for the contour L in (5) the real axis with a detour around the singular point $\omega' = \omega$. In addition, if $\sigma(0) \neq 0$, it is necessary also to detour the point $\omega' = 0$, but only for the sake of simplicity let us put $\sigma(0) = 0$. We shall go around the point $\omega' = \omega$ along a semi-circle having its center at this point. Relationship (5) then obviously assumes the form

$$i\pi[\varepsilon'(\omega) - \varepsilon'(\infty)] + \int_{-\infty}^{+\infty} \frac{\varepsilon'(\omega') - \varepsilon'(\infty)}{\omega' - \omega} d\omega', \tag{6}$$

where, evidently, the need for taking the integral in the principal-value sense results automatically.

Let us now take into account the fact that on the real axis we have

$$\varepsilon'(-\omega) = \varepsilon'^{*}(\omega), \quad \varepsilon(-\omega) = \varepsilon(\omega),$$
$$\sigma(-\omega) = \sigma(\omega); \quad \varepsilon_2(\omega) = -\varepsilon_2(-\omega), \tag{7}$$

where the asterisk (*) denotes the complex conjugate.

Equations (7), with the last three following from the first one and from relationship (1), all result from the requirement that if the field E is real the quantities D and $\underline{j}$ must also be real.

If we now divide expression (6) into its real and imaginary parts and use equations (7) to integrate from 0 to $\infty$ instead of from $-\infty$ to $+\infty$, we readily obtain equations (2) with $\sigma(0) = 0$; here we take furthermore into account that as $\omega$ approaches infinity, the presence of a medium does not affect the propagation of the waves, and therefore

$$\varepsilon'(\infty) = \varepsilon(\infty) = 1, \quad \sigma(\infty) = 0. \tag{8}$$

Let us note that equations (2) do not hold in the presence of super-conductivity, for in that case the function $\epsilon(\omega)$ has a pole at $\omega = 0$, which was not taken into consideration in the derivation [4].

In addition to the function $\epsilon'(\omega)$, many other functions, for example, the function $\omega^{\alpha}\epsilon'(\omega)$ etc., are also regular in the lower half-plane. In addition, one can prove (analogously as above) that the function $\frac{1}{\epsilon'(\omega)}$ is also regular in the lower half-plane. It is possible to obtain for all such regular functions equations that are analogous to (2), provided their behavior at infinity is proper. All such relationships are equivalent to some degree, and the choice of one or the other is dictated by considerations of convenience in the solution of the particular problem.

The arguments given above as applied to $\epsilon'(\omega)$ can be conveniently used in principle also for other analogous quantities, for example, to the complex magnetic permeability $\mu'(\epsilon)$ and to the impedance

$$Z(\omega) = R(\omega) + iX(\omega). \tag{9}$$

If we deal with electric circuits, the impedance is determined from the well-known relationship

$E(\omega) = Z(\omega)\, I(\omega)$, where E is the voltage and I the current; in the case of reflection of electromagnetic waves from metals, the surface impedance is $Z(\omega) = \frac{4\pi}{c}\left[\frac{E_x(\omega)}{H_y(\omega)}\right]_0$, where the fields $E_x$ and $H_y$ are taken on the surface of the metal. For an arbitrary case, R and X are the analogues of $\epsilon_1$ and $-\epsilon_2$, and are related by equations similar to (2):

$$R(\omega) - R(\infty) = -\frac{2}{\pi}\int_0^\infty \frac{\omega'[X(\omega') - X(\infty)]}{\omega'^2 - \omega^2}\, d\omega',$$
$$X(\omega) - X(\infty) = \frac{2\omega}{\pi}\int_0^\infty \frac{[R(\omega') - R(\infty)]}{\omega'^2 - \omega^2}\, d\omega', \tag{10}$$

where it is assumed for simplicity that $Z(\omega)$ has no singularity at $\omega = 0$, as usually occurs. We shall not stop to analyze these equations as applied to individual actual cases. The use of equations (10) may prove quite useful (see, for example, [3]).

If we deal with the impedance, the transition from the electromagnetic to the acoustic case is effected directly, for the physical character of the function $Z(\omega)$ under consideration is to a large extent of no importance from our point of view. True, when equations (10) are used it is necessary to explain separately for each case whether the function $Z(\omega)$ behaves properly enough at large values of $\omega$. This important factor will be dealt with later. Let us now proceed to examine the problem, fundamental for us, of the connection between dispersion and absorption of sound waves propagating in any medium.

It is important to note here that one can speak meaningfully of propagation of sound only as long as the medium remains continuous, so that the equations of hydrodynamics or of the theory of elasticity can be used. In the case of gases, as is known, the sonic approximation is correct as long as the wavelength $\lambda$ exceeds considerably the mean free path $l$ of the molecules, and in the case of liquid and solids the role of $l$ is assumed by the interatomic spacing a. In the sonic approximation the frequency $\omega$ and the wave number $k = \frac{2\pi}{\lambda}$ are connected by definite relationship.*

$$\frac{k}{\omega} = \frac{1}{u(\omega)} = \frac{1}{c(\omega)} - i\frac{\gamma(\omega)}{\omega}, \tag{11}$$

where $u(\omega)$ is the complex velocity of sound, $c(\omega)$ the velocity of sound and $\gamma$ the amplitude-absorption coefficient. All the quantities in the wave are proportional to the factor

$$e^{i(\omega t - kz)} = e^{i\omega(t - z/u)} = e^{i\omega(t - z/c)}\, e^{-\gamma z}.$$

The complex sound velocity $u(\omega)$ is similar to the quantity $\epsilon'(\omega)$ in electrodynamics and is a proportionality coefficient relating the various physical quantities in the sonic field. Thus, in the case of liquid, to which we shall restrict ourselves by way of example:

---

* In many cases, for example, in a solid body and at a given frequency $\omega$, several waves, differing in their polarization or in some other feature, can propagate. Under such conditions, the quantity $\omega$ in (11) may be taken to mean any one of the waves with frequency $\omega$, propagating in a given direction.

$$v = \frac{p'}{\rho_0 u} = \frac{\rho' u}{\rho_0}, \tag{12}$$

where v is the velocity of the liquid in the wave, p' and $\rho'$ the differential pressure and density, and $\rho_0$ the average liquid density. The effects of various processes occurring in the liquid (first and second viscosity, heat conductivity, dissociation, etc.) on the propagation of the sound in the liquid are manifested only in the form of the function u ($\omega$).

For example, at relatively low frequencies we have

$$c = \text{const}$$

and

$$\gamma = \frac{\omega^2}{2\rho_0 c^3}\left[\left(\frac{4}{3}\eta + \zeta\right) = \varkappa\left(\frac{1}{c_v} - \frac{1}{c_p}\right)\right], \tag{13}$$

where the symbols are those commonly used [5].

Putting now, exactly as in the electrodynamic case,

$$v(t) = \frac{1}{\rho_0}\int_{-\infty}^{t} K(t-\tau)\, p'(\tau)\, d\tau$$

and proceeding to consider the relationship $v = v_0 e^{i\omega t}$, we obtain

$$\frac{1}{u(\omega)} = \int_0^{\infty} K(\xi)\, e^{-i\omega\xi} d\xi.$$

Using the assumptions made previously concerning K($\xi$), we therefore reach the conclusion that the function $\frac{1}{u(\omega)}$ has no place in the lower half-plane and on the entire real axis of the variable $\omega$ (when $\omega$ approaches zero, the quantity $\frac{1}{u(\omega)} = \frac{1}{c_0}$ is naturally finite).

Subjecting now the functions $\frac{1}{u(\omega)} = \frac{1}{c(\omega)} - i\,\frac{\gamma(\omega)}{\omega}$ to the same operations performed previously on the functions

$$\varepsilon'(\omega) = \varepsilon_1(\omega) - i\varepsilon_2(\omega) = \varepsilon - i\,\frac{4\pi\sigma}{\omega},$$

we obtain equations analogous to (2) and (10)*

---

* When (14) is compared with (2) one must take into account that in (2) we put $\epsilon(\infty) = 1$ and $\sigma(\infty) = 0$; in addition, in (14) we have $\gamma(0) = 0$.

$$\frac{1}{c(\omega)} - \frac{1}{c(\infty)} = \frac{2}{\pi} \int_0^\infty \frac{\left[\gamma(\omega) - \omega' \left(\frac{\gamma}{\omega}\right)_\infty\right]}{\omega'^2 - \omega^2}\, d\omega',$$

$$\frac{\gamma(\omega)}{\omega} - \left[\frac{\gamma(\omega)}{\omega}\right]_\infty = -\frac{2}{\pi}\, \omega \int_0^\infty \left[\frac{1}{c(\omega')} - \frac{1}{c(\infty)}\right] \frac{d\omega}{\omega'^2 - \omega}, \tag{14}$$

where, as always in such cases, the integrals are taken in the sense of the principal value.

We encounter here a difficulty that at first glance appears to be quite substantial. The fact is that in (14) the integration with respect to $\omega'$ is carried out all the way to $\omega' = \infty$ and in addition, the quantities $c(\infty)$ and $\gamma(\infty)$ are involved. At the same time, as was already noted, the sonic approximation is known to be invalid as $\omega$ approaches infinity, and thus expressions (14), strictly speaking, have no meaning. This remark, incidentally, is not restricted to the acoustic case alone. The same occurs, for example, when equations (10) are applied to electric circuits, since the quasi-stationary approximation used to introduce the impedance is not suitable at sufficiently high frequencies; even in the case of propagation of electromagnetic waves in a medium, the high-frequency region requires special considerations (this is due to the fact that the usual concept of the complex dielectric constant $\epsilon'$ is not suitable for sufficiently high frequencies, and also to other causes). One can remark, however, that the use of infinite integrals in physical problems, or at least in problems in macroscopic physics, has a somewhat arbitrary character. Indeed, it is assumed that the region of sufficiently high frequencies is not important, i.e., that it is possible to carry out the integration up to a certain finite frequency, and such a substitution of the integration limit is insignificant within the limits of accuracy of interest to us. This circumstance in itself is trivial, but is emphasized here owing to its importance from the point of view of the problem that is being discussed.

In the propagation of electromagnetic waves it is readily seen that the use of equations (2) is fully legitimate. This is due to the fact that actually we deal here not with the macroscopic quantity $\epsilon'$, but with a quantity $(n - i\kappa)^2$, which has a definite meaning also at very high frequencies. Furthermore, at high frequencies we have $n \to 1$ and $\kappa \to 0$ (we naturally disregard the frequency region $\omega > \frac{mc^2}{h} \sim 10^{21}$). Finally, and this is the most important, it is clear from the known properties of the function $\epsilon'(\omega)$ that the region of very high frequencies contributes very little to the integrals in (2), and the value of the upper integration limit is thus unimportant to a considerable degree. This is not always so in the propagation of sound waves, and therein lies the principal difference between the two cases. Thus, in a monatomic gas the absorption is given by equation (13), the parameters of which are independent of $\omega$, all the way up to the highest frequencies for which the sonic approximation is still valid. The value of the first integral in (14) is therefore determined by the high-frequency region; the same applies, as can be shown, to the second integral. It is clear from this, that when the velocity of sound in gases is studied, equations of the (14) type can contribute nothing.* The situation is already different in condensed media. In a liquid, for example, equation (13) is valid only for frequencies $\omega < 10^{8} - 10^{10}$; at higher frequencies the coefficient of the second viscosity is first to relax, followed by the first-viscosity coefficient. Thus, in benzol, the characteristic relaxation time for the second viscosity is $\tau \sim 10^{-10}$ sec/cm [6]. The relaxation of the first (ordinary) viscosity is observed only in viscous liquids, where the corresponding time is also approximately $10^{-9} - 10^{-10}$ sec (it is impossible to determine smaller values of the time $\tau$ by studying the fine structure of the scattered light). One must assume, however, that at $\omega \sim 10^{11} - 10^{12}$, the first viscosity relaxes also in low-viscosity liquids such as water or benzol, so that at sufficiently high frequencies the liquid behaves like an isotropic solid body. At any rate, in condensed bodies and at sufficiently high frequencies,

---

* In the Kneser dispersion region one can still employ equations of the (14) type for polyatomic gases within certain limits. In addition, it is possible to employ the function, for example, $1/[\omega^2 u(\omega)]$ in lieu of the function $1/u(\omega)$, thereby improving the behavior of the integrands at high frequencies. We shall not dwell on these factors, for much greater progress can be made in the analysis of gases within the framework of microscopic theory, and there is no need in general to resort to equations similar to (2) or (14).

$\omega > 10^{10} - 10^{12}$, the quantity $\gamma$ increases much slower with frequency than $\omega^2$, and evidently, one can assume $\gamma$ and $\underline{c}$ constant, as follows from the relaxation theory at $\omega\tau >> 1$ [5]. At the same time, the sonic approximation is valid as long as the wavelength $\lambda$ is considerably greater than the interatomic distance $a \sim 10^{-8}$, i.e., at frequencies

$$\omega = 2\pi/\lambda \leqslant \omega_0 \sim 10^{13} - 10^{14} \left(\omega_0 \ll \frac{2\pi c}{a} \sim \frac{6.28\cdot 3\cdot 10^5}{10^{-8}} \sim 2\cdot 10^{14}\right).$$

One can therefore assume that in pure liquids, solutions and emulsions, solids, polymers, etc., equations similar to (14) are suitable, generally speaking, but the integration must be carried out only to frequencies $\omega_0$ on the order of $10^{13} - 10^{14}$. This last conclusion, naturally, follows directly also from the fact that the statement that the function $\frac{1}{u(\omega)}$ has no pole in the lower half-plane is valid only for the sonic approximation, i.e., at $|\omega| \lesssim \omega_0$ (the integral relationships between $\underline{v}$ and $\underline{p}'$, used in the discussion of the properties of $\frac{1}{u(\omega)}$, occur only if there are no Fourier components with $\omega > \omega_0$). Taking the above into consideration, let us examine the integral

$$\oint \frac{\frac{1}{u(\omega')} - \frac{1}{u(\omega_0)}}{\omega' - \omega}\, d\omega' = 0,$$

taken along the real axis within the limits $-\omega_0 \leq \omega' \leq \omega_0$ with a detour around the point $\omega' = \omega$ and along a semicircle with a radius $|\omega'| = \omega_0$ in the lower half-plane of the variable $\omega'$. Here the integral along the semicircle $\delta = \delta_1 + i\delta_2$ may not vanish, for the function $1/u(\omega')$ does not necessarily equal the function $1/u(\omega_0)$ for all values of $\omega' = \omega_0 e^{i\varphi}$ $(-\pi \leq \varphi \leq 0)$. Considering that the ratio $\omega/\omega_0$ is small, we have

$$\delta_1 \leqslant \pi\left[\left(\frac{\gamma}{\omega}\right)_m - \frac{\gamma(\omega_0)}{\omega_0}\right] + \frac{2\omega}{\omega_0}\left[\frac{1}{c_m} - \frac{1}{c(\omega_0)}\right]$$

and

$$\leqslant \pi\left(\frac{1}{c_m} - \frac{1}{c(\omega_0)}\right) - \frac{2\omega}{\omega_0}\left[\left(\frac{\gamma}{\omega}\right)_m - \frac{\gamma(\omega_0)}{\omega_0}\right],$$

where $\frac{1}{c_m}$ and $\left(\frac{\gamma}{\omega}\right)_m$ are the maximum values of the corresponding quantities on the semicircle. Performing now the same operations as on expression (5), we get

$$\left.\begin{aligned} \frac{1}{c(\omega)} - \frac{1}{c(\omega_0)} &= \frac{2}{\pi}\int_0^{\omega_0} \frac{\gamma(\omega') - \omega'\left(\frac{\gamma(\omega_0)}{\omega_0}\right)}{\omega'^2 - \omega^2}\, d\omega' - \frac{\delta_2}{\pi} \\ \frac{\gamma(\omega)}{\omega} - \frac{\gamma(\omega_0)}{\omega_0} &= -\frac{2}{\pi}\,\omega \int_0^{\omega_0} \left(\frac{1}{c(\omega')} - \frac{1}{c(\omega_0)}\right) \frac{d\omega'}{\omega'^2 - \omega^2} - \frac{\delta_1}{\pi} \end{aligned}\right\}. \tag{15}$$

To simplify these equations further, let us recall that

$$\int \frac{d\omega'}{\omega'^2-\omega^2} = \frac{1}{2\omega}\ln\left|\frac{\omega'-\omega}{\omega'+\omega}\right|,$$

$$\int \frac{\omega' d\omega'}{\omega'^2-\omega^2} = \frac{1}{2}\ln|\omega'^2-\omega^2|,$$

where the corresponding expressions are valid also when the integration is over a region containing a singularity, once the integral is taken in the principal-value sense.

It is therefore readily seen that

$$\left.\begin{aligned}\frac{1}{c(\omega)} &= \frac{2}{\pi}\int_0^{\omega_0}\frac{\gamma(\omega')\,d\omega'}{\omega'^2-\omega^2} - \frac{\gamma(\omega_0)}{\pi\omega_0}\ln\left|\frac{\omega_0^2-\omega^2}{\omega^2}\right| - \frac{\delta_2}{\pi} + \frac{1}{c(\omega_0)}\\ \frac{\gamma(\omega)}{\omega} &= -\frac{2}{\pi}\,\omega\int_0^{\omega_0}\frac{1}{c(\omega')}\,\frac{d\omega'}{\omega'^2-\omega^2} + \frac{1}{\pi c(\omega_0)}\ln\left|\frac{\omega_0-\omega}{\omega_0+\omega}\right| - \frac{\delta_1}{\pi} + \frac{\gamma(\omega_0)}{\omega_0}.\end{aligned}\right\} \tag{16}$$

Furthermore, taking the difference between two-values of (16) corresponding to two frequencies $\omega_2$ and $\omega_1$, we finally obtain

$$\left.\begin{aligned}\frac{1}{c(\omega_2)} - \frac{1}{c(\omega_1)} &= \frac{2}{\pi}\int_0^{\omega_0}\gamma(\omega')\left\{\frac{1}{\omega'^2-\omega_2^2} - \frac{1}{\omega'^2-\omega_1^2}\right\}d\omega' + \Delta_1\\ \frac{\gamma(\omega_2)}{\omega_2} - \frac{\gamma(\omega_1)}{\omega_1} &= -\frac{2}{\pi}\int_0^{\omega_0}\frac{1}{c(\omega')}\left\{\frac{\omega_2}{\omega'^2-\omega_2^2} - \frac{\omega_1}{\omega'^2-\omega_1^2}\right\}d\omega' + \Delta_2\end{aligned}\right\}, \tag{17}$$

where

$$\Delta_1 = \frac{2\gamma(\omega_0)}{\omega_0}\ln\frac{\omega_2}{\omega_1} - \frac{\delta_2(\omega_2)-\delta_2(\omega_1)}{\pi}$$

and

$$\Delta_2 = -\frac{2(\omega_2-\omega_1)}{\pi c(\omega_0)\,\omega_0} - \frac{\delta_1(\omega_2)-\delta_1(\omega_1)}{\pi},$$

where for simplicity we assume immediately that the frequencies $\omega_2$ and $\omega_1$ are considerably smaller than the frequency $\omega_0$. From the previously-evaluated estimates $\delta_1$ and $\delta_2$ it is clear that

$$|\delta_1(\omega_2)-\delta_1(\omega_1)| \leqslant \frac{2|\omega_2-\omega_1|}{\omega_0}\left(\frac{1}{c_m} - \frac{1}{c(\omega_0)}\right) \leqslant \frac{|\omega_2-\omega_1|}{\omega_0 c(\omega_0)},$$

$$|\delta_2(\omega_2)-\delta_2(\omega_1)| \leqslant \frac{2|\omega_2-\omega_1|}{\omega_0}\left[\left(\frac{\gamma}{\omega}\right)_m - \frac{\gamma(\omega_0)}{\omega_0}\right] \leqslant \frac{|\omega_2-\omega_1|}{\omega_0}\cdot\frac{\gamma(\omega_0)}{\omega_0}.$$

By virtue of the relatively small dispersion of sound, one can assume $c(\omega_0) \sim c(\omega_2) \sim c(\omega_1) \sim 10^5 - 10^6$, and consequently, $\Delta_2 \sim (10^{-5} - 10^{-6})\ \frac{\omega_2-\omega_1}{\omega_0}$. As to the quantity $\Delta_1$, it is more difficult to estimate it with some reliability and unless special assumptions are made, one can merely say that

$$\Delta_1 \sim \frac{\gamma(\omega_0)}{\omega_0} \ln \frac{\omega_2}{\omega_1} \ll \frac{1}{c(\omega_0)} \ln \frac{\omega_2}{\omega_1},$$

**so that if the sonic approximation is valid, we have $\gamma(\omega_0)\lambda << 1$ and $\frac{\gamma}{\omega} = \frac{\gamma\lambda}{2\pi c}$. At any rate, the frequency dependence of the quantities $\Delta_1$ and $\Delta_2$ is known, and they can be evaluated. Equations (17), particularly the second one, are therefore significant and can be used to estimate the absorption from a known value of dispersion and vice versa. The question of the accuracy and the significance of such estimates must be decided for each case individually, with allowances made for the available data concerning the absorption or dispersion of the sound. We shall not dwell on this important aspect of the matter and we shall restrict ourselves only to the remarks made, which make it possible to judge the character of the general relationship (17) between absorption and dispersion of sound waves.**

## LITERATURE CITED

[1] Propagation of Short Radio Waves, D. E. Kerr, Editor (New York, 1951) Section 8.1.

[2] Ia. L. Al'pert, V. L. Ginzburg, and E. L. Feinberg, Propagation of Radio Waves, (State Tech. Press, 1953) Sec. 83.

[3] W. Nijenhuis and F. L. Stumpfers, Physica 8, 289 (1941).

[4] V. L. Ginsburg, J. Exptl.-Theoret. Phys. (USSR) 29, 2 (1955).

[5] L. D. Landau and E. M. Lifshits,, Mechanics of Continuous Media (State Tech. Press, 1953) Chapt. VIII.

[6] I. L. Fabelinskii, Doklady Akad. Nauk SSSR, 92, 285 (1953).

P. N. Lebedev
Physics Institute of the USSR
Academy of Sciences, Moscow

Received March 6, 1954.

# ON THE PROBLEM OF AXIAL OSCILLATIONS OF POLARIZED BARIUM TITANATE PLATES

I. P. Goliamina

**The frequency dependence of the modulus of electric impedance and the frequency dependence of the radiation from plates of barium-titanate ceramics were investigated in the vicinity of their axial natural frequencies. It was observed that the frequency characteristics in this region exhibit a series of maxima, the locations of which on the frequency scale depend on the geometric parameters of the plate and are independent of the assumed irregularities. It was shown experimentally that the frequency dependence of the radiated sound intensity is uniquely related to the frequency characteristic of the electric impedance.**

**When a plate of polarized barium-titanate ceramic is used to radiate ultrasonic waves, it is essential to know its frequency characteristics, such as the frequency dependence of the sound radiated by the plate or its frequency. Many recently published references [1, 2, 3, 4] give the frequency characteristics of axially excited barium-titanate plates. References [1, 2], report two radiation maxima near the fundamental axial natural frequency of barium-titanate plates. This phenomenon was observed in plates of various thicknesses and of various radii. Reference [3] reports many peaks in the measured frequency dependence of the impedance in the vicinity of the fundamental axial resonance.**

**It is the purpose of this investigation to clear up certain peculiarities of the splitting of the fundamental resonant maximum, particularly to explain the effect of irregularities in a barium-titanate ceramic. We also investigated experimentally the connection between the frequency dependence of the modulus of the electric impedance of the plate and the frequency dependence of the radiated sound intensity.**

## Frequency Dependence of the Modulus of Electric Impedance of Barium-Titanate Plates.

**To determine the natural-frequency spectrum of round barium titanate plates near the fundamental axial natural frequency, we measured the frequency dependence of the modulus of electric impedance $|z|$ or the modulus of the electric admittance $\frac{1}{|z|}$ for free plate oscillations in air. Silver was fused into the end surfaces of the plates to form electrodes. The specimens were excited with a standard signal generator having a low-impedance output. The voltage applied to the plate was measured with a vacuum tube voltmeter; the current in the plate was measured with a thermocouple milliammeter. In many cases the applied voltage was maintained constant regardless of the variations in frequency; in this case a change in voltage from 0.1 to 7 volts did not influence the frequency characteristic of the plate. Tests were also made with the current in the plate kept constant. In both cases identical results were obtained for $|z|$ as calculated from the experimental data. To guarantee**

conditions close to those of free oscillations, the plate was stood on edge on a cork liner. Twenty specimens 4 mm thick and 20 mm in diameter were tested [the ceramics were made by the State Institute for Electroceramic Products (GIEK)]; in addition, seven specimens ranging from 18 to 35 mm in diameter and from 2 to 10 mm in thickness were tested to compare the results of our investigation with the deductions of Reference [1]; these specimens were made by the Dielectric Laboratory of the Physics Institute of the USSR Academy of Sciences and graciously supplied to the author by G. P. Motulevich and I. L. Fabelinskii.

A piezoelectric resonator is expected to exhibit near each of its natural frequencies the following peculiarities of the frequency dependence of the electric impedance: there should exist a so-called resonant frequency $f_r$, at which $|z|$ has a minimum value, and an anti-resonant frequency $f_a$, corresponding to the maximum value of the impedance. This is experimentally confirmed by the curves, particularly those of Figs. 1 and 2. Most plates exhibit one fundamental maximum and many adjacent secondary maxima, of smaller absolute value, with each maximum accompanied by a corresponding minimum.

As a consequence, the electric field excites many natural frequencies in the plate in the vicinity of the fundamental axial natural frequency. The same phenomenon is observed also near the harmonics of the axial oscillations.

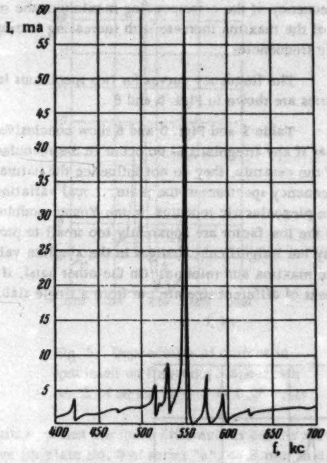

Fig. 1. Dependence of the current flowing in the specimen on the frequency of the exciting voltage. Specimen No. 1, diameter 34.8 mm, thickness 4.6 mm, V = 0.28 volts.

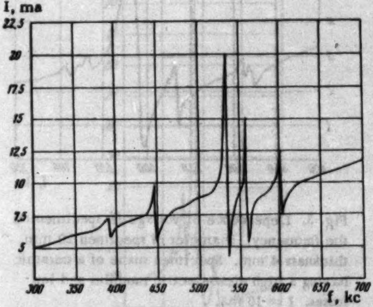

Fig. 2. Dependence of the current flowing through the specimen on the frequency of exciting voltage. Specimen No. 2, diameter 18 mm, thickness 4.5 mm, V = 3 volts.

The quality of the ceramic, in the case of plates of equal size, affects substantially the absolute value of the maxima and minima of $|z|$, but has an only insignificant effect on their position in the frequency scale; this is readily seen, for example, by comparing Figs. 3 and 4. At the same time plates of different dimensions differ substantially in the total number of secondary maxima, in their frequency distribution, and in their relative size. One can thus conclude that for a plate of a specified material the natural-frequency spectrum depends principally on the shape and dimensions of the plate. The distribution of the natural frequencies of a series of specimens obtained by means of an equal manufacturing technology of ceramics and under equal polarization conditions, is but insignificantly affected by variations in the piezoelectric modulus, in the elastic parameters, and in the loss factor of the material.

## Effects of Irregularities in the Material on the Natural-Frequency Spectrum of the Plate.

The fact that the spectral maxima and minima have fixed positions for specimens of equal size indicates apparently that the material within the specimen has sufficient mechanical homogeneity. It was thought of interest to verify further the homogeneity of the material by testing a series of specimens of equal size, cut from the same slab of fired ceramic. Particular care was exercised in the experiments to make the conditions of further heat treatment during the fusion of the electrodes and also the polarization conditions the same for all the specimens in the series. The data for one such series (series "b") are given in Table 1, which lists the fundamental maximum frequency $f_{max}$, the fundamental minimum frequency $f_{min}$, and the positions of each of the additional maxima relative to the fundamental minimum $\frac{(f_{min} - f_n)}{f_{min}}$ %, where $f_n$ is the frequency of the corresponding maximum; the numbers n of the maxima increase with increasing corresponding frequencies.

The frequency curves for two specimens in this series are shown in Figs. 5 and 6 .

Table 1 and Figs. 5 and 6 show conclusively that if any irregularities do occur in the manufacture of the ceramic, they do not influence the natural-frequency spectrum of the plate. Local variations in the piezoelectric modulus, in the Young modulus, and in the loss factor are apparently too small to produce any but insignificant changes in the absolute values of the maxima and minima. On the other hand, if specimens of different size are cut from a single slab, the

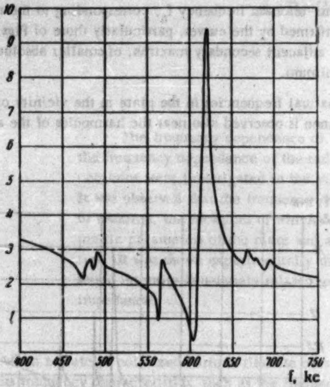

Fig. 3. Dependence of voltage in specimen on the frequency. Diameter of specimen 20 mm, thickness 4 mm. Specimen made of a ceramic having a high piezoelectric modulus and low losses. I = 10 ma.

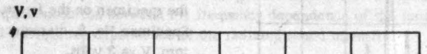

Fig. 4. Dependence of voltage in specimen on frequency. Specimen diameter 20 mm, thickness 4 mm. Specimen made of ceramic having low piezoelectric modulus and high losses. I = 10 ma.

Table 1

| Number of plate | Diameter mm | Thickness mm | $f_{max}$ kc | $f_{min}$ kc | $\frac{f_{min}-f_1}{f_{min}}$ | $\frac{f_{min}-f_2}{f_{min}}$ | $\frac{f_3-f_{min}}{f_{min}}$ |
|---|---|---|---|---|---|---|---|
| 1, "b" | 25.0 | 2.03 | 1172 | 1202 | 4.7% | 2.5% | 1.5% |
| 2, "b" | 25.0 | 2.03 | 1168 | 1200 | 4.7% | 2.7% | 1.3% |
| 3, "b" | 25.0 | 2.03 | 1176 | 1208 | 4.8% | 2.7% | 1.5% |

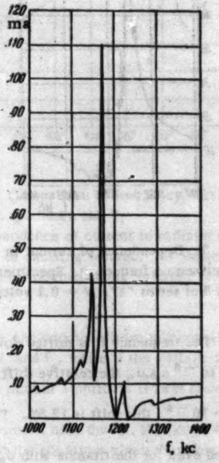

Fig. 5. Dependence of current in specimen on frequency. Specimen No. 1 of series "b". V = 0.26 volts.

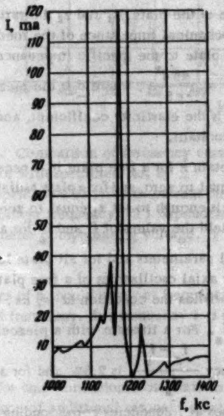

Fig. 6. Dependence of current in specimen on frequency. Specimen No. 3 of series "b". V = 0.26 volts.

results obtained are quite different, as can be seen by comparing Figs. 6 and 7. Figure 7 shows the frequency curve for plate No. 3 of series "a", 48.8 mm in diameter and 2.03 mm thick; the specimens of the "b" were obtained from those of the "a" series by grinding the diameter down.

## Comparison of Frequency Dependence of Radiation Intensity With Frequency Dependence of the Electric-Impedance Modulus.

Measurement of the frequency characteristics of an assembled radiator in a liquid involves certain difficulties, and it is therefore desirable to know beforehand that the plate intended for the assembly of the radiator has the required qualitative and quantitative properties. On the other hand, testing a free plate in air by measuring the modulus of electric impedance is very easy. It was therefore deemed interesting to ascertain to what extent the values of $|z|$ determined for a plate freely oscillating in air can be used to predict the frequency characteristics of sound intensity, produced by a radiator containing the same plate operating in a liquid.

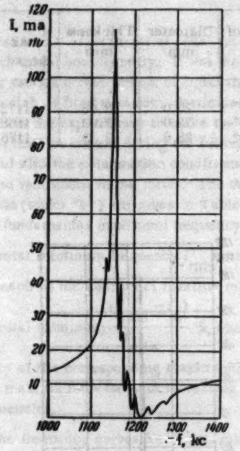

Fig. 7. Dependence of current in specimen on frequency. Specimen No. 3 of series "a". V = 0.1 volts.

A wave theory for a piezoelectric radiator was developed for the one-dimensional case by N. N. Andreev [5]. This reference gives a general equation for the electric impedance of a piezoelectric plate for all load conditions;

$$z = \frac{1}{j\omega c(1-\beta)}\left[1 + \frac{j\beta}{kl}\,\frac{1}{\dfrac{1}{j\sin kl} + \dfrac{(z_1+a)(z_2+a)}{(z_1+a)+(z_2+a)}}\right].$$

Here $\omega$ is the circular frequency, k the wave number, $l$ the plate thickness, $a = j\tan\frac{kl}{2}$, c the capacitance of the plate, $z_1$ and $z_2$ the ratios of the specific mechanical impedance of the media on both sides of the plate to the specific impedance of the plate material, $\beta = \frac{4\pi d^2}{\epsilon S}$, where d is the piezoelectric modulus, S is the elasticity coefficient, and $\epsilon$ the dielectric constant.

To obtain z for a free plate it is necessary to set $z_1$ and $z_2$ equal to zero, and for a plate radiating in one direction it is enough to set $z_1$ equal to zero. These equations yield the values of $f_r$ and $f_a$ for all values of the material parameters and for all plate loading conditions. For axial oscillations of a free plate, the frequency $f_a$ satisfies the condition $kl = n\pi$, where n is an odd interger. The frequency $f_r$ is shifted downward relative to $f_a$. For a titanate with a piezoelectric modulus $d_{33} = 1.2 \cdot 10^{-6}$ e.s.u., the relative shift of the resonant frequency $\frac{f_a - f_r}{f_a}$ is 2.5%, and for a titanate having $d_{33} = 4.5 \cdot 10^{-6}$, this shift is 13.5%. This relative shift decreases at frequencies corresponding to the higher harmonics, and even for the titanate with $d_{33} = 4.5 \cdot 10^{-6}$, $\frac{f_a - f_r}{f_a}$ amounts to merely 1.3% at the third overtone and 0.5% at the fifth one. For a plate loaded on one side (i.e., when the radiator operates in liquid) the radiation losses cause a small increase in the difference between frequencies $f_r$ and $f_a$, in which $f_r$ is shifted downward and $f_a$ upward. This increase, as shown by a calculation based on the above equation, increases with diminishing piezoelectric modulus and with increasing load impedance $z_2$. Thus, for barium titanate with $d_{33} = 1.2 \cdot 10^{-6}$ the value of $\frac{f_a - f_r}{f_a}$ varies from 2.5% in the absence of radiation to 4.8% for one-sided radiation in water. For titanate with $d_{33} = 4.5 \cdot 10^{-6}$, this relative difference in frequencies varies by merely 0.6% compared with the value for the free plate. The sound pressure in the field of the plane wave produced by the radiator is given by

$$p = j\frac{4\pi d\rho c^2}{\varepsilon\omega} z_2 \frac{V}{z} \cdot \frac{\cos kl - 1}{z_2\cos kl + j\sin kl},$$

where $\rho$ is the density of the plate material, $\underline{c}$ the velocity of sound in the plate, $z_2$ the relative mechanical impedance of the medium in which the radiation occurs, and V the voltage applied to the plate.

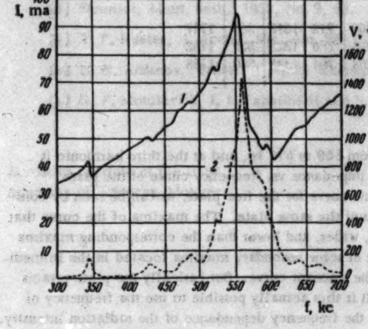

Fig. 8. Comparison of frequency curves of radiator with specimen No. 7:
1) dependence of current in radiator on the frequency of exciting voltage, 2) dependence of radiometer compensating voltage. V = 5 volts.

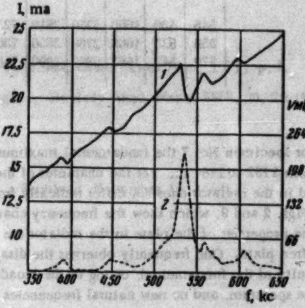

Fig. 9. Comparison of frequency curves of radiator with specimen No. 2:
1) dependence of radiator current on exciting-voltage frequency, 2) dependence of radiometer compensating voltage. V = 6.5 volts.

One can conclude from this equation that the maximum values of $\underline{p}$ should occur at frequencies $\underline{f}$ lying between $f_r$ and $f_a$, while if the voltage is kept constant regardless of frequency, this frequency $\underline{f}$ is closer to $f_r$, but if the current amplitude is kept constant, $\underline{f}$ is closer to $f_a$.

One must note that N. N. Andreev's calculations were made for one-dimensional oscillations of an infinite plate, and the equations given therefore do not explain the appearance of additional resonant maxima. But they do make it possible to explain the experimentally-obtained rules for the relative placement of $f_r$, $f_a$, and $\underline{f}$ of the fundamental maximum.

In the experiments, the titanate plate was placed in a cylindrical metal housing in such a manner as to bring its rear side in contact with a lead cover plate; on the front end the plate was compressed by a metal ring through an annular rubber gasket; this ring served simultaneously as the front cover of the housing. In such a radiator, the free front end of the plate makes direct contact with the liquid. The experiment involved simultaneous measurement of the current in the radiator (determined by its electric impedance) and the radiation pressure in the sound field. The voltage on the radiator was kept constant. The radiation pressure was measured with the micro-radiometer described in Reference [6]. The value of the compensating voltage on the radiometer was directly proportional to the radiation intensity.

Figures 8 and 9 show comparison of the frequency curves of the electric impedance of the radiator and of the radiation pressure. As can be seen, the radiation actually has maxima at the frequencies located between the corresponding resonance and anti-resonance frequencies. Table 2 gives the experimental data of $f_r$, $\underline{f}$, and $f_a$, corresponding to the fundamental maxima for various plates and various overtones.

The results of Table 2 apply to a constant plate voltage, and therefore $\underline{f}$ lies between $f_r$ and $f_a$, closer to $f_r$. If the current is kept constant, the radiation maximum shifts towards the higher frequency, closer to $f_a$.

TABLE 2.

| No. of specimen | 1 | 2 | | | | 3 | 4 | 5 | | | 7 | |
|---|---|---|---|---|---|---|---|---|---|---|---|---|
| No. of harmonic | I | I | III | V | VII | I | I | I | III | V | I | III |
| $f_r$, kc | 548 | 530 | 1660 | 2750 | 3810 | 725 | 1167 | 260 | 772 | 1313 | 553 | 1747 |
| $f$,. kc | 556 | 535 | 1668 | 2760 | 3850 | 736 | 1185 | 263 | 786 | 1325 | 559 | 1752 |
| $f_a$, kc | 570 | 542 | 1683 | 2800 | 3890 | 748 | 1225 | 268 | 794 | 1338 | 580 | 1768 |

Thus, for specimen No. 7 the fundamental maximum shifts from 559 to 570 kc, and at the third harmonic it shifts from 1752 to1764 kc. Yet the character of the electric impedance vs. frequency curve of the plate mounted in the radiator does not differ radically from the same curve for the free plate, as can be seen by comparing Figs. 2 and 9, which show the frequency characteristics of the same plate. The maxima of the curve that shows the properties of the plate in the radiator are less sharp, wider, and lower than the corresponding maxima for the free plate. One frequently observes the disappearance of some secondary maxima located in the immediate vicinity of the fundamental, owing to the broadening of the resonant curve. But basically the plate retains the same spectrum, and no new natural frequencies appear. It is thus actually possible to use the frequency of the impedance of a free plate to determine for such radiators the frequency dependence of the radiation intensity.

## SUMMARY

Based on the above, the following fundamental conclusions can be made:

1. The location of the secondary maxima, observed in the frequency curves of the electric impedance and in the frequency curves of the radiation of titanate plates, depends on the geometry of the plates and on the average parameters of the material; assumed irregularities, if they do exist, have very little effect. One can assume that these irregularities manifest themselves on the average only in the absolute value of the maxima and minima of the frequency curves.

2. A second sharply-pronounced maximum, observed in Reference [1], in which measurements were made at constant voltage, was not observed even in a single specimen, regardless of whether the plate was freely oscillating or operating in a radiator compressed by a rubber gasket. Consequently, the maximum-radiation frequencies should be close to the resonant frequencies. Our calculations show that the harmonics $f_3$, $f_5$ and $f_7$ of this maximum-radiation frequency occur at frequencies for which the plate is an integral number of half waves thick, with an accuracy to within 1% (the same accuracy with which the frequency measurements of Reference [1] were made). The ratios of frequencies $f_3$, $f_5$, and $f_7$ are therefore those of integers. The frequency $\underline{f}$, being equal to $\frac{f_3}{3}$ or $\frac{f_5}{5}$, corresponds therefore to the case when the thickness of the plate is exactly equal to a half wave; the frequency of the first maximum is shifted downward by 4-7%, as can be expected from the calculations. One can therefore conclude that it is indeed the first maximum that corresponds to the fundamental axial oscillation. This frequency is also in approximate agreement with that of the fundamental radiation maximum obtained by our measurements. The origin of the second maximum, however, remains unclear. It may be due to the conditions under which the plate is clamped.

3. From the frequency curves of the electric impedance of a free plate it is possible to judge the character of the frequency curve of the radiation intensity, obtained when a given plate is used in a radiator with a construction similar to that described in this article.

In conclusion, the author takes advantage of the occasion to express gratitude to N. N. Andreev for continuous attention to the work, to G. P. Motulevich and I. L. Fabelinskii for assistance in the work, and to V. S. Grigor'ev for participating in the analysis of the results.

## LITERATURE CITED

[1] G. P. Motulevich and I. L. Fabelinskii, J. Exptl.-Theoret. Phys. (USSR) 25, 605 (1953).

[2] T. F. Hueter and A. Dozois, J. Acoust. Soc. Am. 24, 85 (1952).

[3] Schmidt, Akust. Beih. 1952, No. 2, 83.

[4] T. F. Hueter, J. Acoust. Soc. Am. 25, 152 (1953).

[5] N. N. Andreev, Trans. All-Union Correspondence Power Inst. (State Power Press, 1951). p. 5.

[6] G. P. Motulevich, I. L. Fabelinskii and L. N. Shteingauz, Doklady Akad. Nauk SSSR, 70, 29 (1950).

Acoustics Institute of the USSR
Academy of Sciences, Moscow

Received November 10, 1954.

# EXPERIMENTAL INVESTIGATION OF DIFFRACTION OF ACOUSTIC WAVES BY PERIODIC STRUCTURES

A. N. Leporskii

**An experimental procedure is described for the investigation of the diffraction of acoustic waves by periodic structures. Experimental patterns are given for scattering by sinusoidal and sawtooth surfaces and are compared with the theoretical values calculated with the method developed by L. M. Brekhovskikh [1].**

L. M. Brekhovskikh [1] proposed a method of solving for the diffraction of acoustic waves by a periodic structure with a period that is large compared with the wavelength of the incident sound and having an arbitrary reflection coefficient. This theory is valid in a sector, bounded approximately by the outermost rays directly reflected from the uneven surface; this sector will be called hereinafter the valid sector of the theory.

It was shown in Reference [1] that for a finite area of width D (Fig. 1), the diffracted wave has at distances $R >> kD^2$ a characteristic directivity in the zx plane, consisting of a set of spectra (strips), the maxima of which lie in directions determined by the following expression

$$\cos\alpha_m = \frac{k_x^0 + mp}{k} = \cos\alpha_0 + m\frac{\lambda}{\Lambda}, \quad (1)$$

where k is the wave number, $\Lambda$ the wavelength of the waviness of the scattering area, $\alpha_0$ the elevation* angle of the incident wave, $\alpha_m$ the elevation angle of the m-th order of spectrum, and $\lambda$ the wavelength of the incident sound.

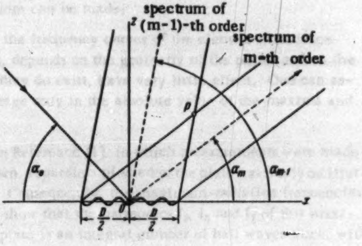

Fig. 1

The angular dependence of the amplitudes of the scattered waves in the zx plane is given by the function

$$f(\alpha_m) = |B_m(\alpha_m)| \cdot \sin\alpha_m. \quad (2)$$

Let us show that these deductions can be used to explain the diffraction pattern at distances R, satisfying the less rigorous relationship:

$$R \geqslant \frac{D\Lambda}{\lambda}.$$

---

* Transl. note – this is the complement of the angle of incidence.

Equation (1) gives the direction of the m-th spectrum, without allowances for the broadening of the beam (in the "projector" zone). The boundary of the (m − 1)-th spectrum facing the m-th one (Fig. 1) is given by the equation

$$z = -\frac{D}{2}\tan\alpha_{m-1} + \tan\alpha_{m-1}\, x.$$

Analogously, the equation of the boundary of the m-th spectrum facing the (m − 1)-th one can be written as

$$z = \frac{D}{2}\tan\alpha_m + \tan\alpha_m \cdot x.$$

The distance $R_s$ separating two neighboring spectra is determined as

$$R = \sqrt{x_p^2 + z_p^2} = \sqrt{\left[\frac{D}{2}\frac{\sin(\alpha_{m-1}+\alpha_m)}{\sin(\alpha_{m-1}-\alpha_m)}\right]^2 + \left[D\frac{\sin\alpha_m \cdot \sin\alpha_{m-1}}{\sin(\alpha_{m-1}-\alpha_m)}\right]^2}.$$

The equation simplifies considerably if we consider that at λ << Λ and Λ << D, we have

$$\left.\begin{aligned} &\sin\alpha_m \sin\alpha_{m-1} \approx \sin^2\alpha_m \\ &\sin(\alpha_m + \alpha_{m-1}) \approx \sin 2\alpha_m = 2\sin\alpha_m\cos\alpha_m \\ &\sin(\alpha_m - \alpha_{m-1}) \approx \alpha_m - \alpha_{m-1} \approx \frac{\lambda}{\Lambda\sin\alpha_m} \end{aligned}\right\}. \tag{3}$$

The equation for $R_s$ then becomes

$$R_p = \sqrt{\left(\frac{D\Lambda}{\lambda}\sin^2\alpha_m\right)^2(\cos^2\alpha_m + \sin^2\alpha_m)} = \frac{D\Lambda}{\lambda}\sin^2\alpha_m.$$

The distance R at which separation of the spectra should be observed must thus satisfy the condition

$$R \geqslant R_p = \frac{D\Lambda}{\lambda}, \tag{4}$$

since $\sin^2\alpha_m$ cannot be greater than unity.

As follows from Reference [1], the scattered wave is given by the expression

$$\varphi = \sum_{m=-\infty}^{+\infty}\int_{-\infty}^{+\infty} B_m(\alpha)\,\Phi(k_x^0 + mp - k\cos\alpha)\cdot e^{ikR}\exp\{iR(k_x\cdot\cos\alpha + \\ + \sqrt{k^2 - k_x^2}\cdot\sin\alpha)\}\,dk_x.$$

In our case, when $R > \frac{D\Lambda}{\lambda} >> 1$, inasmuch as $\Lambda >> \lambda$ and $D >> \lambda$, the exponent under the integral sign will be a rapidly varying function compared with the remaining part of the integrand. This is enough to calculate the integral by the stationary-phase method. Repeating furthermore the derivation given in Reference [1], we obtain expression (2) for the field in the center of the m-th spectrum, with an accuracy to within a constant factor that allows for the finite dimensions of the area.

The calculation equations have the following form:

For a sinusoidal surface

$$f(\alpha_m) = \frac{1 - \cos(\alpha_m + \alpha_0)}{\sin \alpha_m + \sin \alpha_0} I_m(s). \qquad (5)$$

For a sawtooth surface

$$f(\alpha_m) = \frac{ak\,[1 - \cos(\alpha_m + \alpha_0)]}{\left(\frac{m\pi}{2}\right)^2 - S^2} \cdot \sin\left(\frac{m\pi}{2} + S\right), \qquad (6)$$

where $S = ka(\sin \alpha_m + \sin \alpha_0)$, $\underline{a}$ is the amplitude of the waviness of the reflecting surface, and $I_m(S)$ is the Bessel function of order m.

Given below is a description of the method used to investigate the field diffracted from periodic structures, the experimental scattering patterns and their comparison with the theory. The parameters of scattering surfaces, as well as the relative distances between the radiator, the scattering object, and the receiver, were chosen where possible to satisfy the requirement of the theory developed in Reference [1].

## Experimental Set-up.

The sound field scattered by a wavy surface was investigated in a body of water which can be assumed infinite under the experimental conditions. To distinguish the scattered and the direct signals, highly-directional radiators and receivers were used, and transmission was by means of pulses. The pulse durations were chosen long enough to be able to regard the incident wave a sinusoidal one.

Figure 2 shows the block diagram of the experimental set-up, the electric portion being shown in the ordinary block-diagram form with all the individual set-up elements marked, while the mechanical portion is sketched in perspective.

The operation of the individual blocks of the measuring set-up is coordinated by the pulse devices 1, which produce groups of rectangular pulses of various durations, timed in a specified sequence, and following each other at a frequency of 1 – 25 cycles. The first pulse in a group is rectangular, and modulates the oscillations of transmitting device 2. The transmitter thus delivers sinusoidal oscillations of the required frequency, modulated by rectangular pulses. The pulse durations could be varied in steps from 0.2 to 20 milliseconds.

The electric signals from the transmitter were converted by radiator R into ultrasonic pulses, propagating in the water towards the model M. The signals scattered by the models were received by sound receiver S, were converted into electrical signals, and fed to the input of measuring amplifier 4. The sound receiver, mounted on a metal truss, was moved by a geared electric motor along the arc of a circle about the stationary model. The electric signal, amplified and detected by amplifier 4, was applied in the form of a dc pulse through a switching panel 3 to the input of a cathode ray indicator and to the input of a pulse lengthener. The indicator is a double-beam oscilloscope, in which the start of the sweep is synchronized with the start of pulse transmission. The upper beam made it possible to observe the transmitted and received pulses. The lower beam displayed the

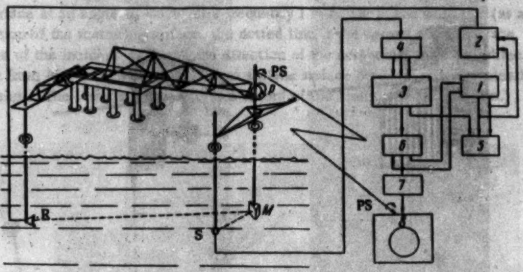

Fig. 2. Block diagram of experimental set-up.
1) pulse equipment, 2) transmitting equipment, R – radiator, M – model,
S – sound receiver, 3) switching panel, 4) measurement amplifier,
5) cathode-ray indicator, 6) pulse-lengthener, 7) dc amplifier,
8) circular-sweep indicator, PS – selsyn power transmission.

so-called "strobe-signal," which was a rectangular pulse, 0.1 millisecond in duration, produced by a pulsing circuit; this pulse was also applied to the input of the pulse lengthener 6. This pulse lengthener marks that time interval, during which the pulse lengthener is open to the passage of the received signal. The delay of the "strobe-signal" relative to the transmitted pulse can be adjusted from 1 to 15 milliseconds. The indicator screen thus displays the time sequence of the transmitted pulse, of the direct and scattered received pulses, and also the "strobe-signal." In controlling the pulse lengthener, the "strobe-signal" cuts out the portion of the received scattered signal needed for the measurement. The pulse lengthener is a "memory" circuit, which retains a voltage proportional to the received signal during almost the entire time up to the arrival of the next pulse, and this voltage is discarded only 0.5 microseconds prior to the arrival of the latter, making the lengthener ready to receive the next pulse.

The signal passes from the pulse lengthener to the dc amplifier 7, and is finally fixed by the beam of the cathode ray tube of the circular sweep indicator 8.

The reading is recorded by photographing the circular-sweep indicator screen. The beam rotation is synchronized with the receiver position by a selsyn power transmission PS. The experimental setup thus made it possible to plot scattering patterns in polar coordinates. The distance R from the radiator to the model was 14 m and the distance $\underline{r}$ from the model to the receiver 3 m; the scattering surface area selected was 15 X 15 cm. To prevent the receiver from blocking the beam incident on the model, the radiator was placed somewhat below the model, and the receiver somewhat above. At these distances the sound wave incident on the model could be assumed plane with sufficient degree of accuracy.

An external view of the model is shown in Fig. 3. It comprises a metal box in the form of a triangular prism. The wavy front surface of the prism was made of glass foil 0.1 mm thick. It can be proven that the impedance of such a thin membrane, and consequently also the reflection coefficient, will be independent of the angle of incidence.

To keep the wavy surface from bending and curving, the small rubber balloon, mounted on a special nipple placed on the rear post of the box, was used to equalize automatically the pressure on both sides of the wavy surface. A weight suspended below the model on a long thin cable kept the model steady in a vertical position.

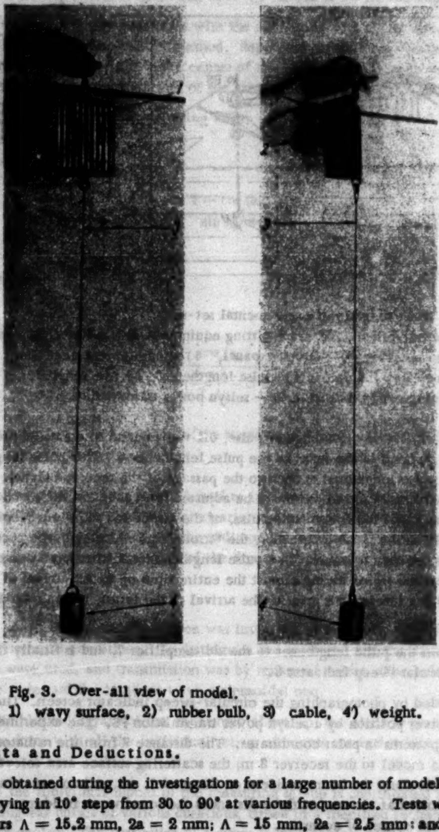

**Fig. 3. Over-all view of model.**
**1) wavy surface, 2) rubber bulb, 3) cable, 4) weight.**

## Experimental Data and Deductions.

Scattering was obtained during the investigations for a large number of models at elevation angles $\alpha_0$ of the incident beam varying in 10° steps from 30 to 90° at various frequencies. Tests were made on sinusoidal models with parameters $\Lambda = 15.2$ mm, $2a = 2$ mm; $\Lambda = 15$ mm, $2a = 2.5$ mm; and $\Lambda = 15$ mm, $2a = 5.5$ mm; the first was tested at 290, 402, and 555 kc, the other two at 305 and 520 kc. Tests were also made on sawtooth models the cross-sections of which in the zx plane, perpendicular to the generatrix, obey the following equations within the confines of one spatial period $\Lambda$

$$z = a\,(1 + 4x\,/\,\Lambda) \quad \text{at} \quad -\frac{\Lambda}{2} \leqslant x \leqslant 0$$

$$z = a\,(1 - 4x\,/\,\Lambda) \quad \text{at} \quad 0 \leqslant x \leqslant \frac{\Lambda}{2}$$

with parameters $\Lambda = 15$ mm, $2a = 1$ mm; $\Lambda = 15$ mm, $2a = 3$ mm; and $\Lambda = 15$ mm, $2a = 1.9$ mm at 290, 402, 496, and 520 kc. In addition, investigations were made with a plane surface, with sinusoidal and sawtooth models having even greater waviness, and also with models having rectangular grooves.

Figure 4 shows samples of photographs of the circular-sweep indicator screen. Figure 4a shows the reflection from a plane surface at an angle $\alpha_0 = 70°$ at a frequency $f = 555$ kc. The solid line (as also in Fig. 4b to 4f) shows the projection of the scattering surface, the dotted line is the normal to this surface, and the arrows indicate the direction of the incident wave and the direction of the zero-order spectrum (directly-reflected wave). It is evident from Fig. 4a that reflection from a plane surface produces only one clearly pronounced directly-reflected beam. The lower strip represents a record of the directly-incident beam.

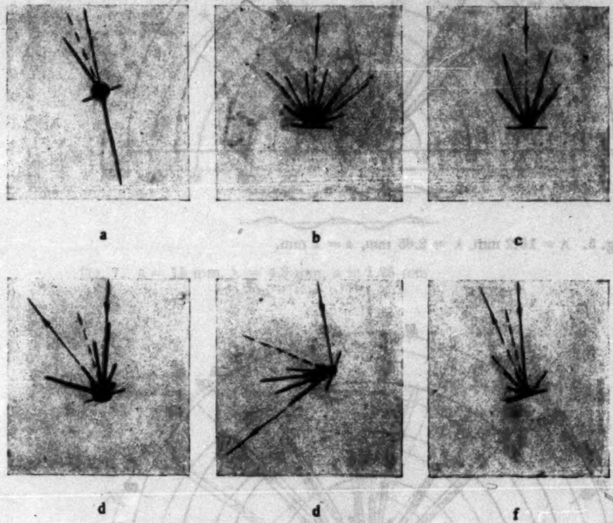

Fig. 4. Examples of photographs of the circular-sweep indicator screen.

One can conclude from Figs. 4b to 4f that under our experimental conditions the diffraction spectra are fully separated. The scattering coefficients, plotted on a linear scale that is convenient for review purposes, are drawn solid in Figs. 5-10.

The dotted lines indicate the theoretically-computed directions of the scattering spectra. The crosses denote the amplitudes calculated from equations (5) and (6) respectively and reduced to the same scale as the experimental patterns by multiplying by a factor K. This factor is defined as the ratio of the sum of the amplitudes of the experimental spectra in the sector in which the theory is valid to the sum of the same spectra, theoretically calculated. The dash-dot lines are tentative boundaries of the sectors within which the theory is valid. The arrows pointing towards the center of the pattern show the direction of the incident wave, the arrows pointing away from the center show the direction of the zero-order spectra. Shown under each pattern is the type of wavy surface.

Figure 5 shows by way of an example the theoretically-computed scattering pattern from a sinusoidal surface at $\Lambda = 15.2$ mm, $2a = 2$ mm at a frequency $f = 555$ kc ($\lambda = 2.65$ mm) at $\alpha_0 = 90°$. Figure 6 shows the same pattern superimposed on the experimental one obtained for the same waviness. The corresponding reading of the circular-sweep indicator is shown in Fig. 4b.

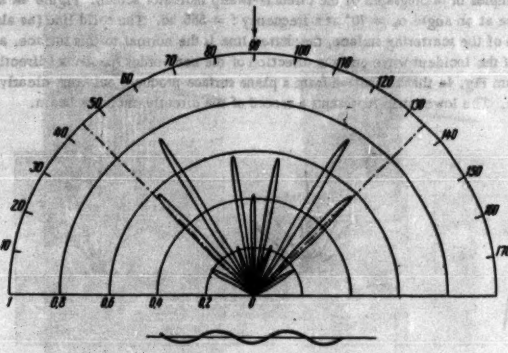

Fig. 5. $\Lambda = 15.2$ mm, $\lambda = 2.65$ mm, $a = 1$ mm.

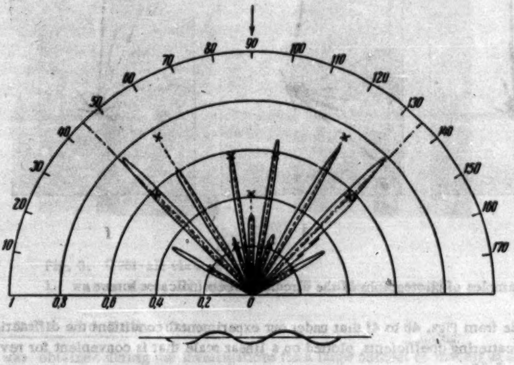

Fig. 6. $\Lambda = 15.2$ mm, $\lambda = 2.65$ mm, $a = 1$ mm.

As can be seen from the plot, the experimental and computed values agree quite well within the region in which the theory is valid.

Figure 7 (see Fig. 4c) shows the comparison of the experimental results with the computed data for a model having $\Lambda = 15$, and $2a = 2.5$ mm at $f = 305$ kc ($\lambda = 4.8$ mm) and $\alpha_0 = 90°$.

Figures 8 and 9 (see Figs. 4d and 4e) give the same information for models having parameters $\Lambda = 15.2$ mm, $2a = 2$ mm, and $\Lambda = 15$ mm, $2a = 1.9$ mm respectively at $\alpha_0 = 70°$, $f = 402$ kc ($\lambda = 3.65$ mm) and $\alpha_0 = 30°$, $f = 520$ kc ($\lambda = 2.8$ mm).

Figure 10 (see Fig. 4f) shows the scattering pattern obtained for a model with $\Lambda = 15$ mm and $2a = 5$ mm at $\alpha_0 = 80°$ and $f = 305$ kc; the figure shows also the comparison with the calculated values.

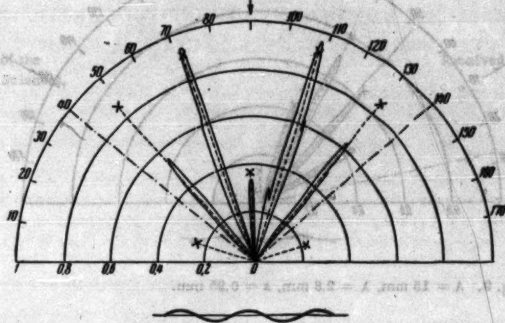

Fig. 7. Λ = 15 mm, λ = 4.8 mm, a = 1.25 mm.

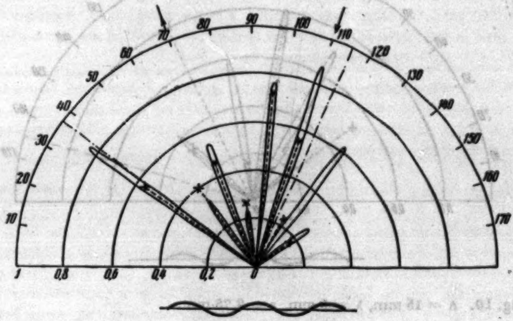

Fig. 8. Λ = 15.2 mm, λ = 3.65 mm, a = 1 mm.

In this case there is a sharp disagreement with the theory, owing to the fact that the radius of curvature of the waviness, $\rho$, is smaller than the wavelength of the incident sound ($\rho = 3$ mm, $\lambda = 5$ mm).

One can conclude from the given scattering patterns that within the sectors where the theory is valid, the theory developed in the reference given above [1] is in good agreement with experiment for sinusoidal surfaces in those cases, when the wavelength of the incident sound $\lambda$ is not less than 2-3 times smaller than the radius of curvature $\rho$ of the irregularity. In case of a sawtooth surface, a good agreement is also seen between theory and experiment (again within the region where the theory is valid). In this case the theory is applicable only for spectra at angles that do not differ much from those made by the rays directly reflected from both slopes of the sawtooth. If the angle between these rays is not too large, the sector within which the theory is valid can be defined in the same manner as for the sinusoidal waviness.

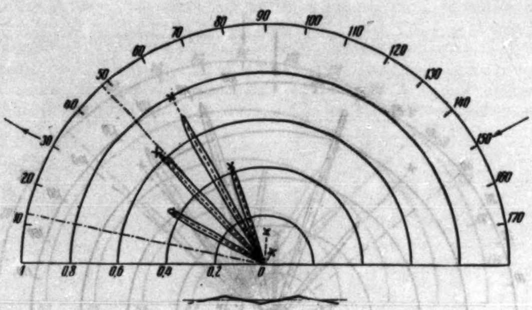

Fig. 9. $\Lambda = 15$ mm, $\lambda = 2.8$ mm, $a = 0.95$ mm.

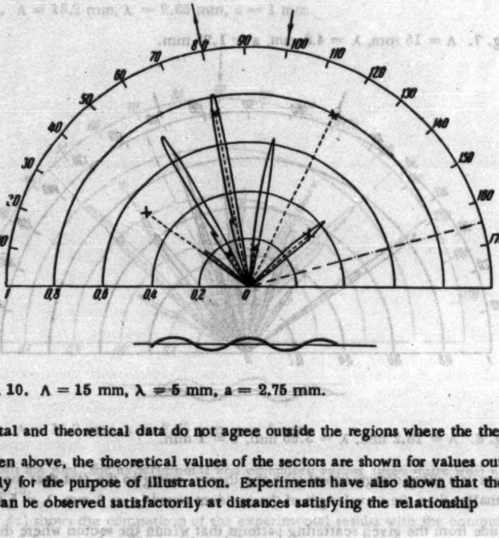

Fig. 10. $\Lambda = 15$ mm, $\lambda = 5$ mm, $a = 2.75$ mm.

The experimental and theoretical data do not agree outside the regions where the theory is valid.

In the plots given above, the theoretical values of the sectors are shown for values outside the region where the theory is valid only for the purpose of illustration. Experiments have also shown that the actually expected separation spectrum can be observed satisfactorily at distances satisfying the relationship

$$R > \frac{\Lambda D}{\lambda}.$$

In conclusion I consider it my obligation to express gratitude to L. M. Brekhovskikh, Associate Member of the USSR Academy of Sciences and V. S. Grigor'ev for valuable advice in the performance of the work, and also for aid in preparing this article for publication.

## LITERATURE CITED

[1] L. M. Brekhovskikh, "Diffraction of waves by rough surfaces," J. Exptl.-Theoret. Phys. (USSR) 23, 3 (1952).

Acoustics Institute of the
USSR Academy of Sciences,
Moscow

Received November 2, 1954.

# SCATTERING OF SOUND FROM PLANE INHOMOGENEOUS SURFACES WITH PERIODICALLY VARYING ACOUSTIC ADMITTANCE

Iu. P. Lysanov

A method is proposed for calculating the scattering of sound from a plane inhomogeneous surface characterized by a normal impedance or acoustic admittance that is independent of the angle of incidence of the sound wave. The solution is given in the form of a series, the $i$-th term of which can be obtained from a recurrence formula.

When a plane sound wave is incident on a plane inhomogeneous surface, a scattered field is produced in addition to the directly-reflected wave. If we restrict ourselves to a consideration of only periodic inhomogeneities, the scattered field will consist of side spectra of various orders. The problem of determining the amplitudes and phases of the scattered-field spectra becomes substantially simplified if approximate boundary conditions can be formulated for the inhomogeneous surface by employing the concept of the normal impedance (or acoustic admittance, independent of the angle of incidence of the sound wave). Boundary conditions in such a form are frequently used in architectural acoustics. A theoretical analysis of the limits within which such boundary conditions can be used is given in Reference [1].

We shall solve this problem for the indicated type of inhomogeneous surface for all ratios between the wavelength of the sound and the spatial period of the inhomogeneity. The results obtained will be compared with an approximate solution, obtained by assuming that the properties of the inhomogeneous surface vary little over distances on the order of the wavelength of sound.

## Derivation of Recurrence Formula for the Field of the Reflected Waves.

Let a plane monochromatic sound wave with a time dependence assumed in the form $e^{-i\omega t}$ be incident on a plane inhomogeneous surface, characterized by an acoustic admittance that is independent of the angle of incidence. Let us find the scattered field at any arbitrary point $M(x, y, z)$. Let us choose the coordinate system such that the $z$ axis coincides with the inward normal to the inhomogeneous surface and makes an obtuse angle with the direction of propagation of the incident wave. We shall characterize the sound field by a sound pressure $p$. The problem reduces to solving the wave equation $\Delta p_s + k^2 p_s = 0$ for the field of reflected waves, satisfying the boundary condition

$$\frac{\partial p}{\partial z} + ik\eta p = 0 \quad \text{at} \quad z = 0, \tag{1}$$

where $p$ is the total field, equal to the sum of the incident ($p_i$) and reflected ($p_s$) waves; $p_s = p_{s1} + p_{s2}$ where $p_{s1}$ is the directly-reflected wave, and $p_{s2}$ are the scattered waves; $\eta$ is the acoustic admittance of the inhomogeneous surface expressed in $\frac{1}{\rho c}$ units, where $\rho$ and $c$ are the constant values of the density and of the velocity of sound in the medium.

The reflected field $p_s$ should satisfy in addition the radiation condition, which requires that the field vanish at infinity. Let the acoustic admittance $\eta$ be specified in the form

$$\eta(x, y) = \eta_0[1 + hW(x, y)], \tag{2}$$

where $\eta_0$ is the average value of the admittance over the surface, $\underline{h}$ the amplitude of the alternating component of the admittance relative to $\eta_0$, and $W(x, y)$ is an arbitrary function, the average value of which is zero.

In general $\eta_0$ and $\underline{h}$ may be complex. We shall restrict ourselves to real $\eta_0$ and $\underline{h}$.

We shall seek an expression for $\underline{p}$ in the form of a series in powers of $\underline{h}$:

$$p = p_0 + p_1h + p_2h^2 + \ldots + p_mh^m + \ldots \tag{3}$$

It is evident that the expansion coefficients $p_m$ must satisfy the wave equation $\Delta p_m + k^2p_m = 0$. Here $p_0$ represents the solution for a homogeneous surface.

Inserting the series (3) into expression (1) and setting the coefficients of the various powers of $\underline{h}$ to zero individually, we obtain a system of equations for the boundary conditions for each individual term of the series:

$$z = 0\begin{cases} \dfrac{\partial p_0}{\partial z} + ik\eta_0p_0 = 0, \\ \dfrac{\partial p_1}{\partial z} + ik\eta_0p_1 + ik\eta_0p_0W = 0, \\ \dfrac{\partial p_m}{\partial z} + ik\eta_0p_m + ik\eta_0p_{m-1}W = 0. \end{cases} \tag{4}$$

The problem reduces thus to solving the system of equations $\Delta p_m + k^2p_m = 0$ ($m = 1, 2, 3, \ldots$) with boundary conditions (4) and with the radiation condition at infinity.

It will be convenient for further calculations to introduce an auxiliary function $U_m(x, y, z)$ defined as follows:*

$$U_m(x, y, z) = \frac{\partial p_m(x, y, z)}{\partial z} + ik\eta_0p_m(x, y, z). \tag{5}$$

It is evident that the function $U_m$ must satisfy the same equation as $p_m$, and the boundary condition:

$$(U_m)_{z=0} = -ik\eta_0p_{m-1}(x, y, 0)\,W(x, y), \tag{6}$$

---

* The use of a function $U_m$ and its subsequent transformations are analogous to the method used in the treatment of the field over an absorbing surface [2].

which follows from (4). Using Green's theorem and boundary condition (6), we obtain the function $U_m$ everywhere in the half space $z > 0$. Green's theorem for this case of a plane boundary surface can be written as [8]:

$$U_m(x, y, z) = -\frac{1}{2\pi}\iint\limits_{-\infty}^{+\infty} U_m(x_1, y_1, 0)\frac{\partial}{\partial z}\frac{e^{ikR}}{R}\,dx_1 dy_1. \tag{7}$$

Then, taking condition (6) into account, we have

$$U_m(x, y, z) = \frac{ik\eta_0}{2\pi}\iint\limits_{-\infty}^{+\infty} p_{m-1}(x_1, y_1, 0)\,W(x_1, y_1)\frac{\partial}{\partial z}\frac{e^{ikR}}{R}\,dx_1 dy_1, \tag{8}$$

where $R = \sqrt{(x - x_1)^2 + (y - y_1)^2 + z^2}$ — is the distance from the running point $(x_1, y_1)$ on the integration surface (plane $z = 0$) to the point of observation $(x, y, z)$. Let us find $p_m$ from equation (5). We first transform it as follows:

$$U_m = e^{-ik\eta_0 z}\frac{\partial}{\partial z}\left(e^{ik\eta_0 z} p_m\right). \tag{9}$$

Multiplying both halves of equation (9) by $e^{ik\eta_0 z}$ and integrating with respect to z, we get the following expression for $p_m$:

$$p_m(x, y, z) = e^{ik\eta_0(\alpha - z)}\,p_m(x, y, \alpha) + e^{-ik\eta_0 z}\int\limits_{\alpha}^{z} e^{ik\eta_0 z}\,U_m(x, y, z)\,dz, \tag{10}$$

where the lower limit $\alpha$ is so chosen as to make $p_m(x, y, z)$ satisfy the wave equation. It turns out that for this purpose it is enough to take $\alpha = i\infty$.

Then

$$p_m(x, y, z) = e^{-ik\eta_0 z}\int\limits_{i\infty}^{z} e^{ik\eta_0 z}\,U_m(x, y, z)\,dz. \tag{11}$$

Inserting equation (8) into (10) we obtain for $p_m$

$$p_m(x, y, z) = \frac{ik\eta_0}{2\pi}e^{-ik\eta_0 z}\int\limits_{i\infty}^{z}\iint\limits_{-\infty}^{\infty} P_{m-1}(x_1, y_1, 0)\,W(x_1, y_1)\,e^{ik\eta_0 z}\times$$

$$\times\frac{\partial}{\partial z}\frac{e^{ikR}}{R}\,dz\,dx_1 dy_1. \tag{12}$$

The resultant equation (12) is a recurrence formula for $p_m$. Knowing $p_0$ by solving for the reflection of the plane sound wave from a homogeneous surface with an acoustic admittance $\eta_0$, and specifying the function W (x, y) in explicit form, we can calculate all the following approximations of the series (3).

## Calculation of Successive Approximations

**First Approximation.** Let us continue our calculations for the case when W is a function of only one of the coordinates (for example, x) and is specified in the form W (x) = cos qx, where $q = \frac{2\pi}{T}$, and T is the spatial period of the inhomogeneity. For $p_1$ we obtain for (12) the following expression:

$$p_1 = \frac{ik\eta_0}{2\pi} e^{-ik\eta_0 z} \int\limits_{i\infty}^{z} \int\limits_{-\infty}^{+\infty} \int\limits_{-\infty} p_0 (x_1,\ y_1,\ 0) \cos qx_1 e^{ik\eta_0 z} \frac{\partial}{\partial z} \frac{e^{ikR}}{R}\, dz dx_1 dy_1. \qquad (13)$$

Let the plane of incidence of the sound wave be the xz plane, then $P_0 (x_1, 0, 0) = (1 + V_0)\, e^{ik^0_x x}$, where $k^0_x = k \sin\theta$, $V_0 = \frac{\cos\theta - \eta_0}{\cos\theta + \eta_0}$ is the reflection coefficient from a homogeneous surface with acoustic admittance $\eta_0$, and $\theta$ is the angle of incidence.

To calculate the resultant integrals it is convenient to expand $\frac{e^{ikR}}{R}$ as a superposition of plane waves in the form [4]:

$$\frac{e^{ikR}}{R} = \frac{i}{2\pi} \iint\limits_{-\infty}^{+\infty} \exp\left\{i\,[k_x(x - x_1) + k_y(y - y_1) + k_z z]\right\} \frac{dk_x dk_y}{k_z}.$$

Hence,

$$\frac{\partial}{\partial z} \frac{e^{ikR}}{R} = \frac{-1}{2\pi} \iint\limits_{-\infty}^{+\infty} \exp\{i\,[k_x(x - x_1) + k_y(y - y_1) + k_z z]\}\, dk_x\, dk_y. \qquad (14)$$

Substituting (14) into (13) and replacing cos $qx_1$ by a sum of two exponents, we obtain for $p_1$

$$p_1 = \frac{-ik\eta_0(1 + V_0)}{8\pi^2} e^{-ik\eta_0 z} \iiiint\!\!\!\int\limits_{i\infty\ -\infty}^{z\ +\infty} \{\exp[i(k^0_x + q - k_x)x_1 - ik_y y_1 + i(k_x x +$$

$$+ k_y y + k_z z)] + \exp[i(k^0_x - q - k_x)x_1 - ik_y y_1 + i(k_x x + k_y y + k_z z)]\} \times$$

$$\times\, dz\, dx_1\, dy_1\, dk_x\, dk_y.$$

The integration with respect to $x_1$ and $y_1$ can be performed immediately, considering that

$$\int\limits_{-\infty}^{+\infty} e^{iat}\, dt = 2\pi\delta(a),$$

where $\delta$ denotes the Dirac $\delta$-function.

**Using the well-known property of the δ-function**

$$\int\limits_{-\infty}^{+\infty} f(t)\,\delta(t-t_0)\,dt = f(t_0),$$

**we can easily also perform the integration with respect to $k_x$ and $k_y$.**

**We then get for $p_1$**

$$p=\frac{-ik\eta_0(1+V_0)}{2}\,e^{-ik\eta_0 z}\left\{e^{i(k_x^0+q)x}\int\limits_{i\infty}^{z}\exp\left\{ik\left[\eta_0+\sqrt{1-\left(\frac{k_x^0+q}{k}\right)^2}\,\right]z\right\}dz+\right.$$

$$\left.+\,e^{i(k_x^0-q)x}\int\limits_{i\infty}^{z}\exp\left\{ik\left[\eta_0+\sqrt{1-\left(\frac{k_x^0-q}{k}\right)^2}\,\right]z\right\}dz\right\}.$$

**Having performed the last integration with respect to $\underline{z}$, we obtain for $p_1$ the following final expression**

$$p_1=\frac{-(1+V_0)}{2}\left\{\frac{\exp\left\{i(k_x^0+q)x+i\sqrt{k^2-(k_x^0+q)^2}\,z\right\}}{1+\frac{1}{\eta_0}\sqrt{1-\left(\frac{k_x^0+q}{k}\right)^2}}+\right.$$

$$\left.+\frac{\exp\left\{i(k_x^0-q)x+i\sqrt{k^2-(k_x^0-q)^2}\,z\right\}}{1+\frac{1}{\eta_0}\sqrt{1-\left(\frac{k_x^0-q}{k}\right)^2}}\right\}. \tag{15}$$

**The first approximation consists thus of a sum of two plane waves, representing the two first side spectra, propagating at angles $\theta=\arcsin\dfrac{k_x^0+q}{k}$ and $\theta=\arcsin\dfrac{k_x^0-q}{k}$ with the $\underline{z}$ axis.**

**Let us simplify the equations that follow by introducing the notation:**

$$\left.\begin{aligned}\left(\frac{k_x^0\pm nq}{k}\right)x+\sqrt{1-\left(\frac{k_x^0\pm nq}{k}\right)^2}\,z&\equiv\psi_{\pm n}(x,z)\\ 1+\frac{1}{\eta_0}\sqrt{1-\left(\frac{k_x^0\pm nq}{k}\right)^2}&=S_{\pm n}\end{aligned}\right\}. \tag{16}$$

**The function $\psi_{\pm n}$ will hereinafter be written without an argument. Using the new notation, $p_1$ can be written as**

$$p_1=\frac{-(1+V_0)}{2}\left[\frac{e^{ik\psi_1}}{S_1}+\frac{e^{ik\psi_{-1}}}{S_{-1}}\right]. \tag{17}$$

Subsequent Approximation. The succeeding terms of the series (3) calculated quite analogously as the first term. We obtain the following expressions for the coefficients $p_m$:

$$p_{2r-1} = \frac{-(1+V_0)}{2^{2r-1}} \sum_{m=1}^{r} \left[ \frac{e^{ik\psi_{2m-1}}}{\prod_{l=1}^{2m-1} S_l} D_{2m-1,\gamma_j} + \frac{e^{ik\psi_{-2m+1}}}{\prod_{l=1}^{2m-1} S_l} D_{-2m+1,\gamma_j} \right],$$

$$p_{2r} = \frac{(1+V_0)}{2^{2r}} \sum_{m=0}^{r} \left[ \frac{e^{ik\psi_{+2m}}}{\prod_{l=1}^{2m} S_l} D_{2m,\gamma_j} + \frac{e^{ik\psi_{-2m}}}{\prod_{l=1}^{2m} S_{-l}} D_{-2m,\gamma_{-j}} \right] \quad (r = 1,2,\ldots), \tag{18}$$

where the following symbols are introduced

$$D_{N\gamma_j} = \begin{cases} 1 \quad \text{at} \quad j=0 \\ \displaystyle\sum_{n_1=0}^{\gamma_1} \frac{1}{S_{n_1} + \delta_1 S_{n_1}} \quad \text{at} \quad j=1 \\ \displaystyle\sum_{n_1=0}^{\gamma_1} \frac{1}{S_{n_1} + \delta_1 S_{n_1}} \sum_{n_2=0}^{\gamma_2} \frac{1}{S_{n_2} + \delta_2 S_{n_2}} \quad \text{at} \quad j=2 \\ \displaystyle\sum_{n_1=0}^{\gamma_1} \frac{1}{S_{n_1} + \delta_1 S_{n_1}} \sum_{n_2=0}^{\gamma_2} \frac{1}{S_{n_2} + \delta_2 S_{n_2}} \sum_{n_\nu=0}^{\gamma_\nu} \frac{1}{S_{n_\nu} + \delta_\nu S_{n_\nu}} \quad \text{at} \quad j=\nu \end{cases} \tag{19}$$

$$\gamma_1 = \begin{cases} N+1 & \text{at} \quad N>0; \\ 2 & \text{at} \quad N=0; \end{cases} \quad \gamma_{-1} = \begin{cases} N-1 & \text{at} \quad N<0; \\ -2 & \text{at} \quad N=0; \end{cases} \quad j = \begin{cases} r-m & \text{at} \quad m \neq 0 \\ r-1 & \text{at} \quad m=0 \end{cases}$$

$$\begin{matrix} \gamma_j = \gamma_{-j} = \\ (j>1) \end{matrix} \begin{cases} n_{j-1}+1 & \text{at} \quad n_{j-1}>0 \\ n_{j-1}-1 & \text{at} \quad n_{j-1}<0 \\ 2 & \text{at} \quad n_{j-1}=0; \quad \gamma_{j-1}<0 \\ -2 & \text{at} \quad n_{j-1}=0; \quad \gamma_{j-1}>0 \end{cases} \qquad \delta_j = \begin{cases} 1 & \gamma_j<0 \\ -1 & \gamma_j>0 \end{cases} \tag{20}$$

Substituting the values of the coefficients $p_r$ from expressions (18) into the series (3) we obtain the solution to a problem in the form of a series in powers of $h$, with the approximation of order $r$ consisting of $2^r$ terms, pertaining to $(r+1)$ different spectra. Let us now group in (3) the terms belonging to the same spectrum. The scattered field together with directly-reflected waves can then be represented by the series:

$$p_s = \sum_{m=0}^{\infty} [A_m e^{ik\psi_m} + A_{-m} e^{ik\psi_{-m}}], \tag{21}$$

which essentially is the expansion of the reflected field in a Fourier series in terms of $x$. Every coefficient $A_{\pm m}$ which defines the amplitude of the corresponding spectrum, is expressed by a series in powers of $h$.

Let us write the expressions for the coefficients $A_{\pm m}$

$$A_0 = V_0 + (1 + V_0)\left(\frac{h}{2}\right)^2 \sum_{r=0}^{\infty}\left(\frac{h}{2}\right)^{2r}\left[\frac{D_{2,\gamma_r}}{S_0 S_1} + \frac{D_{-2,\gamma_{-r}}}{S_0 S_{-1}}\right],$$

$$A_{\pm m} = \frac{(-1)^m (1 + V_0)\left(\frac{h}{2}\right)^m}{\prod\limits_{l=1}^{m} S_{\pm l}} \sum_{r=0}^{\infty}\left(\frac{h}{2}\right)^{2r} D_{\pm m,\gamma_{\pm r}}. \tag{22}$$

The field thus consists of a directly-reflected wave and of side spectra of different orders, the amplitudes of which are given by expressions (22). The series for $A_{\pm m}$ begins here with a term approximately, equal to $\sim\left(\frac{h}{2}\right)^m$ . As the term $\underline{h}$ approaches zero, the field approaches the directly-reflected wave from a homogeneous surface, as is indeed expected.

It is interesting to note that the final equations for the scattered fields become considerably simpler, if the acoustic admittance of the inhomogeneous surface is specified in the form

$$\eta(x) = \eta_0 (1 + he^{iqx}).$$

In this case we obtain for $p_{s2}$ the following simple expression:

$$p_{s2} = (1 + V_0) \sum_{m=1}^{\infty} \frac{(-1)^m h^m e^{ik\psi_m}}{\prod\limits_{l=1}^{m} S_l}. \tag{23}$$

The character of this scattered field is different, for it consists of side spectra located only on one side of the directly-reflected wave.

## Investigation of the Solution

The principal question raised in the investigation of the solution obtained is whether series (3), (18), (21), (22), and (23) are convergent. The only one of these with a simple form is (23), which yields a solution for the case when the admittance of the inhomogeneous surface is of the form $\eta(x) = \eta_0 (1 + he^{iqx})$. Let us first show that the series (23) is absolutely convergent for all finite values of the parameter $\underline{h}$. For this purpose let us consider another series, made up of the moduli of the terms of series (23):

$$(1 + V_0) \sum_{m=1}^{\infty} \frac{|h^m|}{\prod\limits_{l=1}^{m} |S_l|}. \tag{24}$$

It is easily seen that the limit of the ratio of the successive terms vanishes as $\underline{m}$ approaches infinity. In fact,

$$\lim_{m\to\infty}\left\{\frac{|h^m|}{\prod\limits_{l=1}^{m}|S_l|} : \frac{|h^{m-1}|}{\sum\limits_{l=1}^{m-1}|S_l|}\right\} = \lim_{m\to\infty}\frac{|h|}{|S_m|}\to 0,$$

since $\lim_{m\to\infty}|S_m|\to\infty$, as follows from (16). Hence, using the well-known convergence criterion, we can conclude that (24) converges for all finite values of $h$, and consequently, series (23) also converges absolutely under these conditions.

A thorough investigation of the convergence of series (3), (18), (21), and (22) is a difficult task owing to the very complicated structure of these series. However, certain information on the convergence can nevertheless be obtained. Let us consider series (22), which gives an expression for the m-th spectrum. The difficulty in investigating the convergence of the series (22) lies in the fact that the quantities $D_{m,\gamma_r}$ are in turn sums having a number of terms that increases with increasing $r$, and as can be shown, are determined by the number of combinations $C^r_{m+2r}$. Let us now consider a series made up of the moduli of series (22), discarding the factor in front of the summation sign:

$$\sum_{r=0}^{\infty}\left|\left(\frac{h}{2}\right)^{2r}\right|\left|D_{m,\gamma_r}\right|. \tag{25}$$

Let $|D_{m,\gamma_r}|$ in this series be replaced by the sum of the moduli of the terms contained in $D_{m,\gamma_r}$ this operation can only increase every term in the series (25) that corresponds to the given number $r$. We next replace the quantities $|S_{\pm m}|$ in the denominator of each of the terms belonging to $D_{m,\gamma_r}$ by the quantity $|S|$, which is the smallest for all $m$. This evidently will make the convergence conditions of the latter series only worse. We can then write a majorant series with respect to the series (25):

$$\sum_{r=0}^{\infty}\left|\left(\frac{h}{2}\right)^{2r}\right|\frac{C^r_{m+2r}}{|S|^{2r}}, \tag{26}$$

which, as can be seen, will converge at $\left|\frac{h}{S}\right| < 1$. The convergence of series (26) leads to the convergence of series (25), and consequently also to the absolute convergence of series (22) under the condition $\left|\frac{h}{S}\right| < 1$.

Since the least possible value of $|S|$ is unity, the above convergence conditions become: $|h| < 1$. There are cases, however, when $|S| > 1$, and the series will then converge also at $|h| > 1$. The latter can occur under the condition that $\frac{k_x^0 \pm mq}{k} \neq 1$ for all values of $m$. We can show in exactly the same manner that series (3) and (18) converge under this condition. A more accurate estimate of the convergence region requires further investigation.

## Solution of Problem by the Rayleigh Method

The use of approximate boundary conditions makes it possible to obtain a solution to the above problem in the form of a series in powers of $\underline{h}$ using also the Rayleigh method [5]. Let us represent the total field of the incident, directly-reflected, and scattered waves in the upper medium in the form

$$\begin{aligned} p = {} & \exp\{i(k_x^0 x - k_z^0 z)\} + A_0 \exp\{i(k_x^0 x + k_z^0 z)\} + \\ & + \sum_{n=1}^{\infty}{}' \{A_n \exp[i(k_x^0 + nq)x + i\sqrt{k^2 - (k_x^0 + nq)^2}\, z] + \\ & + B_n \exp[i(k_x^0 - nq)x + i\sqrt{k^2 - (k_x^0 - nq)^2}\, z]\}. \end{aligned} \tag{27}$$

Such a representation of the total field denotes its expansion into a sum of spectra with indeterminate amplitudes. For the z component of the oscillation velocity we obtain from (27)

$$\begin{aligned} -V_z = {} & \frac{\cos\theta}{\rho c}[\exp\{i(k_x^0 x - k_z^0 z)\} - A_0 \exp\{i(k_x^0 x + k_z^0 z)\}] - \\ & - \sum_{n=1}^{\infty}\left\{A_n \frac{\sqrt{k^2 - (k_x^0 + nq)^2}}{k\rho c} \exp\{i(k_x^0 + nq)x + i\sqrt{k^2 - (k_x^0 + nq)^2}\, z\} + \right. \\ & \left. + B_n \frac{\sqrt{k^2 - (k_x^0 - nq)^2}}{k\rho c} \exp\{i(k_x^0 - nq)x + i\sqrt{k^2 - (k_x^0 - nq)^2}\, z\}\right\}. \end{aligned} \tag{28}$$

Let, as before, the acoustic admittance of the surface, given in $\frac{1}{\rho c}$ units, be specified as

$$\eta(x) = \eta_0(1 + h\cos qx).$$

Then the following boundary condition should be satisfied at $z = 0$:

$$\frac{-V_z(x, 0)}{p(x, 0)} = \eta(x)/\rho c. \tag{29}$$

Substituting expressions (27) and (28) into condition (29) and cancelling the common factor $e^{ik_x^0 x}$, we get

$$\begin{aligned} & (1 - A_0)\cos\theta - \sum_{n=1}^{\infty}\left\{A_n \sqrt{1 - \left(\frac{k_x^0 + nq}{k}\right)^2} e^{inqx} + B_n \sqrt{1 - \left(\frac{k_x^0 - nq}{k}\right)^2} e^{-inqx}\right\} = \\ & = \eta_0(1 + h\cos qx)\left\{(1 + A_0) + \sum_{n=1}^{\infty}[A_n e^{inqx} + B_n e^{-inqx}]\right\}. \end{aligned} \tag{30}$$

Grouping together in (30) the terms that have as factors an exponential with the same index, and setting these groups individually equal to zero, we obtain a system of equations for the coefficients $A_n$ and $B_n$. Using the symbols of (16) the system can be written as

$$\begin{aligned} -S_0A_0 &= (\eta_0 - \cos\theta) + \frac{h}{2}(A_1 + B_1), \\ -S_mA_m &= \frac{h}{2}(\delta_{m1} + A_{m-1} + A_{m+1}), \\ -S_{-m}B_m &= \frac{h}{2}(\delta_{m1} + B_{m-1} + B_{m+1}), \end{aligned} \tag{31}$$

where

$$A_0 = B_0; \quad \delta_{m1} = \begin{cases} 1 & m = 1 \\ 0 & m \neq 1 \end{cases}$$

The system (31) makes it possible to calculate the coefficients $A_n$ and $B_n$ by successive approximation. We shall seek $A_n$ and $B_n$ in the form of a series in powers of $\underline{h}$:

$$\begin{aligned} A_n &= A_n^{(0)} + A_n^{(1)}h + A_n^{(2)}h^2 + \cdots + A_n^{(m)}h^m + \cdots \\ B_n &= B_n^{(0)} + B_n^{(1)}h + B_n^{(2)}h^2 + \cdots + B_n^{(m)}h^m + \cdots \end{aligned} \tag{32}$$

Inserting Eq. (32) into (31) and collecting terms of equal powers of $\underline{h}$, we obtain for each approximation its own system of equations. When the necessary calculations are made, it is easy to verify directly that the expressions obtained for $A_n$ and $B_n$ are identical with (22).

The Rayleigh method is apparently more general in the sense that it can also be used for scattering from rough surfaces. The first method, however, is more compact in its calculations.

## Comparison of the Kirchhoff Approximation with the Rigorous Solution

If the properties of the scattering inhomogeneous surface are slowly-varying, the scattered field can be calculated approximately under the assumption that the field at each point of the surface is the same as if the whole surface were homogeneous and of the same properties as at the given point. This approximation is analogous to the Kirchhoff approximation in diffraction theory. Recently this approximation was used to obtain many interesting results on the scattering of waves from rough surfaces [4, 6].

It is interesting to compare the solution obtained by this approximation with the rigorous solution. This would make it possible to estimate the applicability limits of the Kirchhoff approximation for sound scattered from a plane inhomogeneous surface. To obtain the scattered field in the Kirchhoff approximation, we employ Green's theorem

$$p_{s\,(x,\,y,\,z)} = \frac{-1}{2\pi}\iint\limits_{-\infty}^{+\infty}\left(\frac{\partial p_s}{\partial z}\right)_{z=0}\frac{e^{ikR}}{R}\,ds.$$

Since we have in this approximation

$$\left(\frac{\partial p_s}{\partial z}\right)_{z=0} = -V(x)\left(\frac{\partial p_i}{\partial z}\right)_{z=0},$$

then

$$p_s(x,\,y,\,z) = \frac{1}{2\pi}\iint\limits_{-\infty}^{+\infty}V(x)\left(\frac{\partial p_i}{\partial z}\right)\frac{e^{ikR}}{R}\,ds, \tag{33}$$

**where $V_{(x)} = \frac{\cos\theta - \eta(x)}{\cos\theta + \eta(x)} = \frac{\cos\theta - \eta_0(1 + h\cos qx)}{\cos\theta + \eta_0(1 + h\cos qx)}$ is the reflection coefficient at the given point on the surface. Let us represent V (x) in a Fourier series**

$$V(x) = \sum_{n=-\infty}^{+\infty} C_n e^{inqx},$$

**where $C_n = \frac{1}{T}\int_0^T V(x)\, e^{-inqx}\, dx,\ q = \frac{2\pi}{T}, T$ T is the spatial period of the inhomogeneity. Representing V (x) under the integral sign as a series in powers of h:**

$$V(x) = \sum_{m=0}^{\infty} b_m h^m.$$

**Upon determining the coefficients $b_m$, we obtain for V (x)**

$$V(x) = V_0 + \sum_{m=1}^{\infty} (1 + V_0)\frac{(-1)^m \cos^m qx}{S_0^m} h^m.$$

**Using the well-known equations for the powers of the cosines in terms of the cosines of multiple angles, we get**

$$V(x) = V_0 - (1 + V_0)\sum_{m=1}^{\infty}\left(\frac{h}{S_0}\right)^{2m-1}\frac{1}{2^{2m-2}}\sum_{n=0}^{m-1} C_{2m-1}^{n}\cos(2m - 2n - 1)\, qx +$$

$$+ (1 + V_0)\sum_{m=1}^{\infty}\left(\frac{h}{S_0}\right)^{2m}\frac{1}{2^{2m}}\sum_{n=0}^{m-1}\left[2C_{2m}^{n}\cos 2(m - n)\, qx + C_{2m}^{m}\right].$$

**Substituting this last equation into the integral (33) and performing calculations analogous to those used to compute integral (12), we obtain the following expressions for the amplitudes of the spectra**

$$A_0^{(k)} = V_0 + (1 + V_0)\sum_{m=1}^{\infty}\left(\frac{h}{2S_0}\right)^{2m} C_{2m}^{m};$$

$$A_{\pm r}^{(k)} = \frac{(-1)^r (1 + V_0)\cos\theta \left(\frac{h}{2S_0}\right)^r}{\sqrt{1 - (\sin\theta \pm rq/k)^2}}\sum_{m=0}^{\infty} C_{2m+r}^{m}\left(\frac{h}{2S_0}\right)^{2m} \quad (r = 1, 2, \ldots), \tag{34}$$

**where $\theta$ is the angle of incidence of the sound wave $A_{\pm r}^{(k)}$ the amplitude of the ±r-th spectrum in the Kirchhoff approximation, with the "plus" sign pertaining to positive spectra, and the "minus" pertaining to the negative spectra.**

The field of reflected waves in this approximation consists thus of a directly-reflected wave and of side spectra of various orders, propagating in the same directions as the corresponding spectra of the rigorous solution. To compare the rigorous and approximate solutions let us find the ratio of the amplitudes of the corresponding spectra. After cancelling out the common factor (assuming that $\cos\theta \neq \frac{\pi}{2}$) we obtain for the r-th spectra

$$\frac{|A_r^{(k)}|}{|A_r|} = \frac{\left|\cos\theta \sum_{n=0}^{\infty} C_{r+2n}^{n} \left(\frac{h}{2S_0}\right)^{2n}\right|}{\left|\sqrt{1-(\sin\theta + rq/k)^2}\right| \left|\sum_{n=0}^{\infty}\left(\frac{h}{2}\right)^{2n} D_{r,\gamma_n}\right|} \left|\frac{\prod_{l=1}^{r} S_l}{S_0^r}\right|. \tag{35}$$

Let us first show that if the ratio of the wavelength of the incident sound to the spatial period of the inhomogeneity approaches zero, the approximate solution approaches the rigorous one. Let us find $\lim\limits_{q/k \to 0} \frac{|A_r^{(k)}|}{|A_r|}$ for normal incidence. Inasmuch as $\lim S_{\pm n} = S_0$ as $q/k \to 0$, and the number of terms contained in $D_{r,\gamma_n}$, as indicated above, is $C_{r+2n}^{n}$, we have in fact

$$\lim_{q/k\to 0} \frac{|A_r^{(k)}|}{|A_r|} \to 1.$$

On the other hand, $\lim \frac{|A_r^{(k)}|}{|A_r|} \to \infty$ as $(\sin\theta + rq/k) \to 1$, and consequently the Kirchhoff approximation can be used to calculate the scattered field only if the condition $(\sin\theta + rq/k) << 1$ is satisfied, i.e., when the properties of the inhomogeneous surface vary little at distances on the order of a wavelength, when the observation direction is sufficiently close to the direction of the mirror image $(rq/k << 1)$, and when the angles of incidence satisfy the above condition at the specified value of rq/k. Let us remark that in general the above limitations on the validity of the Kirchhoff approximation are well-known. In this case, however, it is possible to formulate them quantitatively. Figure 1 shows a plot of the function $f(q/k) = \frac{|A_r^{(k)}|}{|A_r|}$ for $\eta_0 = 10$, $h = \frac{2}{3}$ and $r = 0, 1, 2, 3$, and 4. As can be seen from the graph, the amplitude of the directly-reflected wave obtained by the Kirchhoff approximation is the same as that obtained rigorously for all values of $\frac{\lambda}{T}$, while the amplitude of the first spectrum exceeds the rigorous one by 6 db at $\frac{\lambda}{T} = 0.85$, and the amplitude of the fourth spectrum exceeds the rigorous value by the same amount at $\frac{\lambda}{T} = 0.2$. Figure 2 shows the graph of $f(\theta) = \frac{|A_r^{(k)}|}{|A_r|}$ for $r = 0, 1, 2, 3$, and 4, $\eta_0 = 10$, $h = \frac{2}{3}$, and $q/k = 0.1$. It is evident from the graph that as the angle of incidence increases and as the number $\underline{r}$ of the spectrum increases, the discrepancy between the rigorous and approximate solutions increases for a specified ratio q/k.

Let us remark that the results of this solution can be directly employed for the scattering of electromagnetic waves from a periodically-inhomogeneous surface, if $\underline{p}$ is taken to mean the vertical component of the Hertz vector and $\eta = \sqrt{\frac{\mu}{\epsilon}}$ is taken to be a dimensionless complex constant, characterizing the scattering surface.

In conclusion I consider it my duty to express deep gratitude to Associate Member of the USSR Academy of Sciences, L. M. Brekhovskikh and also to M. A. Isakovich and G. D. Maliuzhinets for attention and interest in this work.

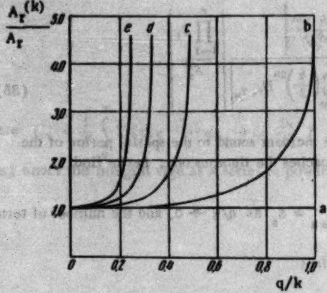

Fig. 1. Ratio of moduli of amplitudes, calculated by the Kirchhoff approximation and by the method of successive approximations for various spectra as a function of q/k;
a) ratio of the mirror-reflected amplitudes,
b) ratio of the amplitudes of the first-order spectra, c) ditto for the second-order spectra, d) ditto for the third-order,
e) ditto for the fourth order.

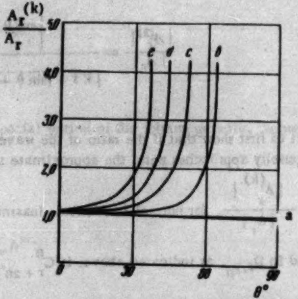

Fig. 2. Ratio of moduli of amplitudes, calculated by the Kirchhoff approximation and by the successive-approximation method for various spectra as a function of the angle of incidence of the sound wave;
a) ratio of the amplitudes of the mirror-reflected waves, b) ratio of amplitudes of the first-order spectra, c) ditto, second-order, d) ditto, third-order,
e) ditto, fourth-order.

## LITERATURE CITED

[1] L. M. Brekhovskikh, Progr. Phys. Sci. 32, 4, 474 (1947).

[2] G. D. Maliuzhinets, Doklady Akad. Nauk SSSR, 3, 367 (1948).

[3] Ia. L. Al'pert, V. L. Ginzburg, and E. L. Feinberg, Propagation of Radio Waves, State Tech. and Theoret. Lit. Press, Sec. 8 (1953).

[4] L. M. Brekhovskikh, J. Exptl.-Theoret. Phys. (USSR), 23, 275 (1952).

[5] Rayleigh, Theory of Sound (State Tech. and Theoret. Lit. Press) Sec. 272a (Russian translation) (1944).

[6] M. A. Isakovich, J. Exptl.-Theoret. Phys. (USSR) 23, 305 (1952).

Acoustics Institute of the
USSR Academy of Sciences,
Moscow

Received October 16, 1954

# ANALYSIS OF GAIN OF CYLINDRICAL SOUND-FOCUSING SYSTEMS

L. D. Rozenberg

**Assuming the length to be small compared with the dimensions of the radiator, general expressions are derived for the amplification coefficients and for the focusing factors of a converging cylindrical front. It is shown to obtain the maximum value of the focusing factor for the pressure, the optimum distribution function is of the form $\Phi(\alpha) = 1$, and for velocity focusing of the form $\Phi(\alpha) = \cos\alpha$. The values of $K_p$, $K_b$, $\kappa$, and $\kappa'$ and their dependence on the aperture angle of the front are calculated for several actual cases. The results obtained can be used to calculate actual focusing systems with an error not exceeding 10%, with the exception of edge segments of length $\sqrt{\lambda f}$.**

In recent times, many technical problems in commercial application of ultrasonics are solved extensively by using cylindrical focusing radiators, representing segments of cylindrical surfaces, oscillating along their thickness and concentrating the energy radiated in a region along the axis of the cylindrical surface [1, 2]. Such radiators are particularly convenient in those cases, when it is necessary to irradiate continuously rather small objects moving on a conveyor, for example, in ultrasonic cleaning.

This article examines the amplification coefficients and focusing factors of several types of cylindrical radiators. The relationships obtained are valid for those cases, when the length of the radiator and its focal distance are considerably greater than the length of the radiated sound wave.

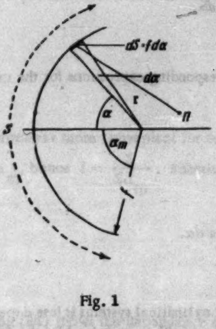

Fig. 1

The sound field of an infinitely long cylindrical surface can be determined (see, for example, [3]) from the expression

$$\varphi_{\Pi} = \frac{i}{4}\int\limits_S H_0^{(2)}(kr)\frac{\partial\varphi}{\partial n}\,ds - \frac{i}{4}\int\limits_S \varphi\frac{\partial}{\partial n}H_0^{(2)}(kr)\,ds. \quad (1)$$

Here $\varphi_{\Pi}$ is the potential of the unknown field at the point Π, $\varphi$ the potential on the surface of the cylinder, n the normal to the cylinder surface, ds an element of the arc, S the arc formed by the segment of the cylinder, r the distance from the surface element of the cylinder to the point Π in which the potential is determined (see Fig. 1), $k = \frac{\omega}{c}$ the wave number, and $H_0^{(2)}(kr)$ the Hankel function of second kind and zero order.

Let the distribution of the potential $\varphi$ over the surface of a cylindrical segment be $\varphi = \Phi(\alpha)\ \varphi_0$, where $\alpha$ is the central angle. For simplicity let us assume that $\Phi(\alpha)$ is a function that is symmetrical about $\alpha = 0$, and that $\Phi(0) = 1$. To determine the sound pressure $p_f$ on the axis of the cylinder, where $r = \text{const} = f$ (focal distance), under the condition $f \gg \lambda$, we employ the well-known relationships from the theory of cylindrical functions

$$\frac{\partial}{\partial x} H_0^{(2)}(x) = -H_1^{(2)}(x),$$

$$\underset{x\to\infty}{H_0^{(2)}(x)} = \underset{x\to\infty}{H_1^{(2)}(x)} \to \left(\frac{2}{\pi x}\right)^{1/2} e^{-i\left(x+\frac{\pi}{4}\right)},$$

and also the expressions $P = \rho \dfrac{\partial \varphi_n}{\partial t}$ and $v = -\dfrac{\partial \varphi_n}{\partial r}$, where $\underline{v}$ is the oscillatory velocity and $\rho$ the density of the medium.

After making some substitutions and simple transformations, we obtain an expression for $p_f$ with an accuracy to within a phase vector:

$$p_f = p_0\left(\frac{2}{\pi} kf\right)^{1/2} \int_0^{\alpha_m} \Phi(\alpha)\, d(\alpha), \tag{2}$$

where $p_0$ is the pressure on the surface of the cylinder at the point $\alpha = 0$ and $\alpha_m$ is the aperture angle of the cylindrical segment.

In an exactly analogous manner we obtain an expression for the velocity at a point on the cylinder axis $v_f$:

$$v_f = v_0\left(\frac{2}{\pi} kf\right)^{1/2} \int_0^{\alpha_m} \Phi(\alpha) \cos\alpha\, d\alpha. \tag{3}$$

Expressions (2) and (3) are very similar in structure to the corresponding expressions for the ordinary axially-symmetrical focusing systems [4]:

$$p_f = p_0 kf \int_0^{\alpha_m} \Phi(\alpha) \sin\alpha\, d\alpha,$$

$$v_f = v_0 kf \int_0^{\alpha_m} \Phi(\alpha) \cos\alpha \sin\alpha\, d\alpha.$$

The basic difference lies in the fact that the focusing effect by cylindrical systems is less dependent on kf. The absence of a term $\sin\alpha$ under the integral sign in expressions (2) and (3) is explained by the fact that the cylindrical-surface element, on which the integration is carried out, equals $f d\alpha$ (per unit length of cylinder), while an element of a spherical surface is

$$f^2 \sin\alpha\, d\alpha.$$

Using the same procedure as for axially-symmetrical systems [5], let us find the optimum distribution functions $\Phi(\alpha)$, i.e., the functions for which the pressure and velocity on the axis of the system will be a maximum at a given energy flux of a converging wave front, equal (per unit length) to

$$W = \frac{p_0^2}{z} 2f \int_0^{\alpha_m} \Phi^2(\alpha)\, d\alpha, \tag{4}$$

where $z$ is the wave impedance of the medium.

Solving the variational problem for the conditional extremum by usual methods, we obtain the optimum pressure distribution in the form

$$\Phi(\alpha) = 1 \tag{5}$$

and for the velocity distribution

$$\Phi(\alpha) = \cos\alpha \tag{5a}$$

It is interesting to note that exactly the same functions were obtained as for the axially-symmetrical systems [5].

Let us now determine the pressure gain that can be obtained from a system with an optimum distribution function. From expressions (2) and (5) we get

$$p_f = p_0 \left(\frac{2}{\pi} kf\right)^{1/2} \alpha_m,$$

from which the pressure coefficient of amplification, defined as $K_p = \frac{p_f}{p_0}$, will be

$$K_p = \left(\frac{2}{\pi} kf\right)^{1/2} \alpha_m. \tag{6}$$

It is somewhat more convenient for further calculations to transform the last equation. We see from Fig. 1 that $S = 2f\alpha_m$, hence $f = \frac{S}{2\alpha_m}$. Substituting this expression into (6) we get

$$K_p = \left(\frac{kS}{\pi}\right)^{1/2} \alpha_m^{1/2}. \tag{6a}$$

Equation (6a) shows the dependence of $K_p$ on the aperture angle for constant value of $S$, corresponding to a constant energy flux in the wave front. If we put $\alpha_m = \pi$, we obtain for the maximum possible amplification coefficient

$$K_{p\,\max} = (kS)^{1/2}. \tag{6b}$$

Let us now introduce the concept of the pressure-focusing factor, considered as a ratio of the actual gain introduced by a given system to the maximum value that can be obtained by using the available energy flux (per unit of actual length of the front), as determined by the value of S:

$$\varkappa = \frac{K_p}{K_{p\,\max}}. \tag{7}$$

For our distribution we obtain from equations (7), (6b), and (6)

$$\varkappa = \left(\frac{\alpha_m}{\pi}\right)^{1/2}. \tag{8}$$

In an exactly analogous manner we obtain from expressions (3) and (5a) for the velocity

$$K_v = \left(\frac{2}{\pi} kf\right)^{1/2} \sin \alpha_m, \tag{9}$$

and from expressions (9) and (6a)

$$\varkappa' = \frac{K_v}{K_{p\,\max}} = \frac{\sin \alpha_m}{(\pi \alpha_m)^{1/2}}. \tag{10}$$

Relationships (6) and (9) are shown in Fig. 2, and (8) and (10) are shown in Fig. 3 (curves 1).

Let us note that expression (6) can also be rewritten as

$$K_p = \left(\frac{S}{\lambda f}\right)^{1/2}. \tag{6c}$$

In this form, it is fully analogous to the generalized well-known Rayleigh expression, derived by us in [7], for the amplification obtained by an axially-symmetrical focusing system

$$K_p = \frac{F}{\lambda f},$$

where F is the surface of the converging wavefront. For the case of cylindrical systems having not too large an aperture angle ($\sin \alpha_m \approx \alpha_m$) we can give a full analogue of the Rayleigh expression in its classical form

$$K_p = K_v = \frac{L}{(\lambda f)^{1/2}}, \tag{6d}$$

where L is the chord joining the arc of the radiating surface.

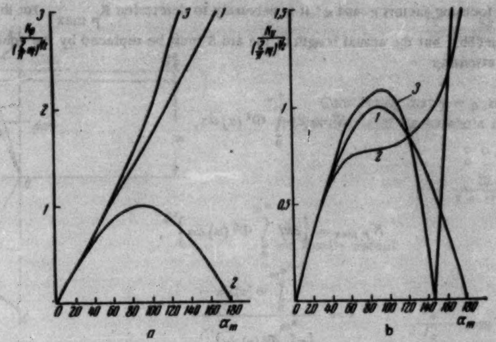

Fig. 2. a) $K_p$ vs. $\alpha_m$: 1) $\Phi(\alpha) = 1$; 2) $\Phi(\alpha) = \cos\alpha$; 3) $\Phi(\alpha) = \cos^{-1}\frac{\alpha}{2}$.

b) $K_v$ vs. $\alpha_m$: 1) $\Phi(\alpha) = 1$; 2) $\Phi(\alpha) = \cos\alpha$; 3) $\Phi(\alpha) = \cos^{-1}\frac{\alpha}{2}$.

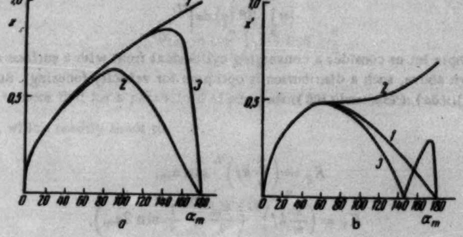

Fig. 3. a) $\varkappa$ vs. $\alpha_m$: 1) $\Phi(\alpha) = 1$; 2) $\Phi(\alpha) = \cos\alpha$; 3) $\Phi(\alpha) = \cos^{-1}\frac{\alpha}{2}$.

b) $\varkappa'$ vs. $\alpha_m$: 1) $\Phi(\alpha) = 1$; 2) $\Phi(\alpha) = \cos\alpha$; 3) $\Phi(\alpha) = \cos^{-1}\frac{\alpha}{2}$.

**Let us now proceed to analyze the inhomogeneous distribution of the amplitude over the surface of the converging wavefront. The pressure amplification coefficients and the velocity amplification coefficients are obtained directly from expressions (2) and (3):**

$$K_p = \left(\frac{2}{\pi}kf\right)^{1/2}\int_0^{\alpha_m}\Phi(\alpha)\,d\alpha, \tag{2a}$$

$$K_v = \left(\frac{2}{\pi}kf\right)^{1/2}\int_0^{\alpha_m}\Phi(\alpha)\cos\alpha\,d\alpha. \tag{3a}$$

To determine the focusing factors $\kappa$ and $\kappa'$ it is necessary to determine $K_{p\,\max}$. For this purpose it is possible to use expression (6b), but the actual length of the arc S must be replaced by the equivalent value S', determined from the relationship

$$S' = 2f\int\limits_0^{\alpha_m}\Phi^2(\alpha)\,d\alpha,$$

hence

$$K_{p\,\max} = \left[2kf\int\limits_0^{\alpha_m}\Phi^2(\alpha)\,d\alpha\right]^{1/2}, \tag{6c}$$

$$\kappa = \frac{\int\limits_0^{\alpha_m}\Phi(\alpha)\,d\alpha}{\left[\pi\int\limits_0^{\alpha_m}\Phi^2(\alpha)\,d\alpha\right]^{1/2}} \tag{7a}$$

and

$$\kappa' = \frac{\int\limits_0^{\alpha_m}\Phi(\alpha)\cos\alpha\,d\alpha}{\left[\pi\int\limits_0^{\alpha_m}\Phi^2(\alpha)\,d\alpha\right]^{1/2}}. \tag{10a}$$

By way of an example let us consider a converging cylindrical front with a surface amplitude distribution $\Phi(\alpha) = \cos\alpha$. As shown above, such a distribution is optimum for velocity focusing. Substituting this distribution into expressions (2a), (3a), (7a), and (10a), we get

$$K_p = \left(\frac{2}{\pi}kf\right)^{1/2}\sin\alpha_m, \tag{2b}$$

$$K_v = \left(\frac{2}{\pi}kf\right)^{1/2}\left(\frac{\alpha_m}{2} + \frac{1}{4}\sin 2\alpha_m\right), \tag{3b}$$

$$\kappa = \frac{\sin\alpha_m}{\left[\pi\left(\frac{\alpha_m}{2} + \frac{1}{4}\sin 2\alpha_m\right)\right]^{1/2}}, \tag{7b}$$

$$\kappa' = \left[\frac{\frac{\alpha_m}{2} + \frac{1}{4}\sin 2\alpha_m}{\pi}\right]^{1/2}. \tag{10b}$$

These dependences are shown in Figs. 2 and 3 (curve 2). As expected, the curves for $K_p$ and $\kappa$ increase monotonically, while the quantities $K_v$ and $\kappa'$, after passing through a maximum, drop to zero.

Another example of a converging cylindrical front with inhomogeneous distribution of amplitude is a front produced by a bent mirror, in the form of a parabolic cylinder. To obtain the amplification of such a mirror let us first find the distribution function. Assume a plane sound wave propagating along the axis of mirror ABC and striking it. Let us isolate a section of width dy on the plane front of the incident wave (see Fig. 4). Then the energy flux per unit length of cylinder will be $I_0 dy$, where $I_0$ is the intensity of the incident wave. On the other hand, the same energy flux passes through the section $f d\alpha$ of the circular cylinder of radius f, where f is the focal distance. Denoting by $I_\alpha$ the intensity in the converging wave, we obtain $I_0 d\alpha = I_\alpha f d\alpha$, hence

$$\frac{I_\alpha}{I_0} = \frac{dy}{f d\alpha}.$$

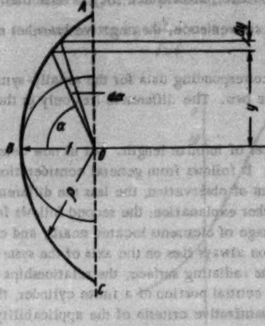

Fig. 4

Considering that $y = \rho \sin \alpha$, and the equation of the generatrix of the parabola is

$$\rho = \frac{2f}{1 + \cos \alpha},$$

we finally obtain

$$\frac{I_\alpha}{I_0} = \cos^{-2} \frac{\alpha}{2}.$$

Since we are not interested in the ratio of the intensities, but in the ratio of the amplitudes, we can assume, recalling that $f >> \lambda$,

$$\Phi_{(\alpha)} = \left(\frac{I_\alpha}{I_0}\right)^{1/2} = \cos^{-1} \frac{\alpha}{2}, \qquad (11)$$

It is interesting to note that for a paraboloid of revolution the distribution function is of the form [2]: $\Phi(\alpha) = \frac{2}{1 + \cos \alpha}$, which readily leads to

$$\Phi_{(\alpha)} = \cos^{-2} \frac{\alpha}{2}.$$

Substituting equation (11) into the general expressions (2a), (3a), (7a), and (10a), and performing the necessary calculations, we get

$$K_p = 2\left(\frac{2}{\pi} kf\right)^{1/2} \ln \frac{1 + \sin \frac{\alpha_m}{2}}{\cos \frac{\alpha_m}{2}}, \qquad (2c)$$

$$K_v = \left(\frac{2}{\pi} kf\right)^{1/2} \left(2 \sin \frac{\alpha_m}{2} - \ln \frac{1 + \sin \frac{\alpha_m}{2}}{\cos \frac{\alpha_m}{2}}\right), \qquad (3c)$$

$$\varkappa = \left(\frac{2}{\pi}\right)^{1/2} \ln \frac{1 + \sin \frac{\alpha_m}{2}}{\cos \frac{\alpha_m}{2}} \cot^{1/2} \frac{\alpha_m}{2}, \qquad (7c)$$

$$\varkappa' = \left(\frac{2}{\pi}\right)^{1/2} \left(2 \sin \frac{\alpha_m}{2} - \ln \frac{1 + \sin \frac{\alpha_m}{2}}{\cos \frac{\alpha_m}{2}}\right) \cot^{1/2} \frac{\alpha_m}{2}. \qquad (10c)$$

The corresponding curves are shown on the same figures (curves 3). Similarly, as for the axially-symmetric paraboloids, the values of $K_v$ and $\kappa'$ pass through zero, but at $\alpha_m = 146°$, after which they reverse their sign; the explanation for this phenomenon is given in Reference [2]. For convenience, the negative branches of the curves are shown in Figs. 2b and 3b in the positive quadrant.

Comparison of the variations shown in Figs. 2 and 3 and the corresponding data for the axially-symmetrical radiators discloses a considerable qualitative agreement between the two. The difference lies only in the quantitative relationships.

The variations obtained above are valid for cylindrical surfaces of infinite length. Let us now determine to what extent they can be applied to real systems, of finite length. It follows from general considerations that the longer a system of finite length is and the closer it is to the point of observation, the less the difference between it and an infinite system. The first condition requires no further explanation; the second follows from the fact that the closer the point of observation, the greater the percentage of elements located nearby and consequently the lesser the role of the ends. Since the point of observation always lies on the axis of the system in the cases considered above, i.e., it is always at a distance f from the radiating surface, the relationships obtained above for an infinite cylinder will be approximately correct for the central portion of a finite cylinder, the length of which is large compared with the focal distance. To establish quantitative criteria of the applicability of the results obtained would require calculation of the field of a finite cylinder, generally a rather complicated and cumbersome task. However, if we are only interested in the field on the axis, we can obtain the desired estimate in a relatively simple manner.*

It follows from the very fact that the converging cylindrical front is axially symmetrical that for a point located on the axis the ratio between the field of a finite and infinite cylindrical front will be the same as the ratio between the field of a finite linear in-phase source (of equal length) and an infinite one, located at a distance f from the reception point. The latter relationship can be readily obtained from the well-known equations, for example, for the diffraction by a slit of finite dimensions [6]. For the amplitude, the ratio is of the form

$$\beta = \frac{1}{\sqrt{2}} \{[C(v_2) - C(v_1)]^2 + [S(v_2) - S(v_1)]^2\}^{1/2}, \tag{12}$$

where $C(r) = \int^{u} \cos \frac{\pi v^2}{2}\, dv$ and $S(v) = \int_0^{u} \sin \frac{\pi v^2}{2}\, dv$ — are the Fresnel integrals.

$$v = \frac{y}{\sqrt{\frac{\lambda f}{2}}}, \tag{13}$$

and $y_1$ and $y_2$ are the distances from the projection of the reception point on the source (or on its continuation) to the ends of the source. For a semi-infinite source $y_2 = \infty$ and consequently $v_2 = \infty$. Since $C(\infty) = S(\infty) = {}^1/_2$, we have

$$\beta = \frac{1}{\sqrt{2}} \{[0.5 - C(v_1)]^2 + [0.5 - S(v_1)]^2\}^{1/2}. \tag{12a}$$

The latter relationship is shown in Fig. 5; the abscissa indicates instead of the variable v the quantity

$$v\sqrt{2} = \frac{y}{\sqrt{\lambda f}}.$$

---

* The author takes this opportunity to thank M. I. Isakovich for pointing out this possibility.

Since $\sqrt{\lambda f}$ is the radius of the first Fresnel zone, the argument of Fig. 5 represents the distance between the projection of the point of observation and the end of the source, expressed in Fresnel-zone values. From the plot it is evident that at $\frac{y}{\sqrt{\lambda f}} \geq 1$, we have $0.9 \leq \beta \leq 1.1$, and at $\frac{y}{\sqrt{\lambda f}} \geq 2.7$, we have $0.95 \leq \beta \leq 1.05$.

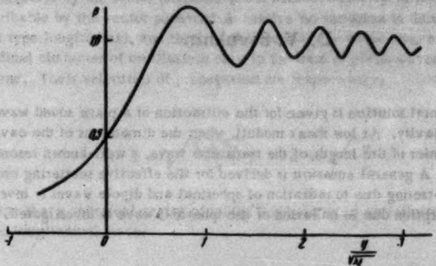

Fig. 5

Since an error of 10% is permissible in most engineering calculations, it follows from Fig. 5 that the relationships obtained for the infinite cylindrical front can be employed for a front of finite length, except for its edge sections, the dimensions of which equal the radius of the Fresnel zone. By way of an example let us take the radiator described in [1], which comprises a cylindrical segment L = 150 mm long with a 60 mm chord. Since the aperture angle is approximately 60°, we have $f = 50$ mm. At an operating frequency of 700 kc the wavelength $\lambda$ in water is approximately 2.0 mm, and the radius of the first Fresnel zone is 10 mm.

The equations obtained by us are thus not suitable for the end portions measuring 10 mm on each side, and can be extended to a central portion 130 mm long, amounting to 87% of the total length of the radiator.

## LITERATURE CITED

[1] T. Kearney, "Uses of ultrasonics in degreasing processes," J. Acoust. Soc. Am. 26, 244-246 (1954).

[2] O. Mattiat, "Ultrasonincs in industry," Radio and T.V. News 50, 6, 5-8 (1953).

[3] Lamb, Hydrodynamics (Moscow-Leningrad) 19 Chapt. 9, (Russian translation).

[4] L. D. Rozenberg, Sound-Focusing Systems (Moscow-Leningrad, 1949).

[5] L. D. Rozenberg, "On the conditions for obtaining maximum concentration of ultrasound," Doklady Akad. Nauk SSSR 94, 845 (1954).

[6] P. Drude, Optics (Leningrad-Moscow, 1935). (Russian translation).

[7] L. D. Rozenberg, "On the concentration of ultrasound," Transactions of Commission on Acoustics 1955, No. 8, 102.

Acoustics Institute of the
USSR Academy of Sciences,
Moscow.

Received October 26, 1954.

# DIFFRACTION OF PLANE SOUND WAVES BY A SPHERICAL CAVITY

D. V. Sivukhin

**A general solution is given for the diffraction of a plane sound wave by a spherical cavity. At low shear moduli, when the dimensions of the cavity are of the order of the length of the transverse wave, a well-known resonance is observed. A general equation is derived for the effective scattering cross-section. Scattering due to radiation of spherical and dipole waves is investigated. Absorption due to radiation of the spherical wave is investigated.**

**1. Diffraction of a sound wave by a spherical cavity is of definite theoretical and practical interest owing to the resonance observed at low shear moduli, to the existence of which attention was called by M. A. Isakovich. We shall characterize the elastic properties of the medium by the Lamé constants $\lambda$ and $\mu$. The resonance is observable when the shear modulus is small compared with the modulus $\lambda$. The conditions for the resonance are that the wavelength of the incident longitudinal wave must be large compared with the dimensions of the cavity, and the length of the excited transverse wave must be of the order of the dimension of the cavity.**

**For monochromatic fields, the equations of the linear theory of elasticity can be written as**

$$\rho\omega^2 \mathbf{s} + \mu\Delta \mathbf{s} + (\lambda + \mu)\,\mathrm{grad\,div}\,\mathbf{s} = 0, \tag{1}$$

**where $\underline{s}$ is the vector displacement of a particle of the medium from its equilibrium position, $\omega$ the angular frequency of oscillations, and $\rho$ the density of the medium.**

**If the medium is absorbing, $\lambda$ and $\mu$ are complex, and generally speaking depend on the frequency $\omega$.**

**Let us put**

$$\mathbf{s} = \mathrm{grad}\,\varphi + \mathrm{rot}\,\mathbf{A}. \tag{2}$$

**The potentials $\varphi$ and A can always be chosen to satisfy the equations**

$$\rho\omega^2\varphi + (\lambda + 2\mu)\,\Delta\varphi = 0,$$

$$\rho\omega^2\mathbf{A} + \mu\Delta\mathbf{A} = 0.$$

**This theorem can be proven exactly in the same manner as an analogous theorem is proven in Reference [1]. We shall omit the proof. Let us introduce the wave numbers for the longitudinal and transverse waves:**

$$k^2 = \frac{\rho\omega^2}{\lambda + 2\mu}; \qquad q^2 = \frac{\rho\omega^2}{\mu}. \tag{3}$$

Then

$$\Delta\varphi = k^2\varphi = 0; \ \Delta \mathbf{A} + q^2\mathbf{A} = 0. \tag{4}$$

The waves describable by the scalar potential $\varphi$ are accompanied by variations in the density of the medium; waves describable by the vector potential **A** involve no variation in density. We shall call for brevity the waves of the first type longitudinal, and those of the second type transverse, although one can speak of a transverse or longitudinal character of oscillations only in the case of plane waves or in the case of spherical waves in the wave zone. Their velocities of propagation are respectively:

$$c = \sqrt{\frac{\lambda + 2\mu}{\rho}}; \quad c' = \sqrt{\frac{\mu}{\rho}}. \tag{5}$$

2. Let us assume that a spherical cavity of radius R is located in an infinite elastic medium, and that a plane monochromatic longitudinal wave;

$$\varphi^\circ = \exp\{i(\omega t - kz)\}, \tag{6}$$

propagates along the Z axis and strikes the cavity. We wish to determine the sound field in the medium.

A unique solution to this problem is obtained from equations (4) and from its boundary conditions. Since the cavity is hollow, the boundary conditions require that the tangential and normal stresses due to the sound vibrations vanish on the boundary of the cavity, and that the radiation condition is satisfied at infinity, which calls for the supplementary sound field that is superimposed on the incident wave to consist of only outgoing waves. The solution obtained is approximately valid when the cavity is filled with air, for the elasticity of air is small compared with the elasticity of all known solid and liquid media, and therefore one can neglect the variations in air pressure inside the cavity, produced by its deformation, as negligible compared with the variations of the elastic stresses in the surrounding medium.

3. Let us locate the origin of coordinates in the center of the cavity and let us introduce the spherical coordinate system r, $\vartheta$, $\alpha$, with the polar axis Z directed along the direction of propagation of the incident wave. By virtue of the axial symmetry, the displacement vector **s**, and also the stress tensor $T_{ij}$, must be independent of the azimuth angle $\alpha$. The normal and tangential stresses

$$\left.\begin{aligned} T_{rr} &= \lambda \operatorname{div} \mathbf{s} + 2\mu \frac{\partial s_r}{\partial r}, \\ T_{r\vartheta} = T_{\vartheta r} &= \mu \left( \frac{\partial s_\vartheta}{\partial r} + \frac{1}{r} \frac{\partial s_r}{\partial \vartheta} - \frac{s_\vartheta}{r} \right) \end{aligned}\right\} \tag{7}$$

should vanish at the boundaries of the cavity.

The vector potential **A** can be so chosen as to have in this coordinate system only one non-vanishing component, namely $A_\alpha$. Actually, the displacement vector **s**, and consequently also curl **A**, are polar vectors. This means that the vector **A** should be axial. The only vectors of which it can be comprised are the radius vector **r** and the wave vector **k** of the incident wave. The same polar vectors can make up only axial vectors that are collinear with the vector product **k** x **r**, i.e., vectors that are tangent to the parallel lines **r** = const., $\vartheta$ = const.

That this statement is true can be verified also from the expressions

$$s_r = \frac{\partial \varphi}{\partial r} + \frac{1}{r \sin\vartheta}\frac{\partial}{\partial\vartheta}(\sin\vartheta A_\alpha)$$

$$s_\vartheta = \frac{1}{r}\frac{\partial\varphi}{\partial\vartheta} - \frac{1}{r}\frac{\partial(rA_\alpha)}{\partial r}, \tag{8}$$

which do not contain the components $A_r$ and $A_\vartheta$. Hereinafter the only component $A_\alpha$ of the vector **A** shall be merely denoted by A: $A_\alpha \equiv A$.

Inserting (8) and (7) we get

$$T_{rr} = -\lambda k^2\varphi + 2\mu\left[\frac{\partial^2\varphi}{\partial r^2} + \frac{\partial}{\partial r}\left(\frac{1}{r}\frac{\partial A}{\partial\vartheta} + \cot\frac{\vartheta A}{r}\right)\right.,$$

$$T_{r\vartheta} = \mu\left[2\frac{\partial}{\partial r}\left(\frac{1}{r}\frac{\partial\varphi}{\partial\vartheta}\right) - \frac{\partial^2 A}{\partial r^2} + \right.$$

$$\left. + \frac{1}{r^2}\left(\frac{\partial^2 A}{\partial\vartheta^2} + \cot\vartheta\frac{\partial A}{\partial\vartheta}\right) + \left(2 - \frac{1}{\sin^2\vartheta}\right)\frac{A}{r^2}\right]. \tag{9}$$

4. Let us expand the incident wave (6) into a series of Legendre polynominals:

$$\varphi^0 = \exp\{-ikr\cos\vartheta\} = \sum_{m=0}^{\infty}(-i)^m(2m+1)\,j_m(kr)\,P_m(\cos\vartheta) \tag{10}$$

(the time factor $e^{i\omega t}$ will be omitted hereinafter). Here $j_m$ is the spherical Bessel function of the m-th order:

$$j_m(x) = (-1)^m x^m \frac{d^m}{(x\,dx)^m}\frac{\sin x}{x}. \tag{11}$$

We shall find useful also the spherical Neumann function

$$n_m(x) = (-1)^{m+1} x^m \frac{d^m}{(x\,dx)^m}\frac{\cos x}{x}, \tag{12}$$

and also the spherical Hankel function of the first and second kind

$$h_m^{(1)}(x) = j_m(x) + in_m(x) = i(-1)^{m+1}x^m\frac{d^m}{(x\,dx)^m}\frac{e^{ix}}{x}, \tag{13}$$

$$h_m^{(2)}(x) = j_m(x) - in_m(x) = i(-1)^m x^m\frac{d^m}{(x\,dx)^m}\frac{e^{-ix}}{x}. \tag{14}$$

The spherical Bessel and Neumann functions have been tabulated relatively recently in Reference [2] for real values of x.

We shall seek the potential $\varphi$ in the form

$$\varphi = \varphi^{\circ} + \Phi(r, \vartheta). \tag{15}$$

**The function $\Phi$ evidently satisfies equation ( 4 ) and therefore a general expression for $\Phi$, satisfying the radiation condition, must be of the form**

$$\Phi = \sum_{m=0}^{\infty} (-1)^m b_m (2m+1) h_m^{(2)}(kr) P_m(\cos\vartheta), \tag{16}$$

**where $b_m$ are constants.**

**To determine A let us note that the vector $\mathbf{A}$, and with it any of its Cartesian components, say $A_x$ satisfies the wave equation**

$$\Delta A_x + q^2 A_x = 0.$$

**$A_x$ should therefore be of a form analogous to (16), except that the Legendre polynomials will be replaced by some other spherical functions $Y_m(\vartheta, \alpha)$. To establish the form of these functions, let us note that $A_x = -A \sin\alpha$, where A can depend only on r and $\vartheta$, but not on $\alpha$. Consequently, the spherical function $Y_m(\vartheta, \alpha)$ should consist of two factors, one being $\sin\alpha$, and the second depending only on $\vartheta$. The general form of such functions, as is known, is:**

$$Y_m(\vartheta, \alpha) = P_{m,1}(\cos\vartheta)\sin\alpha,$$

**where $P_{m,1}(\cos\vartheta)$ is the associated Legendre polynomial:**

$$P_{m,1}(\cos\vartheta) = \sin\vartheta \frac{dP_m(\cos\vartheta)}{d(\cos\vartheta)}.$$

**Thus,**

$$A = \sum_{m=1}^{\infty} (-i)^m a_m (2m+1) h_m^{(2)}(qr) P_{m,1}(\cos\vartheta). \tag{17}$$

**The coefficients $a_m$ and $b_m$ are determined from the condition that the stresses $T_{rr}$ and $T_{r\vartheta}$ vanish at $r = R$.**

**Long and laborious calculations result in the following:**

$$b_0 = -\frac{j_0(kR) + 2\gamma^2\left[j_0(kR) - 2\frac{j_1(kR)}{kR}\right]}{h_0^{(2)}(kR) + 2\gamma^2\left[h_0^{(2)}(kR) - 2\frac{h_1^{(2)}(kR)}{kR}\right]}, \tag{18}$$

$$b_m = -\frac{\Delta'_m}{\Delta_m}, \quad a_m = -\frac{\Delta''_m}{\Delta_m}, \tag{19}$$

**where**

$$\gamma = +\sqrt{\frac{\mu}{\gamma}}, \tag{20}$$

$$\begin{aligned}\Delta_m = &\left\{1 + 2\gamma^2\left[1 - \frac{(m+2)(2m+1)}{k^2R^2}\right]\right\} h_m^{(2)}(kR)\, h_m^{(2)}(qR) + \\ &+ \frac{2\gamma}{kR\sqrt{1+2\gamma^2}}\left\{1 + 2\gamma^2\left[1 + \frac{(m^2-1)(m+2)}{k^2R^2}\right]\right\} h_m^{(2)}(kR)\, h_{m-1}^{(2)}(qR) + \\ &+ \frac{4\gamma^2}{kR}\left[1 + \gamma^2\frac{(m-1)m(m+2)}{k^2R^2(1+2\gamma^2)}\right] h_{m-1}^{(2)}(kR)\, h_m^{(2)}(qR) + \\ &+ \frac{4\gamma^3}{k^2R^2\sqrt{1+2\gamma^2}}\left[2 - m(m+1)\right] h_{m-1}^{(2)}(kR)\, h_{m-1}^{(2)}(qR),\end{aligned} \tag{21}$$

$$\begin{aligned}\Delta'_m = &\left\{1 + 2\gamma^2\left[1 - \frac{(m+2)(2m+1)}{k^2R^2}\right]\right\} j_m(kR)\, h_m^{(2)}(qR) + \\ &+ \frac{2\gamma}{kR\sqrt{1+2\gamma^2}}\left\{1 + 2\gamma^2\left[1 + \frac{(m^2-1)(m+2)}{k^2R^2}\right]\right\} j_m(kR)\, h_{m-1}^{(2)}(qR) + \\ &+ \frac{4\gamma^2}{kR}\left[1 + \gamma^2\frac{(m-1)m(m+2)}{k^2R^2(1+2\gamma^2)}\right] j_{m-1}(kR)\, h_m^{(2)}(qR) + \\ &+ \frac{4\gamma^3}{k^2R^2\sqrt{1+2\gamma^2}}\left[2 - m(m+1)\right] j_{m-1}(kR)\, h_{m-1}^{(2)}(qR),\end{aligned} \tag{22}$$

$$\Delta''_m = \frac{2i}{k^2R^2}\,\frac{\gamma^2}{1+2\gamma^2}\left[1 + 2\gamma^2\left(1 - \frac{(m-1)(m+2)}{k^2R^2}\right)\right]. \tag{23}$$

**At x >> 1, it is possible to employ the asymptotic equation:**

$$h_m^{(2)}(x) = \frac{i^{m+1}}{x}\, e^{-ix}\left[1 + 0\left(\frac{1}{x}\right)\right]. \tag{24}$$

**We therefore have in the wave zone (kr >> 1, qr >> 1)**

$$\Phi = \frac{ie^{-ikr}}{kr}\sum_{m=0}^{\infty}(2m+1)\, b_m P_m(\cos\vartheta), \tag{25}$$

$$A = i\,\frac{e^{-iqr}}{qr}\sum_{m=1}^{\infty}(2m+1)\, a_m P_{m,1}(\cos\vartheta). \tag{26}$$

**The field radiated by the cavity is thus superimposed on the incident wave. The cavity field consists of longitudinal and transverse waves. The waves radiated comprise spherical (m = 0), dipole (m = 1), quadrupole (m = 2) and other multiple waves. The radiated transverse waves do not contain a spherical component. At $\mu = 0$ only longitudinal waves are radiated. In this case**

$$b_m = -\frac{j_m(kR)}{h_m^{(2)}(kR)}, \quad a_m = 0. \tag{27}$$

**In the wave zone, the amplitudes of potentials $\Phi$ and A of all the waves; and also the corresponding displacements and velocities, diminish in inverse proportion to the first power of the distance.**

**5. Let us first assume no absorption ($\lambda$ and $\mu$ real). Let us calculate the average energy scattered by the cavity per second. In the absence of absorption, this energy is evidently equal to the average energy flux through an infinitely-remote sphere surrounding the cavity**

$$\frac{d\overline{W}}{dt} = \oint \overline{S}_r \, df, \tag{28}$$

where $\overline{\mathbf{S}}$ is the vector of the average energy flux density. The linear theory of elasticity yields an expression for $\mathbf{S}$

$$S_r = -T_{ri} v_i = -T_{rr} v_r - T_{r\vartheta} v_\vartheta, \tag{29}$$

where $\mathbf{v}$ is the velocity of the particles of the medium. $T_{ij}$ and $\mathbf{v}$ of equations (28) and (29) represent not the complete stress tensor and velocity of the medium, but only those parts of these quantities related to the radiation from the cavity. In the absence of absorption, the average energy flux through any closed surface surrounding the cavity is zero. This flux consists of three components: the flux produced by the incident plane wave, the radiation-energy flux of the wave, and the mutual flux, produced by their superposition. The first component, averaged over the time, vanishes identically. Equation (28) gives only the third component. Neglecting in (29) the terms of the third and higher powers in $1/r$, we get

$$T_{rr} = \lambda \operatorname{div} \mathbf{s} + 2\mu \frac{\partial s_r}{\partial r} = \lambda \Delta \Phi + 2\mu \frac{\partial^2 \Phi}{\partial r^2},$$

where every small section of the wave radiated by the cavity in the wave zone can be considered as plane and it is therefore possible to write

$$\frac{\partial^2 \Phi}{\partial r^2} = \Delta \Phi = -k^2 \Phi.$$

This yields

$$T_{rr} = -(\lambda + 2\mu) k^2 \Phi = -\rho \omega^2 \Phi.$$

Using the same approximation

$$s_\vartheta = -\frac{\partial A}{\partial r};$$

$$T_{r\vartheta} = \mu \frac{\partial s_\vartheta}{\partial r} = -\mu \frac{\partial^2 A}{\partial r^2} = -\mu \Delta A = \mu q^2 A = \rho \omega^2 A.$$

It is assumed that the calculations are performed in the real form rather than the complex one. To transfer to the complex notation, it is necessary to make the substitution

$$T_{ij} \to \frac{1}{2}(T_{ij} + T_{ij}^*); \quad s_i \to \frac{1}{2}(s_i + s_i^*), \text{ etc.}$$

This yields

$$\frac{d\overline{W}}{dt} = -\frac{1}{4} \oint T_{ri} v_i^* \, df + \text{complex conjugate} =$$

$$= -i \frac{\rho \omega^3}{4} \oint \left( \Phi \frac{\partial \Phi^*}{\partial r} + A \frac{\partial A^*}{\partial r} \right) df + \text{complex conjugate} =$$

$$= \frac{\rho \omega^3}{2} \oint (k \Phi \Phi^* + q A A^*) \, df.$$

Substituting here the equations (25) and (26), and using the orthogonality of the Legendre polynomials, we get

$$\frac{d\overline{W}}{dt} = 2\pi\rho\omega^3\left\{\frac{1}{k}\sum_{m=0}^{\infty}(2m+1)\,|\,b_m\,|^2 + \right.$$

$$\left. + \frac{1}{q}\sum_{m=1}^{\infty} m\,(m+1)\,(2m+1)\,|\,a_m\,|^2\right\}. \tag{30}$$

To characterize the scattering ability of the sphere, let us introduce the effective scattering cross-section $\sigma_s$. This is the ratio of the average energy scattered per unit time to the average energy flux density of the incident wave. The latter is $\frac{1}{2}\,\rho\,\omega^3 k$, and therefore

$$\frac{\sigma_s}{\pi R^2} = \frac{4}{k^2 R^2}\left\{\sum_{m=0}^{\infty}(2m+1)\,|\,b_m\,|^2 + \frac{k}{q}\sum_{m=1}^{\infty} m\,(m+1)\,(2m+1)\,|\,a_m\,|^2\right\}. \tag{31}$$

6. Since equation (31) is complicated, we shall restrict the detailed analysis only to the scattering due to radiation of spherical and dipole waves. Let us consider first the scattering cross-section $\sigma_s^0$ due to radiation from a spherical wave. Transforming to elementary functions, we get

$$\frac{\sigma_s^0}{\pi R^2} = 4\left(\frac{\sin kR}{kR}\right)^2 \frac{\left\{1 + 2\gamma^2\left[1 + 2\,\frac{kR\cot kR - 1}{k^2 R^2}\right]\right\}^2}{\left[1 + 2\gamma^2\left(1 - \frac{2}{k^2 R^2}\right)\right]^2 + \frac{16\gamma^4}{k^2 R^2}}. \tag{32}$$

In particular, if $\gamma = 0$ (i.e., if $\mu = 0$) we have

$$\frac{\sigma_s^0}{\pi R^2} = 4\left(\frac{\sin kR}{kR}\right)^2. \tag{33}$$

Of particular interest is the case of small but non-vanishing values of $\gamma$ ($\mu << \lambda$). Then the spherical oscillations of the cavity and the corresponding radiation of spherical waves are particularly intense in the vicinity of those values of kR, at which the first term in the denominator of (32) vanishes. We deal here with the resonance phenomenon. Setting the first term in the denominator of (32) equal to zero, we find an approximate equation for the position of the maximum:

$$kR = \frac{2\gamma}{\sqrt{1 + 2\gamma^2}}. \tag{34}$$

Bearing in mind that

$$k = \frac{q\gamma}{\sqrt{1 + 2\gamma^2}}, \tag{35}$$

we can write equation (34) as

$$qR = 2. \tag{36}$$

It is seen from this that resonance occurs in the region of such frequencies, at which the length of the transverse sound waves is of the order of the size of the cavity.

If $\gamma^2 << 1$, we can use instead of (32) the approximate equation

$$\frac{\sigma_s^0}{\pi R^2} = 4\left(\frac{\sin kR}{kR}\right)^2 \frac{\left(1+\frac{2}{3}\gamma^2\right)^2}{\left[1+2\gamma^2\left(1-\frac{2}{k^2R^2}\right)\right]^2+\frac{16\gamma^4}{k^6R^6}}. \tag{37}$$

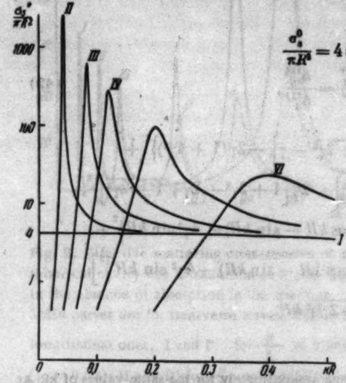

Fig. 1. Effective scattering cross section of a spherical cavity caused by radiation of spherical waves, in the absence of absorption in the medium.

*I* - for $\mu=0$ $(\gamma=0)$; *II* - for $\frac{\mu}{\lambda}=0.0004$ $(\gamma=0.02)$; *III* - for $\frac{\mu}{\lambda}=0.0016$ $(\gamma=0.04)$; *IV* - for $\frac{\mu}{\lambda}=0.0036$ $(\gamma=0.06)$; *V* - for $\frac{\mu}{\lambda}=0.01$ $(\gamma=0.1)$; *VI* - for $\frac{\mu}{\lambda}=0.04$ $(\gamma=0.2)$

This is obtained from (32) by expanding cot kR into a series and terminating the expansion with the third-power term. If $kR >> 2\gamma$, i.e., is considerably to the left of the resonance region, this equation becomes

$$\frac{\sigma_s^0}{\pi R^2} = \frac{\left(1+\frac{2}{3}\gamma^2\right)^2}{4\gamma^4} k^4R^4. \tag{38}$$

In this region the scattering cross-section is proportional to the fourth power of the frequency.

The scattering cross-section has a maximum at approximately $kR = 2\gamma$ with a value

$$\left(\frac{\sigma_s^0}{\pi R^2}\right)_{\max} = \frac{1}{\gamma^2} = \frac{\lambda}{\mu}. \tag{39}$$

The half-width of the resonance curve when plotted on the kR scale is given by the approximate equation

$$\delta(kR) = \frac{4\gamma^2}{1+2\gamma^2} = 4\gamma^2. \tag{40}$$

Figure 1 shows a logarithmic plot of the resonance curves, calculated with equation (37) for five values of $\gamma$. At small values of $\gamma$ the resonance is very sharp. The limiting transition from equation (32) to (33) as $\gamma$ approaches zero is interesting. If $\gamma$ is exactly equal to zero, there is naturally no resonance. But if $\gamma \neq 0$, resonance appears and becomes sharper with decreasing values of $\gamma$. As $\gamma$ approaches zero the resonance curve becomes the ordinate axis for $kR = 0$ and becomes curve (33) for $kR \neq 0$. Naturally, to be able to detect the resonance at very small values of $\gamma$, the incident sound wave must be highly monochromatic. The time constant $\tau$ of the oscillations is related to the half-width $\delta\omega$ of the resonant curve by the usual equation: $\tau\,\delta\omega \approx 1$. From (40) we have

$$\tau \approx \frac{R}{c}\,\frac{1}{4\gamma^2} = \frac{\tau_0}{4\gamma^2}, \tag{41}$$

where $\tau_0$ is the time it takes for the sound to cover the distance R. Incidentally, the above limiting transition is merely formal in nature, since the linear theory of elasticity, on which the solution of the problem is based, is not valid for very large oscillation amplitudes.

7. The scattering cross-section is divided by the dipole-wave radiation into two terms: $\sigma_{sk}^{(1)}$ is the scattering cross-section due to the radiation of the transverse wave, and $\sigma_{sq}^{(1)}$ is the cross-section due to the transverse waves. Here, too, it is desirable to express the spherical Bessel and Hankel functions in terms of the elementary functions. We obtain as a result

$$\frac{\sigma_{sk}^{(1)}}{\pi R^2} = \frac{\Delta_{sk}^{(1)}}{\Delta_s^{(1)}}; \qquad \frac{\sigma_{sq}^{(1)}}{\pi R^2} = \frac{\Delta_{sq}^{(1)}}{\Delta_s^{(1)}}, \tag{42}$$

where

$$\Delta_s^{(1)} = \left\{\left[1 + 2\gamma^2\left(1 - \frac{9}{k^2R^2}\right)\right]\left[k^2R^2\sqrt{1 + 2\gamma^2} - \gamma\right] - 2\gamma(1 + 4\gamma^2)\right\}^2 + $$

$$+ \gamma^2k^2R^2\left\{\left[1 + 2\gamma^2\left(1 - \frac{9}{k^2R^2}\right)\right]\left[\gamma + \sqrt{1 + 2\gamma^2}\right] + 2\gamma\left[1 + 2\gamma^2 + 2\gamma\sqrt{1 + 2\gamma^2}\right]\right\}^2,$$

$$\Delta_{sk}^{(1)} = \frac{12\gamma^2}{(kR)^3}\left[\left\{3\left[1 + 2\gamma^2\left(1 - \frac{3}{k^2R^2}\right)\right](kR\cos kR - \sin kR) - 4\gamma^2\sin kR\right\}^2 + \right.$$

$$\left. + (1 + 2\gamma^2)k^2R^2\left\{\left[1 + 2\gamma^2\left(1 - \frac{9}{k^2R^2}\right)\right](kR\cos kR - \sin kR) - 4\gamma^2\sin kR\right\}^2\right],$$

$$\Delta_{sq}^{(1)} = 384\left(\gamma\sqrt{1 + 2\gamma^2}\right)^3 kR.$$

At small values of $\gamma$ the quantities (42) reach their maxima approximately for the same values of kR, at which the term in the first brace in the expression for the denominator $\Delta_s^{(1)}$ vanishes. Setting this equal to zero, we obtain a quadratic equation in $(kR)^2$ with two positive roots. These correspond to two resonant maxima, the positions of which are determined with sufficient accuracy for small values of $\gamma$ by the following equations:

First maximum:

$$kR = \gamma\sqrt{6}\,(1 - 2\gamma). \tag{43}$$

Second maximum:

$$kR = \sqrt{3\gamma(1 + 4\gamma)}. \tag{44}$$

Incidentally, the first maximum is well pronounced only on the scattering curves of transverse waves; in the case of scattered longitudinal waves, its absolute and relative values are very small. The character of the resonance obtained by scattering of dipole waves can be judged from the curves of Figs. 2 and 3. The solid curves correspond to scattering of transverse waves, and the dotted ones to longitudinal waves.

8. At m ≥ 2, no simplification is gained by converting to elementary functions. It is better to use here the tables of the spherical Bessel functions directly. However, the calculations become too cumbersome. We shall omit the calculations, but merely remark the following. Comparison of the spherical and dipole waves show that at small values of kR the latter do not play an important role. This pertains even to a greater degree to quadrupole radiation and to higher multipole radiation. For small values of kR, which are of greater interest to us, all these radiations are not significant; the principal role is played by the spherical waves.

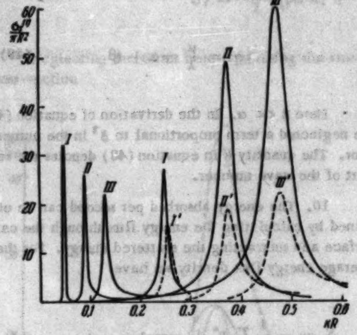

Fig. 2. Effective scattering cross-section of a spherical cavity due to radiation of dipole waves in the absence of absorption in the medium. Solid curves are for transverse waves, dotted for longitudinal ones. I and I' for $\frac{\mu}{\lambda} = 0.004$ ($\gamma = 0.02$); II and II' for $\frac{\mu}{\lambda} = 0.0016$ ($\gamma = 0.04$); III and III' for $\frac{\mu}{\lambda} = 0.0036$ ($\gamma = 0.06$).

9. Let us now proceed to investigate the case of complex $\lambda$ and $\mu$, i.e., when the medium in which the sound propagates is absorbing. In view of the complexity of the calculations, we shall restrict ourselves to investigation of the scattering and absorption of only spherical waves. The equations for the scattering and absorption of multipole radiation could be obtained with relative ease, but they cannot contribute much, since there are no tables of spherical Bessel functions for complex values of the argument. Our results consequently pertained to the region of relatively-low frequencies, for which the multipole radiation can be neglected.

The wave number is now complex:

$$k = k_1 - ik_2. \tag{45}$$

We shall restrict ourselves to the case $k_2 << k_1$. In this case it is reasonable to divide the energy radiated by the cavity into a scattered component and an absorbed component. In fact, near the cavity the field of the incident wave is small compared with the field of the radiated spherical wave. If we neglect this field, and if we also neglect the multipole radiation, the entire field reduces to a spherical wave:

$$\varphi = \frac{i}{kr} e^{-ikr} b_0 P_0(\cos\vartheta) = \frac{ib_0}{kr} e^{-ikr}. \tag{46}$$

Since $k_2 << k_1$, the field is very little attenuated by the exponential factor $e^{-k_2 r}$. In the zone where there are no waves this attenuation can be neglected. In this case the energy flux density reaching the wave zone is proportional to $1/r^2$, and the total flux is independent of r. This portion of the energy radiated by the cavity, i.e., that which reaches the wave zone, will be called the scattered energy. On the other hand, the energy which is lost in the zone where there are no waves, i.e., near the cavity, will be called absorbed. The potential here varies as $1/r$, the velocity and displacement vary as $1/r^2$, and the stress tensor varies as $1/r^3$. Consequently, the energy-flux density is proportional to $1/r^5$, and the total flux is proportional to $1/r^3$. Such a rapid decrease in the energy flux is due to the strong absorption of energy near the cavity; the absorbed energy is inversely proportional to the cube of the cavity radius.

As before, the scattering cross-section is given by the equation

$$\frac{\sigma_s^0}{\pi R^2} = \frac{4}{|kR|^2} |b_0|^2. \tag{47}$$

The complex nature of $\lambda$ and $\mu$ affect the value of $|b_0|$. If we perform the calculations with the same accuracy used in the derivation of equation (37), we get

$$\frac{\sigma_s^0}{\pi R^2} = \frac{4\left(1+\frac{2}{3}\alpha\right)^2\left(\frac{\sin kR}{kR}\right)}{\left[1+2\alpha\left(1-\frac{2}{k^2R^2}\right)+\frac{4\beta}{kR}\right]^2+4\left[\frac{2\alpha}{kR}-\beta+\frac{2\beta}{k^2R^2}\right]^2}, \tag{48}$$

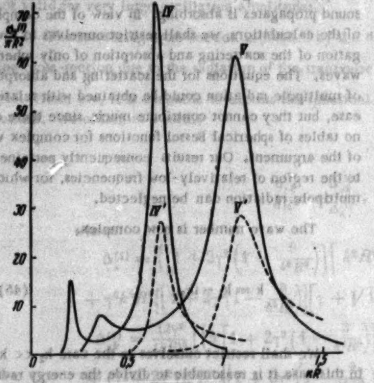

Fig. 3. Effective scattering cross-section of a spherical cavity due to radiation of dipole waves in the absence of absorption in the medium. Solid curves for transverse waves, dotted ones for longitudinal waves. IV and IV' – for $\frac{\mu}{\lambda} = 0.01$ ($\gamma = 0.1$); V and V' – for $\frac{\mu}{\lambda} = 0.04$ ($\gamma = 0.2$).

where α and β are real quantities, the nature of which is clear from the expression

$$\gamma^2 = \frac{\mu}{\lambda} = \alpha + i\beta. \qquad (49)$$

Here $\beta << \alpha$. In the derivation of equation (48) we neglected a term proportional to $\beta^2$ in the numerator. The quantity $\underline{k}$ in equation (48) denotes the real part of the wave number.

10. The energy absorbed per second can be obtained by calculating the energy flux through the cavity surface and subtracting the scattered energy. For the average energy flux density we have

$$\overline{S}_r = -\frac{1}{4} T_{rr} v_r^* + \text{complex conjugate} \qquad (50)$$

Here

$$v_r = \frac{\partial s_r}{\partial t} = \frac{\partial \varphi}{\partial r} = -i\omega\varphi\left(ik + \frac{1}{r}\right),$$

$$T_{rr} = \lambda \operatorname{div} s + 2\mu \frac{\partial s_r}{\partial r} = \left[-\rho\omega^2 + 4\mu\left(\frac{ik}{r} + \frac{1}{2}\right)\right]\varphi.$$

using these equations we readily obtain

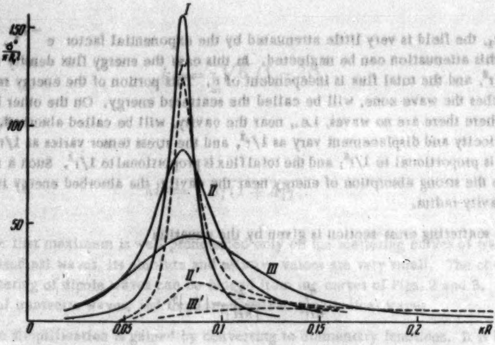

Fig. 4. Effective scattering and absorption cross-sections of a spherical cavity due to excitation of spherical waves in the presence of absorption in the medium at $\alpha = 0.0016$ ($\gamma = 0.04$). Solid curves for absorption, dotted for scattering. α and β are real and imaginary parts of the ratio $\frac{\mu}{\lambda} = \alpha + i\beta$. I and I' – for $\frac{\beta}{\alpha} = 0.1$; II and II' – for $\frac{\beta}{\alpha} = 0.4$; III and III' – for $\frac{\beta}{\alpha} = 1$.

$$\overline{S}_r = \frac{\omega\varphi\varphi^*}{2}\left\{\rho\omega^2 k_1 + \frac{4\mu_2}{r}(k_1^2 + k_2^2) + \frac{8\mu_2 k_2}{r^2} + \frac{4\mu_2}{r^3}\right\}.$$

**Neglecting the terms here containing the small quantity $k_2$. we obtain for the effective absorption cross-section**

$$\sigma_c^0 = \frac{4\mu_2(1 + k^2R^2)}{R^3\rho\omega^2 k}\sigma_s^0. \qquad (51)$$

**This expression can be simplified by taking advantage of the fact that $\mu$ is small compared with $\lambda$. Neglecting the quantity $\mu$ in the first equation of (3) we get $\rho\omega^2 = \lambda k^2$. Substituting this value into (51) we finally get**

$$\sigma_c^0 = \frac{4\beta}{k^4R^4}(1 + k^2R^2)\sigma_s^0. \qquad (52)$$

**The solid lines of Figs. 4 and 5 show the curves for the absorption cross-section, and the dotted lines show the scattering cross-section.**

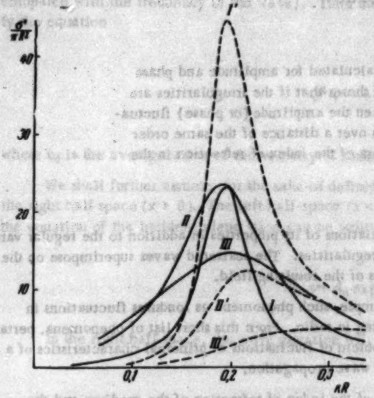

**Fig. 5. Effective scattering and absorption cross-section of spherical cavity due to excitation of spherical waves in the presence of absorption in the medium at $\alpha = 0.01$ ($\gamma = 0.1$). Solid curves for absorption, dotted for scattering, $\alpha$ and $\beta$ real and imaginary parts of the ratio $\frac{\mu}{\lambda} = \alpha + i\beta$. I and I' – for $\frac{\beta}{\alpha} = 0.1$; II and II' – for $\frac{\beta}{\alpha} = 0.4$; III and III' – for $\frac{\beta}{\alpha} = 1$.**

## LITERATURE CITED

**[1] D. V. Sivukhin, J. Exptl.-Theoret. Phys. (USSR) 10, 679 (1940).**

**S. I. Vavilov Institute for Physics Problems,**
**USSR Academy of Sciences, Moscow**

**Received October 2, 1954.**

# CORRELATION OF AMPLITUDE AND PHASE FLUCTUATIONS FOR WAVE PROPAGATION IN A MEDIUM WITH RANDOM IRREGULARITIES

L. A. Chernov

**The coefficient of correlation is calculated for amplitude and phase fluctuations at the reception point. It is shown that if the irregularities are large in scale, the autocorrelation between the amplitude (or phase) fluctuation at different reception points extends over a distance of the same order as the correlation between the fluctuations of the index of refraction in the medium.**

Every real medium has irregular space and time variations of its properties in addition to the regular variations. A propagating wave is scattered by these random irregularities. The scattered waves superimpose on the primary waves and cause amplitude and phase fluctuations of the resulting field.

Random irregularities in the medium cause, for example, such phenomena as loudness fluctuations in acoustics, flickering of stars in optics, and sometimes fading in radio. From this short list of phenomena, pertaining to different branches of physics, it follows that the problem of fluctuations of principal characteristics of a wave field is one of the general problems in the theory of wave propagation.

A relationship should exist between the fluctuations of the index of refraction of the medium and the fluctuations of the wave-field characteristics. The problem is to establish this relationship, from which it would be possible to draw conclusions concerning the statistical properties of the wave fields, knowing the statistical properties of the medium, and vice versa. The study of fluctuations in a wave, a topic interesting in itself, thus uncovers new possibilities of studying the properties of the medium through which the wave propagates.

Many Soviet [1, 2] and foreign [4, 5] works are devoted to the fluctuations of amplitude and phase. There has been little investigation, however, of the correlation of the amplitude and phase fluctuations, a problem of theoretical and practical interest. This, naturally, raises two questions.

1. Is there a correlation between the amplitude and phase fluctuations at the reception point?

2. Is there an autocorrelation between the amplitude (or phase) fluctuations at different reception points and over what distance does this autocorrelation extend?

As far as we know, the first question has never been posed. The second question was examined by several investigators [1, 4] only in the ray approximation. Neither, however, derived the simple law that the autocorrelation between the amplitude (or phase) fluctuations extends approximately over the same distance as the correlation between the random irregularities of the medium itself, provided the dimensions of the latter are large compared with the wavelength.

Both problems are considered below under the assumption that the medium is isotropic, that there are no regular variations of the homogeneity, that the random deviations of the index of refraction of the medium from its average value are small, and that the dimensions of these deviations are large compared with the wavelength.

Let us derive the initial equations for further investigation, repeating here (with slight variations) the corresponding part of the work by A. M. Obukhov [2].

Let the index of refraction fluctuate about an average value equal to unity:

$$n = 1 + \mu, \ |\mu| \ll 1. \tag{1}$$

Here $\mu$ is dependent on the ordinates. We shall disregard the explicit dependence of $\mu$ on the time, assuming that the characteristics of the medium vary very slowly with time (the frequency of the variation is small compared with the frequency of the wave). Then the wave function $\psi$, characterizing the wave field, will satisfy the equation

$$\nabla^2 \psi - \frac{(1+\mu)^2}{c_0^2} \ddot{\psi} = 0, \tag{2}$$

where $c_0$ is the average value of the velocity of sound in the medium.

We shall further assume, for the sake of definiteness, that the random irregularities are contained only in the right half-space ($x > 0$). The left half-space ($x < 0$) contains no random irregularities. In the left half-space the equation of the incident plane wave can be written as

$$\psi_0 = A_0 \exp \{ i (\omega t - kx) \}.$$

In the right half-space, the wave equation will be of the form

$$\psi = A(\mathbf{r}) \exp \{ i [\omega t - S(\mathbf{r})] \}. \tag{3}$$

If the usual method of small perturbations is used to determine $\psi$, as is frequently done in scattering theory, taking $\psi_0$ as the zero approximation, the expressions obtained for the amplitude and phase fluctuations will be restricted to small values, and consequently, to small distances, for the fluctuations increase with distance. It is therefore more advantageous to employ the small-perturbation method in the form presented by S. N. Rytov [3].

In this form, the small-perturbation method, as will be shown below, is not subject to such severe requirements, and this is of importance when theory is compared with experiment, for one frequently observes experimentally large amplitude and phase fluctuations. The essence of the method lies in replacing the wave function $\psi$ by another function $\varphi$, related to the former by

$$\psi = A_0 \exp \{ i [\omega t - \varphi(\mathbf{r})] \}. \tag{4}$$

Comparison of (4) with (3) shows that the function $\varphi(\mathbf{r})$ is defined by the following relationship:

$$\varphi(\mathbf{r}) = S(\mathbf{r}) + i \ln \frac{A}{A_0}. \tag{5}$$

As can be seen, the real and imaginary parts of the function $\varphi(\mathbf{r})$ introduced above determine respectively the phase and the logarithm of the amplitude ratio (sound intensity level), the fluctuations of which are of direct interest to us.

The replacing of $\psi$ in equation (2), by $\varphi$ from expression (4), gives us an equation for the function $\varphi$:

$$(\nabla\varphi)^2 + i\nabla^2\varphi = k^2 n^2, \quad k = \frac{\omega_0}{c_0}. \tag{6}$$

The zero approximation $\varphi_0$ satisfies the equation of the homogeneous medium

$$(\nabla\varphi_0)^2 + i\nabla^2\varphi_0 = k^2. \tag{7}$$

Subtracting (7) from (6) we get for the function $\varphi' = \varphi - \varphi_0$

$$2(\nabla\varphi_0\nabla\varphi') + i\nabla^2\varphi' = 2\mu k^2 + [\mu^2k^2 - (\nabla\varphi')^2].$$

Using the small-perturbation method and assuming that $\nabla\varphi'$ (more accurately speaking, the dimensionless quantity $\frac{1}{k}\nabla\varphi'$) is of the order $\mu$, let us discard the terms in the square brackets, as second-order quantities relative to $\mu$. We then obtain a linear equation for $\varphi'$:

$$2(\nabla\varphi_0\nabla\varphi') + i\nabla^2\varphi' = 2\mu k^2. \tag{8}$$

This equation was obtained under the assumption that

$$\frac{1}{k}\nabla\varphi' \sim \mu_1 \quad \text{or} \quad \frac{1}{k}\left|\nabla\varphi'\right| \ll 1. \tag{9}$$

The latter condition signifies that the variations in phase and the relative variation in amplitude over the wavelength should be small. No limitations are imposed by (9) on the total variation of these quantities. Putting in equation (8) $\varphi_0 = kx$, we get

$$2k\frac{\partial\varphi'}{\partial x} + i\nabla^2\varphi' = 2\mu k^2. \tag{10}$$

An exact solution of this equation is of the form

$$\varphi'(x, y, z) = \frac{ik^2}{2\pi}\iiint\limits_V \frac{\exp\{-ik[r-(x-\xi)]\}}{r}\mu(\xi, \eta, \zeta)\,d\xi\,d\eta\,d\zeta, \tag{11}$$

where V is the region containing the random irregularities.

Separating the real and imaginary parts, we obtain the following equations for the phase fluctuations and for the amplitude fluctuations:

$$S' = \frac{k^2}{2\pi}\iiint\limits_V \frac{1}{r}\sin k[r-(x-\xi)]\,\mu(\xi, \eta, \zeta)\,d\xi\,d\eta\,d\zeta, \tag{12}$$

$$\ln\frac{A}{A_0} = \frac{k^2}{2\pi}\iiint\limits_V \frac{1}{r}\cos k[r-(x-\xi)]\,\eta(\xi, \eta, \zeta)\,d\xi\,d\eta\,d\zeta. \tag{13}$$

In the case of large-scale irregularities, when $ka >> 1$ (where $\underline{a}$ is the dimension of the irregularities), the scattering angles are small and their order of magnitude does not exceed $1/ka$. For this reason, the only irregularities producing a substantial effect will be those concentrated within a cone having its apex at the reception point and having an aperture angle on the order of $1/ka$. Within this cone it is possible to replace the equation $r = \sqrt{(x-\xi)^2 + \rho^2}$, where $\rho^2 = (y-\eta)^2 + (z-\zeta)^2$, by the approximate expression

$$r \approx (x-\xi) + \frac{1}{2}\frac{\rho^2}{x-\xi}. \tag{14}$$

Replacing $r-(x-\xi)$ in equations (12) and (13) in accordance with (14) and replacing $\frac{1}{r}$ by $\frac{1}{(x-\xi)}$, we get

$$S = \frac{k^2}{2\pi}\int_V \frac{\sin\frac{k\rho^2}{2(x-\xi)}}{x-\xi}\,\mu\,dv, \tag{15}$$

$$\ln\frac{A}{A_0} = \frac{k^2}{2\pi}\int_V \frac{\cos\frac{k\rho^2}{2(x-\xi)}}{x-\xi}\,\mu\,dv \tag{16}$$

Let us introduce new symbols, putting

$$\Phi_1\left(\frac{x-\xi}{k},\ \rho\right) \equiv \frac{k}{2\pi(x-\xi)}\sin\frac{k\rho^2}{2(x-\xi)},$$

$$\Phi_2\left(\frac{x-\xi}{k},\ \rho\right) \equiv \frac{k}{2\pi(x-\xi)}\cos\frac{k\rho^2}{2(x-\xi)}.$$

Equations (15) and (16) are then rewritten as

$$S'(x, y, z) = k\int_0^x\int_{-\infty}^{+\infty}\int_{-\infty}^{+\infty}\Phi_1\left(\frac{x-\xi}{k},\ \rho\right)\mu(\xi, \eta, \zeta)\,d\xi\,d\eta\,d\zeta, \tag{17}$$

$$\ln\frac{A(x, y, z)}{A_0} = k\int_0^x\int_{-\infty}^{+\infty}\int_{-\infty}^{+\infty}\Phi_2\left(\frac{x-\xi}{k},\ \rho\right)\mu(\xi, \eta, \zeta)\,d\xi\,d\eta\,d\zeta. \tag{18}$$

Having thus obtained the fundamental initial equations, let us proceed to examine the problem statistically. Let us characterize the statistical properties of the medium by a correlation function $R(r)$:

$$R(r) = \overline{\mu_1\mu_2},$$

where $\mu_1$ and $\mu_2$ are small deviations of the index of refraction from the average value at two points a distance $\underline{r}$ apart. The bar designates the statistical average.

Equations (17) and (18) can be used to decide the problem of correlation between the amplitude and phase fluctuations at the reception point (L, 0, 0). For this purpose let us multiply equations (17) and (18). Let us average them, and obtain by introducing dimensionless variables $\xi' = k\xi$, $\eta' = k\eta$, $\zeta' = k\zeta$, $\rho' = k\rho$. $L' = kL$, $r' = kr$:

$$\left[S' \ln \frac{A}{A_0}\right]_{(L,\,0,\,0)} = \int_0^{L'}\int_0^{L'}\int\int\int_{-\infty}^{+\infty}\int \Phi_1(L' - \xi_1', \rho_1')\,\Phi_2(L' - \xi_2', \rho_2') \times$$
$$\times R(r')\,d\xi_1'\,d\eta_1'\,d\zeta_1'\,d\varsigma_2'\,d\eta_2'\,d\zeta_2'. \tag{19}$$

Transforming to relative coordinates $\eta = \eta'_1 - \eta'_2$, $\zeta = \zeta'_1 - \zeta'_2$, and to the center-of-mass coordinates $y = \frac{\eta'_1 + \eta'_2}{2}$, $z = \frac{\zeta'_1 + \zeta'_2}{2}$, it is possible to integrate with respect to the variables y and z. We then obtain

$$\left[S' \ln \frac{A}{A_0}\right]_{(L,\,0,\,0)} = \frac{1}{2}\int_0^{L'}\int_0^{L'}\iint_{-\infty}^{+\infty}\Phi_2\,[2L' - (\xi_1' + \xi_2'),\,\rho]\,R(r')\,d\eta\,d\zeta\,d\xi_1'\,d\xi_2' -$$
$$- \frac{1}{2}\int_0^{L'}\int_0^{L'}\int\int_{-\infty}^{+\infty}\Phi_2(\xi_1' - \xi_2',\,\rho)\;R(r')\,d\eta\,d\zeta\,d\xi_1'\,d\xi_2', \tag{20}$$

where $\rho^2 = \eta^2 + \zeta^2$. Equation (20) gives the general solution of the problem posed. To use this equation, it is necessary to specify the correlation function R (r'). Assuming, for example, that it is of the form

$$R(r') = R_0 \exp\left\{-\frac{r^2}{a^2}\right\} = R_0 \exp\left\{-\frac{r'^2}{k^2 a^2}\right\}, \tag{21}$$

where $r'^2 = \xi^2 + \eta^2 + \zeta^2$, $\xi = \xi'_1 - \xi'_2$, we obtain after performing the integration in (20)

$$\left[S' \ln \frac{A}{A_0}\right]_{(L,\,0,\,0)} = \frac{\sqrt{\pi}}{16} R_0\, a^3 k^3 \ln\left[1 + \left(\frac{4L}{ka^2}\right)^2\right]. \tag{22}$$

and we obtain for the correlation coefficient $R_{as}$ oh the basis of equations (22), (30), and (31),

$$R_{as} = \frac{1}{2}\,\frac{\sqrt{\ln(1 + D^2)}}{\sqrt{D^2 - \qquad D)^2}}, \tag{23}$$

where $D = \frac{4L}{ka^2}$. At small distances (D << 1), when the ray representation is convenient, equation (23) yields*

$$R_{as} \cong \frac{1}{2}\sqrt{\frac{3}{2}} \cong 0{,}6.$$

At large distances (D >> 1), equation (23) becomes:

$$R_{as} = \frac{\ln D}{D},$$

---

* This result was erroneously reduced by one-half in an article by this author; cf. Dokl. Acad. Nauk USSR 1954, No. 6.

i.e., the coefficient of correlation diminishes with distance, approaching zero. The correlation between the amplitude and phase fluctuations, existing at small distances, thus vanishes at large distances.

Let us now consider the problem of the autocorrelation of the amplitude and phase fluctuations at different reception points.

Let us assume that both receivers lie in the plane x = L a distance $l$ apart.

The receiver coordinates, are (L, 0, 0) and (L, 0, $l$), respectively. The amplitude and phase fluctuations are determined by equations (17) and (18) for either receiver. The only difference is that for the first receiver we have $\rho_1^2 = \eta_1^2 + \zeta_1^2$, and for the second we have $\rho_2^2 = \eta_2^2 + (l - \zeta_2)^2$. The autocorrelation functions for the phase and amplitudes are therefore determined from the following equations

$$\overline{S_1' S_2'} = \frac{1}{2}(I_1 + I_2), \tag{24}$$

$$\overline{\ln\frac{A_1}{A_0}\ln\frac{A_2}{A_0}} = \frac{1}{2}(I_1 - I_2), \tag{25}$$

where

$$I_1 = \int_0^{L'}\int_0^{L'}\iint_{-\infty}^{+\infty} \Phi_1(\xi_1' - \xi_2', \rho) R(r')\, d\eta\, d\zeta\, d\xi_1'\, d\xi_2', \tag{26}$$

$$I_2 = \int_0^{L'}\int_0^{L'}\iint_{-\infty}^{+\infty} \Phi_1[2L - (\xi_1' + \xi_2'), \rho] R(r')\, d\eta\, d\zeta\, d\xi_1'\, d\xi_2',$$

$$\rho^2 = \eta^2 + (\zeta + l')^2,\ l' = kl. \tag{27}$$

Equations (24) – (27) yield a general solution for the autocorrelation of the phases and amplitudes at different reception points. Assuming that the correlation function R(r') is of the form (21), and performing the integration in equations (26) and (27) under the assumption that ka >> 1, L >> a, we get

$$I_1 = \sqrt{\pi}\, R_0 a k^2 L \exp\left\{-\frac{l^2}{a^2} - \left(\frac{l^2}{a^2}\frac{1}{ka}\right)^2\right\}, \tag{28}$$

$$I_2 = \frac{\sqrt{\pi}}{8i} R_0 a^3 k^3 [Ei(\varepsilon_2) - Ei(\varepsilon_1)], \tag{29}$$

where $\epsilon_2 = -\dfrac{i\dfrac{l^2}{a^2}}{D+1}$, $\epsilon_1 = \dfrac{i\dfrac{l^2}{a^2}}{D-i}$, and Ei is the symbol for the integral exponential function. In the particular case of $l = 0$, we obtain equations for the mean-squared fluctuations of amplitude and phase, obtained by A. M. Obukhov [2]

$$\overline{S'^2} = \frac{\sqrt{\pi}}{2} R_0 a k^2 L\left(1 + \frac{1}{D}\operatorname{arc\,tan} D\right), \tag{30}$$

$$\overline{\left(\ln\frac{A}{A_0}\right)^2} = \frac{\sqrt{\pi}}{2} R_0 a k^2 L\Big(1 - \tag{31}$$

$$-\frac{1}{D}\operatorname{arc\,tan} D\Big).$$

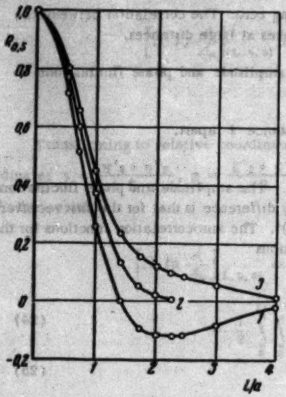

Fig. 1. 1) autocorrelation coefficient for amplitude fluctuations, 2) correlation for index-of-refraction fluctuations, 3) autocorrelation coefficient for phase fluctuations.

From equations (24), (25), (28), (29), (30), and (31) we obtain the following expression for the autocorrelation coefficient

$$R_{a,s} = \frac{\exp\left\{-\frac{l^2}{a^2}-\left(\frac{l^2}{a^2}\frac{1}{ka}\right)^2\right\} \pm \frac{1}{2iD}\left[Ei(\varepsilon_2)-Ei(\varepsilon_1)\right]}{1\pm\frac{1}{D}\operatorname{arc\,tan} D}, \quad (32)$$

where the upper sign must be taken when calculating the autocorrelation coefficient $R_s$ for the phase, and the lower one for the autocorrelation coefficient $R_a$ for the amplitudes. As can be seen from expression (32), the autocorrelation coefficient depends only on the three dimensionless parameters $\frac{l}{a}$, D, and ka. For small and medium distances ($D \lesssim 1$) we obtain an asymptotic value for $R_{a,s}$ at sufficiently large $\frac{l}{a}$, provided we used the asymptotic expression for the Ei functions [7]:

$$R_{a,s} \cong \frac{\exp\left\{-\frac{l^2}{a^2}-\left(\frac{l^2}{a^2}\frac{1}{ka}\right)^2\right\} \pm \left\{\frac{\sin\{(l^2/a^2)[D/(1+D^2)]\}}{(l^2/a^2)D} + \frac{\cos\{(l^2/a^2)[D/(1+D^2)]\}}{l^2/a^2}\right\}\exp\left\{-\frac{l^2}{a^2}\frac{1}{1+D^2}\right\}}{1\pm\frac{1}{D}\operatorname{arc\,tan} D}. \quad (33)$$

The autocorrelation coefficient is small compared with unity by virtue of the presence of exponential factors in the numerator. This means that the correlation between the amplitude and phase fluctuations extends over a distance $l$ of the order of the radius of correlation a in the medium.

For large distances (D >> 1), equation (32) becomes

$$R_{a,s} = \frac{\exp\left\{-\frac{l^2}{a^2}-\left(\frac{l^2}{a^2}\frac{1}{ka}\right)^2\right\} \pm \frac{1}{D}\left[\frac{\pi}{2}-\operatorname{Si}\left(\frac{1}{D}\frac{l^2}{a^2}\right)\right]}{1\pm\frac{1}{D}\operatorname{arc\,tan} D}. \quad (34)$$

The dependence of the autocorrelation coefficients on the distance $l$ between receivers is shown graphically (Fig. 1) for the case $D = 10$; and $ka = 10^2 - 10^4$. The central curve shows the correlation coefficient for the index of refraction in accordance with expression (21). It is seen from the curve that the autocorrelation between the amplitude and phase fluctuations extends over a distance of the order of the correlation radius of the irregularities in the medium. We reach the same conclusion by examining small and medium distances.

I consider it my duty to express gratitude to L. M. Brekhovskikh for valuable advise.

## LITERATURE CITED

[1] B. A. Krasil'nikov, Bull. Acad. Sci. USSR, Geog. and Geophys. Ser. 1949, No. 1, p. 33.

[2] A. M. Obuknov, Bull. Acad. Sci. USSR, Geophys. Ser. 1953, No. 2, p. 155

[3] S. M. Rytov, Bull. Acad. Sci. USSR, Phys. Ser. 1937, No. 2, p. 223.

[4] P. G. Bergmann, Phys. Rev. 70, 7-8 (1946).

[5] D. I. Minzer, J. Acoust. Soc. Am. 25, 5, 922(1953); 6, 1107.

[6] C. L. Pekeris, Phys. Rev. 71, p. 268 (1947).

[7] I. M. Ryzhik and I. S. Gradshtein, "Tables of integrals,sums, series, and products,"(State Tech. and Theor.-Lit. Press, Moscow-Leningrad,1951) p. 324.

Acoustics Institute of the
USSR Academy of Sciences, Moscow

Received October 8, 1954.

# CONFERENCE ON PHYSIOLOGICAL ACOUSTICS

**A conference on physiological acoustics, organized by the Acoustics Commission of the USSR Academy of Science and by the I. P. Pavlov Institute of Physiology of the USSR Academy of Science, was held in Leningrad on July 16-19, 1954. Participating in the conference were acoustical physicists, acoustical engineers, physiologists, and linguists. The principal papers covered work on the physiology of the auditory receptor, pertaining particularly to various effective methods of recording the threshold of audio sensitivity. Papers were delivered on the acoustic structure of the Russian language and on the investigation of the singing voice. Reports of medical nature were also delivered. In addition, the conference devoted a session to problems of manufacturing acoustic apparatus and hearing aids in the USSR.**

**The conference noted the advisability and success of the unified work of representatives of various specialties toward the investigation of the complex problem of hearing and speech.**

**Publication of the transactions and resolutions of the conference is planned.**

## CONFERENCE ON PHYSICAL ACOUSTICS AND ULTRASONICS

**A conference on physical acoustics and ultrasonics, prepared by the Commission on Acoustics jointly with the Acoustics Institute of the USSR Academy of Science, the Moscow State University, and the Leningrad Electrotechnical Institute, was held on March 3-7 1955.**

**The conference was held in two sections; a total of 11 sessions were held, at which 46 papers were read, devoted to various problems in acoustics (non-linear acoustics, modulation-interference methods of measurement, wave propagation, molecular acoustics, ultrasonic defectoscopy, application of ultrasonics, etc.).**

**Abstracts of the papers will be published in the coming issue of "Journal of Acoustics."**

**Collection No. 8 of the "Transactions of the Commission on Acoustics" has just been published. The collection contains a total of 16 articles on sound optics, correlation analysis, and certain problems of acoustics;**

**The collection is sold in the "Akademkniga" stores, and is also mailed COD from the "Akademkniga" office, Moscow, Kuybyshev St. 8.**

# SURVEY OF METHODS USED FOR THE VISUALIZATION OF ULTRASONIC FIELDS

## L. D. Rozenberg

## INTRODUCTION

Problems of visualizing sound fields (in particular, the visualization of sound images) have recently acquired greater and greater significance in various fields of acoustical physics and engineering. The advantage which can be gained from the possibility of studying acoustic fields (especially those of complex shape) by means of direct observation is obvious and does not require any special argumentation. In engineering acoustics visualization is used in defectoscopy where it is important not only to detect the presence of the defect in the body being examined but also to know the shape and dimensions of that defect. Another example of the possible application of visualization in engineering is the ability to "see" in optically opaque media by means of sound fields (in particular, in large bodies of water, lakes and oceans). Thus in 1948 at a television congress the Italian engineer Federichi [41] rather thoroughly analyzed the possibilities of modern acoustical engineering and came to the conclusion that underwater sound visualization was close to being realized in the engineering sense. In subsequent years a series of American patents [42, 43] were published which described various systems for underwater sound visualization by means of a receiving piezoelectric mosaic and a mechanical commutator. Finally, the practical application of visualization is used in medical diagnosis in order to determine the location, shapes and dimensions of both the internal organs and neoplasms (tumors) and other bodies. Acoustical methods can compete with x-ray methods in this field, because their application makes it possible to operate in a pulse regime which considerably increases the sensitivity of the equipment. When x-ray methods are used such brief pulses are required that their generation and reception is impossible in the present state of pulse engineering because of the extremely high propagation velocity of electromagnetic waves in comparison to sonic waves.

At the present time a rather large number of different methods for visualizing ultrasonic fields have been described in the literature. Attempts to classify these methods have been made by various authors [9,27,31]; however the classification systems proposed by them either did not encompass the entire known aggregate of methods or were based upon random and secondary indices.

In our opinion the basis of such a classification must be a separation according to the nature of the effect which operates at the input of the device that converts the acoustic field into a visible field. If we take this point of view, then the known methods can easily be subdivided into three basic groups: the first group encompasses methods which are based upon the effects of the fundamental (linear) quantities which characterize a sound field; the second group encompasses methods which are based upon the utilization of ponderomotive (quadratic) effects, and the third group encompasses methods which are based upon the utilization of various types of secondary effects that are caused by ultrasonic vibrations.

In turn, each of these basic groups can be subdivided into subgroups. The system of classification which is built up according to the principles indicated above is shown in Fig. 1.

In addition to this basic index the methods can be classified according to other less essential indices as well. Thus, for example, all methods can be subdivided into two groups: reversible and irreversible. If we draw an analogy with the photographic process, then reversible methods are analogous to matte glass upon which an image is only visible as long as an external effect is present, and irreversible methods are analogous to a photolayer upon which an image is retained for an indeterminately long time after the exciting field is removed. Another index according to which methods can be subdivided is the magnitude of the reflection coefficient from the input of the transducer. The problem here is that, as Spengler [31] showed, the standing wave pattern which arises for large coefficients of reflection from the input of the converter can distort the field being observed. Therefore the methods which produce a small reflection coefficient are preferable; in addition, it is obvious that when the reflected energy is large, the efficiency of the transducer (and therefore its sensitivity) cannot be great. If we continue the analogy with photographic methods, then the requirement that the reflection coefficient from the transducer be dimished is equivalent to the requirement that the sensitive photolayer must be anti-aureole.

We shall examine the various methods in the order in which they are given in the above classification.

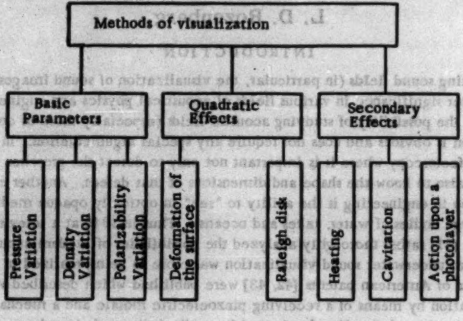

Fig. 1. Classification of visualization methods.

## The Utilization of the Basic Parameters of an Acoustic Field

Methods which make use of pressure variation. When making use of acoustic pressure for visualizing the sound image of a relief, a piezo receiver is used in conjunction with a mechanical or electronic scanning system in all methods that are known at present. Thus Shraiber [1] made use of mechanical scanning which was achieved by moving the investigated part while applying the shadow method of ultrasonic defectoscopy. The signal which appeared at the receiver was fed to a relay after amplication and rectification; the relay cut in a dc voltage to an electrochemical recording pen. Under these conditions a black-on-white (with no half-tones) image of the investigated defect was produced.

Sokolov [2] proposed the scanning of the electrical relief which arose at the surface of the piezoelectric plate upon which the acoustic pressure relief acted; he developed a circuit which achieved scanning by means of a Nipkow disk and reproduced the image upon a neon lamp screen. The principle of the system is obvious from Fig. 2. Analogous systems were subsequently proposed by Dussik [3], Barbie [4] and other authors.

An interesting variant of a mechanical pulse scanning system has been recently described by Wild and Neal [5]. The method proposed by them is designed to obtain images of cross-sections for objects having complex structures, for example, the limbs of animals and humans. A necessary condition for the application

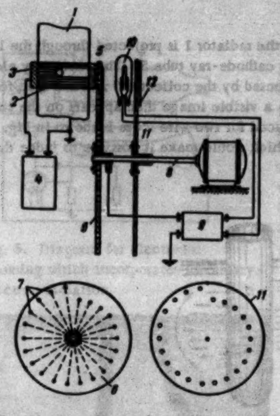

Fig. 2. Diagram for mechanical scanning by a Nipkow disk:
1) part being investigated, 2) defect, 3) ultrasonic radiator, 4) supply oscillator, 5) receiving piezoelectric plate, 6) transmitting disk, 7) commutating elements, 8) axis of rotation, 9) receiving amplifier, 10) neon lamp, 11) receiver disk with apertures, 12) frame window.

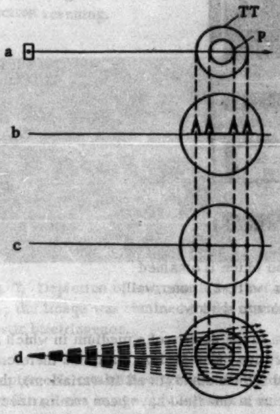

Fig. 3. Circuit for pulse scanning:
a) diagram showing the disposition of the parts (R is the radiator, TT is the test tube, P is a pipe), b) image appearing on the screen for ordinary pulse reception (amplitude modulation), c) image appearing on the screen for intensity modulation, d) image appearing on the screen when the radiator R is rotated.

of this method is the possibility of "penetrating" completely through the investigated object by means of an acoustic ray. Physically this reduces to the requirement that the wave impedances of individual elements of the structure must not differ very greatly in magnitude. The principle of the method is obvious from Fig. 3.

The radiator R which operates at a frequency of 15 megacycles irradiates the object at the right-hand side of the figure with a sharp beam. After a brief pulse has been radiated, the same radiator is converted into a receiver and receives the pulses which are reflected from the boundaries of the sections intersected by the beam. If a saw-tooth sweep is applied to the horizontal deflecting plates of the receiving cathode-ray tube and the amplitudes of the reflected pulses are applied to the vertical deflecting plates, then a picture analogous to the image observed in the usual pulse-defectoscope method is observed upon the screen (Fig. 3,b). However, if the amplitudes of the reflected pulses are fed to the modulator of the tube, then instead of pulses bright points will appear whose intensity will be proportional to the amplitudes of the reflections (Fig. 3,c). We shall now rotate the radiator around an axis perpendicular to the plane of the diagram. Then the ray emanating from the radiator will intersect the entire object which is of interest to us; if under these conditions the rotation of the rays is synchronized with the vertical motion of the electron beam, an image of the scanned cross-section appears upon the screen of the oscilloscope (Fig. 3,d). In Fig. 4 the upper portion shows the picture obtained when a glass test tube immersed in liquid is penetrated by ultrasonic waves; in the center section the image of this test tube is visible upon the screen of the oscilloscope, and the bottom section shows the image which occurs when the test tube is filled with a suspension of insoluble powder and a glass rod is introduced into it.

A circuit which makes use of electron scanning was proposed by Sokolov in 1936 [6]. In the variant described in 1941 [2] the electron beam removes charges from the surface of a quartz plate. In a later variant [7] (which was called an "ultrasonic microscope" by the author) secondary-electron radiation was used; this secondary-electron radiation was caused by the incidence of the electron scanning beam upon the surface of the quartz plate and depended upon the additional charge which was created by the acoustic pressure relief. The circuit for this variant is depicted in Fig. 5.

The acoustic image of the object 2 which is irradiated by the radiator 1 is projected through the lens 3 upon the receiving piezoelectric plate 4 which is a wall of the cathode-ray tube 5. The secondary electrons which are knocked out by the electron scanning beam 6 are collected by the collector 7 and are then fed to the modulator of the receiving kinescope 8 (after amplification); a visible image then appears on the screen of the kinescope. An example of such an image which was produced for two wire loops is shown in Fig. 6. To our regret we do not have any experimental data available which would make it possible to judge the sensitivity and resolving power of this interesting method.

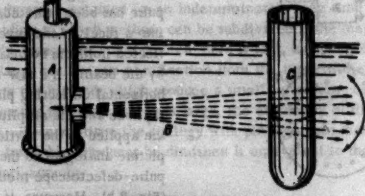

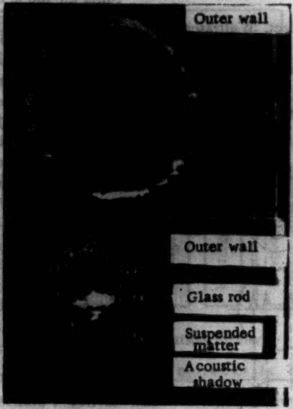

Fig. 4. Image of the test tube cross-section which is obtained by the method of pulse scanning. 1) outer wall, 2) outer wall, 3) glass rod, 4) suspended matter, 5) acoustic shadow.

Methods which make use of density variation. The variation in the density of a medium in which an acoustic wave is being propagated leads to a variation in the refractive index for light rays, and therefore can be shown up by means of purely optical methods such as the shadow method (in all its variations), the method of ultrasonic light diffraction, etc. A large number of papers in this field have been summarized more than once in the form of surveys, and therefore we refer the reader to these surveys. The papers which have been written since 1936 are listed in the survey section of the article by Rzhevkin and Krechmer [8] which contains many convincing photographs of various images of complex acoustic fields in its basic section. Later papers have been systematized in the well-known monograph by Bergmann [9].

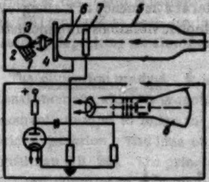

Fig. 5. Diagram for electronic scanning which incorporates secondary-electron radiation.

A certain modification of the classic circuit, which makes it possible to observe the picture of the cross-section of an acoustic ray, is described by Rozenberg [10]. Isakovich and Sirotiuk [11] propose to make use of the variation of the refractive index for the purpose of visualization; this variation occurs in sound-absorbent materials (for example, plexiglass) as a consequence of heating the material while it is absorbing acoustic energy. The quantitative evaluation of the sensitivity of this method which is given by the above authors shows that, for example, for plexiglass the proposed method proves more sensitive than ordinary methods at acoustic pressures which exceed $10^5$ bar.

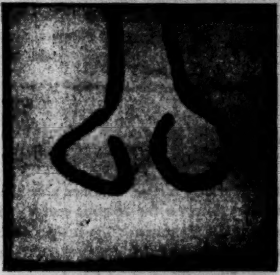

Fig. 6. Image obtained by the method of electron scanning.

Methods which make use of a variation in the nature of the polarization. As a result of so-called acoustic birefringence a medium through which ultrasonic waves are passed can affect the nature of the polarization which obtains in the transmitted ray of light. This effect, which has been known for a comparatively long time, can be utilized for the purposes of visualization. McNamara and Rogers [12] detected an ultrasonic ray in fused quartz glass (Fig. 7) by passing a polarized light beam through the quartz glass in a direction perpendicular to the acoustic ray and by placing an analyzer at the place where the light beam emerged. According to their data it was possible to observe the radiation from a quartz plate which was excited from a voltage of 100 v at a frequency of 10 megacycles. These conditions corresponded to an acoustic intensity of approximately 0.1 watts/ / cm$^2$ in the fused quartz glass.

Hurvitz [45] proposed an analogous circuit which utilized the variation in the nature of polarization in plexiglass for the purposes of the harmonic analysis in the acoustic waves.

## The Utilization of Quadratic (Ponderomotive) Effects

Fig. 7. Depiction of an acoustic ray in fused quartz glass; the image was obtained by the method of acoustic birefringence.

The method of surface relief. Even during the experiments by Wood and Loomis it was noticed that when ultrasonic waves were incident upon the separation boundary between a liquid and a gas a surface deformation arose which first became a breaker and then a fountain. Sokolov [13] proposed to use this effect for the visualization of a defect contour in ultrasonic shadow defectoscopy. For this purpose the surface of the liquid was illuminated by lateral light. Later Sette [14] used an analogous method for investigating ultrasonic focusing, however in his method he made use of the optical system developed by Toepler. He established the fact that at a frequency of 4.2 megacycles and for a plane wave propagated in paraffin oil the image appears when a voltage of 13 volts is applied to the quartz radiator; this voltage is approximately equivalent to an intensity of $3 \cdot 10^{-3}$ watts/cm$^2$ and an acoustic pressure of $5 \cdot 10^4$ bar.

Schuster [15] improved the circuit for the examination of a surface relief by the Toepler method (both the reflection and the transmission methods); the circuit of his device is shown in Fig. 8. Here Q is the acoustic source, O is the examined object, L is the acoustic lens, G is a glass plate which is inclined at an angle of 45°, R is the acoustic image on the surface of the liquid, $P_1$ is the source of light when the transmitted-light system is used, $L_1$ and $L_2$ are objective lenses, $S_1$ and $S_2$ are mirrors, I is a knife and B is the screen. In reflection work a source of light $P_2$, an objective lens $L_3$ and a plane-parallel glass plate H are used. It proves true that the sensitivity for a reflection system exceeds the sensitivity which obtains for a transmission system by a factor of approximately $\frac{2}{n-1}$ where $n$ is the refractive index of the liquid for light rays. If water is used in the capacity of the working liquid, then this factor is ≈6. Figure 9 shows the photographs obtained by Schuster at a frequency of 2.4 megacycles. An analogous method was used by Meier and Trommler [16] for studying piezoelectric vibrations of ammonium dihydrophosphate.

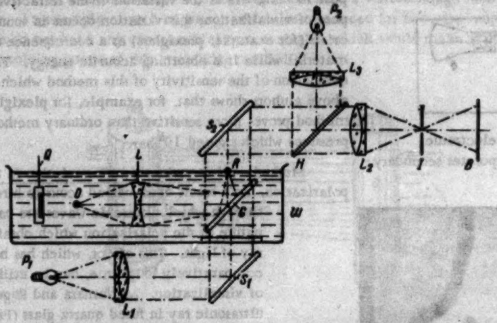

Fig. 8. Diagram of a device for observing surface relief by reflection or by transmission.

Sokolov [17], after having further perfected the method which he described earlier, obtained a number of interesting photographs. The circuit of his device is shown in Fig. 10. Here 1 is the acoustic source, 2 is the object, 3 is a concave mirror, 4 is the liquid present in the vessel 5, 6 is the screen. The images obtained by Sokolov are shown in Fig. 11, a and b. The variant of the optical circuit used for observing the surface relief was proposed by Spengler [31].

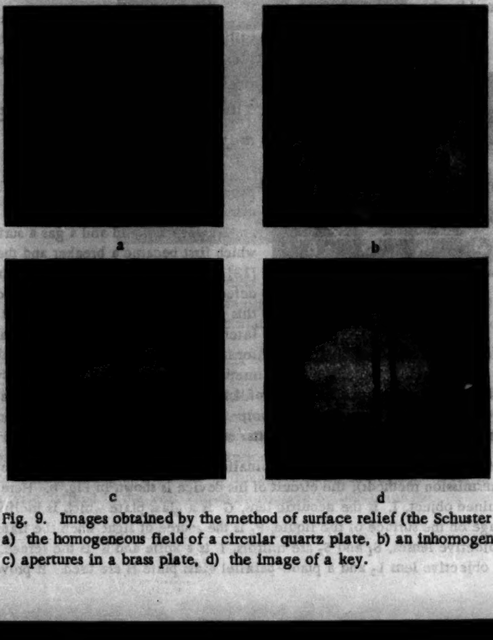

Fig. 9. Images obtained by the method of surface relief (the Schuster method): a) the homogeneous field of a circular quartz plate, b) an inhomogeneous field, c) apertures in a brass plate, d) the image of a key.

Since the sensitivity of the surface relief method is determined in the first place by the height to which the surface of the liquid is deformed, and since this height in turn depends upon the surface tension, Rust and Drubba [18] proposed to decrease the surface tension in order to increase the sensitivity; the surface tension was decreased by depositing an aluminum bronze powder upon the surface of the water.

The suspension method. It is known that when a disk is placed in the path of a plane acoustic wave a rotational moment which is proportional to the square of the wave velocity is applied to the disk by the medium; this moment attempts to rotate the disk in such a way as to make it become perpendicular to the direction of acoustic propagation. The idea of making use of this effect for the vicualization of acoustic images originated with Pohlman [19, 20]. The principle of the method proposed by him is depicted in Fig. 12. A suspension of the smallest lamellas of aluminum* in xylene is present in the adapter; due to the effect of thermal fluxes these particles are in a state of statistical motion. At each instant of time the directions of their axes have equal probabilities. Therefore if this suspension is illuminated through the plate glass which makes up the front wall of the adapter, then the eye of the observer will see a diffusely scattered matte surface (Fig. 13,a). If we now introduce an ultrasonic ray through the thin film which forms the rear wall of the adapter, then the particles which fall in the path of the ray will strive to rotate until their axes are parallel to the surface of the adapter, and as a result the corresponding spots will produce mirror light reflection. Under these conditions the eye of the observer will see a bright image against a grey background (Fig. 13,b).

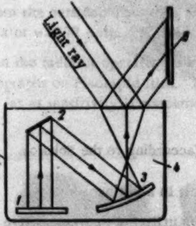

Fig. 10. Diagram of a device for visualization by the method of surface relief (the Sokolov method).

The suspension method is distinguished by its simplicity and good resolving power (the resolving power is determined by the small dimensions of the lamellas). Its shortcomings are a low sensitivity, the considerable time which is required to establish the image, and a gradual settling of the particles due to the effect of gravity. Notwithstanding these shortcomings the suspension method has received wide application for the purposes of ultrasonic defectoscopy in Germany [21, 22], England [23] and the United States [24].

Figure 13 shows images obtained for tinplated iron sheets by the suspension method. For the two sheets at the left the tin layer does not sit tightly upon the iron at all places, whereas in the figure at the right a good adhesion is observable over the entire surface.

## The Utilization of Secondary Effects

The chemical action of ultrasonic waves. Hall, Studt and Rust [25, 26] proposed the utilization of the ultrasonic effect upon the reaction of iodine evolution from a solution of potassium iodide. For this purpose a 10 mm-high raster grating with 4×4 mm cells is placed into a bath containing the solution. A noticeable coloring is observed at 400 kc after a period of 1-2 min when the intensity is 0.5-1.0 watts/cm$^2$.

The sensitivity of this method can be increased somewhat by adding an emulsion of $CCl_4$ in water to the solution. The authors indicate that the bath with the raster grating can be replaced by a gelatinous (or some other type) gel.

Bennett [27] used the acceleration which ultrasonic waves produce in the starch-iodine reaction. A glass plate is covered with a layer of starch paste and (after the paste has dried) is placed into water to which a small amount of 3% solution of iodine in methyl alcohol has been added. At the places which are irradiated by ultrasonic waves the starch film is tinted blue. In the frequency range of 1-3 megacycles at an intensity of 1-2 watts/cm$^2$ several minutes of exposure are required. Bennett assumes that the basic factor which accelerates the reaction is the mixing effect produced by the ultrasonic waves; the result of this mixing effect is that the iodine in the starch film is continually being replenished. The image obtained by Bennett is shown in Fig. 14.

---

* Usually an elutriated aluminum bronze powder is used to provide such lamellas.

Haul, Studt and Rust [25,26], and later Ernst and Hoffman [28] pointed out the possibility of utilizing coloring pigments containing leucobases which change their color when they are oxidized. In particular, Ernst and Hoffman propose the utilization of leucorodamine. They also point out the possibility of making use of the light-sensitive layers which were developed by Eder and which are based upon nitrogen triiodide; they make use of the fact that Richards and Loomis [29] and then Marinesco [30] observed the dissociation of this unstable compound when it was subjected to the effect of ultrasonic waves.

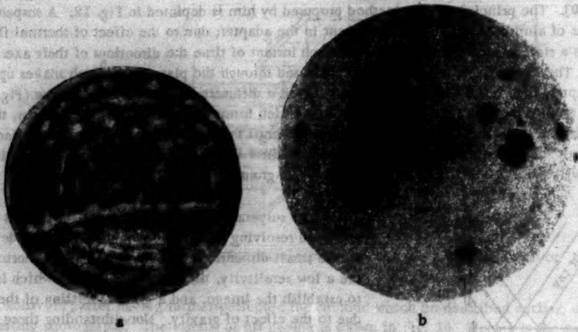
a b

Fig. 11. Images obtained by the method of surface relief (according to the Sokolov method)
a) a signature fashioned from thin wire, b) image of defects in aluminum foil

The thermal effect of ultrasonic waves. The first experiment in utilizing thermosensitive dyes (i.e., dyes which change their color as a function of the temperature) for the purposes of visualization was performed in the middle of 1950 by Anschutz and Spengler [31]. A layer of dye was deposited upon filter paper (the filter paper played the part of an acoustical-thermal transducer). Later experiments which were performed in cooperation with Boshek showed that the best material for this is a rubberized web. Silver tetraiodomecurate was used in the capacity of the pigment; this substance changes its color from straw-yellow through red to black when the temperature is raised above 39.5°C. Analogous experiments were performed by Ernst and Hoffman [28]. Later Rust [32] took up the development of this method, and he proposed to increase the sensitivity by subjecting the dye to preliminary heating up to 36°C and by adding a small amount of $CCl_4$. At a frequency of 566 kc and an intensity of 1 watt/cm$^2$ the required exposure time was 7 sec. According to Spengler [31] it was possible to lower the exposure time to 1 sec. at an intensity of 1 watt/cm$^2$ as a result of later work by Boshek who studied a great number of reversible and irreversible thermodyes.

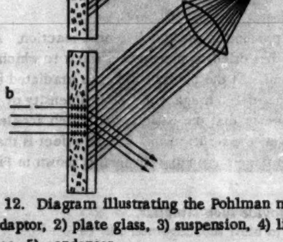

Fig. 12. Diagram illustrating the Pohlman method. 1) adaptor, 2) plate glass, 3) suspension, 4) light source, 5) condenser.

The effect of ultrasonic waves upon the phenomenon of luminiscence was studied by Schreiber and Degner [33] and independently by Eckardt and Lindig [34]. In order to manufacture a screen the authors [33] deposited sulfide phosphors in powder form. The effect of ultrasonic waves upon a weakly shining screen which has been subjected to preliminary excitation led to the rapid disappearance of the phosphorous glow. The resulting image was photographed by the contact method. The best results were obtained with zinc-sulphide phosphorous which was activitated by copper, and with strontium-sulfide phosphorous which was activated by bismuth. The authors assumed that the basis of the effect examined here was the thermal effect of ultrasonic waves. The photographs obtained by these scientists are shown in Fig. 15.

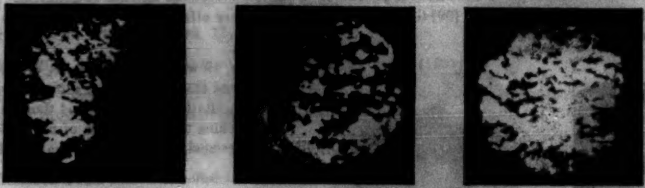

Fig. 13. Images obtained by the suspension method (the Pohlman method).

Eckardt and Lindig made use of zinc-cadmium-sulphide phosphorous which had first been excited by the ultraviolet light of an arc lamp for a period of one minute. The radiating quartz was placed in a vessel with gas-free water; one of the walls of the vessel was made of celluloid foil covered with a layer of phosphorous from the outside. The work was performed at a frequency of 1.42 megacycles, and the power sent to the radiator was 70 watts. The radiator was cut in one-half minute after the arc was cut in.

When the radiator operates for a period of 6-12 sec with an optical distance f: 4,0 it was possible to obtain good photographs on Fluorapid film. The authors assume that this method is substantially worse than the Pohlman method as far as sensitivity is concerned, and thus this method cannot compete with the Pohlman method.

Fig. 14. Image of apertures in a lead plate; the image was obtained by the method of starch iodide plates (the Bennett method).

Peterman [35] somewhat perfected the method described above and as a result he was able to obtain good images for an intensity of 0.1-0.5 watts/cm$^2$ at a frequency of 4.47 megacycles while maintaining the same exposure times. Chomse, Hoffman and Seidel [44] showed that analogous results can be obtained by using organic phosphors.

Along with the methods which are based upon the thermal "quenching" of luminescence, Ernst and Hoffman [28] used phosphors whose glow increased when the temperatures increased. Such phosphors, for example, are strontium selenide or phosphide which have been twice activated with samarium and europium.

The method proposed by Isakovich and Sirotiuk [11], which has already been mentioned above, should also be included in this same group of methods which are based upon the thermal effect of ultrasonic waves; this method is one in which the optical method is used to discover inhomogeneities which arise in a plexiglass layer as a result of ultrasonic heating*.

The effect of ultrasonic waves upon a photolayer. The fact that light-sensitive emulsions become blackened due to the reaction produced by ultrasonic waves was established as far back as 1933 by Marinesco and his associates [36]. The papers by Ernst [37] and Bennett [38] verified the fact that this method had an extremely low sensitivity: for an intensity of 1.5 watts/ $cm^2$ the exposure time lay within the limits of 1-4 hours (Bennett). Ernst obtained exposure times which were somewhat lower (25-30 min), but such values evidently were obtained for greater values of intensity (the intensity numbers are not given in the paper).

---

* After this paper was submitted a paper by Ardenne was published (M. von Ardenne, Nachrichtentechnik 1955, 5, 49) in which he proposed to utilize the heating effect which arises in the layer which absorbs acoustic waves (when it is placed in an acoustic field) in the capacity of the factor which changes the emission from the photocathode of the electronic image converter. When a frequency of five megacycles is utilized the sensitivity of the method is of the order of 0.1 watts/cm$^2$.

As far as the mechanism of this effect is concerned, it has been assumed up until recently that on the basis of the papers by Pinoir and Pouradier [39] that this effect is a secondary effect which is caused by the glow which arises in the cavitation levels.

However a recent paper by Bennett [40] showed that this effect is also observed when no cavitation is present, and thus the problem regarding the mechanism of the ultrasonic effect upon a photolayer remains open.

Bennett assumes that a necessary condition for ultrasonic waves to have an effect upon a photolayer is the softening of the latter. It must be noted that Marinesco also pointed to this fact.

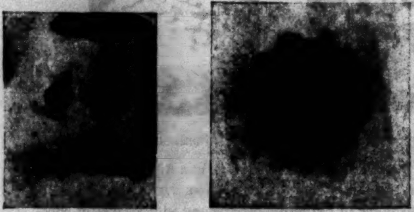

Fig. 15. Images obtained by the method involving the light emitted by a luminescent screen.
a) apertures in a brass plats, b) the field of quartz radiator.

## SUMMARY

From the above discussion it is evident that at present many methods for visualization have been developed which are based upon the most widely differing principles. In addition, if we compare known methods with the classification system given at the beginning of this survey, then it is evident that all of the possibilities are far from being exhausted. Thus we can immediately see that methods based upon utilizing such an essential factor as radiation pressure are completely absent; the broad possibilities presented by the varied chemical effects of ultrasonic waves have been utilized to a very limited degree. There is no doubt that the list of methods and even the catalogue of general lines of development still remain to be intensively developed.

As far as a comparison and critical evaluation of known methods is concerned, many great difficulties present themselves; such an analysis is even impossible because the majority of authors do not provide adequate quantitative characteristics in their papers. For the most part this refers to the threshold intensity, because without a knowledge of this quantity it is impossible to evaluate such an extremely important characteristic of a method as its sensitivity. Even in cases where the authors provide figures which characterize the intensity of the ultrasonic field these figures are not always reliable.

With regard to a qualitative evaluation the following concepts may be used. The methods which utilize pressure receivers and electronic or mechanical scanning must have the greatest sensitivity, since they make it possible to amplify the received signal in an electrical circuit. Their shortcomings are their relative complexity and their limited (although large) resolving power which is determined by the necessity of scanning.

Optical methods yield a resolving power of the order of a light wavelength but are less sensitive than electronic methods.

All methods which are characterized by the application of contact layers are distinguished by extreme simplicity and good resolving power. Their basic shortcoming is their extremely small sensitivity which requires the utilization of intense acoustic fields.

However, notwithstanding the present state of imperfection of the well-known methods, the visualization of acoustic fields is a powerful medium for performing physical research and for solving engineering problems.

## LITERATURE CITED

[1] D. S. Shraiber , Factory Laboratory (U.S.S.R.) 19, 1001 (1940).

[2] S. Ia. Sokolov, J. Tech. Phys. (U.S.S.R.) 11, 160 (1941).

[3] K. Dussik, Z. Neurol. Psych. 174, 153 (1942).

[4] O. Barbie, Alta Frequenza, 11, 383 (1944).

[5] J. Wild, D. Neal, Surgery 27, 183 (1950); Lancet 1, 655 (1951).

[6] S. Ia. Sokolov, Patent Certification No. 49426 awarded August 31, 1936; American Patent No. 2164185, 1937; English Patent No. 477139 awarded May 13, 1937.

[7] S. Ia. Sokolov, Factory Laboratory (U.S.S.R.) 1948, No. 11, p. 1328.

[8] S. N. Rzhevkin and S. I. Krechmer, Trans. P. N. Lebedev Phys. Inst. 1, 43 (1938); Progr. Phys. Sci. 18, 1 (1937).

[9] L. Bergmann, Der Ultraschall, 6 aufl. (Zurich, 1954).

[10] L. D. Rozenberg, Patent Certification No. 91601 awarded Oct. 26, 1950.

[11] M. A. Isakovich, M. G. Sirotiuk, J. Tech. Phys. (U.S.S.R.) 21, 715 (1951).

[12] F. L. McNamara and T. F. Rogers, J. Acoust. Soc. Am. 25, 338 (1953).

[13] S. Ia. Sokolov, Factory Laboratory (U.S.S.R.) 4, 1468 (1935).

[14] D. Sette, J. Acoust. Soc. Am. 21, 375 (1949).

[15] K. Schuster, Jenaer Jahrbuch, 1951, p. 217.

[16] R. Meier and H. Trommler, Ann. Physik. 12 (6), 393 (1953).

[17] S. Ia. Sokolov, Factory Laboratory (U.S.S.R.), 1952, No. 10, p. 1207.

[18] H. Rust and H. Drubba, Kolloid Z. 127, 38 (1952).

[19] R. Pohlman, DRP 1937, No. 710413.

[20] R. Pohlman, Z. Physik. 113, 697 (1939).

[21] R. Pohlman, Z. Angew. Phys. 1, 181 (1948).

[22] R. Pohlman, Die Technik, 3, 465 (1948).

[23] M. W. Thring, J. Sci. Instr. 29, 273 (1952).

[24] L. van Ouwekerek Metalen, 7, 44 (1952).

[25] R. Haul, H. Studt and H. Rust, DRP 1949 No. 842548.

[26] R. Haul, H. Studt and H. Rust, Naturwissenschaften 36, 374, 1949; Angew. Chemie 62, 186 (1950).

[27] G. S. Bennett, J. Acoust. Soc. Am. 24, 470 (1952).

[28] P. Ernst and C. Hoffman, J. Acoust. Soc. Am. 24, 207 (1952).

[29] W. Richards and A. Loomis, J. Am. Chem. Soc. 49, 3086 (1927).

[30] N. Marinesco, Compte Rend. 201, 1187 (1935).

[31] G. Spengler. Nachtrichtentechnik 3, 399 (1953).

[32] H. Rust, Angew. Chemie 64, 308 (1952).

[33] H. Schreiber and W. Degner, Ann. Physik. 7, 275 (1950).

[34] A. Eckardt and O. Lindig, Ann. Physik. 7, 410 (1950).

[35] L. Peterman, Helv. Phys. Acta 24, 596 (1951); J. Acoust. Soc. Am. 24, 416 (1952).

[36] N. Marinesco and J. Trillat, Compte Rend. 196, 858 (1953); N. Marinesco and Reggianai, Compte Rend. 260, 548 (1935).

[37] P. Ernst, J. Acoust. Soc. Am. 23, 80 (1951).

[38] G. Bennett, J. Acoust. Soc. Am. 23, 478 (1951).

[39] R. Pinoir and J. Pouradier, chim. physique 1947, 44, 261.

[40] G. Bennett, J. Acoust. Soc. Am. 25, 1149 (1953).

[41] M. Federici, Bull. Assoc. Suisse Electriciens 40, 657 (1949).

[42] G. Dimmik, USA, Pat. 2453502, 1948.

[43] R. Rines, USA, Pat. 2528725, 2528726, 2528727, 2528728, 2528729, 2528730, 1950.

[44] H. Chomse, W. Hoffman, and P. Seidel. Naturwissenschaften 40, 288 (1953).

[45] H. Hurvitz, USA, Pat. 2643286, 1950.

Acoustics Institute of the Academy of Sciences USSR,
Moscow

Received April 5, 1955

# MEASUREMENT OF THE ACOUSTIC PARAMETERS OF MATERIALS AT ULTRASONIC FREQUENCIES BY MEANS OF A PULSE PIPE

## N. S. Ageeva

The paper analyzes a method for measuring the complex reflection coefficient from a plane surface at ultrasonic frequencies by means of a hydroacoustic device called a "pulse pipe" [1,2].

Applying this method to various types of materials (layers, rods) it becomes possible to determine such acoustic parameters as the acoustic impedance of a specimen, the elasticity coefficients of a material which correspond to various types of deformations, the propagation velocity of sound in a liquid filling the pipe of the device, the propagation velocity of longitudinal waves in rods; it is also possible to determine the sound insulation which is created by plates. The device makes it possible to perform measurements at various temperatures.

### 1. The Relection Coefficient and the Acoustic Input Impedance.

The basic part of the device is a steel pipe which is filled with water. A radiator is attached to one end of the pipe and the test specimen is placed at the other end of the pipe; the diameter of the test specimen is equal to the inside diameter of the pipe. The radiator sends a plane monochromatic wave of ultrasonic frequency through the pipe. The column of water in the pipe can be examined as an acoustically long line, and the test specimen can be viewed as the load at the end of the line. By observing the phase and amplitude of the wave which is reflected from the specimen, it is possible to determine the reflection coefficient of the specimen.

In order to derive the relationships between the load properties which are of interest to us and the quantities which are directly measurable by means of the given device, let us recall certain relationships which obtain in an acoustic field when an acoustically long line is present.

Let a plane monochromatic wave $P = e^{ikx}$ be propagated along the pipe. The wave which is reflected from the surface of the specimen can be written in the form $P_{\text{refl.}} = \beta e^{-ikx}$. Here $\beta$ is the reflection coefficient; $P$ is the pressure in the wave front, $\underline{k}$ is the wave number for acoustic waves of the specified frequency in the water which fills the pipe. In the general case $\beta$ can be a complex quantity

$$\beta = |\beta| e^{-i\varphi}, \tag{1}$$

where $|\beta|$ and $\varphi$ are the modulus and phase of the reflection coefficient respectively. These quantities are usually subjected to direct measurement in the method being examined here.

The acoustic input impedance $Z_{in}$ of the load is associated with the reflection coefficient by the formula

$$Z_{in} = \rho_0 c_0 \frac{1+\beta}{1-\beta} = \rho_0 c_0 \frac{1+|\beta| e^{-i\varphi}}{1-|\beta| e^{-i\varphi}}, \tag{2}$$

Here $\rho_0 c_0$ is the wave impedance in the water which fills the pipe: Here let us remember that the direction into the interior of the specimen is considered the positive direction. Denoting the real and imaginary portions of the impedance by $R_{in}$ and $X_{in}$ respectively, we have:

$$Z_{in} = R_{in} + iX_{in}$$

and

$$R_{in} = \rho_0 c_0 \frac{1-|\beta|^2}{1+|\beta|^2 - 2|\beta| \cos\varphi},$$

$$X_{in} = -\rho_0 c_0 \frac{2|\beta| \sin\varphi}{1+|\beta|^2 - 2|\beta| \cos\varphi}. \tag{3}$$

Formulas (3) provide the relationship between the directly measurable modulus $|\beta|$ and phase $\varphi$ of the reflection coefficient, and the unknown input impedance of the specimen.

The computation of the impedance according to the measured modulus and phase of the reflection coefficient for various types of specimens makes it possible, as we have already said, to determine a series of acoustic and elastic parameters for various types of specimens.

Let us now pass to an examination of specific problems in which finding the acoustic parameters is based upon determining the impedance by the method described above.

## 2. Determining the Velocity and Attenuation of Longitudinal Waves in Rods

In order to measure the velocity and attenuation of longitudinal waves in rods a specimen in the form of a rod is used; the diameter of the rod is made equal to the inside diameter of the pipe. On the basis of the measured modulus $|\beta|$ and phase $\varphi$ of the coefficient of reflection from such a specimen we determine the input impedance of the rod. On the other hand, the impedance of the rod can be expressed in terms of the velocity of longitudinal waves by means of the following expression:

$$Z_{in} = -i\rho c \tan\frac{\omega}{c} h, \tag{4}$$

where $\rho$ is the density of the rod material, $c = \sqrt{E/\rho}$ – is the velocity of longitudinal waves in the rod, E is Young's modulus of the rod * and h is the length of the rod.

This formula makes it possible to express $R_{in}$ and $X_{in}$ in terms of the parameters of the material. Thus, for example, if there are no losses in the material, then $R_{in}$ is always equal to zero. In measuring the coefficient of reflection from such a rod the equation $|\beta| = 1$ will always obtain; the phase $\varphi$ will under these conditions depend upon the length of the rod or (for a rod of specified length) it will depend upon the acoustical frequency. For a rod whose length is equal to one-half the wavelength of a longitudinal wave in the rod (a "half-wave rod") the impedance of the rod is equal to zero; this corresponds to a reflected wave with a phase $\varphi = \pi$. However it is always necessary to deal with materials with one or another amount of loss. Since we are only examining sinusoidal processes, it is sufficient to introduce the concept of a complex modulus of elasticity in order to take the losses in account (in particular, Young's modulus and the shear modulus). For example, we shall write Young's modulus in the form

$$\overline{E} = E(1 - i\eta).$$

---

* In actual fact the measured modulus of the longtiduinal waves is somewhat different from Young's modulus due to the finite diameter of the rod.

Here $\eta$ is the loss coefficient when longitudinal deformations occur.

In a case when losses are present the relationship between the measured quantities and the parameters of the material proves to be more complex.

For the case of small losses ($\eta \ll 1$) the impedance of the rod can be expressed in terms of E and $\eta$ in a comparatively simple manner. In fact, for this case the velocity of longitudinal waves can be assumed equal to

$$\bar{c} = \sqrt{\frac{\bar{E}}{\rho}} = c\left(1 - i\frac{\eta}{2}\right). \tag{5}$$

with an accuracy up to terms involving second-order infinitiesimals.

The formula for the impedance of the rod will be of the form:

$$Z_{\text{in}} = R_{\text{in}} + iX_{\text{in}} = -i\rho c\left(1 - i\frac{\eta}{2}\right)\tan\left[\frac{\omega}{2}\left(1 + i\frac{\eta}{2}\right)h\right]. \tag{6}$$

The values of $R_{\text{in}}$ and $X_{\text{in}}$ can be determined from the data resulting from the direct measurements of the quantities $|\beta|$ and $\varphi$; further, by solving Equations (6) with respect to c and $\eta$, we can compute c and therefore find the unknown parameters of the material. However more accurate results are obtained if we select a frequency at which the phase of the reflected wave is $\varphi = \pi$. Under these conditions the length of the rod is exactly a half-wavelength, and the relationships

$$\frac{\omega}{c}h = \pi; \qquad X_{\text{in}} = 0; \qquad R_{\text{in}} = \pi\rho c\frac{\eta}{2}. \tag{7}$$

will be fulfilled (with an accuracy of up to the quadratic terms). In that case when the same condition $\eta \ll 1$, is observed we obtain

$$c = 2fh, \tag{8}$$

$$\eta = \frac{2}{\pi}\frac{\rho_0 c_0}{\rho c}\frac{1 - |\beta|}{1 + |\beta|}. \tag{9}$$

Formulas (8) and (9) associate the parameters of the the rod material c and $\eta$ with the directly measured quantities $|\beta|$ and f.

In the case of rods with large losses we shall have

$$Z_{\text{in}} = R_{\text{in}} + iX_{\text{in}} = -i\rho c\sqrt{1 - i\eta}\tan\frac{\omega h}{c\sqrt{1 - i\eta}}. \tag{10}$$

instead of Formulas (6).

In principle the problem remains the same as it is for $\eta \ll 1$, but in this case the computation of c and $\eta$ according to the data for $R_{\text{in}}$ and $X_{\text{in}}$ must be performed according to a special chart described in [3].

## 3. Determining the Shear Modulus and the Loss Coefficient for Shear Deformation in Rubbery Materials

In order to determine the shear modulus and loss coefficient for shear deformations in rubbery materials on the basis of measuring $|\beta|$ and $\varphi$ by means of the device described above, we use a solid "half-wave" rod as a load for the pipe. First we determine the velocity and attenuation of longitudinal waves in the rod, i.e., we find the complex sound velocity in it:

$$c = \sqrt{\frac{\overline{E}}{\rho}} = c\sqrt{1 - i\eta}.$$

A sample of the rubbery test material which is shaped in the form of a ring is glued onto the lateral surface of the rod; the coefficient of reflection from such a rod is measured and its input impedance is determined. From this impedance the input impedance for shear vibrations in the ring-shaped specimen is computed, and then the shear modulus and loss coefficient for shear deformation (which are both associated with the input impedance) are determined in the test material. Here the input impedance of the specimen is determined as the ratio between the shear stress at the gluing boundary between the specimen and the rod and the tangential velocity component at the boundary along the generant of the cylindrical rod.

In order to obtain the relationships between the measured quantities and the investigated parameters we first examined the vibrations of a solid rod whose entire lateral surface has a rubbery material glued to it. When longitudinal vibrations are excited in the rod shear vibrations will arise in the rubbery material. The reaction of the rubbery specimen which is glued to the rod (henceforth we shall simply call the rubbery material the specimen) is proportional to the input impedance of the specimen to shear vibrations.

In deriving the equation of motion for the element of a rod to which the rubbery material is glued we shall assume the following postulates to be fulfilled. In order that the velocity of particles can be considered to vary only a small amount over the cross-section of the rod, we shall assume that the diameter of the rod is small in comparison to a half-wavelength of a longitudinal wave in the rod. Since the wavelength of a shear wave in the rubbery material is considerably less than the wavelength of a longitudinal wave in the rod, it can be assumed that the amplitude of the rod's surface displacement varies little over a shear wavelength measured along the rod in the specimen. In that case the reaction of the specimen upon the rod can be characterized as the impedance of the specimen.

When longitudinal vibrations are present in the rod a cylindrical shear wave will be propagated in the specimen. But when the condition obtains which requires the thickness of the specimen $l_r$ (Fig. 1) to be many times smaller than the radius of the rod, it is possible to assume that the shear wave which is propagated in the specimen from the gluing surface of the specimen towards its outer surface is plane. In that case the amplitude of the vibrations at each point in the specimen is proportional to the amplitude of the rod vibrations in the corresponding cross-section which is perpendicular to its axis.

When the postulates indicated above are valid the equation for the vibrations of an element dx of the rod will be of the form:

$$\pi a^2 \rho \frac{\partial^2 \xi}{\partial t^2} dx = \pi a^2 \overline{E} \frac{\partial^2 \xi}{\partial x^2} dx - \frac{\partial \xi}{\partial t} 2\pi a \, dx Z_r, \tag{11}$$

where $\xi$ is the displacement of the cross-section of the rod, $\rho$ is the density of the rod material, $\overline{E} = E(1 - i\eta)$ is Young's modulus for the rod material, a is the radius of the rod, $Z_r$ is the input impedance when the specimen is subject to shear vibrations.

Provided that a plane shear wave is propagated in the specimen, it can be examined as a transmission-line segment which has a length equal to the thickness $l_r$ of the specimen. Under these conditions the impedance $Z_r$ to shear waves can be expressed in terms of the parameters of the specimen material in the following manner:

$$Z_r = -i\rho_r c_r \tan\left(\frac{\omega}{c_p} l_p\right) = r_r + iX_r. \tag{12}$$

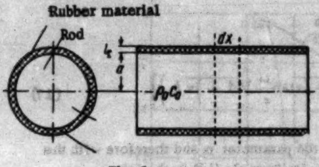

Fig. 1

Here $\rho_r$ is the density of the specimen material, $c_r = \sqrt{\frac{\mu_r (1 - i\eta)}{\rho_r}}$ is the propagation velocity of waves in the specimen, $\mu_r$ and $\eta_r$ are respectively the shear modulus and the shear loss coefficient in the material of the specimen.

For sinusoidal vibrations of the rod Equation (11) can be written in the form

$$\frac{\partial^2 \xi}{\partial x^2} + \bar{k}_1^2 \xi = 0,$$

where

$$\bar{k}_1^2 = \frac{\omega^2 \rho (1 + i\alpha)}{\bar{E}}. \tag{13}$$

Here we have introduced the definition $\alpha = \frac{2Z_r}{\omega \rho a}$.

Thus it follows from the equation that when a rod with a specimen of rubbery material attached to it performs sinusoidal vibrations the rod will have effective parameters which depend upon the impedance of the specimen. These effective parameters are the density and the velocity of a longitudinal wave (and therefore the wave number); these parameters will differ from the corresponding parameters of a rod with no specimen attached to it. The effective parameters of a rod with a specimen are expressed in the following manner in terms of a rod without a specimen and its input impedance [according to Equation (13)]:

$$\rho_1 = \rho (1 + i\alpha), \tag{14}$$

$$\bar{c}_1 = \bar{c} \frac{1}{\sqrt{1 + i\alpha}}. \tag{15}$$

We examined a rod which has a rubbery material glued to it over its entire length, and we found the effective parameters of such a rod. As we have already said above, in making measurements we made use of a rod with a specimen of rubbery material shaped in the form of a ring which was glued onto the rod.

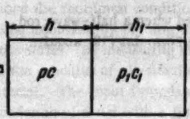

Fig. 2

In computing the input impedance of such a rod it is convenient to consider the entire rod as if it were composed of two rods (Fig. 2): a rod of length h consisting of material that has a density $\rho$ and in which the velocity of longitudinal waves is $\bar{c} = c\sqrt{1 - i\eta}$ (the portion of the rod which has no specimen glued onto it), and a rod of length $h_1$ consisting of a material which has the effective parameters $\rho_1$ and $\bar{c}_1 = \bar{c}\frac{1}{\sqrt{1 + i\alpha}}$ (the portion of the rod which has the specimen glued onto it). From the theory of long transmission lines it is known that the formula for the input impedence of such a composite rod can be written in the form

$$Z_{in} = \frac{-i\rho\bar{c}\tan\frac{\omega}{\bar{c}} h - i\rho_1 \bar{c}_1 \tan\frac{\omega}{\bar{c}_1} h_1}{1 - \frac{\rho_1 \bar{c}_1 \tan\frac{\omega}{\bar{c}_1} h_1}{\rho\bar{c} \cot\frac{\omega}{\bar{c}} h}}. \tag{16}$$

It is convenient to transform Formula (16) into the expression

$$Z_{\text{in}} = R_{\text{in}} + iX_{\text{in}} = -i\rho\bar{c}\tan\left[\frac{\omega}{\underline{c}}h + \arctan\left(\sqrt{1+i\alpha}\tan\frac{\omega}{\underline{c}}\sqrt{1+i\alpha}\,h_1\right)\right]. \tag{17}$$

This formula correlates the input impedance of the rod with the parameter $\alpha$ and therefore with the input impedance $Z_r$ of the specimen. In order to determine $\alpha$ we write Formula (17) in the form:

$$\frac{\omega}{\underline{c}}h_1\sqrt{1+i\alpha}\,\tan\left[\frac{\omega}{\underline{c}}h_1\sqrt{1+i\alpha}\right] = \frac{\omega}{\underline{c}}h_1\tan\left[\operatorname{arc\,tan}\left(\frac{iZ_{\text{in}}}{\rho\underline{c}}\right) - \frac{\omega}{\underline{c}}h\right].$$

Introducing the definition

$$\frac{\omega}{\underline{c}}h_1\sqrt{1+i\alpha} = L_1\sqrt{1+i\eta_1},$$

where $L_1$ and $\eta_1$ are real numbers, we obtain

$$-iL_1\sqrt{1+i\eta_1}\tan(L_1\sqrt{1+i\eta}) = -i\frac{\omega}{\underline{c}}h_1\tan\left[\operatorname{arc\,tan}\left(\frac{iZ_{\text{in}}}{\rho\underline{c}}\right) - \frac{\omega}{\underline{c}}h\right] = r - iX. \tag{18}$$

Knowing $\underline{r}$ and X, it is possible to determine the parameters $L_1$ and $\eta_1$ graphically by means of a chart which is plotted in accordance with Equation (18) (Fig. 3). Taking Equation (13) into account, it is possible to determine the real and imaginary portions of the impedance of the specimen:

$$r_r = \frac{\omega\rho a}{2}\left(\frac{L_1}{\frac{\omega}{c}h_1}\right)^2(\eta_1 - \eta), \qquad X_r = -\frac{\omega\rho a}{2}\left[\left(\frac{L_1}{\frac{\omega}{c}h_1}\right)^2 - 1\right]. \tag{19}$$

Knowing $r_r$ and $X_r$, it is possible to use Formula (12) to determine the elastic parameters $\mu_r$ and $\eta_r$ which are associated with them. The determination of $\mu_r$ and $\eta_r$ can be performed according to the chart described in [3] (as we have done in Section 2 of this paper).

It can be shown that the maximum accuracy in measuring $\mu_r$ and $\eta_r$ is achieved when a half-wave rod is used upon whose lateral surface the test specimen is glued. Under these conditions Formulas (19) acquire the form:

$$r_r = \frac{\omega\rho a}{2}\left[\frac{L_1(h_1+h)}{\pi h_1}\right]^2(\eta_1 - \eta), \qquad X_r = -\frac{\omega\rho a}{2}\left[\left(\frac{L_1(h_1+h)}{\pi h_1}\right)\right]^2 - 1. \tag{20}$$

By measuring the coefficients of reflection from a half-wave rod with a ring-shaped specimen glued onto it and from a half-wave rod without a specimen, it is possible to use Formulas (3) to compute $Z_{\text{in}}$ of the rod with the specimen, and Formulas (8) and (9) to compute $\underline{c}$ and $\eta$ of a free rod. Based upon the computed values of $Z_{\text{in}}$, $\underline{c}$ and $\eta$, Formula (20) is used to determine the values of $r_r$ and $X_r$ for the ring-shaped specimens; based on these values the values of $\mu_r$ and $\eta_r$ are determined for the rubbery material.

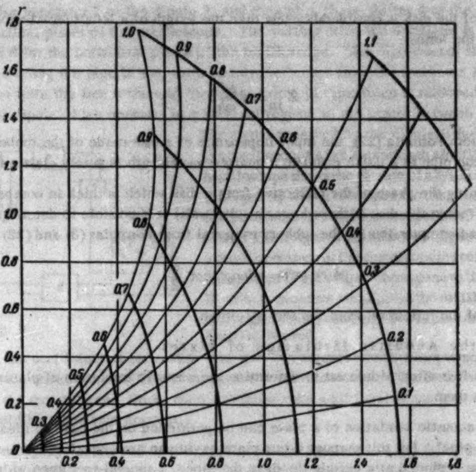

Fig. 3

## 4. Determining the Modulus of All-Sided Compression for Rubbery Materials.

As we know, the modulus of all-sided compression for materials is expressed in terms of the Lamé coefficients in the following manner:

$$K = \lambda + \frac{2}{3}\mu.$$

Since $\mu \ll \lambda$ for rubbery materials, it follows that the modulus of all-sided compression is almost the same as the modulus for a plane wave (the modulus for a plane wave is $\lambda + 2\mu$). It is precisely the quantity $\lambda + 2\mu$ which is determined by means of the device which is described in this paper. For this purpose a specimen of rubbery material shaped in the form of a disk is used in the capacity of the measured object; the disk has a diameter which is equal to the inside diameter of the pipe. The specimen is placed into the pipe, and beyond the specimen conditions are created which correspond to an absolutely rigid wall. Such conditions can be achieved by placing the specimen in the pipe at a depth of a quarter-wavelength below the surface of the water. By measuring the phase of the reflection from the specimen we determine the input impedance and the modulus of all-sided compression (which is associated with the input impedance) of the rubbery material. The input impedance of such a specimen is determined in accordance with the formula for the impedance of a rod with a fixed end:

$$Z_{in} = i\rho c \cot \frac{\omega}{c} h, \qquad (21)$$

where $\rho$ is the density of the specimen material, $\underline{h}$ is the thickness of the disk,

$$c = \sqrt{\frac{\lambda + 2\mu}{\rho}} \approx \sqrt{\frac{\lambda}{\rho}}.$$

If the thickness of the disk is considerably less than the length of a longitudinal wave in the disk, then Formula (21) acquires the form:

$$Z_{\text{in}} = i\frac{\rho c^2}{\omega h}. \tag{22}$$

As can be seen from Formula (22), the input impedance of a disk made of the rubbery test material which is immersed in the pipe to a depth equal to a quarter-wavelength is purely elastic in nature.

Thus be determining the phase of the reflection from a disk which is thick in comparison to the length of a longitudinal wave (when the disk is placed near a solid wall) it is possible to determine the coefficient $K = \lambda = \rho c^2$ of all-sided compression for the rubbery material from Formulas (3) and (22) by using the formula

$$\lambda = \rho c^2 = \omega h\, \rho_0 c_0 \cot \frac{\varphi}{2},$$

where $\varphi$ is the phase of the reflection from the test specimen.

## 5. Determining the Acoustic Insulation of Plates

In hydroacoustics it is often of interest to determine the acoustic insulation of plates when waves are normally incident upon them.

Determining the acoustic insulation of a plate can be performed on the basis of measurements which are made in the "pulse pipe". For this purpose a test plate having an area equal to the area of the inside cross-section of the pipe is placed at a certain depth in the pipe. A special specimen which has an impedance equal to the wave impedance of the water is placed upon the surface of the water. Such a specimen reflects nothing, and thus the plate is in a travelling-wave field. Using the same method as before to determine the reflection coefficient $\beta$ from the plate under these conditions, it is easy to find the energy which has passed through the plate and therefore the acoustic insulation of the plate):

$$\alpha = 1 - |\beta|^2.$$

## 6. Description of the Device and of the Process of Measuring the Reflection Coefficient

The "pulse pipe" metering device consists of a thick-walled vertical pipe filled with water (Fig. 4). A dipole is mounted in the lower portion of the pipe, and the test specimen is placed at the top of the pipe. The entire length of the pipe is surrounded by a sleeve inside of which a cooled or heated solution circulates. The temperature of the solution is controlled in a manner which depends upon the temperature required inside the pipe. From the outside the pipe is covered with thermal insulation so that the temperature established within the pipe will not change during the metering process. The top of the pipe is closed by a cover which is shaped in the form of a double-walled bucket; the same solution which circulated between the walls of the bucket, thus creating the required temperature within the pipe and around the test specimen. The block diagram of the electrical section of the device is shown in Fig. 5. A sinousidal voltage of ultrasonic frequency is fed from the oscillator 1 to the input of the pulse generator 2; a signal in the form of rectangular pulses which are "filled" with oscillations of ultrasonic frequency is simultaneously fed from

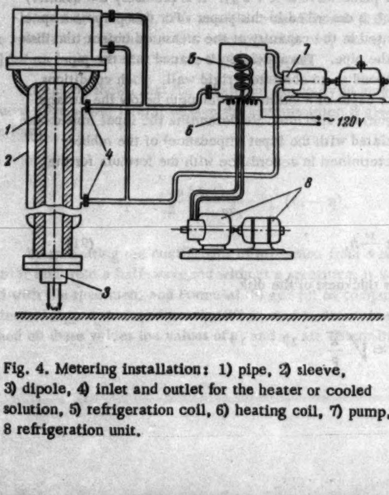

Fig. 4. Metering installation: 1) pipe, 2) sleeve, 3) dipole, 4) inlet and outlet for the heater or cooled solution, 5) refrigeration coil, 6) heating coil, 7) pump, 8 refrigeration unit.

the output of the pulse generator 2 to the dipole 3, and through a phase-shifter 4 to the input of the amplification channel 5 for the vertical plates of the oscilloscope. The voltage from the oscillator is fed to the input of the amplication channel 6 for the horizontal plates of the oscilloscope. The dipole sends the pulses into the pipe which are propagated along the pipe in the water and are reflected from the specimen located in the upper portion of the pipe or from the free surface of the water (when the specimen is removed); the pulses then are reflected back to the dipole which operates in a receiver regime in the pauses between pulse-sending intervals. The signal received by the dipole is fed to the vertical plates of the oscilloscope after appropriate amplification. The screen of the oscilloscope shows the picture of a system of various ellipses (Lissajous figures) which correspond to the successive reflection of pulses from the radiator and from the specimen or the free surface of the water. The height of the Lissajous figures is proportional to the acoustic pressure of the corresponding reflection; the shape and orientation of the ellipse correspond to the phase of the reflection. In order to measure amplitudes the oscilloscope screen is equipped with a grid scale, and only the ellipse corresponding to the first reflection is used.

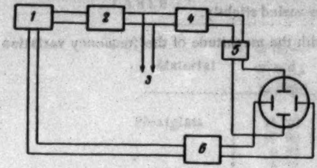

Fig. 5

The fact that the coefficient of reflection from the free surface of the water is equal to (-1) makes it possible to measure the reflection coefficient as the ratio between the amplitudes of waves reflected from the specimen and from the free surface. Under these conditions the additional phase $\varphi = \pi$ of the reflection from the free surface should be taken into account.

The modulus and phase of the reflection coefficient are measured in the following manner. For a specimen immersed in water the picture of the ellipse upon the screen of the oscilloscope is reduced to a straight line by means of a phase-shifter, and the scale indication $\varphi_1$ on the phase-shifter scale is recorded; then the amplitude $a_1$ of the reflected signal is read. When the specimen is removed the straight line is restored to an ellipse by means of the phase-shifter, and the quantity $\varphi_2$ is read from the phase-shifter scale and the signal amplitude $a_2$ is measured.

Based upon the magnitude of the signal amplitude ratio $\left|\frac{a_1}{a_2}\right| = |\beta|$ which represents the modulus of the reflection coefficient, and based upon the phase difference combined with the additional half-wave $\varphi = \varphi_1 - \varphi_2 + \pi$ (the two measurements are made with and without the specimen), the acoustic output impedance of the test specimen is determined according to Formulas (3).

It should be noted that in measuring the modulus of all-sided compression for rubbery material a specimen in the form of a disk is immersed at a depth which is exactly equal to a quarter-wavelength in water. Here the phase of the reflection from a quarter-wave column of water is equal fo $\pi$. As a result the phase of the reflection from such a disk is determined as the phase difference between measurements taken with and without the specimen (without adding a half-wavelength).

When measuring the shear modulus in rubbery materials it is necessary to use rods consisting of material which has losses; in these rods the time required to establish vibrations in a half-wave rod is considerably less than the duration of a pulse. In our measurements we used plexiglass rods. The measurements were performed in the following sequence. A specimen of the test material was glued onto one of two completely identical rods. The rods were first checked by measurements made in the pipe to see if their resonant frequencies were identical (i.e., the frequencies which correspond to a phase $\pi$ for the reflections from the rods). The rods must have identical resonant frequencies. The second rod was used in order to monitor the frequency. The resonant frequency of the rod was determined in the following manner. The tuning knob of the oscillator was adjusted to establish a frequency for which the Lissajous pattern on the screen of the oscilloscope remained constant when the rod was immersed in water and when it was not; such conditions corresponded to a reflection phase $\pi$. Next, the coefficient of reflection $|\beta|$ from the basic rod was measured at the resonant frequency of the control rod; on the basis of this measurement we determined $Z_{in} = R_{in}$ of a rod without a specimen, and then determined $\underline{c}$ and $\eta$ of the rod. At the same frequency we measured $|\beta|$ and $\varphi$ for a rod with a specimen. We determined $\underline{Z_{in}} = R_{in} + iX_{in}$ for a rod with a specimen. Then we computed the parameters of the rubbery material according to the formulas given in Section 3.

It should also be noted that in order to compute the input impedance it is necessary to know the wave impedance of the water in the pipe. The wave impedance $\rho_0 c_0$ in the general case differs from the wave impedance of water in a free medium because of the decrease in the propagation velocity of sound in the pipe which is caused by the pliability of the pipe walls. [4]. Therefore here it is necessary to determine the actual value of the propagation velocity of sound in the pipe directly. The experimental measurements of the velocity of sound in the pipe were performed in the following manner. The variation in the phase of the reflection from the free surface of the water was observed when the frequency was varied slightly.

The variation in the phase of the reflection is associated with the magnitude of the frequency variation by the following relationship:

$$\Delta\varphi = \frac{4\pi l}{c_0}\Delta f,$$

where $l$ is the length of the column of water in the pipe, $c_0$ is the velocity of sound in the pipe, $\Delta f$ is the frequency variation in cps.

From this formula it follows that

$$c_0 = \frac{4\pi l}{\Delta\varphi}\Delta f.$$

In order to assure a greater accuracy in measuring the velocity of sound $c_0$ in water the quantity $\Delta f = \Delta f_n$ is chosen so that the phase variation $\Delta\varphi$ is equal to a multiple of $\pi$ (i.e., $\Delta\varphi = n\pi$, where $n$ is a whole number).

Then we shall have

$$c_0 = \frac{4l}{n}\Delta f_n$$

## 7. The Number in Which Specimens are Mounted in the Pipe and the Effect of the Slot

The accuracy requirements for measuring the impedance of the specimens are rather high. Therefore it is necessary to take into account the possibility of systematic errors. One of the sources of error is the inescapable presence of a ring-shaped slot which is filled with water; this slot is formed around the circumference of the specimen when it is placed into the pipe. The shunting action of the slot depends upon the height of the slot [i.e., upon the depth to which the specimen (the rod) is immersed]. In our measurements, which were made at frequencies of 10-20 kc with a pipe diameter of 22mm, the rods were immersed to a depth of 7-10mm. For such a slot height and at the indicated frequencies the effect of the slot is negligible and can be ignored. Since the diameter of the rod is taken to be 0.1mm less than the diameter of the pipe, The rod is encompassed by a wire ring (in order to maintain the rod at the required level) which lies against the end-face of the pipe when the rod is loaded into the pipe; thus the rod is suspended in the wire ring.

It should be noted that the accuracy with which measurements can be made by means of the device described here is basically limited by the errors introduced by the presence of air bubbles and films which are formed when the surfaces of the specimens and the walls of the pipe are insufficiently moistened with water. Therefore special care is required when the specimens are immersed in the water. When all possible precautions are taken the dispersal of the results of reflection phase measurements does not exceed 2-3°, and the dispersal of the values for the reflection coefficient modulus does not exceed 2-3%.

## 8. Results of Measurements

Below we provide certain experimental results. By means of the "pulse pipe" we measured the velocity of sound and the loss coefficient in plexiglass and ebonite rods. The experiments were performed at frequencies of 9.5-18.5 kc for the purpose of using the indicated rod for subsequent measurements of the complex shear modulus of rubber. In making the measurements we used rods with a diameter of 2.18cm (this diameter corresponds to the inside diameter of the pipe). We prepared a set of half-wave rods for use at various frequencies.

The table shows the results of measuring the velocity $\underline{c}$ of longitudinal waves, Young's modulus E, and $\eta$ the loss coefficient at a temperature of 25°C. Assuming that the velocity of sound in the rods does not depend upon frequency in the indicated frequency range, we conclude that the maximum deviation from the median value of the velocity does not exceed ± 2 %, and for the loss coefficient the deviation does not exceed ± 4 %.

We also performed measurements of the complex shear modulus of rubber.

TABLE

| Material | Length of rod $l$ in cm | Frequency $f$ kc | $c \times 10^{-5}$ cm/sec | $\eta$ | $E \times 10^{-10}$ dynes/cm² |
|---|---|---|---|---|---|
| Plexiglass | 11.70 | 9.50 | 2.22 | 0.0380 | 5.85 |
| | 10.90 | 10.10 | 2.20 | 0.0390 | 5.72 |
| | 9.82 | 11.10 | 2.18 | 0.0395 | 5.62 |
| | 8.75 | 12.40 | 2.17 | 0.0395 | 5.57 |
| | 8.36 | 13.00 | 2.17 | 0.0395 | 5.57 |
| | 7.76 | 14.00 | 2.17 | 0.0395 | 5.57 |
| | 7.50 | 14.80 | 2.22 | 0.0386 | 5.85 |
| | 6.39 | 16.90 | 2.16 | 0.0395 | 5.52 |
| | 6.50 | 17.80 | 2.15 | 0.040 | 5.48 |
| | 5.86 | 18.40 | 2.15 | 0.044 | 5.48 |
| Ebonite | 7.5 | 10.75 | 1.62 | 0.045 | 3.16 |

The graph in Fig. 6 gives an example of the results of measuring the temperature dependence of $\mu_r$ and $\eta_r$ for one type of synthetic rubber in the temperature range of +5° to +25°. On the graph the values of $\mu_r$ and $\eta_r$ are given in relative units. As can be seen from the graphs, the shear modulus decreases with an increase in the temperature, and the loss coefficient varies insignificantly with temperature.

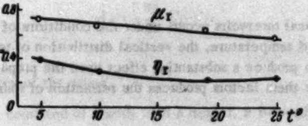

Fig. 6

In conclusion the author expresses his appreciation to Junior Science Associate V. I. Kashina who performed the measurements.

## LITERATURE CITED

[1] H. Kuhl, Oberst and Skudrzyk, Akust. Beih. 3, 421-433 (1953).

[2] E. Meyer and H. Oberst, Akust. Beih. 3, 149-170 (1952); Problems of Modern Physics, Acoustics, (U.S.S.R.) 1953, No. 9, 171.

[3] N. S. Ageeva, I. P. Zhukov, M. A. Isakovich, A. L. Sosedova, Iu. M. Sukharevskii, J. Tech. Phys. (U.S.S.R.) 22, 6, (1952).

[4] D. J. Korteweg, Ann. Physik 5, 525 (1878).

Acoustics Institute of the Academy of Science USSR,
Moscow

Received January 31, 1955

# INVESTIGATION OF ACOUSTIC SHADOW IN A MEDIUM WHICH HAS A VERTICAL SOUND VELOCITY GRADIENT

**A. N. Barkhatov**

**The paper shows the possibility of simulating the vertical distribution of sound velocity in water. The method described here is used for investigating acoustic shadow.**

**The propagation of sound in natural reservoirs occurs under the conditions of an inhomogeneous medium. Besides local fluctuations of density and temperature, the vertical distribution of temperature, of various impurities and of hydrostatic pressure also produce a substantial effect upon the propagation of sound. The vertical sound velocity gradient which is due to these factors produces the refraction of sound (and the various phenomena associated with this refraction).**

**Along with studying the propagation of sound in an inhomogeneous medium under natural conditions, where it becomes necessary to take into account the effect of many factors, it is of interest to perform laboratory investigations for which it is possible to create artificially various types of inhomogeneities which are similar to the inhomogeneities which occur in a natural medium and to study the effect of these inhomogeneities upon the propagation of sound in a purer physical sense.**

**In our experiments we showed that it was possible to simulate a number of cases of the vertical distribution of sound velocity in water by means of thermal effects and by using salt solutions of varying concentrations. In this paper we describe a device for simulating a constant vertical temperature gradient in a water bath and its use for investigating acoustic shadow.**

**Let the water be considered as a laminarly-inhomogeneous medium in which the velocity of sound decreases with depth according to the linear law**

$$c = c_0(1 + \eta z); \ \eta < 0,$$

Acoustics Institute of the Academy of Sciences USSR, Moscow. Received January 30, 1958

where $c_0$ is the velocity of sound at the surface of the water. In that case rays which emanate from the point source S (Fig. 1) at an angle of slip $\chi$ are bent along circular arcs with a radius

$$\rho = \frac{1}{\eta \cos\chi}\,.$$

The ray which is tangent to the surface of the water (the surface is assumed to be plane and to produce mirror-reflection) forms a region of acoustic shadow according to geometric theory.

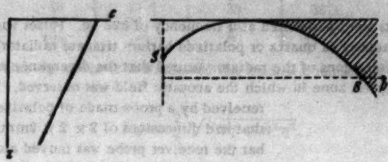

Fig. 1

By means of wave theory [1] it is possible in this case to derive an approximate formula for the intensity of sound in the region of geometric shadow:

$$I_P = I_B \frac{R_0}{R_0 + r} e^{-Ar}, \tag{1}$$

where $I_p$ and $I_B$ are the sound intensities at the points P (shadow) and B (the boundary of the shadow), $R_0$ is the horizontal distance from the point B to the source (Fig. 1), $r$ is the distance BP and

$$A = \frac{5.93}{c_0} \xi^{2/3} f^{1/3},$$

where $\xi = \frac{dc}{dz}$; $f$ is the frequency of the sound.

The experimental device consisted of a bath with a heater, a moveable thermometer, a metering unit, a sound radiator with an oscillator, and a receiver with an amplifier (Fig. 2). The tub was made of organic glass (its length was greater than 300 cm, its width and depth were both 60 cm) and was filled with water. By uniformly heating the surface of the water, a vertical temperature gradient was produced over the depth of the water. The heating unit consisted of an aluminum plate whose dimensions were the same as the surface dimensions of the water; the plate was hung at a small distance (5-10cm) above the surface. Heating coils were uniformly distributed over the plate and the output voltage from an autotransformer was applied to the coils. The required heating regime (i.e., the law governing the time variation of the voltage applied to the coils) was experimentally determined after numerous experiments.

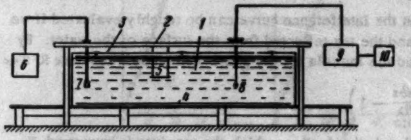

Fig. 2. Experimental device:
1) bath with water, 2) stand with a crossbar, 3) heater, 4) cooling system, 5) moveable thermometer, 6) pulse generator, 7) radiator, 8) probe-receiver, 9) amplifier, 10) electronic oscilloscope.

In a number of tests the water was cooled from the bottom in addition to being heated at the top surface; the cooling was accomplished by a battery of narrow pipes which were laid along the bottom of the tub and through which water at a temperature of 2-4°C flowed. When the cooling and heating units operated together for a period of ~40 hours a stable constant temperature gradient was formed throughout the entire depth of the tub. The temperature of the water at various depths was measured with an accuracy of up to 0.1°C by a laboratory thermometer which was placed at the required height. It is also possible to use several electrical resistance detectors which are connected to an automatic pen in order to record the time variation of the temperature at various depths.

The measurement of temperature in horizontal planes showed that the horizontal temperature gradient was 2-3 times less than the vertical gradient, with the exception of sectors which were adjacent to the front and back of the tub where vertical tubes with cold flowing water were located. Therefore it is possible to consider the water in the tube as a laminarly-inhomogeneous medium and to apply the above-indicated theory to it.

The acoustic measurements were performed at a frequency of 528 kc. Pulses with a duration of 100 microseconds were emitted from the radiator (a quartz or polarized barium titanate radiator) with a repetition frequency of 200 pulses per second. The dimensions of the radiator assured that the divergence of the beam would be approximately 20° in the Frauenhofen zone in which the acoustic field was observed. The acoustic waves were received by a probe made of polarized barium titanate ceramic that had dimensions of 2 x 2 x 2mm. By means of the crossbar the receiver probe was moved along the bath at the required depth. After the voltage obtained from the probe had been amplified it was applied to the vertical plates of the electronic oscilloscope. The acoustic pressure at the place where the probe was located was measured in scale divisions on the screen of the oscilloscope (on the screen of the oscilloscope the direct acoustic signal was clearly segregated from the signals reflected from the bottom and the walls of the tub). Figure 3 shows the experimental distribution curve for the acoustic pressure along the length of the tub. The distribution curve for the pressure along the length of the tub (including the interference region) can in principle also be plotted theoretically. The solution for the wave function then appears [1] in the form of an infinite series whose convergence improves to the degree that we advance into the shadow region. Thus at the shadow boundary a consideration of three terms of the series introduces a correction of the order of only 10% to the result which is obtained if we limit ourselves to just one term. As far as the region of direct sound is concerned, a greater number of terms of the series should be used in order to obtain a correct result. This conclusion agrees qualitatively with the computations of the field in the vicinity of the geometric shadow boundary formed by radiowaves which are propagated in the vicinity of the earth's surface [2].

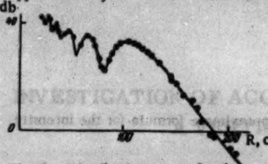

Fig. 3. Distribution curve for the acoustic pressure along the length of the bath when the radiator and receiver are immersed at a depth of 4 cm; $R_0$ = 193 cm; a = 0.5°/cm

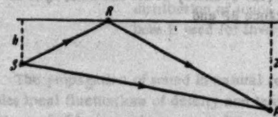

Fig. 4

The positions of the maxima and of the minima on the interference curve can be roughly evaluated if we examine the interference of two rays - the direct ray and the ray reflected from the surface of the water. By assuming that these rays are rectilinear (Fig. 4), we find the formula for the phase difference when $h \ll R$, $z \ll R$:

$$\varphi = \pi\left(\frac{4hz}{R\lambda} - 1\right),$$

where h is the depth at which the radiator is immersed, z is the depth at which the receiver is immersed, R is the horizontal distance between the radiator and receiver, λ is the acoustic wavelength.

In the table the positions of the maxima and of the minima of the interference curve (as calculated according to this formula for the case corresponding to Fig. 3) are compared with experimental data. The divergence between the experimental and theoretical values increases to the degree that the shadow boundary is approached ($R_0$ = 193 cm).

The graphs in Fig. 5 show the sound attenuation in decibels in the geometric shadow region. The distance from the boundary of the shadow is plotted along the horizontal axis. The position of the shadow boundary when a constant velocity gradient is present is computed in an elementary manner, since in that case the sound rays are circular.

TABLE

| Maxima in cm | | Minima in cm | |
|---|---|---|---|
| Experimental | Theoretical | Experimental | Theoretical |
| $R = 22$ | 20.8 | $R = 20$ | 19.0 |
| 27 | 25.4 | 23 | 22.9 |
| 34 | 32.6 | 29 | 28.6 |
| 46 | 45.7 | 38 | 38.1 |
| 64 | 76.2 | 54 | 57.2 |
| 105 | — | 80 | 114.4 |

At the depth h to which the radiator is immersed the shadow boundary is at a distance

$$R_0 = \frac{2}{\eta}\sqrt{2h\eta + h^2\eta^2}.$$

from the radiator.

In our experiments the temperature gradient (and not the velocity gradient) remained constant. Let us make use of the following empirical formula for the dependence of the velocity of sound in fresh water upon temperature:*

$$c = 1410 + 4.21t - 0.037t^2 \ (\text{m/sec}).$$

The sound velocity gradient along the height of the tub is equal to

$$-\xi = \frac{\Delta c}{\Delta z} = (4.21 - 0.074t)\frac{\Delta t}{\Delta z}.$$

If $a = -\frac{\Delta t}{\Delta z}$, then the temperature diminishes with depth according to a linear law,.and the absolute value of the velocity gradient increases according to the same law. Therefore the rays are not bent along the circumference of a circle but are bent according to a more complex curve which can be found graphically or analytically. From the formulas written above it is evident that in order to obtain a constant velocity gradient $\xi$ it is necessary to have a temperature gradient a which decreases with depth in a definite manner.

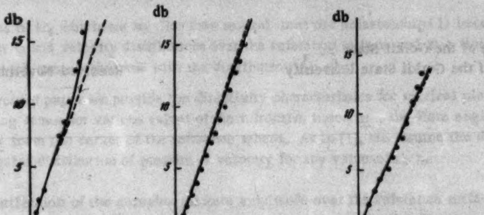

Fig. 5. Curves for the sound attenuation in the region of geometric shadow. I) h = 4 cm, z = 6 cm, $a = 1.2°$/cm; II) h = 4 cm, z = 4 cm, $a = 1.2°$/cm; III) h = 4 cm, z = 6 cm, $a = 0.95°$/cm.

---

* This formula yields values of the velocity which coincide with the experimental values [3] to an accuracy of 1-1.5 m/sec in the region of temperatures close to 30° at which the measurements were performed. The values of $\frac{\Delta c}{\Delta t}$ in the indicated temperature region (computed according to the formula given for the velocity of sound) do not differ by more than 5-10% from the experimental values. Such an error is within the limits of accurary of the experiment.

However in those cases when the velocity gradient along the depth of the tub varies little within the limits of the performed measurements it is possible to make use of its mean value. Computation shows that in our experiments the maximum error in determining the shadow boundary by this method does not exceed 5%. On the graphs the dashed line shows the attenuation as computed according to Formula (1). The experimental data are in good agreement with the theory. Thus we have proven that it is also possible to use the method described here in order to investigate the propagation of sound in other cases of laminarly-inhomogeneous media.

In certain experiments (Fig. 5,I ) we detected an increase in the attenuation of sound as the distance from the shadow boundary increased. The explanation for this phenomenon evidently consists of the fact that when the edge of the tub is approached the horizontal nature of the isotherm is disrupted; this leads to a complication of the entire picture of sound propagation in that region. This conclusion is verified by an investigation of the temperature distribution in the tub for various operating regimes.

Under laboratory conditions an inescapable feature of the work described here is the utilization of large temperature gradients per unit length for the purpose of obtaining a geometric shadow boundary which is within the limits of the tub. However in order to compare the values of the gradients when acoustic waves of varying frequency are propagated it is necessary to examine the temperature gradient over an acoustic wavelength λ:

$$G = a\lambda.$$

Problems involving the propagation of sound in a medium with a constant temperature gradient should be considered similar if the dimensionless temperature gradients G are equal:

$$a_1\lambda_1 = a_2\lambda_2.$$

Thus the investigations which we have performed for comparatively large temperature gradients can be considered useful for smaller gradients as well if the acoustic wavelength is increased proportionally.

## LITERATURE CITED

[1] C. L. Pekereis, J. Acoust. Soc. Am. 18, 295 (1946).

[2] H. Bremmer, Terrestrial Radio Waves, (1949).

[3] N. N. Zubov and N. I. Chigirin, Oceanological Tables (HydrometerologyPress, 1940).

Physico-Engineering Institute of the Gorkii State
University. Acoustics Staff of the Gorkii State University

Received November 9, 1954

# DIRECTIONAL PROPERTIES OF ACOUSTIC SCATTERING LENSES

L. N. Bondareva and M. I. Karnovskii

**The paper computes the angular distribution of the acoustic pressure created by plane-elliptic and plane-hyperbolic acoustic lenses for various values of the refractive index, the flare angle and the imaginary focal distance of the lens.**

[1] provided a method for computing the pressure distribution $P(\varphi)$ and the velocity distribution $V(\varphi)$ on the sperical reference surface of acoustic scattering lenses. It was shown that for sperical plane-elliptic scattering lenses the following relationship holds true for values of $kr_0$ which are greater than several units:

$$\frac{P(\varphi)}{P(0)} \approx \frac{V(\varphi)}{V(0)} \approx \sqrt{\frac{I(\varphi)}{I(0)}}, \tag{1}$$

where $I(\varphi)$ is the acoustic intensity upon the reference surface at the angle $\varphi$, $r_0$ is the radius of the reference sphere and is equal to the focal distance $f$ [1, 2, 3], $k = \omega/c$.

The distribution represented by $I(\varphi)$ was obtained by L. D. Rozenberg [2, 3].

For values of $kr_0$ which are smaller than several units the Relationship (1) becomes non-real, and in that case the pressure and velocity distributions over the reference surface and at a finite distance from the lens do not coincide with one another and with the distribution $\sqrt{I(\varphi)}$.

In this present paper we provide the directivity characteristics for sperical plane-elliptic and plane-hyperbolic scattering lenses for various values of the refractive index $m$, the flare angle $\varphi_m$, the frequency $\omega$ and the distance $r$ from the center of the reference sphere. As in [1], we assume the directivity characteristic to mean the angular distribution of pressure or velocity for any value of $r > r_0$.

If the distribution of the complex pressure amplitude over the reference surface, $\bar{P}_m(\varphi)$, can be written [1, 4] in the form of the series

$$\bar{P}_m(\varphi) = \sum_n C_n P_n(\cos\varphi)\,\bar{\mathfrak{h}}_n = \sum_n C'_n P_n(\cos\varphi), \tag{2}$$

then at a distance $r$ from the center of the reference sphere we have

$$\bar{P}_{rm}(\varphi) = \bar{A} \sum_n C'_n P_n(\cos\varphi) \frac{f_n(jkr)}{f_n(jkr_0)}, \tag{3}$$

where $P_n(\cos\varphi)$ is a Legendre polynomial (a zonal spherical function) of the n-th order, $f_n(jkr)$ is a Stokes polynomial of the n-th order, and $\bar{A} = \frac{r_0}{r}\exp[-jk(r - r_0)]$.

Since $f_n(jkr) \approx 1$ for sufficiently large values of kr, it follows that at great distances from the lens we have

$$\bar{P}_{\infty m}(\varphi) = \bar{A} \sum_n \frac{C'_n P_n(\cos\varphi)}{f_n(jkr_0)}. \tag{4}$$

The directivity characteristic with respect to the pressure is determined by the angular distribution of the effective value of the pressure:

$$P_r(\varphi) = \frac{1}{\sqrt{2}} \, |\bar{P}_{rm}(\varphi)|. \tag{5}$$

As was shown in 1940 by one of the authors of this paper [4], if the expansion of Equation (2) contains spherical functions of orders which do not differ by much, then beginning with the values of $kr_0$ which are of the order of several units the normalized directivity characteristic is practically independent of kr and approaches the angular pressure distribution on the surface $r = r_0$. However if Equation (2) contains components of orders which differ radically, then in practice the indicated stability of the directivity characteristics appears for considerably greater values of $kr_0$.

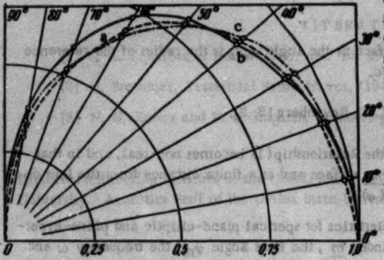

Fig. 1. a) pressure distribution upon the reference sphere according to L. D. Rozenberg, b) the same on the basis of Formula (8), c) the directivity characteristic when kr = ∞ for a plane-elliptic lens and for the conditions m = 0 and $kr_0 = 3$

For sperhical plane-elliptic scattering lenses the pressure distribution on the reference sphere approaches the distribution obtained by L. D. Rozenberg [2] for values of $kr_0$ which are greater than several units (in this paper it is assumed that $kr_0 = 3$):

$$\left.\begin{aligned} \frac{P(\varphi)}{P(0)} &= \frac{(1-m)(\cos\varphi - m)^{1/2}}{(1-m\cos\varphi)^{3/2}} \quad \text{when } \varphi \leqslant \varphi_m, \\ \frac{P(\varphi)}{P(0)} &= 0. \quad \text{when } \varphi > \varphi_m. \end{aligned}\right\} \tag{6}$$

For lenses which are not fully open we have

$$\varphi_m < \varphi_{lim} = \arccos m,$$

where $\varphi_{lim}$ is the limiting flare angle. For fully open lenses we have $\varphi_m = \varphi_{lim}$.

Taking Equation (6) into account we obtain

$$C'_n = P(0)\, \frac{2n+1}{2} \int\limits_{\cos\varphi_m}^{1} \frac{(1-m)(\cos\varphi - m)^{1/2}}{(1-m\cos\varphi)^{3/2}} P_n(\cos\varphi)\, d(\cos\varphi). \tag{7}$$

The integration of (7) was performed by the approximate Simpson method.

Computations show that the Series (2) is a good approximation to the specified Distribution (6) when the Legendre polynomials are taken into account up to the fourth-seventh orders inclusive.

Thus for a fully open plane-elliptic lens with a refractive index of m = 0 the Distribution (6) (Fig. 1, a) can be approximated by a series (Fig. 1, b) in which the essential polynomials are those up to the fourth-fifth orders inclusive:

$$\frac{P(\varphi)}{P(0)} = 0.333P_0 + 0.6P_1 + 0.239P_2 - 0.156P_3 - \\ - 0.119P_4 + 0.093P_5 + 0.08\,P_6 - 0.06P_7. \tag{8}$$

When m = 0.3 the pressure distribution on the reference sphere (Fig. 2, a) can be approximated by the series

$$\frac{P(\varphi)}{P(0)} = 0.198P_0 + 0.440P_1 + \\ + 0.364P_2 + 0.102P_3 - \\ - 0.091P_4 - 0.084P_5 + \\ 0{,}025P_6 + 0.077P_7. \tag{9}$$

For greater values of m, when the pressure distribution becomes more directional, the specific weight of the higher order components increases. Thus for m = 0.8 the Distribution (6) (Fig. 3, a) can be represented by the series (Fig. 3, b)

$$\frac{P(\varphi)}{P(0)} = 0.046P_0 + 0.128P_1 + 0.185P_2 + 0.206P_3 + 0.194P_4 + 0.153P_5 + \\ + 0.096P_6 + 0.041P_7. \tag{10}$$

The normalized directivity characteristics at large distances from the system are given in Figs. 1, 2, and 3 [the curves (c) ] as determined on the basis of Relationships (4) and (5). Figure 2 also shows the normalized directivity characteristic for kr = 6 (i.e., at a distance $r = 2r_0$).

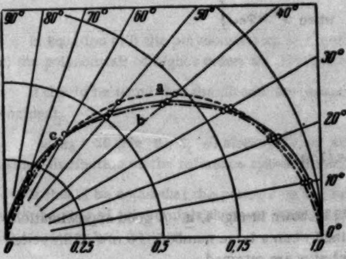

Fig. 2. a) Pressure distribution on the reference sphere according to Formula (9), and the directivity characteristics for kr = 6 (b) and kr = ∞ (c) for a plane-elliptic lens when m = 0.3 and $kr_0 = 3$

Figures 1, 2 and 3 illustrate an interesting property of plane-elliptic scattering lenses - the independence of the directivity characteristics $S_r(\varphi)$ from kr, beginning with values of $kr_0$ of the order of several units; these characteristics are practically coincident with the pressure distribution on the reference sphere. The indicated positions are explained by the fact [4] that in expanding the Series (2) the essential terms are the components which have orders that are close to one another, as well as by the fact that for values of $kr_0$ which are greater than several units the pressure distribution (or the velocity distribution) on the reference sphere is practically determined by the refractive index alone.

For values of m which are close to unity the number of components of the Series (2) that are essential in order to approximate the pressure distribution on the reference sphere increases; under these conditions the stability of $S_r(\varphi)$ is attained at considerably greater values of $kr_0$.

On the basis of the same concepts it follows that the stability of $S_r(\varphi)$ for lenses which are not completely open must also be attained at greater values of $kr_0$. Thus for flare angles of the order of 15-20° the practical onset of stability begins at values of $kr_0$ of the order of 20-25. For small values of $kr_0$ a considerable variation of directivity is observed with a variation in kr.

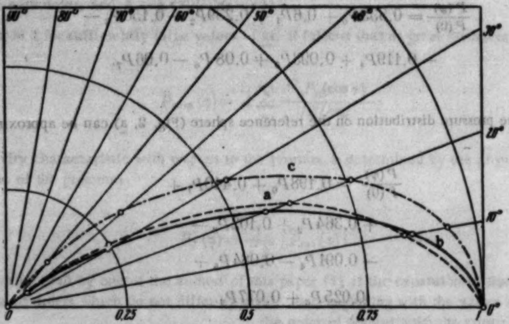

Fig. 3. a) Pressure distribution on the reference sphere according to L. D. Rozenberg, b) the same in accordance with Formula (10), c) directivity characteristic when kr = ∞ for a plane-elliptic lens when m = 0.8 and $kr_0 = 3$.

The energy distribution at the output of a plane-hyperbolic lens is such that the angular distributions of pressure and velocity on the reference sphere differ substantially from one another. However for the purpose of simplifying the computations of $S_r(\varphi)$ we assume here that $P(\varphi)$ and $V(\varphi)$ on the reference sphere are expressed by the relationships obtained by L. D. Rozenberg [3]:

$$\left.\begin{aligned} \frac{P(\varphi)}{P(0)} &= \frac{(m-1)(m-\cos\varphi)^{1/2}}{(m\cos\varphi-1)^{3/2}} && \text{when } \varphi \leqslant \varphi_m, \\ \frac{P(\varphi)}{P(0)} &= 0 && \text{when } \varphi > \varphi_m, \end{aligned}\right\} \tag{11}$$

where

$$\varphi_m \leqslant \varphi_{\lim} = \arccos(1/m).$$

The Pressure Distribution (11) [when m = 3 and $\varphi_m$ = 33°] is shown in Fig. 4, a. A good approximation to this distribution by means of the Series (2) can only be obtained when a large number of terms of the series is used. Thus when the polynomials up to the seventh-order inclusive are retained -

$$\frac{P(\varphi)}{P(0)} = 0.166P_0 + 0.427P_1 + 0.530P_2 + 0.560P_3 + \\ + 0.162P_4 - 0.135P_5 - 0.350P_6 - 0.403P_7 \tag{12}$$

we obtain the curve shown in Fig. 4, b.

It should be noted that when polynomials up to the sixteenth order inclusive are retained in the expansion of (2) the approximation of Equation (11) is still not good enough.

Although Equation (12) is only a very rough approximation of Equation (11), Equation (12) retains the characteristic feature of plane-hyperbolic scattering lenses; this characteristic feature is that the pressure maximum is displaced with respect to the axis by a certain angle. An analysis of the directionality for the pressure distribution described by Equation (12) permits us to draw a series of conclusions which are characteristic for plane-hyperbolic lenses.

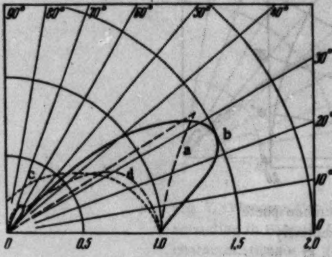

Fig. 4. a) Pressure distribution on the reference sphere according to L. D. Rozenberg, b) the same according to Formula (12), and the directivity characteristics for $kr_0 = 3$ (c) and $kr_0 = 20$ (d) and for a plane-hyperbolic lens when $m = 3$, $\varphi_m = 33$ and $kr = \infty$.

Figure 4 also shows the directivity characteristics at great distances from the system on the basis of assuming that Equation (12) is specified on the reference sphere when $kr_0 = 3$ and $kr_0 = 20$. In Figs. 5, 6 and 7 we have shown $S_r(\varphi)$ for various values of kr and $kr_0$. Analogous curves for a lens with $m = \infty$ and $\varphi_m' = 35°$ are shown in Fig. 8. From the graphs shown here it follows that the $S_r(\varphi)$ of spherical plane-hyperbolic scattering lenses differ substantially from the assumed pressure distribution on the reference sphere for different values of kr. This difference is the greater, the smaller the value of $kr_0$. Thus when $kr_0 = 3$, the directivity characteristic (Fig. 5, b) differs sharply from Equation (12) even in the direct vicinity of the lens ($kr = 6$, i. e., $r = 2r_0$), but does not vary greatly when kr is further increased.

This is caused by the fact that for small values of $kr_0$ a decrease in the components of the Series (3) occur more rapidly with an increase in distance for the components that have the greater values of n. Thus, for $kr_0 = 3$ and $kr = 6$ the directivity characteristic is proportional to the modulus of a complex series for which the real (R) and imaginary (J) components are of the form:

$$\begin{aligned} R &= 0.166P_0 + 0.406P_1 + 0.408P_2 + 0.197P_3 - 0.033P_4 + 0.174P_5 + 0.025P_6 + 0.010P_7, \\ J &= 0.064P_1 + 0.215P_2 + 0.376P_3 + 0.64P_4 - 0.021P_5 - 0.013P_6 - 0.003P_7 \end{aligned} \qquad (13)$$

In Equation (13) the polynomials up to the third order are of fundamental importance, whereas in Equation (12) the polynomials of higher orders are also essential.

It should be noted that the directivity characteristics for $kr > (3 - 5)\, kr_0$ and $kr \to \infty$ are practically coincident.

For $kr_0 = 20$ (Fig. 6), $S_r(\varphi)$ already do not acquire a maximum on the axis and only approach the assumed pressure distribution on the reference sphere for $kr_0 = 50$ (Fig. 7); they are practically independent of kr.

It should be noted that the pressure on the reference sphere is actually expressed by a series with a greater number of polynomials than was assumed above. Therefore the actual functions $S_r(\varphi)$ vary still more with frequency and distance.

On the basis of the computations which we have made, it can be asserted that the directivity characteristics of plane-hyperbolic scattering lenses do not depend upon frequency and distance and approach the pressure distribution on the reference surface beginning with values of $kr_0$ which are not less than 50-100.

The stability of the directivity characteristics of the indicated lenses decreases when

$$m \to 1, \ \varphi_m \to 0 \text{ and } \varphi_m \to \varphi_{lim}$$

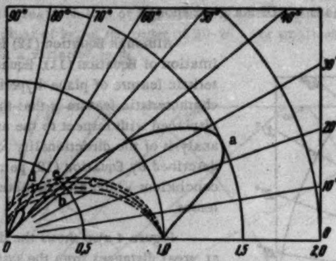

**Fig. 5. a) Pressure distribution on the reference sphere according to Formula (12), and the directivity characteristics for kr = 6 (b), kr = 9 (c), kr = 50, (d) and kr = ∞ (e) for a plane-hyperbolic lens when m = 3, $kr_0$ = 3, $\varphi_m$ = 33°**

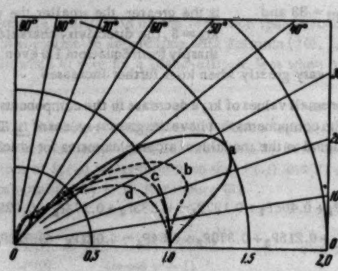

**Fig. 6. a) Pressure distribution on the reference sphere according to Formula (12), and the directivity characteristics for kr = 50 (b), kr = 100 (c), kr = ∞ (d) for a plane-hyperbolic lens when m = 3, $kr_0$ = 20 , $\varphi_m$=33°**

**Figures 9 and 10 compare the theoretical (a) and experimental (b) directivity characteristics of a spherical plane-hyperbolic scattering lens with m = 5 and a flare angle of $\varphi_m$ = 35° when $kr_0$ = 3, kr = 15 (Fig. 9), and $kr_0$ = 20, kr = 100 (Fig. 10).**

**The experimental investigation of various spherical and cylindrical plane-hyperbolic scattering lenses which are made from inclined metallic plates proves the practicability of using such lenses for improving the directional properties of loudspeakers in the high-frequency region.**

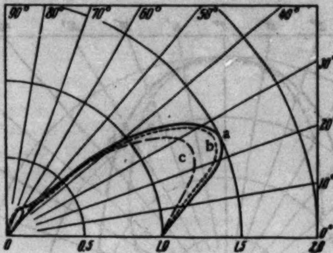

Fig. 7. a) Pressure distribution on the reference sphere according to Formula (12), and the directivity characteristics for $kr = 100$ (b), and kr = oo (c), for a plane-hyperbolic lens when $m = 3$, $kr_0 = 50$ (c) and when $\varphi_m = 35°$.

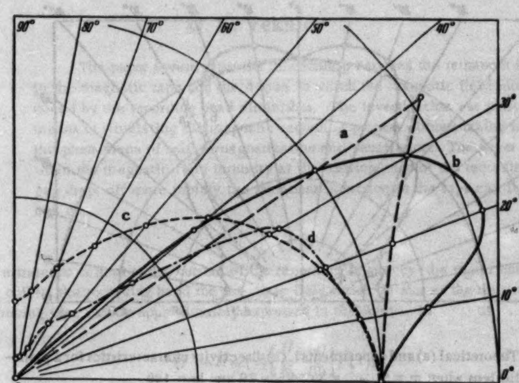

Fig. 8. a) Pressure distribution on the reference sphere according to L. D. Rozenberg, b) the same function as approximated by the Series (2), and the directivity characteristics of a plane-hyperbolic lens with a refractive index of $m = \infty$ and a flare angle of $\varphi_m = 35°$ when $kr_0 = 3$ and $kr = \infty$ (c), and when $kr_0 = 20$ and $kr = \infty$ (d).

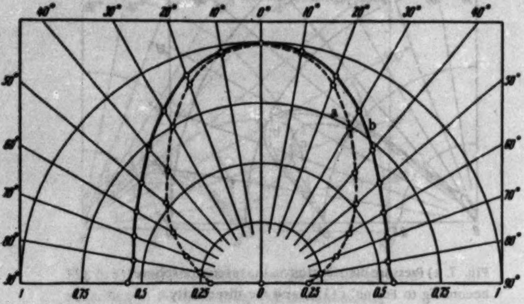

Fig. 9. Theoretical (a) and experimental (b) directivity characteristics for a plane-hyperbolic lens when m = 5, $\varphi_m$ = 35°, $kr_0$ = 3, and kr = 15.

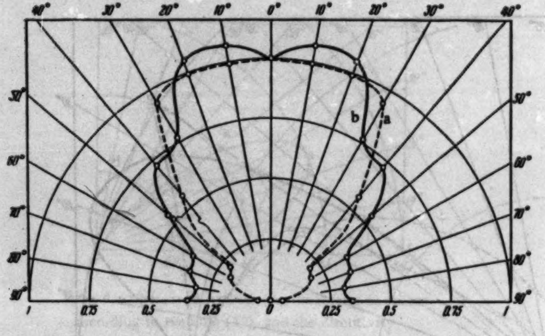

Fig. 10. Theoretical (a) and experimental (b) directivity characteristics for a plane-hyperbolic lens when m = 5, $\varphi_m$ = 35°, $kr_0$ = 20 and kr = 100.

## LITERATURE CITED

[1] L. N. Bondareva and M. L. Karnovskii, Directional Properties of Acoustic Scattering Lenses, I, Trans. Acoustics Comm. 1955, 8, 114-124.

[2] L. D. Rozenberg, Plane-Elliptic Acoustic Lenses, Trans. Acoustics Comm. 1950, 5, 114-119.

[3] L. D. Rozenberg, Plane-Hyperbolic Acoustic Lenses, Trans. Acoustics Comm. 1951, 6, 114-124.

[4] M. L. Karnovskii, Directional Properties of Spherical Radiators, J. Tech. Phys (U.S.S.R.) 10, 12, 970-979, 1940.

Kiev Polytechnical Institute

Received November 15, 1954

# THE EFFECT OF THE MAGNETIC FIELD DISTRIBUTION AT THE RECORDING-HEAD GAP UPON THE LOSS OF REMANENT INDUCTION IN THE TAPE

G. S. Veksler

The paper investigates the relationship between the remanent induction in the magnetic tape and the degree to which the magnetic field intensity produced by the recording head diminishes. The investigation was performed by means of simulating the magnetic recording process without taking into account the phenomena of self-demagnetization and penetration. The paper shows that when the magnetic field intensity at the trailing edge of the recording-head gap drops off more rapidly the remanent induction in the tape can increase by 5-6 db.

When an ultrasonic current and a current of the recording frequency (the signal current) are simultaneously fed through the coil of the recording head the magnetic field which obtains at the trailing edge of the gap and acts upon the moving tape can be approximately expressed in the form ·

$$H = H_m(0)\left[\frac{H_m(x)}{H_m(0)}\right] f(x),$$

where $\underline{x}$ is the path traversed by an element of the tape (this path is measured from the edge of the recording-head gap in the direction of motion of the tape), $H_m(x)$ is the amplitude of the magnetic field intensity at the distance $\underline{x}$ from the edge of the gap when the head is magnetized by the dc ampere-turns $aw_0$, $f(x)$ is the instantaneous value of the sum of the signal ampere-turns and the ultrasonic frequency ampere-turns as normalized to the quantity $aw_0$.

Figure 1 shows the ideal (rectangular) shape for the drop-off of the magnetic field intensity; this drop-off curve leads to the maximum possible remanent induction $B_{ru}$, in the tape for the specified regime (this is evident from Fig. 2,a).

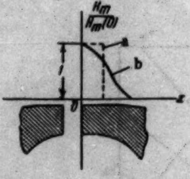

Fig. 1. Magnetic field distribution at the recording-gap: a) ideal, b) actual

The actual shape of the drop-off curve for the magnetic field intensity is shown in Fig. 1 (curve b); from Fig. 2, b which corresponds to the drop-off curve 1, b for the magnetic field it follows that under actual operating conditions the magnitude of the remanent induction $B_{rp}$ will always be less than $B_{ru}$. The difference $B_{ru} - B_{rp}$ shall be defined by $B_{rn}$ and shall be called the loss of remanent induction during the recording process.*

A special paper [2] was devoted to the clarification of the manner in which $B_{rn}(y)$ depends upon the signal frequency; however this paper did not investigate the dependence of $B_{rn}$ upon the quantity $\underline{y}$** (the nature of the magnetic field distribution at the recording-head gap).

A knowledge of the function $B_{rn}(y)$ makes it possible to establish the practicability of manufacturing special recording heads with a decreased value of $\underline{y}$. The importance of studying this problem was indicated by the author of this paper in 1951.

Let us note that a recording head which creates a field with a smaller value of $\underline{y}$ not only makes it possible to obtain a high recording input to the tape at all frequencies but also to improve the recording frequency response.

In this paper we analyze a method for investigating the function $B_{rn}(y)$ and provide the results of such an analysis.

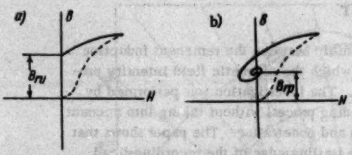

Fig. 2. Remanent induction in the tape for various magnetic field distributions at the trailing edge of the recording-head gap:
a) for an ideal field distribution, b) for an actual field distribution

The investigation was made by means of simulating the magnetic recording process [4]; the simulation method did not require the reproduction of the recorded signal and made it possible to eliminate the effects of the phenomena of self-demagnetization and penetration. All of this made it possible to obtain the relationship between the remanent induction in the tape and the quantity $\underline{y}$ directly during the recording process.

The experimental unit has been described in detail in an earlier paper [4].

As we know [2,4] the magnitude of $B_r$ in the tape depends upon: 1) the tape material, 2) the distribution pattern of the magnetic field and the gap in the recording head, 3) the magnitude of the signal current, 4) the magnitude of the ultrasonic-frequency current, 5) the phase of the signal current, 6) the phase of the ultrasonic-frequency current, 7) the wavelength of the signal on the tape and 8) the wavelength of the ultrasonic bais current on the tape.

In our investigation the wavelength of the signal on the tape was equal to 100 micrometers, and the bias wavelength on the tape was equal to 12.5 micrometers.

The tape material was reproduced with an accuracy of the order of 5% [4] by the simulating substance.

Since for ordinary heads $\underline{y}$ is of the order of 0.5, we investigated fields for which $\underline{y}$ = 0.65, 0.3 and 0.1. The fields which were characterized by a value $y < 0.1$ were not of any particular interest, since in the first place the curve B(H) did not enter the steep portion of the hysteresis loop in this case, and therefore the remanent induction in the tape differed little from the value which obtained when the magnetic field intensity had a rectangular drop-off curve [4], and secondly the practical realization of a head with $y < 0.1$ posed considerable difficulties.

---

* The phenomenon which is associated with the effect of the actual magnetic field distribution at the recording-head gap and which decreases $B_{ru}$ to $B_{rp}$ is also called [1,2] the recording demagnetization.

** $\underline{y}$ is the ratio between adjacent ultrasonic intensity amplitudes which have the same sign (when there is no signal) at the trailing edge of the recording-head gap [4].

Taking into account the quantities which are enumerated in points 3-5 leads to a considerable complication of both the experiment and the analysis of the results because of their diversity and independence of one another. A certain limitation of these quantities over the investigated region was established by taking into account the fact that during the recording process any arbitrary phases of the signal and bias waves were possible and that no recording with noticeable nonlinear distortion was permissible. On this basis the analysis was performed

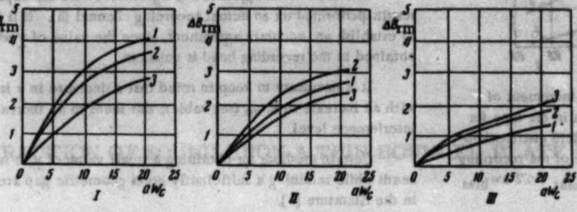

Fig. 3. Family of curves for the dependence of the increment of maximum remanent induction in the tape upon the signal ampere-turns for various bias ampere-turns and various magnetic field distributions at the trailing edge of the recording-head gap.
I) for $y = 0.1$: 1) 55 $aw_{bias}$, 2) 64 $aw_{bias}$, 3) 97 $aw_{bias}$; II) for $y = 0.3$: 1) 40 $aw_{bias}$, 2) 55$aw_{bias}$, 3) 64$aw_{bias}$; III) for $y = 0.65$: 1) 40$aw_{bias}$, 2) 55 $aw_{bias}$, 3) 64 $aw_{bias}$.

within the limits of the comparatively linear sector of the characteristic $\Delta B_{rm} = \varphi(aw_c)$ and for signal and bias wave phases which were such that they yielded the maximum value of the remanent induction increment $aw_C$ for the specified signal ampere-turns $aw_s$ and bias ampere-turns $aw_{bias}$. When there was no signal the remanent induction in the tape which was caused by $aw_{bias}$ was equal to $B_{ro}$. When the bias and signal waves were applied the remanent induction in the tape was $B_r$. The increment due to the signal was $\Delta B_r = B_r - B_{ro}$.

TABLE

Maximum Remanent Induction in the Tape when there is no Signal

| y | $B_{rom}$ in relative units | | |
|---|---|---|---|
| | 40 $aw_{bias}$ | 55 $aw_{bias}$ | 64 $aw_{bias}$ |
| 0.1 | 1.2 | 3.7 | 5.0 |
| 0.3 | 0.8 | 2.1 | 2.5 |

If $B_{ro} \neq 0$, then $B_{rn} = \Delta B_{rm_{y=o}} - \Delta B_{rm}$. However due to the fact that it is not possible to perform a measurement at $y = 0$, it is necessary to determine not the absolute value of $B_{rn}$ but its increment $\Delta B_{rn}$ which is determined as the difference between two values of $\Delta B_{rm}$ or two values of $\underline{y}$ ($\Delta B_{rn} = \Delta B_{rm1} - \Delta B_{rm2}$).

The measurements which were performed for $\Delta B_{rm} = \varphi(aw_c)$ for values of $y = 0.65$, 0.3 and 0.1 permitted us to establish the range of $aw_s$ within which excessive nonlinear distortion did not occur in the simulated tape. This sector was investigated in detail in the range (40-97) of $aw_{bias}$.

The functions $\Delta B_{rm} = \varphi(aw_c)$ for this data are shown in Fig. 3, and Fig. 4 shows the function $\Delta B_{rm} = \psi(y)$. (Here and above, $\Delta B_{rm}$ is plotted in relative units).

The table shows the values of the maximum remanent induction $B_{rom}$ (when there is no signal) for two values of $\underline{y}$ and different values of $aw_{bias}$.

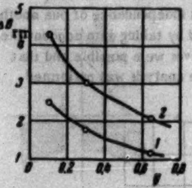

Fig. 4. Maximum increment of remanent induction in the tape for various magnetic field distributions at the trailing edge of the recording-head gap. 1–7 $aw_{bias}$, 2–22 $aw_{bias}$.

From the curves shown in Fig. 4 it follows that when $\gamma$ is decreased from 0.5 to 0.1 in the recording head the output (due to the decrease in $B_{rn}$) increases by 5-6db (at a tape speed of 0.5m/sec, a signal frequency of 5,000 cps and an ultrasonic frequency of 40,000 cps).

The result is in approximate agreement with the experimental results performed on an actual recording channel [5]. It is impossible to establish an accurate agreement, since the value of $\gamma$ which Camras obtained in the recording head is unknown.

It is necessary to keep in mind that a decrease in $\gamma$ is associated with an increase in $B_{rom}$ (see table); this leads to an increase in the interference level.

Certain methods for obtaining a small value of $\gamma$ in recording heads while retaining a sufficiently great geometric gap are given in the literature [5].

In conclusion the author considers it his duty to express his appreciation to N. D. Radomskii for his help in performing the measurements.

## LITERATURE CITED

[1] C. N. Porto, The Basic Factors Which Determine the Frequency Response in Magnetic Recording, Trans. Acoustics Comm. Acad. Sci. USSR, Collection 1951 No. 6.

[2] O. W. Muckenhirn, Recording Demagnetization in Magnetic Tape Recording, P.I.R.E. 1951, 39, 8.

[3] G. S. Veksler, "The visualization of the dynamic processes which occur in ferromagnetic material during magnetic recording," Radiotekhnika 1952, 7, No. 1.

[4] G. S. Veksler, "Oscillographic investigation of the elements involved in the process of magnetic recording when AC biasing current is used," Radiotekhnika 1953, 8, No. 6.

[5] M. Camras, New Magnetic - Recording Head J. S. M. P. T. E. 1952, 58, No. 1.

Kiev Institute of Cinema Engineers

Received March 5, 1954

# DIFFRACTION OF SOUND UPON A THIN BOUNDED PLATE IN LIQUID

L. M. Liamshev

**The paper examines the problem involved in the diffraction of sound upon a thin bounded plate in liquid; the analysis takes into account the longitudinal and flexural vibrations of the plate.**

**It is shown that at certain angles of incidence the passage of the sound through the plate is observed, as well as intense scattering in a direction opposite to the direction of the incident wave (this constitutes so-called non-mirrorlike reflection).**

**In papers which have been published up to now on the subject of sound scattering by plates [1, 2, 3] the authors only took into account flexural vibrations of the plate and did not take into account its transverse compression vibrations. In this paper we take both types of vibrations into account.**

**Let a plane monochromatic wave $\exp[ik_x x - ik_z z]$, where $k_x = k\sin\theta$, $k_z = k\cos\theta$ (the factor $\exp[i\omega t]$ is omitted) be incident at a certain angle upon a thin plate (see figure) which is fastened to an immovable infinite screen and is placed in liquid in the half-space $z > 0$.**

**Let us find the wave fields $p_1(x, z)$ and $p_2(x,z)$ which correspond to the upper and lower half-spaces respectively.**

**The rectangular system of coordinates $x$, $y$, $z$ is selected as shown in the figure; we assume that the plate is infinite in the $y$ direction and occupies the interval $-d > \xi > d$ along the $x$ axis.**

**The velocity of the normal displacements of the upper surface of the plate is described by the following equation of motion [4] for flexural or antisymmetrical vibrations:**

$$g\frac{\partial^4 v}{\partial x^4} - \omega^2 m_s v = -i\omega(p_1 - p_2)_{z=0} \qquad (1)$$

and for transverse compression vibrations or symmetrical vibrations the equation [5]

$$c_1^2 \frac{\partial^2 v_1}{\partial x^2} + \omega^2 v_1 = \frac{-i\omega^2\sigma_1^2 a}{E_1}\left(\frac{p_1 + p_2}{2}\right)_{z=0} \tag{2}$$

applies, provided certain boundary conditions at the points x = ± d are satisfied. For simplicity we shall assume that these conditions are self-conjugate.

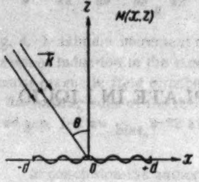

In Formulas (1) and (2) $\rho_s$ is the density of the plate material, 2a is its thickness; $E_1$ is Young's modulus, $\sigma_1$ is the Poisson coefficient of the plate material, $c_1$ is the velocity of longitudinal waves in the plate, $m_s = 2a\rho_s$ is the mass of the plate per unit area, $g = \frac{2}{3}E_1a^3$ is the cylindrical rigidity of the plate.

The boundary conditions on both surfaces of the plate (as well as the quenchability requirements [6] can be satisfied if we seek a solution for the wave equation $\Delta p + k^2 p = 0$ in the form

$$p_1 = \exp[ik_x x - ik_z z] + \exp[ik_x x + ik_z z] - X(x, z) - X_1(x, z), \tag{3}$$

$$p_2 = +X(x, -z) - X_1(x, -z), \tag{4}$$

where

$$X(x, z) = \frac{\omega\rho}{4}\int_{-d}^{+d} v(\xi) H_0^{(1)}(kR)\, d\xi, \tag{5}$$

$$X_1(x, z) = \frac{\omega\rho}{4}\int_{-d}^{+d} v_1(\xi) H_0^{(1)}(kR)\, d\xi, \tag{6}$$

$$R = \sqrt{(x-\xi)^2 + z^2}. \tag{7}$$

Thus the problem of determining the wave fields $p_1$ and $p_2$ reduces to finding the velocity of the normal displacements of the plate surfaces.

Substituting (5) and (6) into (3) and (4) and then into (1) and (2), we obtain the following integro-differential equations for the velocities v(x) and $v_1$(x):

$$g\frac{\partial^4 v}{\partial x^4} - \omega^2 m_s v = -i\omega\left[2\exp(ik_x x) - \frac{\omega\rho}{2}\int_{-d}^{+d} v(\xi) H_0^{(1)}(kr)\, d\xi\right], \tag{8}$$

$$c_1^2 \frac{\partial^2 v_1}{\partial x^2} + \omega^2 v_1 = -\frac{i\omega^2\sigma_1^2 a}{E_1}\left[\exp(ik_x x) - \frac{\omega\rho}{4}\int_{-d}^{+d} v_1(\xi) H_0^{(1)}(kr)\, d\xi\right], \tag{9}$$

where

$$r = |x - \xi|. \tag{10}$$

The solution of these integro-differential equations can be reduced to the solution of linear algebraic equations if we expand the displacement velocities and the pressures into series based upon the intrinsic vibration functions of the plate in a vacuum.

Let $\psi_n(x)$ and $\psi_{(1)n}(x)$ be normalized intrinsic functions which satisfy the equations

$$g\,\frac{\partial^4\psi_n(x)}{\partial x^4} - \omega_n^2\, m_s\psi_n(x) = 0, \tag{11}$$

$$c_1^2\,\frac{\partial^2\psi_{(1)n}(x)}{\partial x^2} + \omega_{(1)n}^2\psi_{(1)n}(x) = 0 \tag{12}$$

and the selected boundary conditions.

In Equations (11) and (12) $\omega_n$ and $\omega_{(1)n}$ are the intrinsic frequencies of the flexural vibrations and the transvense compression vibrations for the plate in a vacuum.

Expanding the velocities of the normal displacements $v(x)$, $v_1(x)$ and the pressures $p_1$ and $p_1$ into series based upon the intrinsic functions, we have

$$v(x) = \sum_{n=1}^{\infty} b_n\psi_n(x), \tag{13}$$

$$v_1(x) = \sum_{n=1}^{\infty} b_{(1)n}\psi_{(1)n}x, \tag{14}$$

$$2\exp[ik_x x] = \sum_{n=1}^{\infty} G_n\psi_n(x), \tag{15}$$

$$\exp[ik_x x] = \sum_{n=1}^{\infty} G_{(1)n}\psi_{(1)n}(x), \tag{16}$$

where

$$G_n = 2\int_{-d}^{+d}\psi_n(x)\exp(ik_x x)\,dx, \tag{17}$$

$$G_{(1)n} = \int_{-d}^{+d}\psi_{(1)n}(x)\exp(ik_x x)\,dx \tag{18}$$

Substituting these series into Equations (8) and (9) we obtain:

$$\sum_{n=1}^{\infty} m_s(\omega_n^2 - \omega^2)\,b_n\psi_n(x) = -i\omega\Big[\sum_{n=1}^{\infty} G_n\psi_n(x) - \\ - 2\sum_{n=1}^{\infty} b_n\frac{\omega\rho}{4}\int_{-d}^{+d}\psi_n(\xi)\,H_0^{(1)}(kr)\,d\xi\Big], \tag{19}$$

$$\sum_{n=1}^{\infty}(\omega_{(1)n}^2-\omega^2)\,b_{(1)n}\psi_{(1)n}(x)=\frac{i\omega^2\sigma_1^2 a}{E_1}\Big[\sum_{n=1}^{\infty}G_{(1)n}\psi_{(1)n}(x)-$$
$$-\sum_{n=1}^{\infty}b_{(1)n}\frac{\omega\rho}{4}\int_{-d}^{+d}\psi_{(1)n}(\xi)\,H_0^{(1)}(kr)\,d\xi\Big]. \tag{20}$$

Expanding the integrals in the right-hand side into series with respect to the intrinsic functions, we obtain

$$\frac{\omega\rho}{4}\int_{-d}^{+d}\psi_n(\xi)\,H_0^{(1)}(kr)\,d\xi=\sum_{k=1}^{\infty}Z_{kn}(\omega)\,\psi_k(x), \tag{21}$$

$$\frac{\omega\rho}{4}\int_{-d}^{+d}\psi_{(1)n}(\xi)\,H_0^{(1)}(kr)\,d\xi=\sum_{k=1}^{\infty}Z_{(1)kn}(\omega)\,\psi_{(1)k}(x), \tag{22}$$

where

$$Z_{kn}(\omega)=\frac{\omega\rho}{4}\int_{-d}^{+d}\int_{-d}^{+d}\psi_n(\xi)\,\psi_k(x)\,H_0^{(1)}(k\,|x-\xi|)\,d\xi\,dx, \tag{23}$$

$$Z_{(1)kn}(\omega)=\frac{\omega\rho}{4}\int_{-d}^{+d}\int_{-d}^{+d}\psi_{(1)n}(\xi)\,\psi_{(1)k}(x)\,H_0^{(1)}(k\,|x-\xi|)\,d\xi\,dx. \tag{24}$$

Substituting (21) and (22) into (19) and (20) and then multiplying both sides of the equations by $\psi_n(x)$ and $\psi_{(1)n}(x)$ respectively and integrating with respect to $\underline{x}$ over the limits of the plate, we shall have:

$$m_s(\omega_n^2-\omega^2)\,b_n=-i\omega\Big[G_n-2\sum_{k=1}^{\infty}b_kZ_{kn}(\omega)\Big], \tag{25}$$

$$(\omega_{(1)n}^2-\omega^2)\,b_{(1)n}=\frac{i\omega^2\sigma_1^2 a}{E_1}\Big[G_{(1)n}-\sum_{k=1}^{\infty}b_{(1)k}Z_{(1)kn}(\omega)\Big]. \tag{26}$$

Equations (25) and (26) can be rewritten thus:

$$b_nZ_n=G_n-2\sum_{k=1}^{\infty}b_kZ_{kn}(\omega), \tag{27}$$

$$b_{(1)n}Z_{(1)n}=G_{(1)n}-\sum_{k=1}^{\infty}b_{(1)k}Z_{(1)kn}(\omega), \tag{28}$$

where

$$Z_n = i\frac{m_s}{\omega}(\omega_n^2 - \omega^2), \tag{29}$$

$$Z_{(1)n} = -i\frac{E_1}{\omega^2\sigma_1^2 a}(\omega_{(1)n}^2 - \omega^2). \tag{30}$$

The coefficients $b_n$, $b_{(1)n}$, $G_n$ and $G_{(1)n}$ which obtain for the intrinsic functions $\psi_n(x)$ and $\psi_{(1)n}(x)$ shall be called "amplitudes". Then $Z_n$ and $Z_{(1)n}(\omega)$ can be called inpedances, and $Z_{kn}(\omega)$ and $Z_{(1)kn}(\omega)$ can be called "mutual impedances"; here the latter quantities characterize the mutual coupling between the normal vibrations of the plate (this coupling is due to the presence of the liquid).

It is possible to segregate terms with the number $k = n$, in the expressions $\sum\limits_{k=1}^{\infty} b_k Z_{kn}(\omega)$ and $\sum\limits_{k=1}^{\infty} b_{(1)k} Z_{(1)kn}(\omega)$, i.e.,

$$\sum_{k=1}^{\infty} b_k Z_{kn} = b_n Z_{nn} + \sum{}' b_k Z_{kn}, \tag{31}$$

$$\sum_{k=1}^{\infty} b_{(1)k} Z_{(1)kn} = b_{(1)n} Z_{(1)nn} + \sum{}' b_{(1)k} Z_{(1)kn}. \tag{32}$$

In the case where the dimensions of the plate are large in comparison to the wavelength in the liquid and where, practically speaking, only normal vibrations of a relatively high order are excited, the mutual interaction between the vibrations can be neglected [7]. Then

$$\sum{}' b_k Z_{kn} \to 0 \text{ and } \sum{}' b_{(1)k} Z_{kn} \to 0. \tag{33}$$

Substituting (33) into (27) and (28), we obtain the following approximate expressions for the coefficients $b_n$ and $b_{(1)n}$:

$$b_n = \frac{G_n}{Z_n + 2Z_{nn}}, \tag{34}$$

$$b_{(1)n} = \frac{G_{(1)n}}{Z_{(1)n} + Z_{(1)nn}}. \tag{35}$$

Now it is possible to write the final expressions for the fields $\chi(x,z)$, and $\chi_1(x,z)$. Substituting (34) and (35) into (13) and (14) and then into (5) and (6), and making use of (17) and (18), we obtain

$$\begin{aligned} \mathrm{X}(x, z) \approx \frac{\omega\rho}{2}\sum_{n=1}^{\infty}\frac{1}{Z_n + 2Z_{nn}}\int_{-d}^{+d}\psi_n(\xi')\exp(ik_x\xi')\,d\xi' \times \\ \times \int_{-d}^{+d}\psi_n(\xi)\,H_0^{(1)}\left(k\sqrt{(x-\xi)^2 + z^2}\right)d\xi, \end{aligned} \tag{36}$$

$$X_1(x, z) \approx \frac{\omega\rho}{4} \sum_{n=1}^{\infty} \frac{1}{Z_{(1)n} + Z_{(1)nn}} \int_{-d}^{+d} \psi_{(1)n}(\xi') \exp(ik_x\xi')\, d\xi' \times$$
$$\times \int_{-d}^{+d} \psi_{(1)n}(\xi)\, H_0^{(1)}\left(k\sqrt{(x-\xi)^2 + z^2}\right) d\xi. \tag{37}$$

In the particular case of a hinge-connected plate the intrinsic functions are of the form:

$$\psi_n(x) = \frac{1}{\sqrt{d}} \sin\left(\frac{\pi n x}{2d}\right), \qquad \psi_{(1)n} = \frac{1}{\sqrt{d}} \sin\left(\frac{\pi n x}{2d}\right). \tag{38}$$

Examining the field at a distance $R \gg d$, it is possible to assume that

$$H_0^{(1)}(kR) \approx \sqrt{\frac{2}{\pi k R_0}} \exp\left[i\left(kR_0 - \frac{\pi}{4}\right)\right] \exp(-i\varkappa_x\xi), \tag{39}$$

where

$$R_0 = \sqrt{x^2 + z^2}, \qquad \varkappa_x = k\frac{x}{R_0} = k \sin\theta'. \tag{40}$$

then

$$X(x, z) \approx \frac{i\omega\rho}{4} \sqrt{\frac{2}{\pi k R_0}} \exp\left[i\left(kR_0 - \frac{\pi}{4}\right)\right] \sum_{n=1}^{\infty} \frac{\omega}{m_s} \frac{-2d}{\omega_n^2 - 2\frac{i\omega}{m_s} Z_{nn} - \omega^2} \times$$
$$\times \left[\frac{\sin\left(\frac{\pi n}{2} + k_x d\right)}{\frac{\pi n}{2} + k_x d} - \frac{\sin\left(\frac{\pi n}{2} - k_x d\right)}{\frac{\pi n}{2} - k_x d}\right] \left[\frac{\sin\left(\frac{\pi n}{2} + \varkappa_x d\right)}{\frac{\pi n}{2} + \varkappa_x d} - \frac{\sin\left(\frac{\pi n}{2} - \varkappa_x d\right)}{\frac{\pi n}{2} - \varkappa_x d}\right], \tag{41}$$

$$X_1(x, z) \approx \frac{i\omega\rho}{4} \sqrt{\frac{2}{\pi k R_0}} \exp\left[i\left(kR_0 - \frac{\pi}{4}\right)\right] \sum_{n=1}^{\infty} \frac{a}{E_1} \frac{\omega^2 \sigma_1^2 d}{\omega_{(1)n}^2 + i\omega^3 \frac{a}{E_1} \sigma_1^2 Z_{(1)nn} - \omega^2} \times$$
$$\times \left[\frac{\sin\left(\frac{\pi n}{2} + k_x d\right)}{\frac{\pi n}{2} + k_x d} - \frac{\sin\left(\frac{\pi n}{2} - k_x d\right)}{\frac{\pi n}{2} - k_x d}\right] \left[\frac{\sin\left(\frac{\pi n}{2} + \varkappa_x d\right)}{\frac{\pi n}{2} + \varkappa_x d} - \frac{\sin\left(\frac{\pi n}{2} - \varkappa_x d\right)}{\frac{\pi n}{2} - \varkappa_x d}\right]. \tag{42}$$

From Expressions (41) and (42) it is evident that a portion of the wave is scattered and a portion of the wave passes through the plate. A considerable portion of the energy is scattered in a direction which is opposite to the direction of the incident wave. This direction corresponds to the condition $\omega = \omega_n$, $\pi n = k_x d = -\varkappa_x d$, or $\omega = \omega_{(1)n}$, $\pi n = k_x d = -\varkappa_x d$.

The scattering in this direction is so-called non-mirrorlike reflection [5].

Thus, in contrast to an absolutely rigid immovable plate, a plate which is capable of performing vibrations when an acoustic wave is incident upon it at certain angles not only produces scattering in the "mirror" direction but also in the direction which is opposite to the direction of the incident wave; it also allows a portion of the acoustic energy to pass through it.

In conclusion I express my deep appreciation to G. D. Maliuzhinets for his valuable advice.

## LITERATURE CITED

[1] G. D. Maliuzhinets and N. S. Ageeva, Report of the Supervisory Board for the Construction of the Palace of Soviets, 1946.

[2] V. G. Volkov, J. Tech. Phys. (U.S.S.R.) 23, 5, 853-864 (1953).

[3] J. Joung, J. Acoust. Soc. Am. 26, 485-492 (1954).

[4] F. Morz, Vibrations and Sound (State Tech. and Theor. Lit. Press, Moscow-Leningrad, 1949).

[5] L. M. Liamshev, Doklady Akad. Nauk SSSR, 99, No. 5, 719-721 (1954).

[6] G. D. Maliuzhinets, Doklady Akad. Nauk SSSR 78, 3, 439 (1951)

[7] M. Lax, J. Acoust. Soc. Am. 16, 5-14 (1944).

Acoustics Institute of the Academy of Science, USSR, Moscow

Received Marcy 17, 1955

# THE RADIATION OF SOUND BY THE VIBRATING BOUNDARIES OF AN ARBITRARY WEDGE. PART I.

G. D. Maliuzhinets

**The Sommerfeld integral is used to obtain an accurate solution for the sound pressure field which is caused by the vibrations of the boundaries of a wedge-shaped region. The case when the velocity of the vibratory motion on each of the two boundaries is constant is examined in greater detail. The relationship between the solutions of the given problem and the problem of diffraction upon a rigid wedge is indicated.**

## 1. Posing the Problem

Let two rigid half-planes form the boundary of a wedge-shaped region, $-\Phi < \varphi < \Phi$, and let this region be filled with a medium in which acoustic waves can be propagated (Fig. 1).

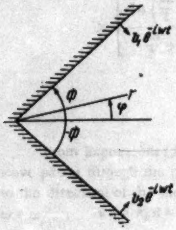

Fig. 1

Each of the boundary half-planes performs small sinusoidal vibrations in such a way that acoustic waves are radiated in the region $\Phi < \varphi < \Phi$.

Let the velocity of the vibratory motion of the boundary $v_1 e^{-i\omega t}$ be equal to $\varphi = \Phi$, and the vibratory velocity for the boundary $v_2 e^{-i\omega t}$; be equal to $\varphi = \Phi$; the positive direction for both velocities is assumed to be into the region. The velocity amplitudes $v_1$ and $v_2$ shall be assumed constant along each boundary, although the method of solution used below is also applicable to the case of a sinusoidal velocity distribution along the boundaries.

The problem being examined here consists of finding the forced vibration which is excited in the region $-\Phi < \varphi < \Phi$ by the vibrations of the boundaries.

In the case of forced vibrations the unknown sound pressure field must be of the form $P = pe^{-i\omega t}$, where p is a function solely of the spacial coordinates, so that the problem can be directly formulated for the complex amplitude p which satisfies the differential equation $\Delta p + k^2 p = 0$ ($\frac{\omega}{c} = k$, c is the velocity of sound).

In the sound field the relationship between the pressure P and the velocity $v = Ve^{-i\omega t}$ in the direction n is given by the basic acoustics equation

$$\rho \frac{\partial V}{\partial t} = -\frac{\partial P}{\partial n} \quad (\rho \text{ is the density of the medium})$$

and therefore, since we have assumed a time dependence which obeys the law $e^{-i\omega t}$, we have

$$v = \frac{1}{ik\rho c}\frac{\partial p}{\partial n}.$$

Assuming n is the internal normal to the boundary and noting that $\frac{\partial}{\partial n_{(\varphi=\Phi)}} = -\frac{1}{r}\frac{\partial}{\partial \varphi}$, for the upper boundary and $\frac{\partial}{\partial n_{(\varphi=-\Phi)}} = \frac{1}{r}\frac{\partial}{\partial \varphi}$, for the lower boundary, we can write the boundary conditions for our problem in the following way:

$$-\frac{1}{ik\rho c r}\frac{\partial p}{\partial \varphi} = v_1, \quad \text{when} \quad \varphi = \Phi,$$

$$\frac{1}{ik\rho c r}\frac{\partial p}{\partial \varphi} = v_2, \quad \text{when} \quad \varphi = -\Phi.$$

The problem being examined here is a particular case of the general problem involving forced vibrations in an arbitrary region for which a singular solution requires the imposition of still another supplementary condition which consists of the quenchability principle [1,2].

In accordance with this principle the solution of the problem p (x, y, z; k) which represents an analytical function of the parameter k must be bounded in the region $\Phi \le \varphi \le \Phi$ for some complex value of k (and for values which lie in a certain proximity of this value) which is located in the region

$$|k| > 0; \; 0 < \arg k < \pi^*$$

The equation, the boundary conditions, the bounding requirements and the requirement of single-valuedness on the boundary of the wedge determine a singular solution of the problem which has been posed here.

Due to the linearity of the problem the unknown sound pressure $p(r, \varphi)$ can be represented in the form $p = p_1 + p_2$, where $p_1$ is the pressure caused by the vibrations of the upper boundary $\varphi = \Phi$ alone, and $p_2$ is the pressure due to the vibrations of the lower boundary $\varphi = -\Phi$ alone. Here $p_1$ satisfies the boundary conditions

$$-\frac{1}{ikr\rho c}\frac{\partial p_1}{\partial \varphi} = v_1, \quad \text{when } \varphi = \Phi; \qquad \frac{\partial p_1}{\partial \varphi} = 0, \quad \text{when} \quad \varphi = -\Phi,$$

and $p_2$ satisfies the conditions

$$\frac{\partial p_2}{\partial \varphi} = 0, \quad \text{when } \varphi = \Phi; \qquad \frac{1}{ik\rho c r}\frac{\partial p_2}{\partial \varphi} = v_2, \quad \text{when} \quad \varphi = -\Phi.$$

It is convenient to find the function $S(r, \varphi)$, (which is proportional to $p_1$) first instead of finding $p_1$ and $p_2$; the result is that we obtain

$$p_1(r, \varphi) = v_1 \rho c S(r, \varphi)$$

---

* In the case of an arbitrary region the solution could prove to be unbounded outside of the region $\frac{\pi}{4} < \arg k < \frac{3\pi}{4}$.

The function $S(r, \varphi)$, which represents the pressure caused by the vibrations of the boundary $\varphi = \Phi$ (these vibrations occur with a velocity that corresponds to the unit amplitude of the pressure in the travelling plane wave), satisfies the boundary conditions

$$-\frac{1}{ikr}\frac{\partial S}{\partial \varphi} = 1, \text{ when } \varphi = \Phi; \qquad \frac{\partial S}{\partial \varphi} = 0, \text{ when } \varphi = -\Phi. \tag{1}$$

In view of the symmetry of the problem with respect to $\varphi$, the function $S(r, -\varphi)$ is proportional to the function $p_2(r, \varphi)$; thus we have

$$p_2(r, \varphi) = v_2 \rho c S(r, -\varphi).$$

Therefore the unknown solution $p(r, \varphi)$ can be expressed by the formula

$$p(r, \varphi) = \rho c\,[v_1 S(r, \varphi) + v_2 S(r, -\varphi)] \tag{2}$$

in terms of the function $S(r, \varphi)$ which also satisfies the equation

$$\Delta S + k^2 S = 0, \tag{3}$$

the quenchability condition and the Boundary Conditions (1).

The function $S(r, \varphi)$ shall be sought in the form of a Sommerfeld [3] integral

$$S(r, \varphi) = \frac{1}{2\pi i}\int_{\gamma} \exp\,[-ikr\cos(\varphi - z)]\,s(z)\,dz, \tag{4}$$

which represents a superposition of the plane waves $s(z)\exp[-ikr\cos(\varphi - z)]dz$ that are incident from infinity upon the edge $r = 0$ of the wedge at the complex angles $\varphi = z$. The path of integration (which consists of two loops) is shown in Fig. 2, where the lined areas indicate the regions within which the real portion of the quantity $-ik\cos(\varphi - z)$ is negative for real positive $\underline{k}$.

The path of integration $\gamma$ depends upon $\varphi$ and is displaced when this quantity varies. Therefore we should write $\gamma_\varphi$ instead of $\gamma$. However for brevity in notation we shall assume the subscript $\varphi$ without writing it explicity.

In order to solve the problem it is necessary to find a function which correlates the amplitude $s(z)$ with the angle in such a way that the integral (4) satisfies the differential equation, the boundary conditions and the quenchability principle.

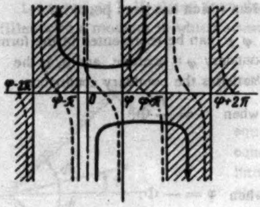

Fig. 2

In order to satisfy Equation (3) and the quenchability principle it is sufficient to impose very simple limitations upon the function $s(z)$; we shall proceed to do this first. After that it is still necessary to find a specific form of this function that will satisfy the boundary conditions. This will be done in the next section.

Since the plane waves $\exp[-ikr\cos(\varphi - z)]$ from which the Sommerfeld integral is composed are themselves solutions of Equation (1), then in order for Integral (4) to become a solution as well it is only necessary to make it converge for various values of the parameters $\underline{r}$ and $\varphi$.

Let the amplitude $s(z)$ be an analytical function which is regular in the half-planes $|\operatorname{Im} z| > c$, where $\underline{c}$ is a sufficiently large positive number. Then it is possible to assume that the path of integration is completely located within these half-planes and can be freely displaced (when $\varphi$ varies) in such a way that its sides (as they go to infinity) always lie within the lined areas; this guarantees the uniform convergence of the integral in the region $r > 0$; $-\infty < \varphi < \infty$. Then Integral (4) is a solution of Equation (1).

Now we shall turn to the quenchability principle. First we shall insure that the solution is bounded for $r = 0$. Since $s(z)$ is regular for $|\operatorname{Im} z| > c$, then it follows that in any band of finite width $A < \operatorname{Re} z < B$ the function $s(z)$ goes to constant limits when the imaginary portion of z goes to plus or minus infinity.

Let us denote these limits by $s(i\infty)$ and $s(-i\infty)$ respectively. Since they do not depend upon $\varphi$ it is sufficient to perform the computation for $\varphi = 0$. Let us examine the integral over the upper loop of the integration path which is drawn as shown in Fig. 3. The integral over this loop can be represented in the form of a sum of three integrals:

$$\frac{1}{2\pi i}\int\limits_{\frac{\pi}{2}+i\sigma}^{\frac{\pi}{2}+ia} \exp(-ikr\cos z)\,s(z)\,dz + \frac{1}{2\pi i}\int\limits_{\frac{\pi}{2}+ia}^{-\frac{3\pi}{2}+ia} \exp(-ikr\cos z)\,s(z)\,dz +$$

$$+\frac{1}{2\pi i}\int\limits_{-\frac{3\pi}{2}+ia}^{-\frac{3\pi}{2}+i\infty} \exp(-ikr\cos z)\,s(z)\,dz.$$

For a sufficiently large a it is possible to assume that $s(z) = s(i\infty)$ and to bring it out from under the integral sign. After that the first and third integrals mutually cancel one another due to the periodicity of the function $\exp[-ikr\cos z]$. The remaining second integral (and therefore the entire integral over the upper loop of the integration path for $r = 0$ and $a \to \infty$) becomes equal to the value $is(i\infty)$. In the same manner we compute the integral over the lower loop for $r = 0$; this integral is equal to $-is(-i\infty)$. Therefore for the acoustic pressure at the very apex of the wedge-shaped region we obtain the finite value

$$S(0, \varphi) = i[s(i\infty) - s(-i\infty)]. \tag{5}$$

which does not depend either upon the angle $\varphi$ or upon the wave number k. This formula will be necessary in the subsequent analysis.

Let us now assume that $r > 0$, and let us examine the complex values $k = |k|e^{i\delta}$. Under these conditions the lined regions in Fig. 2 (where the real portion of the quantity $-ikr\cos(\varphi - z)$ is negative) are deformed in the manner shown in Fig. 4 (as well as in Fig. 2) by means of the dashed lines *, and when $\delta = \pi/2$ this causes the Sommerfeld integral to acquire the form

$$S(r, \varphi) = \frac{1}{2\pi i}\int\limits_{\gamma} \exp[|k|r\cos(\varphi - z)]\,s(z)\,dz, \tag{6}$$

they approach the rectilinear lined regions which are shown in the same Fig. 4.

For finite values of r and $|k|$ a solution of the form (6) remains bounded. However the quenchability principle requires that the solution be bounded in the region $-\Phi < \varphi < \Phi$ for $r \to \infty$ as well. In order to guarantee this we impose the additional requirement that the function $s(z)$ must be regular everywhere in the band $(\Phi + \pi/2 + \epsilon) < \operatorname{Re} z < (\Phi + \pi/2 + \epsilon)$ [except, perhaps, for a finite number of poles located outside of the band $(\Phi + \pi/2) < \operatorname{Re} z < (\Phi + \pi/2)$]. In such a case it is possible (for each angle $\varphi$ associated with our region $\Phi < \varphi < \Phi$ to connect both loops of the intergration path $\gamma$ in such a way that the poles are not intersected and that the integration

---

* In order to make the transition to the case of a time dependence which obeys the law $e^{i\omega}$ it is sufficient to place $\delta = \pi$ in the final solution while taking into account the corresponding deformation of the lined regions.

path will lie (almost everywhere) within the lined bands (this is shown by the dotted line in Fig. 4). Then Solutions (6) will also be bounded at infinite distances $r \longrightarrow \infty$. Thus in order to satisfy the quenchability principle we imposed the additional requirement of regularity upon the function $s(z)$.

Incidentally we note that in the problem involving the diffraction of a plane wave upon a wedge the corresponding function $s(z)$ must definitely have poles which are located within the band $-(\Phi + \pi/2) < \operatorname{Re} z < (\Phi + \pi/2)$. These poles correspond to the incident wave and to those reflected waves whose rays are incident upon the center $r = 0$ at angles which fall within the interval $-(\Phi + \pi/2) < \varphi < (\Phi + \pi/2)$.

If we subtract those waves which can easily be computed according to the laws of geometric reflection from the resultant solution of the diffraction problem, then we can apply the quenchability principle to the remainder in the same form that we have used in this paper.

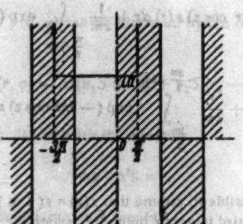

Fig. 3

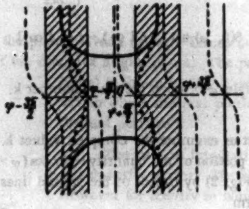

Fig. 4

## 2. Functional Equations

In order to find the form of the function $s(z)$ it is necessary to represent the Boundary Conditions (1)

$$-\frac{1}{ikr}\frac{\partial S}{\partial \varphi} = 1, \quad \text{when} \quad \varphi = \Phi; \qquad \frac{\partial S}{\partial \varphi} = 0, \quad \text{when} \quad \varphi = -\Phi$$

in the form of Sommerfeld integrals.

The left-hand sides are immediately obtained by differentiating the Integral (4) with respect to the parameter, since for any value of $\varphi$ we have

$$\frac{\partial S}{\partial \varphi} = \frac{ikr}{2\pi i} \int_{\gamma} \exp\left[-ikr\cos(\varphi - z)\right] \sin(\varphi - z)\, s(z)\, dz. \tag{7}$$

In order to represent the right-hand side we must make use of a somewhat artificial but convenient method. It is possible to conceive of the problem involved in radiation from a vibrating half-plane as a problem,in the reflection of a certain auxiliary wave from a stationary and rigid half-plane. In fact, let us imagine that a plane wave

$$S^{*}(r, \varphi) = -\exp\left[-ikr\cos\left(\varphi - \Phi + \frac{\pi}{2}\right)\right]. \tag{8}$$

is incident upon the half-plane $\varphi = \Phi$ (and only upon this half-plane) from within the region.

Then the boundary condition

$$-\frac{1}{ikr\rho c}\frac{\partial S}{\partial \varphi} + \frac{1}{\rho c} S^{*}(r, \varphi) = 0, \quad \text{when} \quad \varphi = \Phi, \tag{9}$$

which formally coincides with the first of Boundary Conditions (1) signifies the cancellation of the resulting normal velocity on the rigid boundary.

However it is possible to represent the plane wave $S^{*}(r,\varphi)$ in the form of a Sommerfeld integral on the basis of the formula

$$\exp\left[-ikr\cos(\varphi - \varphi_0)\right] = \frac{1}{2\pi i}\int_{\gamma} \exp\left[-ikr\cos(\varphi - \varphi_0 - z)\right] \frac{i}{1 - e^{-iz}}\, dz \tag{10}$$

and therefore, making use of the Formulas (1), (7), (8), (9) and (10), it is possible to write the boundary conditions in the form

$$\left.\begin{aligned} -\frac{1}{2\pi i}\int_{\gamma} \exp\left[-ikr\cos(\Phi - z)\right] \sin(\Phi - z)\, s(z)\, dz - \\ -\frac{1}{2\pi i}\int_{\gamma} \exp\left[-ikr\cos\left(\frac{\pi}{2} - z\right)\right] \frac{i}{1 - e^{-iz}}\, dz = 0, \\ \frac{1}{2\pi i}\int_{\gamma} \exp\left[-ikr\cos(-\Phi - z)\right] \sin(-\Phi - z)\, s(z)\, dz = 0. \end{aligned}\right\} \tag{1*}$$

In this form the terms in the first boundary condition have different arguments in the cosine expression in the core of the integral. Correspondingly the integration paths $\gamma$ are displaced with respect to one another.

However, making use of the identity

$$\int_{\gamma} \exp\left[-ikr\cos(\alpha - z)\right] s(z)\, dz = \int_{\gamma} \exp\left[-ikr\cos z\right] s(z + \alpha)\, dz,$$

we can reduce both integrals to an identical core and an identical path of integration. After that both terms in the boundary condition join into one integral and the boundary conditions acquire the form

$$\left.\begin{aligned} &\int_{\gamma} \exp(-ikr\cos z)\left[\sin z s(z+\Phi) - \frac{i}{1+ie^{-iz}}\right] = 0, \\ &\int_{\gamma} \exp(-ikr\cos z)\sin z s(z-\Phi)\,dz = 0. \end{aligned}\right\} \qquad (1^{\bullet\bullet})$$

The following theorem which has been proven by the author in a dissertation [2] is valid.

Theorem 1. If an analytical function $f(z)$ is regular for $|\operatorname{Im} z| > c$, then in order to fulfill the identity

$$\int_{\gamma} \exp(-ikr\cos z) f(z)\,dz \equiv 0 \quad (z > 0)$$

it is necessary and sufficient that the function $f(z)$ be even (i.e., that

$$f(z) - f(-z) = 0. \qquad (11)$$

The proof of this theorem will be given in the supplement to the second part of the paper.

On the basis of Equation (11) [having taken the contents of the brackets in the integrands of $(1^{\bullet\bullet})$ in the capacity of $f(z)$] we obtain two functional equations:

$$s(z+\Phi) + s(-z+\Phi) = -\frac{1}{\cos z}, \qquad (12)$$

$$s(z-\Phi) + s(-z-\Phi) = 0. \qquad (13)$$

The solution of the problem as posed in the form of Integral (4) will be found if we determine the function $s(z)$ from these functional equations [the function $s(z)$ is regular for $|\operatorname{Im} z| > c$ and for $|\operatorname{Re} z| < \Phi + \pi/2$]. Such a function is simply expressed in terms of function $\eta_{\Phi}(z)$, (this function is examined in the supplement) on the basis of the formula

$$s(z) = \eta_{\Phi}(z+\Phi).$$

so that it would be possible for us to pass over directly to an investigation of the accurate solution for $S(r, \varphi)$ given by Formula (28). However in order to make our analysis complete we shall here provide a direct derivation of the solution for the functional Equations (12), (13); if desired this derivation can be omitted by the reader.

In order to solve such equations it is convenient to make use of Fourier integrals which are written in a somewhat modified form and for which the following theorem is valid.

Theorem 2. Let $f(z)$ be an analytical function which is regular in the interval $a < \operatorname{Re} z < b$ and which goes to the constant limits $f(i\infty)$ and $f(-i\infty)$ in this interval when $\operatorname{Im} z \longrightarrow \pm\infty$; thus

$$f(z) = f(i\infty) + O[\exp(-\lambda \operatorname{Im} z)] \quad \text{when } \operatorname{Im} z \to \infty,$$
$$f(z) = f(-i\infty) + O[\exp(\mu \operatorname{Im} z)] \quad \text{when } \operatorname{Im} z \to -\infty;$$

where $\lambda$ and $\mu$ are positive numbers.

Then the function f(z) can be represented in the following manner in the indicated band:

$$f(z) = \frac{1}{2}[f(i\infty) + f(-i\infty)] + \frac{i}{2\sqrt{2\pi}}\left\{\int_{-\alpha-i\infty}^{-\alpha+i\infty} F(w)\exp(-iwz)\,dw + \right.$$

$$\left. + \int_{\beta-i\infty}^{\beta+i\infty} F(w)\exp(-iwz)\,dw\right\}, \tag{14}$$

$$(0<\alpha<\lambda), \quad (0<\beta<\mu),$$

or

$$f(z) = \frac{1}{2}[f(i\infty) + f(-i\infty)] + \frac{i}{\sqrt{2\pi}}\, P\int_{-i\infty}^{i\infty} F(w)\exp(-iwz)\,dw, \tag{15}$$

(the symbol $P\int$ denotes the chief value of the integral), where F(w) is an analytical function which can be represented by the integral

$$F(w) = \frac{i}{\sqrt{2\pi}}\int_{-i\infty}^{i\infty} [f(z) - f(i\infty)]\exp(iwz)\,dz \tag{16}$$

in the band $-\lambda < \mathrm{Re}\,w < 0$ and by the integral

$$F(w) = \frac{i}{\sqrt{2\pi}}\int_{-i\infty}^{i\infty} [f(z) - f(-i\infty)]\exp(iwz)\,dz, \tag{17}$$

in the band $0 < \mathrm{Re}\,w < \mu$; here the function f (w) is regular over the entire band $-\lambda < \mathrm{Re}\,w < \mu$[*]; precisely speaking, this is true everywhere except for the pole which exists at the point w = 0 and which has a deduction

$$\frac{1}{\sqrt{2\pi}}[f(-i\infty) - f(i\infty)].$$

The method of proving this theorem differs little from the method utilized for ordinary Fourier integrals [6]. Therefore we shall not give the proof here.

Let us note that in applying a Fourier integral in its given form to some appropriate function we can always assume that the limiting values f(i∞) and f (−i∞) are equal and opposite in sign, i.e.,

$$f(-i\infty) = -f(i\infty). \tag{18}$$

---

[*] As a particular case, when f( i ∞) = f(−i ∞) = 0, we obtain a pair of mutual transformations:

$$f(z) = \frac{i}{\sqrt{2\pi}}\int_{-i\infty}^{i\infty} F(w)\exp(-iwz)\,dz, \quad F(w) = \frac{i}{\sqrt{2\pi}}\int_{-i\infty}^{i\infty} f(z)\exp(iwz)\,dz.$$

After a simple substitution of variables these formulas become ordinary Fourier integrals or (for a different substitution) they become formulas for a two-sided Laplace transformation.

In fact, if that were not so it would be possible to analyze the function $f_1(z) = f(z) - \frac{1}{2}\,[f(i\infty) + f(-i\infty)]$ instead of $f(z)$; Equation (18) is always observed for the function $f(z)$.

When Condition (18) applies, the first term in Formulas (14) and (15) of Theorem 2 disappears and the function $f(z)$ can be written in the form:

$$f(z) = \frac{i}{2\sqrt{2\pi}}\left\{\int\limits_{-\alpha-i\infty}^{-\alpha+i\infty} F(w)\exp(-iwz)\,dw + \int\limits_{\beta-i\infty}^{\beta+i\infty} F(w)\exp(-iwz)\,dw\right\} \tag{19}$$

or

$$f(z) = \frac{i}{\sqrt{2\pi}}\,P\int\limits_{-i\infty}^{i\infty} F(w)\exp(-iwz)\,dw. \tag{20}$$

Turning to the solution of the Functional Equations (12) and (13); we make use of the fact that the unknown function $s(z)$ must be determined with an accuracy of up to an arbitrary additive constant.

In fact, the addition of any constant to the function $s(z)$ does not change the value of the Sommerfeld integral (this result follows from Theorem 1 and from the fact that the integral $\int\limits_{\gamma}\exp(-ikr)\cos(z-\varphi)\,dz$ does not depend upon $\varphi$).

In such a case this arbitrary constant can always be selected in such a way that

$$s(-i\infty) = -s(i\infty)$$

and therefore the function $s(z)$ can be represented in the following way according to Formula (19):

$$s(z) = \frac{i}{2\sqrt{2\pi}}\left\{\int\limits_{-\epsilon-i\infty}^{-\epsilon+i\infty} F(w)\exp(-iwz)\,dw + \int\limits_{\epsilon-i\infty}^{\epsilon+i\infty} F(w)\exp(iwz)\,dw\right\}, \tag{22}$$

where $\epsilon$ is the sufficiently small positive quantity. Since the function $s(z)$ is regular in the band $|\operatorname{Re} z| < \varphi + \frac{\pi}{2}$, Formula (22) (on the basis of Theorem 2) represents this function over the entire band. Therefore all the terms in the left-hand sides of the Functional Equations (12) and (13) can be expressed according to this formula for sufficiently small values of (Re z). For example, the term $s(z+\varphi)$ can be expressed thus:

$$s(z+\Phi) = \frac{i}{2\sqrt{2\pi}}\left\{\int\limits_{-\epsilon-i\infty} F(w)\,e^{-iw\Phi}e^{-iwz}\,dw + \int\limits_{\infty} F(w)\,e^{iw\Phi}e^{-iwz}\,dw\right\}$$

and the term $s(-z+\varphi)$ can be expressed thus:

$$s(-z+\Phi) = \frac{i}{2\sqrt{2\pi}}\left\{\int\limits_{-\epsilon-i\infty}^{-\epsilon+i\infty} F(w)\,e^{-iw\Phi}e^{iwz}\,dw + \int\limits_{\epsilon-i\infty}^{\epsilon+i\infty} F(w)e^{-iw\Phi}e^{iwz}\,dw\right\} =$$

$$= \frac{i}{2\sqrt{2\pi}}\left\{\int\limits_{-\epsilon-i\infty}^{-\epsilon+i\infty} F(-w)\,e^{iw\Phi}e^{-iwz}\,dw + \int\limits_{\epsilon-i\infty}^{\epsilon+i\infty} F(-w)\,e^{iw\Phi}e^{-iwz}\,dw\right\}.$$

In order to express the right-hand sides of the functional equations we shall represent the function $1/\cos z$ by the same type of Fourier integral:

$$\frac{1}{\cos z} = \frac{i}{\sqrt{2\pi}} \int\limits_{-i\infty}^{i\infty} G(w)\, e^{-iwz}\, dw =$$

$$= \frac{i}{2\sqrt{2\pi}} \left\{ \int\limits_{-\varepsilon-i\infty}^{-\varepsilon+i\infty} G(w) e^{-iwz}\, dw + \int\limits_{\varepsilon-i\infty}^{\varepsilon+i\infty} G(w)\, e^{-iwz}\, dw \right\},$$

where

$$G(w) = \frac{i}{\sqrt{2\pi}} \int\limits_{-i\infty}^{i\infty} \frac{e^{iwz}}{\cos z}\, dz = -\frac{2}{\sqrt{2\pi}} \int\limits_{0}^{\infty} \frac{t^{w}\, dt}{1+t^{2}} = -\frac{\sqrt{2\pi}}{2\cos\frac{\pi w}{2}}.$$

Substituting the expressions found above into the first Functional Equation (12), we obtain

$$\frac{i}{2\sqrt{2\pi}} \left\{ \int\limits_{-\varepsilon-i\infty}^{-\varepsilon+i\infty} \left[ F(w)\, e^{-iw\Phi} + F(-w)\, e^{iw\Phi} - \frac{\sqrt{2\pi}}{2\cos\frac{\pi w}{2}} \right] e^{-iwz}\, dw + \right.$$

$$\left. + \int\limits_{\varepsilon-i\infty}^{\varepsilon+i\infty} \left[ F(w)\, e^{-iw\Phi} + F(-w)\, e^{iw\Phi} - \frac{\sqrt{2\pi}}{2\cos\frac{\pi w}{2}} \right] e^{-iwz}\, dw \right\} \equiv 0.$$

A necessary condition for the observation of this identity is the requirement that the contents of the square brackets in the integrand must be equal to zero. Therefore for the functions F(w) and F( −w) we obtain the following algebraic equation:

$$F(w)\, e^{-iw\Phi} + F(-w)\, e^{iw\Phi} = \frac{\sqrt{2\pi}}{2\cos\frac{\pi w}{2}}.$$

Proceeding in an analogous manner with the second Functional Equation (13), we obtain the equation

$$F(w)\, e^{iw\Phi} + F(-w)\, e^{-iw\Phi} = 0.$$

From these two equations we find that

$$F(w) = \frac{i\sqrt{2\pi}}{4} \frac{e^{-iw\Phi}}{\cos\frac{\pi w}{2}\sin 2\Phi w}, \tag{23}$$

whence we have

$$s(z) = -\frac{1}{8}\left\{\int_{-\varepsilon-i\infty}^{-\varepsilon+i\infty} + \int_{\varepsilon-i\infty}^{\varepsilon+i\infty}\right\} \frac{e^{-iw(z+\Phi)}}{\cos\frac{\pi w}{2}\sin 2w\Phi}\,dw. \tag{24}$$

on the basis of Formula (22).

The substitution of this expression into the Sommerfeld Integral (4)

$$S(r, \varphi) = \frac{1}{2\pi i}\int_{\gamma} \exp\left[-ikr\cos(\varphi - z)\right] s(z)\,dz$$

yields the unknown function $S(r, \varphi)$.

The Expression (24) obtained for f (z) requires a certain manipulation. However, before we proceed with this let us examine the simplest problem: determining the sound pressure upon the apex ($r = 0$) of a wedge-shaped region.

As we have shown in Section 1, this pressure (or, more precisely, the amplitude of this pressure) is equal to (5):

$$S(0, \varphi) = i\left[s(i\infty) - s(-i\infty)\right],$$

but since Theorem 2 applies, the quantity $-\frac{1}{\sqrt{2\pi}}\left[(s(i\infty) - s(-i\infty)\right]$ is equal to the deduction from the function $F(w)$ at the point $w = 0$. This deduction, as can be seen from Expression (23), is equal to $\frac{i\sqrt{2\pi}}{8\Phi}$, and therefore

$$S(0, \varphi) = \frac{\pi}{4\Phi}. \tag{25}$$

In order to find the pressure of the given boundary vibration velocities $v_1$ and $v_2$ upon the apex it is sufficient to make use of Formula (2):

$$p(r, \varphi) = \rho c\left[v_1 S(r, \varphi) + v_2 S(r, -\varphi)\right].$$

In accordance with Equation (25) we obtain

$$p(0, \varphi) = \frac{\pi\rho c}{4\Phi}(v_1 + v_2). \tag{26}$$

It is natural that the right-hand side of the equation does not depend upon $\varphi$, since one cannot have different pressures at one and the same point.

Let us now examine the function $s(z)$ which is given by Expression (24). The formula

$$s(z) = \eta_{\Phi}(z + \Phi) \tag{27}$$

correlates this formula with the function of $\eta_{\Phi}(z)$ of two variables which was examined by the author in his dissertation while solving the problem of diffraction upon an absorbent wedge [2]. The basic properties of the function $\eta_{\Phi}(z)$ are given in the supplement.

Making use of Equation (27) in Equation (24), we obtain an expression for the function $S(r, \varphi)$ in terms of $\eta_{\Phi}(z)$:

$$S(r, \varphi) = \frac{1}{2\pi i}\int_{\gamma} \exp\left[-ikr\cos(\varphi - z)\right]\eta_{\Phi}(z + \Phi)\, dz. \tag{28}$$

We shall make use of this formula for further investigations, but first[(in order to underline the meaning of the function $\eta_{\Phi}(z)$ )]we shall rewrite Expression (28) in the form

$$S(r, \varphi_1 - \Phi) = \frac{1}{2\pi i}\int_{\gamma} \exp\left[-ikr\cos(\varphi_1 - \alpha)\right]\eta_{\Phi}(\alpha)\, d\alpha, \tag{29}$$

which can easily be obtained by substituting the variable of integration $z + \Phi = \alpha$.

The quantity $\varphi_1 = \varphi + \Phi$ is the angle measured from the lower stationary boundary $\varphi = -\Phi$ of the angular region. Thus $\eta_{\Phi}(z)$ is a function of the angular distribution of the plane wave amplitudes in the Sommerfeld integral which determines the forced vibrations of the sound pressure in the wedge-shaped region $0 < \varphi_1 < 2\Phi$, $r > 0$, if for a stationary boundary $\varphi_1 = 0$ the boundary $\varphi_1 = 2\Phi$ performs vibrations which have velocity amplitudes equal to the unit pressure divided by the wave impedance $\rho c$ of the medium (i.e., with a velocity amplitude which corresponds to a unit pressure amplitude in the travelling plane wave).

Under these conditions the positive direction for the velocity is assumed to be the direction of the internal normal to the boundary $\varphi_1 = 2\Phi$. From this it is evident that the function $\gamma_{\Phi}(z)$ which plays an auxiliary role in other problems as far as the mathmatical operations are concerned, acquires a meaning which permits direct simplification in this problem.

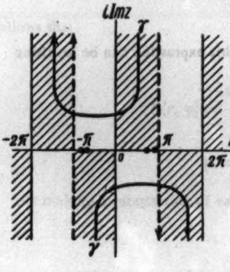

Fig. 5

Since in the physical problem the velocities of both boundaries of the wedge are different from zero in the general case, it follows that for subsequent analysis it is more convenient for us to use Expression (28) for $S(r, \varphi)$.

By means of Formula (2)

$$p(r, \varphi) = \rho c\left[v_1 S(r, \varphi) + v_2 S(r, -\varphi)\right]$$

we obtain the following formula by a simple substitution for the variable of integration:

$$p(r, \varphi) = \frac{\rho c}{2\pi i}\int_{\gamma} \exp\left[-ikr\cos(\varphi - z)\right]\left[v_1\eta_{\Phi}(z + \Phi) + v_2\eta_{\Phi}(z - \Phi)\right] dz. \tag{30}$$

This is the accurate solution for the proposed problem in the form of a Sommerfeld integral. The derivation of approximate representations of the field which are convenient for computations when the values of kr are large or small can also be performed initially for the auxiliary function $S(r, \varphi)$, with a subsequent transition to the general case by means of Formula (2).

In order to make the transition from the contour integral (28)

$$S(r, \varphi) = \frac{1}{2\pi i}\int_{\gamma} \exp\left[-ikr\cos(\varphi - z)\right]\eta_{\Phi}(z + \Phi)\, dz$$

to a simple integral we proceed in the following manner. We rewrite this integral in the form

$$S(r, \varphi) = \frac{1}{2\pi i}\int_{\gamma} \exp(-ikr\cos z)\,\eta_{\Phi}(z+\varphi+\Phi)\,dz. \tag{31}$$

The path of integration $\gamma$ in this integral is depicted in Fig. 5 in the form of two loops.

By deforming this path it is possible to convert it into two vertical straight lines $\operatorname{Re} z = \pm\pi$ which are shown in the same figure by the dashed lines. However, in doing this we obtain deductions at those poles of the expression under the integral sign which are disposed within the interval $|\operatorname{Re} z| < \pi$.

The function $\eta_{\Phi}(z)$ can be represented * as follows:

$$\eta_{\Phi}(z) = 2z\sum_{m=1}^{\infty}(-1)^{m-1}\sum_{n=1}^{\infty}\frac{1}{z^2-\left[2\Phi(2n-1)+\frac{\pi}{2}(2m-1)\right]^2}.$$

The poles which lie in the indicated interval can belong only to the first term (m = 1) of the external sum (i.e., they can only belong to the expression

$$A_{\Phi}(z) = 2z\sum_{n=1}^{\infty}\frac{1}{z^2-[2\Phi(2n-1)+\pi/2]^2}.$$

In our case, where the argument is not z but the quantity $z+\varphi+\Phi$, this expression can be rewritten thus:

$$A_{\Phi}(z+\varphi+\Phi) = \sum_{\nu=0}^{\infty}\frac{1}{z+\varphi-(-1)^{\nu}[(2\nu+1)\Phi+\pi/2]}.$$

We shall obtain deductions only at the first N + 1 poles

$$z_{\nu} = -\varphi + (-1)^{\nu}[(2\nu+1)\Phi+\pi/2] \quad (\nu = 0, 1, \ldots, N)$$

of this expression which satisfy the condition $|z_{\nu}| < \pi$. The sum of the deductions from the integrals (31) at these poles is of the form:

$$S_0(r, \varphi) = \sum_{\nu}\exp\{-ikr\cos[(2\nu+1)\Phi+\pi/2-(-1)^{\nu}\varphi]\}, \tag{32}$$

and represents the plane wave aggregate which corresponds to the geometric-optical solution of the problem. The term with the number $\nu = 0$ corresponds to a plane wave which is directly radiated by the vibrating upper boundary $\varphi = \Phi$. The subsequent numbers correspond to geometrically reflected waves. Only the terms for which $\nu \leq \frac{\pi}{4\Phi}$ appear in the series written above; the terms with the largest number $\nu$ that satisfies this condition

---

* See supplement at the end of the paper.

are different from zero only for those values of the angle $\varphi$ ($|\varphi| \leq \Phi$) for which $(2\nu + 1)\Phi + \pi/2 - (-1)^{\nu}\varphi < \pi$. In particular, if $\Phi > \pi/4$, then out of the entire sum only the zero term $\exp[-ikr\cos(\Phi + \pi/2 - \varphi)]$ is retained; even if this term is absent if $\varphi < -\dfrac{\pi}{2}$.

As a result of the deformation of the integration path the function $S(r, \varphi)$ acquires the form:

$$S(r, \varphi) = S_0(r, \varphi) + I(r, \varphi), \tag{33}$$

where

$$I(r, \varphi) = \frac{1}{2\pi i}\left(\int\limits_{-\pi-i\infty}^{-\pi+i\infty} + \int\limits_{\pi+i\infty}^{\pi-i\infty}\right)\exp(-ikr\cos z)\,\eta_{\Phi}(z + \varphi + \Phi)\,dz =$$

$$= \frac{1}{2\pi i}\int\limits_{-i\infty}^{i\infty} \exp(ikr\cos z)\,[\eta_{\Phi}(z + \varphi + \Phi - \pi) - \eta_{\Phi}(z + \varphi + \Phi + \pi)]\,dz,$$

or, since the function $\eta_{\Phi}(z)$ satisfies the identity*

$$\eta_{\Phi}(z - \pi) - \eta_{\Phi}(z + \pi) = \frac{\pi}{2\Phi}\,\frac{\sin\dfrac{\pi^2}{4\Phi}}{\cos\dfrac{\pi^2}{4\Phi} + \cos\dfrac{\pi z}{2\Phi}},$$

it follows that

$$I(r, \varphi) = \frac{\sin\dfrac{\pi^2}{4\Phi}}{4\Phi i}\int\limits_{-i\infty}^{i\infty} \exp(ikr\cos z)\,\frac{dz}{\cos\dfrac{\pi^2}{4\Phi} - \sin\dfrac{\pi(z + \varphi)}{2\Phi}}.$$

By making a substitution of variables we obtain

$$I(r, \varphi) = \frac{\sin\dfrac{\pi^2}{4\Phi}}{4\Phi}\int\limits_{-\infty}^{\infty} \frac{\exp(ikr\cosh z)}{\cos\dfrac{\pi^2}{4\Phi} - i\sinh\dfrac{\pi}{2\Phi}(z - i\varphi)}\,dz. \tag{34}$$

A substitution of this expression into Equation (33) yields the final expression for $S(r, \varphi)$ in terms of an ordinary integral:

$$S(r, \varphi) = \sum_{\nu}\exp\left\{-ikr\cos\left[(2\nu + 1)\Phi + \frac{\pi}{2} - (-1)^{\nu}\varphi\right]\right\} +$$

$$+ \frac{\sin\dfrac{\pi^2}{4\Phi}}{4\Phi}\int\limits_{-\infty}^{\infty} \frac{\exp(ikr\cosh z)\,dz}{\cos\dfrac{\pi^2}{4\Phi} - i\sinh\dfrac{\pi(z - i\varphi)}{2\Phi}}. \tag{35}$$

---

* See supplement at end of paper.

The sum yields an approximation of geometric optics; the integral yields the correction to it.

## 3. Approximate Expressions for Large Distances

In order to obtain an approximate expression for the function S(r, $\varphi$) at large distances it is possible to make use of the fact that S is an analytical function of the wave number, and thus to place k = i$\mu$ while temporarily assuming that $\mu$ is real and positive. Then Integral (34) acquires the form:

$$I(r,\varphi)=-\frac{\sin\frac{\pi^2}{4\Phi}}{4\Phi}\int_{-\infty}^{\infty}\frac{\exp(-\mu r\cosh z)}{\cos\frac{\pi^2}{4\Phi}-i\sinh\frac{\pi(z-i\varphi)}{2\Phi}}\,dz.$$

After making the substitution of variables cosh z = 1 + 2t$^2$, this integral can be rewritten thus:

$$I(r,\varphi)=\frac{1}{2\Phi}e^{-\mu r}\sin\frac{\pi^2}{4\Phi}\int_{-\infty}^{\infty}e^{-2\mu rt^2}f(t)\,dt,$$

where

$$\frac{1}{f(t)}=\sqrt{1+t^2}\left\{\cos\frac{\pi^2}{4\Phi}-i\sinh\frac{\pi}{\Phi}\left[\mathrm{Ar}\cosh(1+2t^2)-\frac{i\varphi}{2}\right]\right\}. \tag{36}$$

In order to obtain an approximate expression for large r we shall replace the function f(t) by its expansion into a power series:

$$f(t)=\sum_{n=0}^{\infty}f^{(n)}(0)\frac{t^n}{n!}=\sum_{n=0}^{\infty}\left(f^{(2n)}(0)\frac{t^{2n}}{(2n)!}+f^{(2n+1)}(0)\frac{t^{2n+1}}{(2n+1)!}\right). \tag{36*}$$

Then

$$I(r,\varphi)\sim\frac{e^{-\mu r}}{2\Phi}\sin\frac{\pi^2}{4\Phi}\sum_{n=0}^{\infty}\frac{f^{(2n)}(0)}{(2n)!}\int_{-\infty}^{\infty}e^{-2\mu rt^2}t^{2n}\,dt.$$

The odd terms of the series are not written out, since they disappear upon integration.

Carrying out the integration, we obtain

$$I(r,\varphi)\sim\frac{\pi}{2\Phi}\sin\frac{\pi^2}{4\Phi}\frac{e^{-\mu r}}{\sqrt{2\pi\mu r}}\left(f(0)+\sum_{n=1}^{\infty}\frac{(2n-1)!!}{(2n)!}\frac{f^{(2n)}(0)}{(4\mu r)^n}\right). \tag{37}$$

The series which we have written is divergent, since we have utilized the series (36*) to obtain it [series (36*) diverges for $|t| = 1$]. However, by limiting ourselves to a finite number of terms in the series we obtain an expression which approaches the true value of the integral asymptotically as r increases.

In accordance with Equation (36),

$$f(0)=\frac{1}{\cos\frac{\pi^2}{4\Phi}-\sin\frac{\pi\varphi}{2\Phi}},$$

$$f''(0)=\frac{1}{\cos\frac{\pi^2}{4\Phi}-\sin\frac{\pi\varphi}{2\Phi}}\left[1-\left(\frac{\pi}{\Phi}\right)^2\frac{\sin\frac{\pi\varphi}{2\Phi}}{\cos\frac{\pi^2}{4\Phi}-\sin\frac{\pi\varphi}{2\Phi}}-2\left(\frac{\pi}{\Phi}\right)^2\left(\frac{\cos\frac{\pi\varphi}{2\Phi}}{\cos\frac{\pi^2}{4\Phi}-\sin\frac{\pi\varphi}{2\Phi}}\right)^2\right]$$

etc.

Substituting these values and making the substitution $\mu = -ik$, we obtain

$$I(r,\varphi)\sim\frac{\pi}{2\Phi}\frac{\sin\frac{\pi^2}{4\Phi}}{\cos\frac{\pi^2}{4\Phi}-\sin\frac{\pi\varphi}{2\Phi}}\frac{\exp\left[i\left(kr+\frac{\pi}{4}\right)\right]}{\sqrt{2\pi kr}}\Bigg\{1+$$

$$+\frac{i}{4kr}\left[1-\left(\frac{\pi}{\Phi}\right)^2\frac{\sin\frac{\pi\varphi}{2\Phi}}{\cos\frac{\pi^2}{4\Phi}-\sin\frac{\pi\varphi}{2\Phi}}-2\left(\frac{\pi}{\Phi}\right)^2\left(\frac{\cos\frac{\pi\varphi}{2\Phi}}{\cos\frac{\pi^2}{4\Phi}-\sin\frac{\pi\varphi}{2\Phi}}\right)+\cdots\right]\Bigg\}. \qquad (37^\bullet)$$

It is not difficult to compute the subsequent terms of Expansion (37) by finding the fourth, sixth, etc., derivative functions of $f(t)$.

Since $S(r,\varphi) = S_0(r,\varphi) + I(r,\varphi)$, it is possible to use Formula ($37^\bullet$) in order to compute the correction to the geometric-optical solution at distances which are large in comparison to a wavelength. The formula is inapplicable only in a certain vicinity of the zeros of the denominator which correspond to the shadow boundaries of one or another geometric reflection. The closer we are to the shadow boundary, the greater the distance $r$ required for the formula to be valid.

For sufficiently large values of $r$ we obtained the formula

$$I(r,\varphi)\sim A_\Phi(\varphi)\frac{\exp\left[i\left(kr+\frac{\pi}{4}\right)\right]}{\sqrt{2\pi kr}}, \qquad (38)$$

where

$$A_\Phi(\varphi)=\frac{\pi}{2\Phi}\frac{\sin\frac{\pi^2}{4\Phi}}{\cos\frac{\pi^2}{4\Phi}-\sin\frac{\pi\varphi}{2\Phi}}. \qquad (39)$$

A criterion for the validity of the formula is the smallness of the modulus of the discarded second term in the square brackets of Expression ($37^\bullet$) in comparison with unity.

The angular dependence of the field at great distances in the region of the geometric shadow is plotted in Fig. 6 for several angular dimensions of a wedge which is radiating from one boundary; the dashed half-lines depict the shadow boundaries for the corresponding cases.

For convenience in plotting, the angle is measured not from the center of the angular region $\varphi = 0$ but from the stationary boundary $\varphi_1 = 0$ ($\varphi_1 = \varphi + \Phi$) according to the formula

$$A_\Phi(\varphi_1-\Phi)=\frac{\pi}{2\Phi}\frac{\sin\frac{\pi^2}{\Phi}}{\cos\frac{\pi^2}{4\Phi}+\cos\frac{\pi\varphi_1}{2\Phi}}. \qquad (39^\bullet)$$

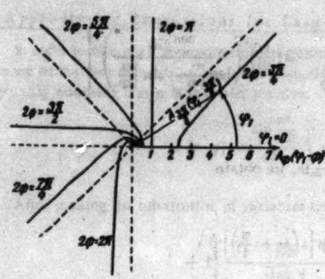

Fig. 6

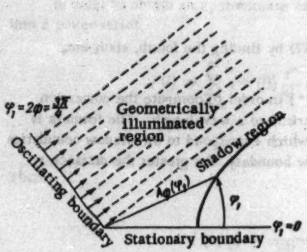

Fig. 7

The vibrating boundaries $\varphi_1 = 2\Phi$ are not depicted in Fig. 6. For the purposes of clarification Fig. 7 depicts the case of a wedge-shaped region with an aperture of $2\Phi = 3\pi/4 = 135°$ separately.

The fact that $A_\Phi(\varphi)$ tends to go to infinity in the vicinity of the geometric shadow boundary is quite natural in view of the fact that on this boundary the cylindrical wave $I(r, \varphi)$ (which decays with distance) is forced to compete with the field of a non-decaying plane wave produced by geometric reflection.

In order to compute the field at large distances for given velocities $v_1$ and $v_2$, it is possible to make use of the formula

$$p(r, \varphi) = \rho c \{v_1 S_0(r, \varphi) + v_2 S_0(r, -\varphi) + \\ + \frac{\exp\left|i\left(kr + \frac{\pi}{4}\right)\right|}{\sqrt{2\pi kr}} [v_1 A_\Phi(\varphi) + v_2 A_\Phi(-\varphi)]\}. \tag{40}$$

It is easy to verify the fact that for the case $2\Phi = \pi$, $v_2 = v_1$ which corresponds to an infinite radiating plane the quantity enclosed in the square brackets becomes zero and a plane wave $p(r, \varphi) = \rho c v_1(\exp[ikt \cos \varphi])$ remains.

## 4. The Representation of the Solution by an Infinite Series of Bessel Functions

In order to compute the field at small distances it is convenient to make use of a representation of the function $S(r, \varphi)$ in the form of a series containing Bessel functions:

$$S(r, \varphi) = \frac{\pi}{4\Phi} J_0(kr) + \frac{\pi}{2\Phi} \sum_{s=1}^{\infty} (-1)^s \exp\left(-\frac{is\pi^2}{4\Phi}\right) \frac{\cos\frac{s\pi(\varphi+\Phi)}{2\Phi}}{\cos\frac{s\pi^2}{4\Phi}} J_{\frac{s\pi}{2\Phi}}(kr) + \\ + 2 \sum_{s=1}^{\infty} (-1)^s \exp\left[-\frac{i\pi(2s-1)}{2}\right] \frac{\cos[(2s-1)(\varphi+\Phi)]}{\sin[(2s-1)2\Phi]} J_{2s-1}(kr). \tag{41}$$

The acoustic pressure at the given amplitudes of the vibration velocities which exist upon the boundaries is obtained from this expression according to Formula (2):

$$p(r, \varphi) = \rho c [v_1 S(r, \varphi) + v_2 S(r, -\varphi)].$$

In order to obtain the Series (41) we rewrite Equation (29) in the form:

$$S(r, \varphi_1 - \Phi) = \frac{1}{2\pi i} \int_\gamma \exp(-ikr\cos z)\, \eta_\Phi(z+\varphi_1)\, dz, \tag{42}$$

**TABLE**

The values of $A_\Phi(\varphi_1-\Phi)=\frac{\pi}{2\Phi}\,\frac{\sin\frac{\pi^2}{4\Phi}}{\cos\frac{\pi^2}{4\Phi}+\cos\frac{\pi\varphi_1}{2\Phi}}$

| $\varphi_1$ | Angular size of the wedge $2\phi$ | | | | | |
|---|---|---|---|---|---|---|
| | $\frac{3\pi}{4}$ | $\pi$ | $\frac{5\pi}{4}$ | $\frac{3\pi}{2}$ | $\frac{7\pi}{4}$ | $2\pi$ |
| 0 | 2.30 | 1.00 | 0.582 | 0.384 | 0.275 | 0.207 |
| $\pi/8$ | 3.15 | 1.08 | 0.608 | 0.393 | 0.279 | 0.209 |
| $\pi/4$ | | 1.42 | 0.682 | 0.420 | 0.292 | 0.217 |
| $\pi/2$ | | | 1.233 | 0.576 | 0.358 | 0.250 |
| $3\pi/4$ | | | | 1.152 | 0.528 | 0.324 |
| $\pi$ | | | | | 1.113 | 0.502 |
| $5\pi/4$ | | | | | | 0.990 |
| $3\pi/2$ | | | | | | |

where the integration path consists of two loops $\gamma=\gamma_1+\gamma_2$ which are depicted in Fig. 8. But

$$\int_{\gamma_2}\exp(-ikr\cos z)\,\eta_\Phi(z+\varphi_1)\,dz=-\int_{\gamma_1}\exp(-ikr\cos z)\,\eta_\Phi(-z+\varphi_1)\,dz,$$

and since* $\eta_\Phi(-z)=-\eta_\Phi(z)$ it follows that

$$S(r,\varphi_1-\Phi)=\frac{1}{2\pi i}\int_{\gamma_1}\exp(-ikr\cos z)\,[\eta_\Phi(z+\varphi_1)+\eta_\Phi(z-\varphi_1)]\,dz. \tag{43}$$

Making use of a representation of the function $\eta_\Phi(z)$ in the form of a Fourier * integral:

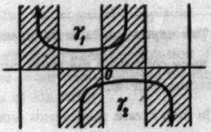

Fig. 8

$$\eta_\Phi(z)=-\frac{1}{8}\left(\int_{-a-i\infty}^{-a+i\infty}+\int_{a-i\infty}^{a+i\infty}\right)\frac{e^{-iwz}}{\cos\frac{w\pi}{2}\sin 2w\Phi}\,dw,$$

we can write

$$\eta_\Phi(z+\varphi_1)+\eta_\Phi(z-\varphi_1)=-\frac{1}{4}\left(\int_{-a-i\infty}^{-a+i\infty}+\int_{a-i\infty}^{a+i\infty}\right)\frac{\cos w\varphi_1 e^{-iwz}}{\cos\frac{w\pi}{2}\sin 2w\Phi}\,dw=$$

$$=\frac{1}{4}\left(\int_{-a-i\infty}^{-a+i\infty}+\int_{a-i\infty}^{a+i\infty}\right)\frac{\cos w\varphi_1}{\cos\frac{w\pi}{2}\sin 2w\Phi}\,e^{iwz}dw.$$

---

* See supplement at the end of the paper.

Or, by displacing the path of integration of the first integral to the right until it coincides with the second path of integration, we have:

$$\eta_\Phi(z+\varphi_1)+\eta_\Phi(z-\varphi_1)=\frac{\pi}{4\Phi i}+\frac{1}{2}\int\limits_{a-i\infty}^{a+i\infty}\frac{\cos w\varphi_1}{\cos\frac{w\pi}{2}\sin w\Phi}e^{iwz}dw.$$

In this form the integral represents the examined function only in the convergence band$|\operatorname{Re} z|<\frac{\pi}{2}+2\Phi-|\varphi_1|$. However, if the path of integration is deformed in the manner shown in Fig. 9, then the expression

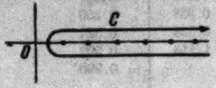

Fig. 9

$$\eta_\Phi(z+\varphi_1)+\eta_\Phi(z-\varphi_1)=\frac{\pi}{4\Phi i}+$$
$$+\frac{1}{2}\int\limits_{c}\frac{\cos w\varphi_1}{\cos\frac{w\pi}{2}\sin 2w\Phi}e^{iwz}dw$$

becomes valid over the entire upper half-plane $\operatorname{Im} z>\epsilon$. Under these conditions the integral reduces to the sum of the deductions at all the poles of the integrand.

If the functions $\cos\frac{w\pi}{2}$ and $\sin 2w\Phi$ do not have common zeroes (this is the case, for example, if $2\Phi=\frac{\pi n}{2m}$, where $\frac{n}{2m}$ is an irreducible fraction) then all of the poles of the denominator are simple ones and are located at the points $w=2k-1$ $(k=1,2,3,\ldots)$ and $w=\frac{s\pi}{2\Phi}$ $(s=1,2,3,\ldots)$.

Under these conditions we have

$$\eta_\Phi(z+\varphi_1)+\eta_\Phi(z-\varphi_1)=\frac{\pi}{4\Phi i}+\frac{\pi}{2\Phi i}\sum_{s=1}^{\infty}(-1)^s\frac{\cos\frac{s\pi\varphi_1}{2\Phi}}{\cos\frac{\pi^2 s}{4\Phi}}\exp\left(\frac{i\pi sz}{2\Phi}\right)+$$
$$+\frac{2}{i}\sum_{k=1}^{\infty}(-1)^k\frac{\cos(2k-1)\varphi_1}{\sin(2k-1)2\Phi}\exp[i(2k-1)z]. \tag{44}$$

This expression loses its meaning only in the case where the flare angle of the wedge is $2\Phi=\pi\frac{n}{2m-1}$ Under these conditions the terms corresponding to $s=n(2r-1)$; $2k-1=(2m-1)(2r-1)$ under the summing sign become infinite.

In such a case these terms should be omitted under the summing sign, but the term

$$-\frac{4(2m-1)}{n\pi}z\sum_{r=1}^{\infty}(-1)^{m(r-1)}\cos[(2m-1)(2r-1)]\exp\{i[(2m-1)(2r-1)z]\}. \tag{45}$$

must be added to the right-hand side.

Leaving aside this special case which can be examined more easily by another method, we make use of the Series (44) which converges absolutely and uniformly for $\operatorname{Im} z>\epsilon$.

Substituting this series into (43) and changing the sequence of summing and integrating, we obtain

$$S(r,\ \varphi_1-\Phi)=\frac{\pi}{4\Phi}J_0(kr)+\frac{\pi}{2\Phi}\sum_{s=1}^{\infty}(-1)^s\exp\left[-\frac{is\pi^2}{4\Phi}\right]\frac{\cos\frac{s\pi\varphi_1}{2\Phi}}{\cos\frac{s\pi^2}{4\Phi}}J_{\frac{s\pi}{2\Phi}}(kr)+$$

$$+2\sum_{k=1}^{\infty}(-1)^k\exp\left[-\frac{i(2k-1)\pi}{2}\right]\frac{\cos[(2k-1)\varphi_1]}{\sin[2\Phi(2k-1)]}J_{2k-1}(kr),\tag{46}$$

where $J_p(\rho)$ is a Bessel function which is expressed in terms of a Sommerfeld integral:

$$J_p(\rho)=-\frac{\exp\left(-\frac{ip\pi}{2}\right)}{2\pi}\int_{\gamma_1}\exp(-i\rho\cos z)\exp(ipz)\,dz.$$

Making the substitution $\varphi_1=\varphi+\Phi$ in Equation (46), we obtain the unknown Series (41).

## 5. The Relationship Between the Solutions for the Problem of Radiation From the Boundary of a Wedge and the Problem of Diffraction Upon a Rigid Wedge.

Let $u(r,\varphi)$ be the sound pressure field in the wedge-shaped region $|\varphi|<\Phi$ which is produced as a result of the diffraction of a plane wave $u_0(r,\varphi)=p_0\exp[-ikr\cos(\varphi-\Phi)]$ upon a rigid wedge (Fig. 10). The incident plane wave $u_0$ slips along the boundary $\varphi=\Phi$.

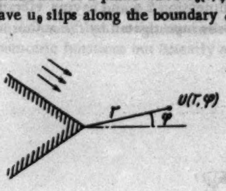

Fig. 10

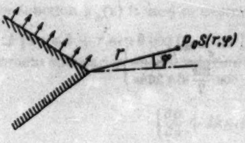

Fig. 11

On the other hand, we have a sound pressure field (which was examined above) that is expressed by $p_0S(r,\varphi)$ and which creates vibrations at the boundary $\varphi=\Phi$ (Fig. 11) that have a velocity $p_0/\rho c$.

It can be shown that

$$p_0S(r,\ \varphi+\pi/2)+p_0S(r,\ \varphi-\pi/2)=\frac{1}{2}u(r,\ \varphi).\tag{47}$$

That is, as a result of adding two angularly displaced solutions of the radiation problem (analytically extended beyond the boundary of the wedge) we obtain an accurate solution for the diffraction problem. In fact, the Sommerfeld solution for the examined diffraction problem is of the form:

$$u(r,\ \varphi)=\frac{p_0}{4\Phi i}\int_{\gamma}\exp[-ikr\cos(\varphi-z)]\frac{\cos\frac{\pi z}{2\Phi}}{\sin\frac{\pi z}{2\Phi}-1}dz.\tag{48}$$

On the other hand, since Equation (28) is valid we have

$$p_0\left[S\left(r,\ \varphi+\frac{\pi}{2}\right)+S\left(r,\ \varphi-\frac{\pi}{2}\right)\right]=\frac{p_0}{2\pi i}\int_{\gamma}\exp[-ikr\cos(\varphi-z)][\eta_{\Phi}(z+\Phi+$$

$$+\pi/2)+\eta_{\Phi}(z+\Phi-\pi/2)]\,dz,$$

but*

$$\eta_\Phi(z+\Phi+\pi/2)+\eta_\Phi(z+\Phi-\pi/2)=-\frac{\pi}{4\Phi}\tan\frac{\pi(z+\Phi)}{4\Phi}=$$
$$=\frac{\pi}{4\Phi}\,\frac{\cos\frac{\pi z}{2\Phi}}{\sin\frac{\pi z}{2\Phi}-1}\,.$$

Substituting this expression into the preceding integral, we verify the validity of (47).

In the particular case of $2\Phi=\pi$ when the field $u(r, \varphi)$ reduces to a plane wave $u=p_0\exp\left[-ikr\cos\left(\varphi-\frac{\pi}{2}\right)\right]=p_0\exp(-ikr\sin\varphi)$, we obtain the following expression from Equation (47):

$$S\left(r,\ \varphi+\frac{\pi}{2}\right)+S\left(r,\ \varphi-\frac{\pi}{2}\right)=\frac{1}{2}\exp\left[-ikr\sin\varphi\right].$$

## SUPPLEMENT

### The Properties of the Function $\eta_\Phi(z)$

The function $\eta_\Phi(z)$ determines the angular distribution of the plane wave amplitudes in the Sommerfeld integral which expresses the wave field in a wedge having the angular dimension $2\Phi$ and having vibrating boundaries. Let us give the basic properties of this function which have been investigated by the author in solving another problem.

1) The integral representations are

$$\eta_\Phi(z)=\frac{e^{-iz}}{4i\Phi}\int_0^\infty\frac{(t^{\pi/2\Phi}-1)\,dt}{(t^{\pi/2\Phi}+1)(t^2+e^{-2iz})}\,, \tag{1}$$

$$\eta_\Phi(z)=\frac{1}{8i\Phi}\int_{-\infty}^{\infty}\frac{\tanh\frac{\pi t}{4\Phi}}{\cosh(t+iz)}\,dt\,, \tag{2}$$

$$\eta_\Phi(z)=-\frac{1}{8}\left\{\int_{-\varepsilon-i\infty}^{-\varepsilon+i\infty}\frac{e^{-iwz}\,dw}{\cos\frac{\pi w}{2}\sin 2\Phi w}+\int_{\varepsilon-i\infty}^{\varepsilon+i\infty}\frac{e^{-iwz}\,dw}{\cos\frac{\pi w}{2}\sin 2\Phi w}\right\}. \tag{3}$$

2) The functional relationships are

$$\eta_\Phi(z)+\eta_\Phi(-z)=0, \tag{4}$$

$$\eta_\Phi(z-2\Phi)-\eta_\Phi(z+2\Phi)=\frac{1}{\cos z}, \tag{5}$$

$$\eta_\Phi\left(z+\frac{\pi}{2}\right)+\eta_\Phi\left(z-\frac{\pi}{2}\right)=-\frac{\pi}{4\Phi}\tan\frac{\pi z}{4\Phi}, \tag{6}$$

---

* See supplement at end of paper.

$$\eta_{\Phi}(z-\pi)-\eta_{\Phi}(z+\pi)=\frac{\pi}{2\Phi}\,\frac{\sin\frac{\pi^2}{4\Phi}}{\cos\frac{\pi^2}{4\Phi}+\cos\frac{\pi z}{2\Phi}}, \tag{7}$$

$$\eta_{\Phi}(z+\Phi)+\eta_{\Phi/2}(z-\Phi)=\eta_{\Phi/2}(z). \tag{8}$$

3) The representation in the form of a series is

$$\eta_{\Phi}(z)=2z\sum_{l=1}^{\infty}\sum_{k=1}^{\infty}\frac{(-1)^{l+1}}{z^2-\left[\frac{\pi}{2}(2l-1)+2\Phi\,(2k-1)\right]^2}. \tag{9}$$

4) Particular cases.

If $\Phi = \frac{\pi}{4}\cdot\frac{n}{m}$, where $\frac{n}{m}$ is an irreducible rational faction, the integral (58) is taken in finite form.

If n is odd, then

$$\eta_{\pi n/4m}(z)=\frac{m}{2n}\sum_{l=1}^{n}(-1)^l\tan\frac{n}{m}\left[z-\frac{\pi}{2}\,(2l-1)\right]+\frac{1}{2}\sum_{k=1}^{m}\sec\left[z+\frac{n}{m}\,\frac{\pi}{2}\,(2k-1)\right]. \tag{10}$$

If n is even, then in the expression for the function $\eta_{\Phi}(z)$ the variable z appears not only under the signs of trigonometric functions but linearly as well. For example,

$$\eta_{\pi/2}(z)=\frac{z}{2\pi\cos z}-\tan\frac{z}{4}, \tag{11}$$

$$\eta_{\pi}(z)=\frac{\cos\frac{\pi}{4}\sin\frac{z}{2}-\frac{z}{2\pi}}{2\cos z}-\tan\frac{z}{8}. \tag{12}$$

5) Another application of the function $\eta_{\Phi}(z)$.

The function $\eta_{\Phi}(z)$ is used to express the solution for the diffraction problem involving the plane wave $\exp\{-ik\,[z\cos\theta+r\sin\theta\cos(\varphi-\varphi_0)]\}$ in a wedge-shaped region $(|\varphi|<\Phi,\ |z|<\infty,\ 0\leq r<\infty)$ with absorbent boundaries when the following boundary conditions obtain:

$$\left[\frac{\partial p}{\partial n}+ikg_1p\right]_{\varphi=\Phi}=0;\ \left[\frac{\partial p}{\partial n}+ikg_2p\right]_{\varphi=-\Phi}=0. \tag{13}$$

If the admittances of the boundaries are expressed in terms of the auxiliary angles $\vartheta_1$ and $\vartheta_2$, and if it is assumed that $g_1 = \sin\theta\sin\vartheta_1$; $g_2 = \sin\theta\sin\vartheta_2$ while using the definitions

$$\begin{aligned}f(t)=\eta_{\Phi}\left(t+\Phi-\frac{\pi}{2}+\vartheta_1\right)-\eta_{\Phi}\left(t+\Phi-\frac{\pi}{2}-\vartheta_1\right)+\\+\eta_{\Phi}\left(t-\Phi+\frac{\pi}{2}-\vartheta_2\right)-\eta_{\Phi}\left(t-\Phi+\frac{\pi}{2}+\vartheta_2\right).\end{aligned} \tag{14}$$

$$s(\alpha) = \frac{\pi}{2\Phi} \frac{\cos \frac{\pi \varphi_0}{2\Phi}}{\sin \frac{\pi \alpha}{2\Phi} - \sin \frac{\pi \varphi_0}{2\Phi}} \times$$

$$\times \frac{\sin \frac{\pi}{4\Phi}(\alpha - \Phi - \vartheta_1) \sin \frac{\pi}{4\Phi}(\alpha + \Phi + \vartheta_2)}{\sin \frac{\pi}{4\Phi}(\varphi_0 - \Phi - \vartheta_1) \sin \frac{\pi}{4\Phi}(\varphi_0 + \Phi + \vartheta_2)} \exp \left[ \int_{\varphi_0}^{\alpha} f(t) dt \right], \qquad (15)$$

then the solution obtained by the author for the problem of [2] in 1949 is given by the Sommerfeld integral

$$p(r, \varphi, z) = \frac{e^{-ikz \cos \theta}}{2\pi i} \int_{\gamma} e^{-ikr \sin \theta \cos(\varphi - \alpha)} s(\alpha) \, d\alpha. \qquad (16)$$

## LITERATURE CITED

[1] G. D. Maliuzhinets, Doklady Akad. Nauk SSSR 60, 3, 307-311 (1948). Doklady Akad. Nauk SSSR 78, 3, 439-442 (1951); J. Tech. Phys. (U.S.S.R.) 21, 8, (1951).

[2] G. D. Maliuzhinets, Dissertation, Phys. Inst. Acad. Sci (U.S.S.R.); Authors' Index (Acad. Sci. USSR Press, 1950).

[3] A. Sommerfeld, from the book Differential and Integral Equations of Mathematical Physics by F. Frank and G. Mizes (United Sci. Tech. Press, 1937).

Acoustics Institute of the Academy of Science USSR, Moscow

Received March 1, 1955

# NONLINEAR DISTORTION OF A NONPERIODIC SIGNAL IN AN ELECTROACOUSTIC CHANNEL

A. V. Rimskii-Korsakov

**For the purposes of an approximate evaluation of the nonlinear distortion in an electroacoustic channel it is assumed that the transmitted signal is a stationary random process and that its spectral density at the output can be computed according to the spectral density at the input and according to the nonlinearity characteristic of the channel. The nonlinear transformation of the spectrum is examined when the nonlinearity characteristic is approximated by an exponential polynomial. For the particular case of "rectangular" and "bell-shaped" spectra, expressions are given for the spectral density of the nonlinear products of the second and third and second-through-fifth orders respectively.**

The computation of nonlinear distortion is usually performed on the basis that a periodic wave acts at the input of the nonlinear system. The computation is usually limited to two cases: a) a sinusoidal perturbation at the input, and, as a consequence of the low nonlinearity of the system, a wave of the same frequency at the output having more or less sharply expressed harmonics; b) the sum of two or several (a finite number) sinusoidal waves at the input, and the same frequencies, their harmonics and their modulation frequencies appearing correspondingly at the output. In the final analysis the nonlinearity coefficients, according to which the quality of the electroacoustic channel is estimated, are computed. However, these nonlinearity coefficients poorly characterize the phenomena which take place in the electroacoustic channel in its normal operating regime. In this latter case the elements of the channel are subjected to a nonperiodic input signal which has a continuous spectrum, considerable signal energy fluctuations in the critical audiofrequency bands, and extremely long duration of the entire perturbation in comparison to the periods which correspond to the region occupied by the spectrum.

Therefore, it seems rational to assume that the signal has the properties of a stationary random oscillatory process under the operating conditions which obtain for an electroacoustic channel. In that case it is possible to evaluate the channel according to the magnitude of the nonlinear distortion products which arise for a signal having a continuous spectrum.

For this purpose we should use the known method for computing the nonlinear transformation of a signal; this method is based upon the relationships between the probability and spectral characteristics of a random stationary oscillation.

By developing one particular case involving the computation of a nonlinear transformation for a detector with an exponential nonlinearity characteristic (this case is developed in a paper by V. A. Bunimovich [1]), it is possible to obtain the correlation function of the signal at the output for a nonlinear characteristic of the form

$$I=\sum_{1}^{n} A_k e^{\frac{u}{u_k}}. \tag{1}$$

Here u is the input signal, I is the output signal, $A_k$, $u_k$ are approximation coefficients which make it possible to represent the experimentally obtained nonlinearity characteristic in the form of (1). These coefficients can be computed by known methods which are described in the literature [2]. If the correlation coefficient of the input signal is equal to $R(\tau)$, then the correlation function of the output signal is written thus:

$$\overline{\Pi}_\tau = \sum_{(k)}^{n} \sum_{(i)}^{n} A_k A_i \int_{-\infty}^{+\infty}\int_{-\infty}^{+\infty} \frac{\exp\left[\frac{u}{u_k} + \frac{u_\tau}{u_i} - \frac{u^2 + u_\tau^2 - 2uu_\tau R(\tau)}{2\sigma^2[1 - R^2(\tau)]}\right]}{2\pi\sigma^2\sqrt{1 - R^2(\tau)}}\, du\, du_\tau .$$

Here $\sigma^2 = \overline{u^2}$. By making the following substitutions:

$$u = \frac{\sigma}{\sigma_1}(z - \alpha), \qquad u_\tau = \frac{\sigma}{\sigma_2}(z_\tau - \alpha),$$

$$\frac{1}{\sigma_1} = -\frac{\sigma}{\alpha}\left(\frac{R}{u_i} + \frac{1}{u_k}\right), \qquad \frac{1}{\sigma_2} = -\frac{\sigma}{\alpha}\left(\frac{R}{u_k} + \frac{1}{u_i}\right)$$

it is possible to eliminate the integral in the right-hand side of the expression; thus we obtain

$$\overline{\Pi}_\tau = \sum_{(k)}^{n} \sum_{(i)}^{n} A_k A_i \exp \frac{\sigma^2(u_k^2 + u_i^2 + 2Ru_k u_i)}{2u_k^2 u_i^2}. \tag{2}$$

The spectral density of the output signal is obtained as usual and is written as:

$$S(\omega) = \frac{2}{\pi}\int_0^\infty \left(\overline{\Pi}_\tau - \overline{\Pi}_{\tau\, R=0}\right)\cos\omega\tau\, d\tau =$$

$$= \sum_k \sum_i A_k A_i \exp\left[\frac{\sigma^2}{2u_i^2} + \frac{\sigma^2}{2u_k^2}\right] \times \frac{2}{\pi}\int_0^\infty \left[\exp\left(\frac{\sigma^2 R}{u_k u_i}\right) - 1\right]\cos\omega\tau\, d\tau. \tag{3}$$

The integrand can be substantially simplified if $\sigma^2 << u_k u_i$. In practice this is always the case if the investigated system has low nonlinearity. Precisely such a case is of interest when it is required to evaluate the quality of an electroacoustical tract which is designed for the transmission of an audiosignal containing nonlinear distortion which is unnoticeable (or hardly noticeable) to the ear. Then, assuming that $\frac{\sigma^2 R}{u_k u_i}$ is a quantity that is small in comparison with unity, one can expand $\exp \frac{\sigma^2 R}{u_k u_i}$ into a series so that

$$S(\omega) = \sum_k \sum_i A_k A_i \exp\left[\frac{\sigma^2}{2u_i^2} + \frac{\sigma^2}{2u_k^2}\right] \times \sum_m^\infty \frac{2}{\pi}\frac{1}{m!}\left(\frac{\sigma^2}{u_k u_i}\right)^m \int_0^\infty R^m(\tau)\cos\omega\tau\, d\tau.$$

By decomposing $S(\omega)$ into components which represent spectra of the m-th order, and which have a specified number m (so that the component with $m = 1$ is the undistorted portion of the transmitted signal, the component with $m = 2$ is the spectrum of the "quadratic" distortion, the component with $m = 3$ is the spectrum of the "cubic" distortion, etc.), we obtain

$$S(\omega) = \sum_{m}^{\infty} S_m \ldots$$

$$S_m = \sum_{k}\sum_{l} A_k A_l \exp\left[\frac{\sigma^2}{2u_k^2} + \frac{\sigma^2}{2u_l^2}\right] \frac{2}{\pi} \frac{1}{m!} \left(\frac{\sigma^2}{u_k u_l}\right)^m \int_0^{\infty} R^m(\tau) \cos \omega\tau \, d\tau. \tag{4}$$

**Further computations can only be performed for a definite type of input signal spectrum. Let us examine the case when the spectral density of the input signal is constant in the band $\omega_2 - \omega_1$ and is equal to zero outside of this band. Then**

$$R(\tau) = \frac{\sin \frac{\omega_2 - \omega_1}{2} \tau \cos \frac{\omega_1 + \omega_2}{2} \tau}{\frac{\omega_2 - \omega_1}{2} \tau}.$$

**The integral in Equation (4) acquires the form:**

$$\int_0^{\infty} \frac{\sin^m \left(\frac{\omega_2 - \omega_1}{2} \tau\right) \cos^m \left(\frac{\omega_1 + \omega_2}{2} \tau\right) \cos \omega\tau}{\left(\frac{\omega_2 - \omega_1}{2} \tau\right)^m} d\tau. \tag{5}$$

**By means of the formula for integration by parts the power of the denominator of the integrand can be lowered to the second power, and the numerator can be transformed to a product of $\sin^2 \alpha\tau$ and a cosine sum:**

$$\frac{\sin^2 \alpha\tau}{\alpha^2\tau^2} [b_1 \cos \beta_1\tau + b_2 \cos \beta_2\tau + \ldots].$$

**Here $\alpha = \frac{\omega_2 - \omega_1}{2}$, and $b_1, b_2, \ldots$ and $\beta_1, \beta_2, \ldots$ are linear combinations of the frequencies $\omega_2, \omega_1, \omega$. As a result it is necessary to integrate a function of the form**

$$\frac{\sin^2 \alpha\tau}{\alpha^2\tau^2} \cos \beta\tau d\tau.$$

**in order to solve Equation (5).**

**The substitution of $\alpha\tau = x$ and $\frac{\beta}{2\alpha} = p$ reduces the integrals to forms which can be found in the Tables [3]:**

$$\frac{b}{\alpha} \int_0^{\infty} \frac{\sin^2 x}{x^2} \cos 2px \, dx = \frac{\pi b}{2\alpha} (1 - |p|)_{0<|p|<1}. \tag{6}$$

**The Integral (6) is equal to zero outside of the region $0 < |p| < 1$. Thus, the inequality $0 < |p| < 1$ determines the boundary of the spectrum for nonlinear products of a given type, and the quantity $\frac{\pi b}{2\alpha}(1 - |p|)$**

determines the frequency dependence of the spectral density of the nonlinearity products. As an example, let us examine the spectra of the second-and third-order products.

1) m = 2.

$$S_2=\sum_k\sum_l\frac{\sigma^4 A_k A_l}{\pi u_k^3 u_l^3}\ \exp\left[\frac{\sigma_k^2}{2u_k^2}+\frac{\sigma^2}{2u_l^2}\right]\int_0^\infty\frac{\sin^2\alpha\tau}{4\alpha^2\tau^2}\,[2\cos\omega\tau+$$

$$+\cos(\omega_1+\omega_2+\omega)\tau+\cos(\omega_1+\omega_2-\omega)\tau]\,d\tau. \tag{7}$$

Transforming the integrand in Expression (7) to the form given in (6), we obtain three integrals:

$$\begin{gathered}\frac{\pi}{2}\left(1-\left|\frac{\omega}{\omega_2-\omega_1}\right|\right),\\ \frac{\pi}{4}\left(1-\left|\frac{\omega_1+\omega_2+\omega}{\omega_2-\omega_1}\right|\right),\\ \frac{\pi}{4}\left(1-\left|\frac{\omega_1+\omega_2-\omega}{\omega_2-\omega_1}\right|\right).\end{gathered}\tag{8}$$

The limits within which the first of these expressions exists are evident. As far as the other two are concerned, the inequality with a plus sign in front of $\omega$ is impossible when $\omega > 0$, and therefore the integral corresponding to it disappears. The remaining (third) integral can exist in the region $2\omega_1 < \omega < 2\omega_2$ (it is assumed from the outset that $\omega_2 > \omega_1$). The spectrum of the nonlinear second-order products increases linearly up to the frequency $\omega_1 + \omega_2$ and then decreases in the same manner, reaching the value $2\omega_2$.

2) m = 3.

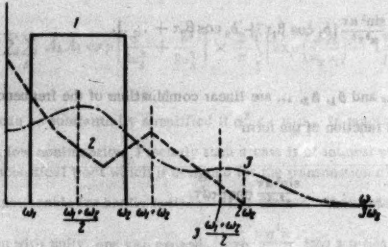

Fig. 1. Computed spectra $S_m$.

1) The spectrum $S_1$ of the input signal ($\omega_2 = 5\omega_1$),
2) the spectrum $S_2$ of the quadratic distortion products,
3) the spectrum $S_3$ of the cubic distortion products.

The method of computation has been indicated above. Omitting the trigonometric transformations and the investigation which is required to determine the existence of the integrals of the type (6) which are obtained, we provide the final result:

$$S_3=\sum_k\sum_l\frac{\sigma^6A_kA_l}{3\pi u_k^3u_l^3}\exp\left[\frac{\sigma}{2u_k^2}+\frac{\sigma^2}{2u_l^2}\right]\Bigg\{\underset{\substack{0<\omega<\omega_2-2\omega_1\\ \omega_2>2\omega_1}}{\frac{3(\omega_2-2\omega_1-\omega)^3}{(\omega_2-\omega_1)^3}}+\underset{\substack{0<\omega<\omega_1\\ \omega_2>2\omega_1}}{\frac{3(\omega_2-2\omega_1+\omega)^3}{(\omega_2-\omega_1)^3}}+$$

$$+\underset{\omega_1<\omega<\omega_2}{\frac{3\left[(\omega_1-\omega_2)^3-2(\omega_1-\omega)(\omega_2-\omega)\right]}{(\omega_2<\omega_1)^3}}+\underset{\omega_2<\omega<2\omega_2-\omega_1}{\frac{3(2\omega_2-\omega_1-\omega)^3}{(\omega_2-\omega_1)^3}}+$$

$$+\underset{3\omega_1<\omega<2\omega_1+\omega_2}{\frac{(\omega-3\omega_1)^3}{(\omega_2-\omega_1)^3}}+\underset{2\omega_1+\omega_2<\omega<2\omega_2+\omega_1}{\frac{6(\omega_1+\omega_2)\omega-3(\omega_1+\omega_2)^3-2\omega^3-6\omega_1\omega_2}{(\omega_2-\omega_1)^3}}+\underset{2\omega_2+\omega_1<\omega<3\omega_2}{\frac{(3\omega_2-\omega)^3}{(\omega_2-\omega_1)^3}}\Bigg\}. \qquad (9)$$

In this expression the first two terms within the braces are written for the case of a comparatively wide spectrum band at the input, where $\omega_2 > 2\omega_1$. If $\omega_2 < 2\omega_1$, then the first of these components disappears, and the second exists within the limits $2\omega_1 - \omega_2 < \omega < \omega_1$.

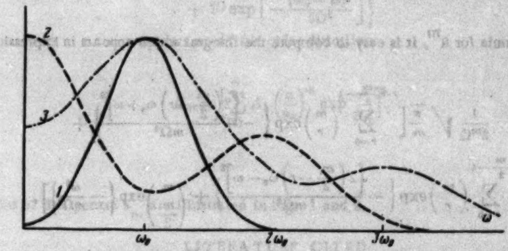

Fig. 2. Computed spectra $S_m$.

1) The spectrum $S_1$ of the input signal ($\frac{\omega_0}{\omega_1} = 2$), 2) the spectrum $S_2$ of the quadratic distortion products, 3) the spectrum $S_3$ of the cubic distortion products.

It is essential that the distribution of the nonlinear products of a definite order depends upon the nature of the spectrum at the input and not upon the form of the nonlinearity. Only the amplitudes of the spectra of various orders relative to one another depend upon the type of nonlinearity. For the case of low nonlinearity, when $\frac{\sigma^2}{u_k^2} \ll 1$, the expression determining the amplitude of the m-th spectrum can be considerably simplified if we assume that $\exp\left[\frac{\sigma^2}{2u_k^2}+\frac{\sigma^2}{2u_l^2}\right]\approx 1$:

$$S_m\approx\frac{2}{\pi m!}\left[\sum_{(k)}^{n}A_k\frac{\sigma^m}{u_k^m}\right]^2\int_0^\infty R^m\cos\omega\tau d\tau.$$

A convenient special form of $S_m$ is obtained when it is assumed that $R = \exp\left\{-\frac{\tau^2\Omega^2}{4}\right\}\cos\omega_0\tau$. Such a correlation coefficient corresponds to an input signal which has the spectrum

$$S(\omega)=\overline{u^2}\sqrt{\frac{\pi}{\Omega^2}}\left[\exp\left\{-\frac{(\omega_0-\omega)^2}{\Omega^2}\right\}+\exp\left\{-\frac{(\omega_0+\omega)^2}{\Omega^2}\right\}\right],$$

where $\Omega$ is the bandwidth of the spectrum, and $\omega_0$ is the central frequency. The convenience of such a selection lies in the fact that $R^m$ and the integrals of $R^m \cos \omega\tau$ can be expressed in terms of easily readable and comparatively compact formulas:

$$\exp\left\{-\frac{\tau^2 m\Omega^2}{4}\right\}\cos^m\omega_0\tau =$$

$$= \begin{cases} \dfrac{1}{2^m}\left[\sum\limits_{r=0}^{r=\frac{m}{2}-1} 2\binom{m}{r}\exp\left\{-\dfrac{m\tau^2\Omega^2}{4}\right\}\cos 2\left(\dfrac{m}{2}-r\right)\omega_0\tau + \dbinom{m}{\frac{m}{2}}\exp\left\{-\dfrac{m\tau^2\Omega^2}{4}\right\}\right] \\ \qquad\qquad m - \text{ even} \\ \dfrac{1}{2^m}\sum\limits_{r=0}^{\frac{m+1}{2}-1} 2\binom{m}{r}\exp\left\{-\dfrac{m\tau^2\Omega^2}{4}\right\}\cos(m-2r)\,\omega_0\tau \\ \qquad\qquad m - \text{ odd} \end{cases}$$

Utilizing this formula for $R^m$, it is easy to compute the integral which appears in Expression (4): its value is

$$\frac{1}{2^m\Omega}\sqrt{\frac{\pi}{m}}\left[\sum_{r=0}^{r=\frac{m}{2}-1}\binom{m}{r}\exp\left\{-\frac{\left[2\left(\frac{m}{2}-r\right)\omega_0+\omega\right]^2}{m\Omega^2}\right\}+\right.$$

$$\left.+\sum_{r=0}^{\frac{m}{2}-1}\binom{m}{r}\exp\left\{-\frac{\left[2\left(\frac{m}{2}-r\right)\omega_0-\omega\right]^2}{m\Omega^2}\right\}+\binom{m}{\frac{m}{2}}\exp\left\{-\frac{\omega^2}{m\Omega^2}\right\}\right],$$

when $m$ is even and

$$\frac{1}{2^m\Omega}\sqrt{\frac{\pi}{m}}\left[\sum_{r=0}^{\frac{m+1}{2}-1}\binom{m}{r}\exp\left\{-\frac{[(m-2r)\,\omega_0+\omega]^2}{m\Omega^2}\right\}+\right.$$

$$\left.+\sum_{r=0}^{\frac{m+1}{2}-1}\binom{m}{r}\exp\left\{-\frac{[(m-2r)\,\omega_0-\omega]^2}{m\Omega^2}\right\}\right].$$

when $m$ is odd.

As an example we provide expressions for spectra of the first five orders:

$$S_1 = \frac{2}{\Omega\sqrt{\pi}}B_1\left\{\exp\left[-\frac{(\omega_0-\omega)^2}{\Omega^2}\right]+\exp\left[-\frac{(\omega_0+\omega)^2}{\Omega^2}\right]\right\}$$

Fundamental undistorted wave

$$S_2 = \frac{1}{4\Omega\sqrt{2\pi}}B_2\left\{\exp\left[-\frac{(2\omega_0+\omega)^2}{2\Omega^2}\right]+\exp\left[-\frac{(2\omega_0-\omega)^2}{2\Omega^2}\right]+2\exp\left[-\frac{\omega^2}{2\Omega^2}\right]\right\}$$

Spectrum of quadratic distortion

$$S_3=\frac{1}{24\Omega\sqrt{3\pi}}B_3\left\{\exp\left[-\frac{(3\omega_0+\omega)^2}{3\Omega^2}\right]+\exp\left[\frac{3\omega_0-\omega)^2}{3\Omega^2}\right]+\right.$$
$$\left.+3\exp\left[-\frac{(\omega_0+\omega)^2}{3\Omega^2}\right]+3\exp\left[-\frac{(\omega_0-\omega)^2}{3\Omega^2}\right]\right\}$$

**Spectrum of cubic distortion**

$$S_4=\frac{1}{192\,\Omega\sqrt{4\pi}}B_4\left\{\exp\left[-\frac{(4\omega_0+\omega)^2}{4\Omega^2}\right]+\exp\left[-\frac{(4\omega_0-\omega)^2}{4\Omega^2}\right]+\right.$$
$$\left.+4\exp\left[-\frac{(2\omega_0+\omega)^2}{4\Omega^2}\right]+4\exp\left[-\frac{(2\omega_0-\omega)^2}{4\Omega^2}\right]+6\exp\left[-\frac{\omega^2}{4\Omega^2}\right]\right\}$$

**Spectrum of fourth-order distortion**

$$S_5=\frac{1}{480\,\Omega\sqrt{5\pi}}B_5\left\{\exp\left[-\frac{(5\omega_0+\omega)^2}{5\Omega^2}\right]+\exp\left[-\frac{(5\omega_0-\omega)^2}{5\Omega^2}\right]+\right.$$
$$+5\exp\left[-\frac{(3\omega_0+\omega)^2}{5\Omega^2}\right]+5\exp\left[-\frac{(3\omega_0-\omega)^2}{5\Omega^2}\right]+10\exp\left[-\frac{(\omega_0+\omega)^2}{5\Omega^2}\right]+$$
$$\left.+10\exp\left[-\frac{(\omega_0-\omega)^2}{5\Omega^2}\right]\right\}$$

**Spectrum of fifth-order distortion**

**Here**

$$B_m=\left[\sum_{(k)}^{n}A_k\left(\frac{\sigma}{u_k}\right)^m\exp\frac{\sigma^2}{2u_k^2}\right]^2.$$

**The computations of the spectra $S_m$ are illustrated in Figs. 1 and 2.**

## LITERATURE CITED

**[1] V. I. Bunimovich, Fluctuating Processes In Radio-Receiving Units (Soviet Radio Press, Moscow, 1951).**

**[2] Ia. S. Bezikovich, Approximate Computations (State Tech. Press. Moscow-Leningrad, 1949).**

**[3] I. M. Ryzhik and I. S. Gradshtein, Tables Of Integrals, Sums, Series and Products (State Tech. and Theor. Lit. Press, Moscow-Leningrad, 1951).**

**Leningrad Bonch-Bruevich Electrical-Engineering**
**Communications Institute**

**Received February 9, 1954**

# TONAL METHOD FOR DETERMINING THE INTELLIGIBILITY OF SPEECH TRANSMITTED BY COMMUNICATIONS CHANNELS

A. D. Tkachenko

**A new method is analyzed for determining the intelligibility of speech which is transmitted by communications channels; this method does not require articulation tests.**

**The theoretical bases of the method is given as well as the necessary data for its practical utilization; results are given from comparisons of intelligibility as determined by the method described and by articulation tests.**

Recently the problem of evaluating the quality of speech which is transmitted by telephone systems has acquired special significance. There are a great variety of known methods for making such an evaluation, and these methods have been adopted by one or another group of organizations; however, the method of evaluating the quality of transmitted speech according to intelligibility occupies a very important place among these methods.

The intelligibility of speech which is transmitted by telephone systems is determined in practice by the method of articulation. The essence of the articulation method, as we know, consists in the transmission and reception of definite speech material through the test channel. The intelligibility is determined by the percentage of properly received sound combinations. Depending upon the nature of the transmitted sound material, we can determine intelligibility with respect to meaning (i.e., phrase intelligibility) I, work intelligibility W, syllabic intelligibility S and sound intelligibility D.

It is also known that among all of the indicated types of intelligibility there exists a definite relationship which is characteristic for a given language. Therefore, for the purpose of an all-sided evaluation of the telephone system being tested, it is sufficient to perform a determination of intelligibility for only one of the indicated types of speech material. In the practice of articulation tests the most economical methods prove to be the methods of determining syllabic and sound intelligibility; therefore, they have become the ones most widely used.

In order to determine intelligibility by the articulation method we selected a working group of four-five persons who had the necessary development and characteristics of speech and hearing that satisfied definite requirements. Such a group must first be taught and systematically trained in the transmission and reception of speech material.

The process of performing articulation tests is a prolonged one. It has been established, for example, that in order to determine the syllabic intelligibility assured by the test channel it is necessary for the indicated working group of people to receive 1600-2000 syllables [1, 2]. In order to obtain the result of the tests (i.e., the results of the transmission, reception and calculation of the properly received syllables) a time which is usually greater than 3-4 hours is required.

However, notwithstanding the prolonged nature of articulation tests, their results may depend to a considerable degree upon the subjective peculiarities of the people making up the group – namely upon the pronounciation and the maintenance of constant loudness of speech during transmission, and upon the intensity of attention, comprehension and fatigue during reception. The results obtained by direct experiment need to be manipulated so as to eliminate data which deviates appreciably for individual pairs of participants to completely eliminate the results obtained by testing individual operators. This shows how difficult it is to obtain comparable test results for the same channels when the tests are conducted for definite constant conditions but at different times and (even more important) by different working groups. Therefore, the articulation method has up to this time achieved only a limited practical application, notwithstanding the universally acknowledged importance of the characteristics which are obtained as the result of articulation tests.

Another method, which is based upon computation, is known to be usable for the purpose of determining the intelligibility which is assured by telephone channels. In [2, 3, 4, and 5] it is shown that the intelligibility which is assured by communications channels can in principle be determined by computation. For this purpose it is necessary to know the characteristics of the channel as measured by objective instruments, the noise and interference characteristics, and the auditory and speech characteristics. However, for actual channels such a computation proves to be complex and difficult, and due to the effect of many variable factors, its results only approximately agree with the data obtained from practical tests.

The proposed tonal method which does not require the performance of cumbersome articulation tests is considerably freer from the effects of the subjective peculiarities of the operators who take part in the tests, does not require the creation of working groups, and in comparison to the articulation method takes 8-10 times less time.

In order to clarify the essence of the proposed method it is necessary to examine the basic relationships which exist between the characteristics of the channel, the noise and interference, and the speech and auditory characteristics on the one hand, and the intelligibility of the transmitted speech on the other hand. In this regard the method is based upon known theoretical and experimental assumptions which deal with the reception of speech by the human auditory apparatus and the recognition of individual speech sounds [2, 3, 4, 5, and 6].

It is well-known that intelligibility is governed by the intensity levels of the speech sounds as well as by the levels of interference and noise which affect the ear (both directly and through the transmission channel) at the point of speech reception. The intensity level of speech sounds depends upon the properties of the speaker's voice and upon the electroacoustic characteristics of the channel; the intensity level of noise and interference depends upon the reception conditions and upon the properties of the channel. However, for each of the two persons carrying on a conversation, the intelligibility is determined not by the absolute magnitude of the speech and noise intensity levels but by the level of speech perception (i.e., the degree to which the speech components exceed the auditory threshold). Generally speaking, the subjective factors noted above also affect the intelligibility of speech, but in evaluating the quality of channels they can be excluded to one or another degree by selecting definite average values for these factors.

Besides the forms of intelligibility indicated above, the concept of formant intelligibility (A) is introduced. Formant intelligibility for a given channel cannot be determined by direct measurement, but can be computed according to the corresponding characteristics of speech, noise and hearing. Having obtained the value of formant intelligibility by computation, it is possible to determine any practically required form of intelligibility (sound, syllabic, word, phrase) by means of known functions.

The formant intelligibility has one property which none of the other forms of intelligibility has – namely, the property of additivity of individual particular values whose arithmetic sum yields an over-all intelligibility. This property makes it possible to find the over-all formant intelligibility which is guaranteed by the channel if the intelligibility corresponding to individual frequency bands is known.

For each national language the entire frequency range of speech can be subdivided into twenty such frequency bands, each of which guarantees 5% formant intelligibility under optimum transmission conditions. Thus, the transmission of the entire frequency range (i.e., the transmission of twenty bands) guarantees 100% formant intelligibility (A) under these conditions. However, if the perception level for the frequency band ($E'_n$) is not optimum, then the formant intelligibility will differ from 5%; this will be taken into account by the perception coefficient $P_n$, of a band, where $P_n = \varphi(E'_n)$. The formant intelligibility A of a band will in this case be $A_n = 0.05\,P$ when the perception coefficient P is taken into account.

The formant intelligibility A of the entire speech range will be equal to the sum of the formant intelligibilities of all the received bands;

$$A = 0.05 \sum_{n=1}^{n=20} P_n = 0.05 (P_1 + P_2 + P_3 + \ldots + P_n).$$

As we have indicated above, it is possible to use the formant intelligibility A to determine all other forms of intelligibility on the basis of the functions established for a given language. From what has been said above it is evident that the magnitude of the formant intelligibility (and therefore, the magnitude of all other forms of intelligibility) is determined by the sensation level of a formant in each of the twenty frequency bands.

In a number of papers it was shown that the formant spectrum can be expressed with a small error in terms of a mean (during the course of a prolonged period of time) level $B_{av}$ of the spectrum [3]. The sensation level of the formant $E'_n$ in each band will then be determined on the basis of the expression;

$$E'_n = B_{av.} - (b + M) - x,$$

where $B_{av}$ is the mean level (over a long period of time) of the speech spectrum per 1 cps, b is the attenuation of the channel, M is the masking factor which is the result of the noise and interference effects, x is the audibility threshold of the spectrum.

Since

$$x = \beta_0 - 10 \log \Delta f_{cr.}$$

where $\beta_0$ is the audibility threshold of a pure tone and $\Delta f_{cr.}$ is the width of the critical frequency band, we have

$$E'_n = B_{av.} - (b + M) - \beta_0 + 10 \log \Delta f_{cr.}$$

Usually this expression is basic in computing intelligibility. Under these conditions $B_{av.}$, $\beta_0$, $\Delta f_{cr.}$ are known quantities, b is determined by measuring the characteristics of individual elements in each channel or by computing the attenuation of the channel, M is computed according to the data on the spectrum of the acoustical and electrical noises and according to the characteristics of the channel.

The idea of the proposed new method consists of determining the sensation level of speech $E'_n$ (henceforth, we shall call this quantity the excess) in individual frequency bands by means of direct measurements involving human hearing.

In principle the problem of measuring the excess reduces to determining the speech components by listening at the output of the channel while all interference factors operate simultaneously (these interference factors are acoustical noises, electrical interference, etc.). For this purpose one of the frequency bands of the speech spectrum must be fed to the input of the channel under given conditions of acoustical noise and electrical interference, and then the level in this band must be brought to the audibility threshold by some method (for example, the amount of attenuation $b_{a.b.}$ which is established in the attenuation box in this case will be the magnitude of the excess for the components corresponding to the specified frequency band. By successively feeding all of the frequency spectrum bands into the input of the channel it is possible to determine the values of excess which correspond to them.

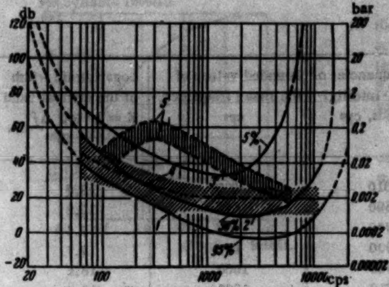

Fig. 1. The effect of noise upon the levelling of the audibility thresholds.

It is possible to simplify considerably the performance of the indicated measurements if the frequency bands of the spectrum are replaced by individual pure tones which correspond to the specified frequency bands in terms of their position in the speech spectrum and in terms of level, and which are fed to the input of the channel by means of an artificial voice. From the expression for $E'_n$ it is evident that if at a given frequency a pure tone with a level equal to the level of the speech spectrum $B_{av.}$ for that frequency is created in front of a microphone, then all of the factors which are included in that expression will be actually taken into account when we measure the magnitude of the excess (with the exception of the logarithmic width 10 log $\Delta f_{cr.}$ of the critical band). Therefore, in measuring the magnitude of the excess for a pure tone it is necessary to create a sound pressure of a level

$$B_{a.v.} = B_{av.} + 10 \log \Delta f_{cr.}$$

in front of the microphone.

In order to achieve a more accurate reproduction of the actual speech spectrum by means of an artificial voice it is necessary to subdivide the entire speech range in such a manner that the greatest possible number of frequency bands approximate critical bands, and then to establish corresponding values of $B_{av.}$ corresponding to the mean frequencies of these bands. In practice it is more convenient to have only one measuring point in each band that has equal intelligibility. Therefore, it is more practicable to utilize the mean frequencies of the bands which have equal intelligibilities, the more so since the width of these bands is small and modern channels have a relatively uniform frequency response.

Since a definite speech spectrum is specified for all the measurements (this spectrum must be assumed identical for all cases of measurement), the application of an artificial voice makes the specified method completely objective from the point of view of transmission, since it completely eliminates the participation of human speakers from the transmission process.

The work of the operators at the reception point is also considerably simplified in comparison to the reception of syllables in articulation tests. The problem of the operators in this method is solely the determination of the audibility boundary of the tone. Although there is a considerable divergence in the audibility thresholds of various people, it is nevertheless true that the presence of the noise which obtains during ordinary operation (and which therefore must also exist during the tests of the equipment) leads to the reduction of this difference. The effect of noise upon the levelling of the audibility thresholds is evident from Fig. 1 which is taken from [6]. The curves (1), (2), (3) are the result of generalizing the measurements of audibility thresholds in silence, as measured on more than one-half million people. Here the numbers 5, 50, 95, denote respectively that 5, 50, 95% of the people did not hear tones which had a level below the indicated boundary. Curve (4) gives values of the masking level which is due to the presence of room noise whose over-all level comprised 43 db. Even for this case the audibility thresholds for the majority of the people actually overlap in a wide range of frequencies (from 200 to 6,000 cps). On the other hand, in testing telephone equipment the acoustical noise in the speech (continuous) spectrum is usually established at an intensity level which is not less than 60 db. Curves (5) in Fig. 1 show the values of the masking level as normalized to a noise level of 65-75 db. In that case the audibility thresholds for practically all people who do not have obvious auditory defects overlap over a wide frequency range. The levelling of the audibility thresholds of various participants in the tests leads to the fact that the necessity of

**TABLE 1**

**Frequency Bands of Equal Intelligibility for Formants.**

| Bands of equal intelligibility, cps | Width of the equal-intelligibility bands, cps | Mean frequencies of the equal-intelligibility bands, cps | Rounded values of the mean frequency, cps | Logarithmic width of the critical band $K = 10 \log \Delta f_{cr.}$, db |
|---|---|---|---|---|
| 117 – 510 | 393 | 310 | 300 | 17.0 |
| 510 – 670 | 160 | 590 | 600 | 17.2 |
| 670 – 820 | 150 | 740 | 750 | 17.4 |
| 820 – 975 | 155 | 900 | 900 | 17.7 |
| 975 – 1130 | 155 | 1050 | 1050 | 18.1 |
| 1130 – 1290 | 160 | 1210 | 1200 | 18.4 |
| 1290 – 1445 | 155 | 1370 | 1400 | 18.6 |
| 1445 – 1600 | 155 | 1520 | 1550 | 19.0 |
| 1600 – 1760 | 160 | 1680 | 1700 | 19.3 |
| 1760 – 1925 | 165 | 1840 | 1850 | 19.6 |
| 1925 – 2100 | 175 | 2010 | 2000 | 20.0 |
| 2100 – 2300 | 200 | 2200 | 2200 | 20.4 |
| 2300 – 2540 | 240 | 2420 | 2400 | 20.7 |
| 2540 – 2820 | 280 | 2680 | 2700 | 21.0 |
| 2820 – 3160 | 340 | 2990 | 3000 | 21.5 |
| 3160 – 3530 | 370 | 3340 | 3400 | 22.1 |
| 3530 – 3930 | 400 | 3730 | 3750 | 22.8 |
| 3930 – 4400 | 470 | 4160 | 4100 | 23.0 |
| 4400 – 5400 | 1000 | 4900 | 5000 | 24.4 |
| 5400 – 10000 | 4600 | 7700 | 8000 | - |

having a large number of operators at the reception point is removed when noise is present; this is true since in determining the excesses such subjective features of the operators as, for example, the attentiveness, the speed of reaction, fatigue, etc., produce a substantially lesser effect than they do in determining intelligibility by the method of transmission and reception of syllables. This guarantees the possibility of the participation of only one (and as a maximum, two) operators in all measurements of excesses.

The basic original data concerning the characteristics of Russian speech was obtained from [1].

In accordance with this paper it is necessary to transmit a frequency range of from 120 to 10,000 cps in order to obtain 100% formant intelligibility of Russian speech when this speech is received at an optimum sensation level. This range is subdivided into 20 frequency bands each of which guarantees an identical five-percent formant intelligibility at an optimum sensation level $E'_n$ of the speech spectrum in the specified band.

The frequency limits of the equal-intelligibility bands and the mean frequencies of these bands are given in Table 1. The same table provides the values of the logarithmic width of the critical bands as normalized to the mean frequencies.

The relationship between the formant and syllabic intelligibility, $S = \varphi(A)$, for Russian speech is given in Fig. 2 in accordance with [1]. The relationship between the perception probability and the sensation level, $P = \varphi[E'_n]$, (Fig. 3) was established on the basis of the material cited in [1] with additional experimental refinement. The relationship $P = \varphi[E'_n]$ given in the indicated paper was only a first approximation and therefore, could not be used directly.

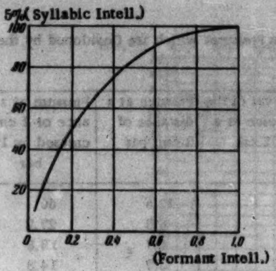

Fig. 2. The relationship between the formant and syllabic intelligibility for Russian speech.

The frequency spectrum $\dot{B}_{av.}$ of Russian speech is shown in Fig. 4 in accordance with [1]. It is determined as the mean (taken over a long period of time) speech level per one cps in the frequency bands at a distance of 8 cm from the mouth of the speaker and yields an average value for ten people (5 men and 5 women).

The mean level of the speech spectrum at another distance $r$, which is different from R = 8, can be determined according to the formula

$$B'_{av.} = B_{av.} + 20 \log \frac{R}{r}.$$

On the basis of what has been said above concerning the replacement of the speech spectrum in the critical band by one tone, the pressure developed by the artificial voice at a distance $r$ must correspond to a level of

$$B'_{a.v.} = B_{av.} + 20 \log \frac{R}{r} + 10 \log \Delta f_{cr.}$$

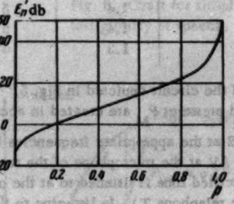

Fig. 3. Relationship between the perception probability and the sensation level.

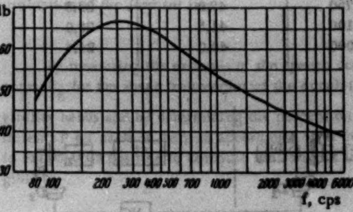

Fig. 4. Frequency spectrum of Russian speech.

In Table 2 we have shown the values of the pressures which must be developed by the artificial voice in order to reproduce the spectrum $B'_{av}$ of Russian speech at a distance of 2 cm from the mouth. In Graph (6) of Table 2 the pressures are varied in accordance with a 12 db variation in $B'_{av}$. This was done for the purpose of simplifying the work of the operators in determining the excesses (we shall speak of this below).

In fact, this is how the value of the speech peakfactor is taken into account and how the peak values of the speech levels are obtained instead of the mean levels; as a consequence of this the corresponding 12 db corrections must be made on the coordinates of the graph $P = \varphi(E'_n)$ in Fig. 3 (i.e., for example, the level $-12$ db in Fig. 3 must now correspond to 0 db).

Let us now pass on to an examination of the practical side of using the proposed methods. In order to measure the speech components above the audibility thresholds (i.e., in order to determine the sensation level) we

**TABLE 2**

**Values of the Pressures Which are Equivalent to the Speech Spectrum Pressures Which are Developed by the Artificial Voice.**

| Mean frequency, cps | Mean level of the speech spectrum (at a distance of 8 cm), db | Logarithmic width of the critical band $K = 10 \log \Delta f_{cr}$, db | Intensity level of the artificial voice at a distance of 2 cm, db | Pressure at a distance of 2 cm, bar | Pressure at a distance of 2 cm (increased by 12 db), bar |
|---|---|---|---|---|---|
| 300 | 67 | 17.0 | 96 | 12.5 | 50 |
| 600 | 61.5 | 17.2 | 90.6 | 6.8 | 27.2 |
| 750 | 58 | 17.4 | 87.5 | 4.7 | 18.8 |
| 900 | 56 | 17.7 | 85.4 | 3.7 | 14.8 |
| 1050 | 55 | 18.1 | 85.0 | 3.5 | 14 |
| 1200 | 52 | 18.4 | 82.6 | 2.7 | 10.8 |
| 1400 | 51 | 18.6 | 81.6 | 2.4 | 9.6 |
| 1550 | 50 | 19.0 | 81.0 | 2.2 | 8.8 |
| 1700 | 48 | 19.3 | 79.0 | 1.8 | 7.2 |
| 1850 | 47.8 | 19.6 | 79.2 | 1.8 | 7.2 |
| 2000 | 47 | 20.0 | 79.1 | 1.8 | 7.2 |
| 2200 | 46 | 20.4 | 78.7 | 1.7 | 6.8 |
| 2400 | 45.5 | 20.7 | 78.2 | 1.6 | 6.4 |
| 2700 | 44 | 21.0 | 77.6 | 1.5 | 6.0 |
| 3000 | 43.5 | 21.5 | 77.2 | 1.4 | 5.6 |
| 3400 | 42.5 | 22.1 | 76.6 | 1.35 | 5.4 |
| 3750 | 42.0 | 22.8 | 76.8 | 1.4 | 5.6 |
| 4100 | 41.5 | 23.0 | 76.7 | 1.4 | 5.6 |
| 5000 | 40.0 | 24.4 | 76.4 | 1.3 | 5.2 |

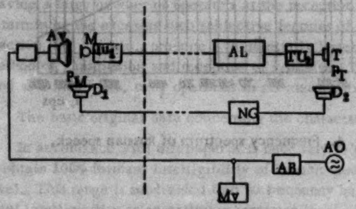

Fig. 5. Circuit for determining the sensation level. AV) artificial voice, M) microphone of the test unit, $TU_1$) transmitting telephone unit, AL) artificial line, T) telephone of the test unit, $TU_2$) receiving telephone unit, NG) noise generator, $D_1$ and $D_2$) dynamic units for the reproduction of acoustic noise, AO) audio-oscillator, AB) attenuation box, MV) metering voltmeter.

made use of the circuit depicted in Fig. 5. The required sound pressures $P_M$ are created in accordance with Table 2 at the appropriate frequencies by the artificial voice AV at the microphone of the test channel M. The specified tone is listened to at the output of the channel (the telephone T). In listening to the tone the operator establishes the threshold value of the tone by means of the attenuation box AB, which is connected into the artificial voice circuit, and determines the excess according to the readings of the box.

As can be seen from the circuit of Fig. 5 in order to measure the excesses it is necessary to have two separate sound-insulated rooms and to guarantee that the necessary noises have characteristics and levels which are such that they satisfy the imposed requirements.

All of the instruments are disposed in such a way that one operator can perform the measurements without outside help. The artificial voice must first be calibrated in order to establish a pressure $P_{a.v.}$ which corresponds to the voltage fed to the artificial voice and is measured by means of the voltmeter MV. Here it is practical to correct the characteristic of the artificial voice in such a way that the required values of $P_{a.v.}$ are obtained at constant voltage.

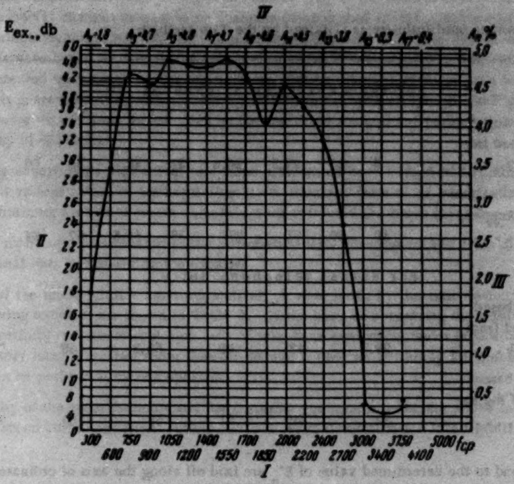

Fig. 6. Chart for simplifying the determination of the formant intelligibility of speech.

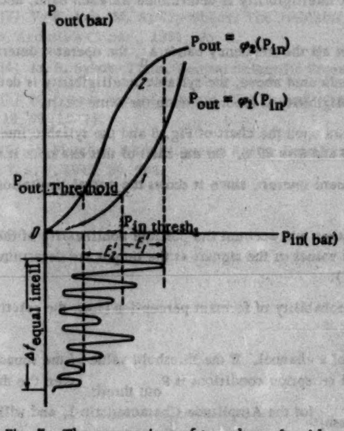

Fig. 7. The comparison of two channels with different amplitude characteristics.

By measuring the excesses of the speech components $E'_n$ for the mean frequencies of the equal-intelligibility bands and by determining the perception coefficients P for each of them in accordance with the graph in Fig. 3, it is possible to compute the formant intelligibility:

$$A = 0.05 \sum_{n=1}^{n=20} P,$$

and then it is possible to find the syllabic intelligibility S according to the graph $S = \varphi(A)$ (Fig. 2).

In order to simplify the determination of the formant intelligibility it is more practicable to make use of the chart shown in Fig. 6 which is prepared for that purpose. The mean frequencies of the equal-intelligibility bands are laid off on the bottom scale of the axis of abscissas, the sensation levels (the excesses) $E'_n$ ($E_{ex.}$) are laid off along the axis of ordinates at the left, and the values of the formant intelligibilities for the

TABLE 3

Results of the Comparison of Intelligibility as Obtained by the Two Methods.

For the experimental channel

| | | | | | | | | | | | |
|---|---|---|---|---|---|---|---|---|---|---|---|
| Syllabic intelligibility according to the data obtained from articulation tests, in % . . . . . . . . | 8 | 17 | 27.5 | 26.4 | 33 | 48 | 58 | 60 | 77 | 86 | 97 |
| Syllabic intelligibility obtained from measuring the excesses, in % . . . . . . . . . . . . . . . . . . . | 10 | 20 | 31 | 27 | 36 | 46.5 | 57 | 64 | 73 | 85 | 98 |

For actual telephone units

| | | | | | | | |
|---|---|---|---|---|---|---|---|
| Syllabic intelligibility based upon the data obtained from articulation tests, in % . . . . . . . . | 28.5 | 43 | 49 | 55.3 | 58 | 73.5 | 85 |
| Syllabic intelligibility based upon measurements of the excesses, in % . . . . . . . . . . . . . . . | 32 | 42 | 51 | 58 | 60 | 77.5 | 89 |

band $A_n$ which correspond to the determined value of $E'_n$ are laid off along the axis of ordinates at the right. At the top of the chart the values of the formant intelligibility for the given band are written for the value of $E'_n$ which has been found. In making use of such a chart it is possible to record the excess on the chart opposite the corresponding frequency and level $E'_n$ after having measured the excess. After determining the entire characteristic on the basis of the measured excesses the formant intelligibility is determined for each band, and its value is written opposite to the corresponding frequency.

Having summed the values of formant intelligibility for all the frequency bands $A_n$, the operator determined the over-all formant intelligibility. Further, as has been indicated above, the syllabic intelligibility is determined on the basis of the graph in Fig. 2; this syllabic intelligibility is recorded upon the same chart.

As an example, one of the excess characteristics is drawn upon the chart of Fig. 6 and the syllabic intelligibility is determined for it. For the given case, $\Sigma A_n = 58.3$ and $S = 89\%$. On the basis of this example it is evident that the characteristic of the excesses is of independent interest, since it shows the actual limitation of the transmitted frequency band.

The indicated circuit for measuring the excesses also takes into account the possible nonlinearity of the amplitude characteristic of the channel (when the threshold values of the signals at the output are determined by the threshold value of the signal at the input of the channel).

By measuring the excesses we actually determine the probability of formant perception (i.e., the relative number of audible formants).

Figure 7 shows two arbitrary amplitude characteristics of a channel. If the threshold value of the sound pressure at the output (in the telephone) under the specified reception conditions is $P_{\text{out thresh.}}$, then the threshold value of the sound pressure at the input will be $P_{\text{in thresh}_1}$ for the Amplitude Characteristic 1, and will be $P_{\text{in thresh}_2}$ for the Amplitude Characteristic 2. It is evident that the channel having the amplitude characteristic which is similar to Characteristic 2 assures the passage of audiosignals which correspond to a sound pressure which is smaller than that required for a channel with the Characteristic 1.

For the purposes of practical verification of the universality of the method developed here we conducted experiments on a special channel as well as on channels composed of actual telephone units. The experimental channel with an electrodynamic microphone and telephone permitted us to vary the frequency band and transmission level over wide limits by means of filters, a discriminator and an attenuation box. In performing the experiments we created speech-spectrum acoustic noise with an intensity level of from 65 to 90 db at the point of reception. This guaranteed a variation of from 8 to 98% in the syllabic speech intelligibility. For each type of frequency response we obtained the excesses by the indicated method and performed articulation measurements with a group of operators.

In performing experiments with actual telephone units which have carbon microphones the measurements were performed at various values of artificial-line attenuation and for a noise intensity level of 65-90 db. For the purposes of obtaining a more accurate comparison we measured the mean level $B_{av.}$ of the speech spectrum of the speaker (a man) who participated in the articulation test. The speech spectrum of the given speaker was taken as the original data in measuring the excesses.

The results of the intelligibility measurements which were made by the articulation method and by the method of measuring excesses are shown in Table 3. On the basis of comparing the results we see that the tonal method can successfully replace articulation tests of telephone equipment under laboratory conditions and under conditions of factory reception. Not more than 30-40 min is used for obtaining the measurements, and the measurements can be performed by one operator.

The simplicity of the measurements and the metering equipment make the above method a convenient one for performing tests on communications equipment in order to determine the intelligibility of the transmitted speech.

## LITERATURE CITED

[1] Transactions of the All-Union Commission on Audio-communications, 1951, Nos. 29-30.

[2] The Computation and Measurement of the Intelligibility of Russian Speech, Transactions of the All-Union Commission on Audio-communication, 1952, No. 33.

[3] V. K. Iofe, M. A. Sapozhkov, The Problems Involved in the Method of Computing Speech Intelligibility, Trans. Acoustics Comm., 1951, No. 6.

[4] Iu. S. Bykov, Trans. Central Scientific Research Institute of Communications, 1948, No. 1.

[5] N. French and I. Steinberg, The Factors Which Determine the Intelligibility of Speech, J. Acoust. Soc. Am. 19, 91 (1947).

[6] H. Fletcher, Audibility as a Factor Determining the Accuracy with Which Sounds are Reproduced, Proc. I. R. E. 1942, 30, 266.

Moscow

Received April 14, 1952

# CHRONICLE

## CONFERENCE OF THE FOURTH RESEARCH COMMISSION OF THE INTERNATIONAL CONSULTATIVE COMMITTEE ON TELEPHONY (ICCT)

In September-October of 1954 the regular conferences of the Research Commissions and of the 17th Plenum of the International Consultative Committee on Telephony (ICCT) took place in Geneva. A delegation from the Soviet Union took part in these conferences.

This summary discusses the work solely of the Fourth Research Commission which devoted itself to the problems of transmission quality and of all problems associated with it, including acoustical problems.

At the September conference of the Fourth Research Commission the following subjects were discussed:

1) The establishment of limiting norms for the quality index of telephone transmission for national telephone systems which participate in international communications.

2) The refinement of the method for measuring the equivalent intelligibility attenuation (AEN).

3) The selection of a standard artificial ear for use in the laboratory of the ICCT by administrations and private companies that participate in the work of the ICCT, until such time as the international electrical-engineering commission or the international organization on normalization make a decision.

4) The interchange of information between members of the administration on the development of methods for computing the quality index of transmission on the basis of the original parameters (measured by objective methods) of telephone systems.

5) A discussion of methods for evaluating the transmission quality deterioration which is caused by noise that is reproduced by telephones, the limiting norms for noise, and the corrections which must be introduced into the readings of a psophometer for the purposes of taking the nature of the measured noise into account.

The greatest attention of the conference participants was directed to the problem involved in determining the limiting norms for the transmission quality index of national telephone systems. In the opinion of certain administrations the index of transmission quality which takes into account the equivalent intelligibility attenuation (AEN) cannot serve as a criterion for the quality of telephone transmission in its assumed form due to the conditional nature of the method for measuring this latter quantity.

Professor West from the English delegation indicated that according to the data obtained by the English administration under conditions where the values of line attenuation were large, the evaluation of telephone systems as performed on the basis of the magnitude of AEN contradicts the evaluation obtained on the basis of direct conversation.

As a result of the discussions the commission adknowledged that it was possible to recommend limiting norms for the transmission quality index of national telephone systems that are included in international communication only as desirable norms, and to establish them temporarily as equal to:

| | |
|---|---|
| For transmission | 24 db |
| For reception | 18 db |
| International line | 7 db |

With regard to the methods for measuring the equivalent intelligibility attenuation (AEN), the commission introduced changes into the recommendations of the ICCT in the form of changing the room noise at the reception point of a standard ARAEN system by electrical noise (a Khot spectrum and a psophometric electromotive force of 2 mv).

When such a change is made the errors which arise as a result of the variable degree to which telephones of the ARAEN system are pressed to the ear of the operators are eliminated.

For the purpose of obtaining comparable results in performing tests on telephone units in the laboratories of the ICCT and in the laboratories of the administrations of various countries, the commission considered it practical (on the basis of its preceding meetings) to recommend a unified type of "artificial ear" instrument. For the purposes of selecting such a standard instrument the ICCT laboratory performed tests on the same types of telephones from various countries by means of the "artificial ear" instruments. These tests showed that in the frequency range of from 300 to 4000 cps the frequency responses of the telephones as measured by the different instruments had shapes which were sufficiently identical. Based on these results and using the additional concept that it was necessary to recommend an instrument which could easily be reproduced in the various countries, the September conference of the commission considered it possible to temporarily recommend an "artificial" ear instrument which had a simple closed chamber with a volume of 6 $cm^3$. The decision of the commission rigorously determined the basic dimensions of this chamber.

The problem of computing the transmission performance index on the basis of objective measurements gave rise to great interest among the members of the Fourth Commission. The Soviet delegation explained the results of work done on this problem in the Soviet Union. The Commission considered it necessary to continue its studies in that direction, and in its decisions it turned its attention to the methods of computation which were described in the responses of the Soviet and Japanese delegations.

The problems associated with the effects of noise upon the quality of telephone transmission are of considerable practical interest. These problems were examined at a joint meeting of the Third and Fourth Research Commissions.

At this meeting the noises which occur in telephone systems were listened to and recorded on magnetic tape by various administrations. Listening to these recordings brought out the fact that the noise in coaxial systems, as well as in radio-relay systems, has the characteristics of almost "white" noise and therefore, can be measured by a psophometer which satisfies the requirements of the ICCT.

Commutation noise has a clearly defined pulse character and cannot be measured by the usual method. In this regard a new problem was posed which was associated with the development of a method for measuring pulse noise in such a way that the effects of this noise upon a human being are taken into account. It is possible to judge the necessity of modifying the method for measuring noise as a function of the nature of that noise according to the results obtained from investigating the degree to which "white" noise and rectified noise (as obtained in the laboratory of the ICCT) affects the intelligibility of speech. These investigations established that when the psophometric electromotive forces are equal the loss in transmission quality for "white" noise is 6 db greater than for rectified noise.

As a result of the discussion it was decided to exclude commutation noise from further investigations, since because of the short duration of this type of noise one could expect that it would have an insignificant effect upon speech intelligibility; it was therefore decided that these investigations should be limited to typical noise in the following systems: radio-relay systems, coaxial systems, and 60-channel systems.

In regard to psophometer parameters it was decided to retain the recommendations of the ICCT for the time being as they were formulated in 1949. At the same time the new problem was posed concerning the necessity of reexamining the curve for broadcast channels.

During the work of the commission on the solution of problems associated with the establishment of limiting norms for the transmission performance index special experiments were performed in the laboratory of the ICCT in which all members of the conference participated. These experiments allowed each of the participants to establish for himself the maximum value of attenuation in a ARAEN system in which he still considered it possible to carry on a conversation. As a result of the statistical manipulation of the data obtained by all delegations, the limiting norm for the transmission performance index was established as equal to 49 db.

In concluding its work the Commission proposed an enumeration of the problems which are up for study in the laboratory administrations of various countries and in the laboratory of the ICCT. The next conference of the Fourth Research Commission is designated for March-April, 1956.

## Conference on Physical Acoustics and Ultrasonics

### Moscow, March 3-7, 1955

From March 3 to March 7, 1955, a conference on physical acoustics and ultrasonics took place in Moscow; this conference was organized by the Acoustics Commission, the Acoustics Institute of the Acad. Sci. USSR, the Moscow Order of Lenin and Order of the Red Banner of Labor, M. V. Lomomosov State University and the V. I. Ul'ianov (Lenin) Institute of Electrical Engineering. In number of reports and participants this conference was the most impressive of the entire post-war period. Below we provide brief annotations from the papers read at the conference, as well as from the resolutions adopted by the conference.

N. N. Andreev. Second-order Quantities in Acoustics (Acoustics Institute of the Acad. Sci. USSR).

Such quantities include the energy, energy density, energy flux, radiation pressure, momentum, etc. The paper showed that the formulations which are accepted at the present time contain a number of misunderstandings and errors which had already been discovered in a preceding paper (1940) by the author; a proper analysis of all these quantities is given. The general formulation of solutions for second-approximation problems are given, and these are applied to certain particular phenomena which are of interest.

O. L. Babikov. Methods of Ultrasonic Analysis [V. I. Ul'ianov (Lenin) Leningrad Electrical-Engineering Institute].

The general principles of physico-chemical ultrasonic analysis are formulated for liquid media, and the essence of pulse methods for measuring the velocity and absorption of ultrasonic waves is analyzed. Block diagrams are given for instruments, and an analysis of the basic relationships which determine the sensitivity (precision) of the instruments is made.

Experimental data is given on the application of ultrasonic monitoring to various fields in industry.

D. K. Balabukha, L. L. Miasnikov, E. N. Plotnikova. The Modulation Method for Measuring Small Voltages in the Audio-Frequency Range (Leningrad Shipbuilding Institute).

The paper gives a detailed description of the construction of an audio-frequency microvoltmeter with capacitive modulation which is designed for measuring weak signals over the entire audio-frequency range when these signals have an intensity that is ten times lower than the intrinsic noise intensity of the equipment for large values of input impedance (greater than 100 megohms). By means of this instrument investigations are made of the intrinsic noise in Rochelle-Salt piezoelements and capacitors. It is established that the intrinsic noise of Rochelle-Salt piezoelements is not purely thermal noise, and this indicates that additional noise sources are present (in particular, it indicates the generation of noise as a consequence of the "Barkhausen effect").

L. N. Barsukov. The Utilization of High-Frequency Mechanical vibrations in agriculture (All-Union Scientific-Research Institute of Fertilizers, Agricultural Engineering and Soil Conservation of the Lenin All-Union Academy of Agricultural Science).

The paper examines the problems involved in the stimulation of seed growth due to the action of high-frequency vibrations and discusses the methods by which these vibrations affect the earth; the discussion is from the point of view of raising the harvest yield. Experimental results are given.

A. N. Barkhatov. Laboratory Unit for Studying the Propagation of Sound in Water (Gor'kii State University).

The paper describes a laboratory unit for investigating the process of sound propagation in water. The paper demonstrates the possibility of simulation in water by means of thermal action or by the utilization of table salt solutions having various concentrations in order to create a vertical distribution of sound velocity. The investigation of the sound field was performed in an undeadened basin by an acoustical probe at various points or by means of equipment which automatically records the sound. The described method is utilized for investigating acoustic shadow in a medium with a constant vertical temperature gradient, and for the measurement of sound attenuation in a surface isothermal layer of water when the medium below it has a negative vertical sound velocity gradient.

Iu. V. Bogoslovskii. The Development and Perfection of Ultrasonic Equipment by the CSRITM (Central Scientific-Research Institute of Technology and Machine Building).

The ultrasonic UZD-7N defectoscope which was developed in the CSRITM is an instrument which can be universally used.

Improvements have been made in the circuit of the defectoscope in comparison with the earlier UZD-7N model; in particular, a receiving-amplifier sensitivity is provided which is variable in time. Included in the piezoelectric probe complex of the defectoscope are plane probes with a protective bottom cup soldered onto it and prismatic probes which make it possible for the instrument to operate with a single-probe circuit. Pulse-type ultrasonic defectoscopes find limited use in monitoring metal which is less than 10-7 mm thick. For these purposes resonant ultrasonic defectoscopes are more practical; these defectoscopes make it possible to monitor the thickness of a part and to show up its lamination zones, poor welds, etc., when the part is accessible only from one side.

The resonant ultrasonic UZT-R defectoscope-thickness meter which was developed in the CSRITM makes it possible to monitor metal with a thickness ranging from 1 to 22 mm. The relative error involved in measuring the thickness of parts does not exceed ± 1.5%.

L. M. Brekhovskikh. Certain Problems Involved in the Propagation of Waves in Layers (Acoustics Institute of the Acad. Sci. USSR). A simple method is described for attaining the frequency equation (the dispersion equation) for sound waves which are propagated in layers. Both liquid layers and layers having shear elasticity are examined.

I. S. Vainshtok. A Unit for Drilling Glass and Ceramic.

The paper gives a detailed description of the construction of a unit devised for drilling apertures of any shape in glass, ceramic and stone casting by means of ultrasonic waves.

V. L. Ginzburg. The General Relationship Between the Absorption and Dispersion of Acoustic Waves. (P. N. Lebedev Physics Institute of the Acad. Sci. USSR).

A general relationship is established between the absorption and dispersion of electromagnetic and sound waves. The results of the investigations made by the author reduce to the relationships

$$\frac{1}{c(\omega_2)} - \frac{1}{c(\omega_1)} = \frac{2}{\pi} \int_0^{\omega_0} \gamma(\omega') \left\{ \frac{1}{\omega'^2 - \omega_2^2} - \frac{1}{\omega'^2 - \omega_1^2} \right\} d\omega' + \Delta_1,$$

$$\frac{\gamma(\omega_2)}{\omega_2} - \frac{\gamma(\omega_1)}{\omega_1} = -\frac{2}{\pi} \int_0^{\omega_0} \frac{1}{c(\omega')} \left\{ \frac{\omega_2}{\omega'^2 - \omega_2^2} - \frac{\omega_1}{\omega'^2 - \omega_1^2} \right\} d\omega' + \Delta_2,$$

where $c(\omega)$ is the real velocity of the sound having the frequency $\omega$, $\gamma(\omega)$ is the amplitude coefficient of sound absorption at the frequency $\omega$, $\omega_1$ and $\omega_2$ are two frequencies which are of interest to us, $\omega_0$ is the maximum frequency at which the acoustic approximation is still applicable, $\Delta_1$ and $\Delta_2$ are corrections for which the evaluation is performed, and finally, the integrals in both formulas are interpreted in the sense of the chief value.

The formulas given in the paper can be utilized for the evaluation of absorption according to a known dispersion and vise versa. The problem of the accuracy and meaning of such evaluations must be solved for each individual case while taking into account the totality and accuracy of the available data on dispersion or absorption of sound in the medium being examined.

**G. S. Gorelik.** The Measurement of Acoustic Waves with Very Small Amplitudes (Moscow Physics-Engineering Institute).

The paper provides a brief survey of papers which discuss the optical modulation-interference method for measuring very small oscillations. The method is based upon the detection and measurement of extremely small periodic variations in the path difference of two light rays.

The periodic path difference can be obtained if one of the interfering rays is reflected from a vibrating mirror. In that case we are able to measure very small periodic displacements. The periodic path difference can also be obtained if one of the interfering rays passes through a transparent (optically transparent) medium in which the acoustic wave is propagated. In that case it is possible to measure very small periodic variations in the refractive index (and therefore, in the density as well).

This method also makes it possible to measure comparatively large acoustic vibrations with a high absolute accuracy. Periodic variations in the path difference which are of the order of several light wavelengths can be measured with an accuracy of up to hundredths and even thousandths of an angstrom.

**A. K. Gurvich.** An Ultrasonic Defectoscope for a Welded Seam and Several Problems of Designing the Radio-Engineering section of Ultrasonic Defectoscopes (All-Union Scientific Research Institute of Bridgebuilding).

A method for detecting defects in butt-welded seams is described; the method employs a specially designed ultrasonic defectoscope of the type NIIM-2 and includes additional units for the automatic displacement of the probe and for recording the location of the defects upon the paper.

The problem involved in the computation and design of individual elements of the radio-engineering section of the defectoscope is analyzed.

**N. A. Dmitrieva.** Optical Methods For the Investigation of the Dependence of the Propagation Velocity of Ultrasonic Waves in Mixtures of Normal Organic Liquids Upon Temperature and Composition (Moscow Regional Pedagogical Institute).

The paper analyzes the results of investigating the propagation velocity of ultrasonic waves in mixtures of normal organic liquids over a wide range of temperatures and concentrations. The paper shows that it is possible to apply the law of corresponding states to the mixtures being studied. A theoretical foundation is provided for applying Rao's rule to normal mixtures, and this possibility is experimentally verified.

**V. P. Dremina.** Dispersion of Sound in Certain Organic Liquids.

Results are given as obtained from an experimental investigation of sound velocity in carbolic acids and their derivatives in the direct vicinity of the crystallization temperature. An explanation is proposed for the possible mechanism of the anomalous sound dispersion which was observed. The boundaries for applying Rao's rule are indicated.

**I. S. Zheludev.** Piezoelectric Properties of Heterogeneous Systems Which Contain Barium Titanate (Crystalogrophy Institute of the Acad. Sci. USSR).

Results are given for measurements of the piezoelectric moduli of heterogeneous systems (matrix systems and mixtures) that contain barium titanate in various concentrations. A method is described for manufacturing large piezoelements of various shapes from such systems. The results of exciting flexural vibrations in metallic plates by means of mixtures containing barium titanate are given.

**V. A. Zverev.** Certain New Methods for Investigating a Sound Field. (Gor'kii State University).

The paper describes measurements of the sound pressure at the surface of a radiator by the radiation-modulation method, and results are given for the theoretical and experimental investigation of this problem. The reception of a sound field is examined by measuring the permittivity of the medium at radio frequencies. The application of a specially designed analyzer for investigating the properties of various media is indicated here. A description is given of the method used for detecting the mutual interaction of sound fields, and experimental results are cited.

**V. S. Krygov.** The Absorption of Ultrasonic Waves in Metals.

The paper analyzes the manner in which ultrasonic losses in polycrystalline metals are caused by absorption, both as a consequence of elastic hysteresis and by scattering due to the crystalline lattices. It is shown that at low frequencies (the wavelength exceeds the dimensions of the crystallite by more than 20 times) the absorption effect which is due to elastic hysteresis predominates; at high frequencies (the wavelength is less than one-eighth of the crystallite dimension) scattering predominates. Data concerning the dependence of the absorption coefficient upon various factors is given.

**B. B. Kudriavtsev.** Ultrasonic Velocity in Liquids and the Physico-Chemical Properties of Liquids.

The paper develops a thermodynamic computation of sound velocity in pure liquids and binary liquid mixtures. The theoretical computations are compared with experimental results. The possible applications of ultrasonic measurements in the study of the liquid state of matter are indicated.

**Iu. P. Lysanov.** Sound Scattering From an Inhomogeneous Surface with a Periodically Varying Normal Impedance (Acoustics Institute of the Acad. Sci. USSR).

When a plane sound wave is incident upon an inhomogeneous surface whose normal impedance is a periodic function of the surface points, a scattered field appears in addition to the wave which is subject to mirror reflection; this scattered field consists of the sideband spectra of various orders. A method is given for determining the amplitudes and phases of sideband spectra of the scattered field. Certain particular cases of periodic impedance are examined.

**L. M. Liamshev.** The Reflection of Sound by Thin Plates in Water (Acoustics Institute Acad. Sci. USSR).

As a result of an experimental investigation of the reflection of sound by thin plates in water, a new effect arises involving a strong non-mirrorlike reflection that is due to the longitudinal waves which appear along the surface of the plate and which are excited by the incident soundwave. The new effect is analogous to the effect, noted earlier in Finney's paper, which is due to the flexural vibrations of the plate. The theory of the reflection and transmission of sound by a thin plate of finite dimensions is developed while taking into account both longitudinal and flexural waves in the plate. The theory is in good agreement with the experimental data.

**G. I. Makarov and N. N. Shaposhnikov.** Nonstationary Radiation From a Sphere and from a Spherical Segment (Leningrad Shipbuilding Institute).

The paper analyzes the problems of the theory of nonstationary radiation and those features of the directivity patterns which arise when brief ultrasonic pulses are radiated. The rigorous solution of this problem, even for radiators of the simplest types, has not been obtained to this day. As a result of obtaining a solution by asymptotic methods for a spherical radiator with a vibrating sector, it is possible to explain the nature of the field growth in the vicinity of the wave front. The paper also provides methods for computing fields at any point in space. It is shown beyond doubt that the basic regularities which obtain during the operation of such a radiator can also be observed during the operation of radiators which are constructed in various other ways.

**L. C. Melkonian and B. B. Kudriavtsev.** Velocity of Sound in Mixtures Whose Components Form Chemical Compounds (Erevan Karl Marx Polytechnical Institute).

The paper analyzes the results of an experimental investigation of ultrasonic propagation in binary mixtures whose components form chemical compounds; the tests were made at various temperatures and concentrations of the mixtures. These results are compared with data obtained from physico-chemical analysis. On the basis of the resultant data certain conclusions were drawn concerning the physico-chemical properties of the systems studied.

**I. G. Mikhailov.** The Relaxation of Volume and Shear Viscosity in Certain Viscous Liquids (Leningrad Order of Lenin A. A. Zhdanov State University).

The paper analyzes the results obtained from investigating the relaxation mechanism of ultrasonic absorption in castor oil and mixtures of castor oil with benzine and cottonseed oil. Confirmation of the intramolecular mechanism of the relaxation processes is obtained.

Certain features of absorption in mixtures of viscous liquids are indicated.

M. E. Mokeev. An Experiment in the Application of Ultrasonic Defectoscopes to Railroad Transport (All-Union Scientific Research Institute of Railroad Transport).

Data is given concerning the application of ultrasonic defectoscopes on railroads in order to check the butt-joints of rails without removing the cover plates; the most typical defects which are shown up by this method are illustrated. The reason for the great effectiveness of defectoscopes is clarified and the perspectives for their further development are noted. Analogous data is given on an ultrasonic defectoscope for checking the crank pins and the axles of steam-engine wheel-pairs.

L. L. Miasnikov and G. K. Ul'ianov. The Magnetoacoustic Effect in Para-and Diamagnetic Metals (Leningrad Shipbuilding Institute).

The dispersion of sound in ferromagnetic materials when a magnetic field is present (the magneto-acoustic effect) has been discussed in a considerable number of papers; the magneto-acoustic effect in para-and diamagnetic metals has remained an uninvestigated subject up to the present time.

In this paper the magneto-acoustic effect in aluminum, copper and magnesium plates is subjected to a detailed experimental investigation. It is established that the magneto-acoustic effect in aluminum and other plates is actually present for longitudinal vibrations, but is expressed considerably more weakly than the Robey theory would indicate. A very strongly expressed (and theoretically unanalyzed) magneto-acoustic effect is detected when the plates are subjected to torsional vibrations. The investigations show that the phase velocity of the sound increases with a decrease in the frequency; the logarithmic attenuation decrement increases by a factor of tens in this range. The dependence of the relative variation of the phase velocity upon the magnitude of the magnetic induction (right up to $B = 10^4$ gauss) follows a quadratic law.

The paper also investigates the distribution of the alternating magnetic field components which are due to eddy current fluxes which obtain along the length of the plates when they are excited in various ways.

V. F. Nozdrev, A. K. Sultanov, V. Zakurenov, Iu. Bormosov. The Absorption of Ultrasonic Waves in Ethers of Acetic amd Formic Acids by Means of Pulse and Optical Methods. The authors were successful in establishing and investigating two complete relaxation regions of volume viscosity. The dependence of the relaxation time upon temperature is studied. The results are discussed on the basis of relaxation theory.

A. N. Obrosov. The Application of Ultrasonic Waves for Curative Purposes (State Scientific-Research Physiotherapy Institute).

The paper discusses the characteristics of three basic ultrasonic effects; the specific mechanical effect, the nonspecific thermal effect and the chemical effect. Data is provided on the equipment used for ultrasonic therapy and on the most useful curative methods. The paper enumerates the diseases for which the application of ultrasonic waves is indicated. The one-sidedness and limited nature of the theoretical explanations of the effects produced upon the human organism by ultrasonic waves are noted, and the paths for fruitful scientific research in this field are pointed out.

L. M. Plotnikov and L. I. Gnesin. The Application of Ultrasonic Waves in Curing Dieupiuitren's disease, scar-tissue changes after trauma and unresolved hematomas. The positive experimental results which have been obtained are cited. The equipment and methods used at present are described.

A. S. Povalishnikova. Investigation of the Propagation of Ultrasonic Waves in Satured Vapors of Monoatomic Alcohols (Moscow Regional Pedagogical Institute).

The paper describes the methodological features of measuring the velocity of ultrasonic waves in the saturated vapors of liquids. The results of measuring the ultrasonic velocity in the saturated vapors of alcohol are given, including data for the critical region, and a thermodynamic examination of the results is made. The computed specific heats of the saturated vapors under study are given.

I. G. Polotskii and Z. L. Khodov. Velocity of Ultrasonic Waves in Certain Liquid Systems and their Compressibility (Institute of Metallophysics of the Acad. Sci. USSR).

Data on measurements of ultrasonic velocity are used to analyze the problem involved in creating liquid and metallic systems.

It is shown that the nature of the isotherm of adiabatic compressibility for certain binary liquid systems is determined by the relationship between the forces of molecular interaction between the components.

It is established that for liquids with metallic, Van-der-Vaals and hydrogen bonds, the magnitude of the forces of interaction is characterized not only by the absolute value of the adiabatic compressibility coefficient, but also by the temperature coefficient of ultrasonic velocity and by the relative variation of the compressibility.

An investigation of the temperature variation of the ultrasonic velocity and the adiabatic compressibility for salol alloys, orthochloronitrobenzine and thymol showed that the compressibility increases with an increase in temperature (in the range 30-90°) and obeys an almost linear law. The linear law which is detected in these experiments indicates the absence of any substantial structural variations in salol, orthochloronitrobenzine and thymol when they make the transition from a stable to a metastable state.

A relationship is found between the adiabatic compressibility for metals in the liquid phase and their interatomic distances within the limits of individual subgroups of the periodic system; when the interatomic distance increases for alkali metals and for the zinc, gallium and germanium subgroups, the compressibility of these elements increases.

**S. N. Rzhevkin.** Travelling-Wave Acoustic Radiators (Moscow Order of Lenin and Order of the Red Banner of Labor M. V. Lomonosov State University).

The paper examines spherical, cylindrical and plane travelling-wave sound radiators and provides expressions for the acoustic field and the radiated energy in cases of spherical and cylindrical radiators. The papers show that travelling-wave radiators and rotational radiators are equivalent to one another within known limits of approximation. It is also demonstrated that travelling-wave radiators yield a sharp increase in the radiated power when the velocity of the travelling-waves increases beyond the velocity of sound in the surrounding medium. Results are given for an experimental investigation of a cylindrical travelling-wave radiator, and these results are in satisfactory agreement with the theoretical computations.

**L. D. Rozenberg.** Survey and Comparative Evaluation of Methods for Converting Sound Fields into a Visible Image (Acoustics Institute of the Acad. Sci. USSR).

Sound visualization and its characteristic. The role and application of sound visualization in various fields of physics, engineering and medicine; the study of sound fields, defectoscopy, medical diagnosis. Classification of conversion methods. Methods which are based on scanning; mechanical scanning, electronic scanning, scanning by means of a radiator ray. The suspension method. Optical methods; the simple shadow method, the shadow method for examining deformations in the surface of a liquid, the shadow method for examining a layer. Contact methods (sensitive layers): the direct effect of ultrasonic waves upon a photolayer, phosphorescent screens, light emission by phosphors, the evolution of iodine from solution, the method of starch plates, the method of thermoreactive colors.

The requirements which the conversion method must satisfy are; sensitivity, contrast, reversibility, resolving power, simplicity. The role of the input acoustic impedance of the converter. A comparison of various methods.

**L. D. Rozenberg.** Cylindrical Acoustic Focusing Systems (Acoustics Institute of the Acad. Sci. USSR).

Cylindrical focusing systems are examined. An equation is derived for the field of a cylinder segment. General formulas are given for the gain coefficient and focusing factor in terms of the pressure and the velocity. The paper examines concrete cases of trough-shaped ceramic radiators, cylindrical-parabolic mirrors and cylindrical lenses.

**I. Skards.** A High-Power Ultrasonic Unit for Irradiating Microorganisms (Institute of Microbiology of the Acad. Sci. of the Latvian SSR).

The paper describes the construction of a high-power ultrasonic unit with a cooling system and with an automatic circuit to protect the quartz piezocrystal from damage when the oil breaks down. The basic characteristics of the unit are; an ultrasonic intensity of 100 v/cm$^2$, the temperature of the irradiated liquid does not exceed the temperature of the cooling water by more than 5°, the ultrasonic intensity is maintained constant within 4% limits, the instant at which cavitation is brought about in the irradiated substratum is accurately determined.

S. Ia. Sokolov. The Application of Ultrasonics in Engineering and Physics [Leningrad V. I. Ul'ianov (Lenin) Electrical-Engineering Institute].

An experimental method is developed for determining the orbital-spin constant by means of the effect of ultrasonic waves upon crystals whose atoms (which have a magnetic moment and which are in a constant magnetic field) precess at the Larmor frequency. When the ultrasonic frequency coincides with the precession frequency of the vector magnetic moment of the atom around the magnetic field vector the probability of an atom making the transition from one state to another increases, the work necessary for such a transition is done on account of the ultrasonic energy, and therefore, an increase in ultrasonic absorption can be expected at the resonant frequency.

The paper also develops a new frequency-modulation method of ultrasonic defectoscopy; this method is meant for use in cases when the surface of the investigated metal has not been processed. This new method consists of sending ultrasonic waves of a continuously varying frequency through the investigated body and simultaneously receiving vibrations at the receiver which have passed through the medium and have encountered an inhomogeneity or defect in their path. The depth of the defect or inhomogeneity is determined on the basis of the difference between the frequency of the reflected pulse and the instantaneous value of the original propagated frequency at the instant the reflected pulse arrives at the receiver.

B. N. Suslov. The Investigation of Liquid Binary Systems with Different Types of Molecular Interaction Between Components.

The paper analyzes the results of an experimental investigation of ultrasonic propagation in four binary mixtures, which have different types of interaction between the molecules, at various temperatures and pressures. The paper discusses the problem of the relationship between the sound velocity and the types of molecular interaction, the problem of the additivity of sound velocity in mixtures, the problem of Rao's rule being applied to a mixture, and the problem of applying the law of corresponding states to the computation of the sound velocity in the liquids.

Iu. M. Sukharevskii and A. G. Sokolinskii. The Radiation of a Quartz Dipole into a Solid Medium.

The acoustical characteristics of a quartz dipole which radiates into a solid medium depends substantially upon the mechanical parameters of the intermediate layer between the dipole and the medium; this intermediate layer makes possible "acoustical contact" (i.e., it makes possible the transmission of the vibrations). On the basis of a theoretical investigation of the problem it is made clear that a relatively large mechanical compliance on the part of the liquid and semi-solid transition layers which are used (even those of very small thickness) leads to a sharp decrease in the transmitted frequency band and to an upward shift of the resonant frequency of the entire system. The results of the experimental investigation, which was performed for quartz sheets with resonant frequencies of 8 and 10 megacycles and a liquid transition layer, are in good agreement with the computed data.

B. D. Tartakovskii. Ultrasonic Filters (Acoustics Institute of the Acad. Sci. USSR).

The paper develops certain problems involved in the computation of ultrasonic filters which are used in instruments that serve as intermediate elements for the transmission of sound in liquids.

The paper points out the possibility of creating a filter which permits the segregation of plane waves which are propagated in a given direction and to suppress waves which are propagated in the undesirable direction (this can be done both in the case of a constant and in the case of a smoothly varying frequency). The basic concepts are given with regard to the selection of materials for filters which employ half-wave and quarter-wave plates; the attenuation, the dimensions of the plates and the effect of transverse waves are all taken into account. In conclusion the results of both the computation of filters and their experimental investigation are given.

V. V. Tiutekin. Measurement of the Shear Modulus and the Loss Coefficient of Rubbery Materials by Means of a Solid Long Acoustical Line at Sonic and Ultrasonic Frequencies (Acoustics Institute of the Acad. Sci. USSR).

This new method which has been developed for investigating properties of rubbery materials is based upon measuring the reflection from the end of a solid long acoustical line which is loaded by a test specimen of rubbery material. An advantage of this method is the possibility of making measurements during the smooth variation of the frequency. Results of measurements taken on various types of rubber are given.

V. M. Fridman. The Application of Sonic and Ultrasonic Vibrations in Light Industry.

The paper describes a large number of possible applications for sonic and ultrasonic vibrations in light industry, namely, in the production of leather, in fur technology, in washing wool, in cleaning cloth, for obtaining various emulsions, for coloring cloth, for the dispersion of dyes, for the treatment of materials, for degassing viscose masses and also for the defectoscopy of the glued layer between a sole and an upper shoe. Data is given on the semi-production utilization of the results obtained from the analysis in the paper.

N. V. Khimchenko. Ultrasonic Monitoring of Cast Iron (All-Union Scientific-Research and Construction Institute of Chemical Machine Building).

The paper examines the special features of ultrasonic monitoring during the defectoscopy of cast iron. The paper shows that the optimum ultrasonic frequency must be selected as a function of the magnitude of the graphite inclusions, and that the sensitivity of the method depends upon the structure of the cast iron. The effect of the structure of the basic metallic mass upon the scattering of ultrasonic waves in cast iron is clarified, and the possibility of ultrasonically monitoring the graphite inclusions in the cast iron layer is established.

L. A. Chernov. Correlation of the Amplitude and Phase Fluctuations Which Occur When Waves are Propagated in a Statistically Inhomogeneous Medium (Acoustics Institute of the Acad. Sci. USSR).

The paper examines the problem of the correlation of amplitude and phase fluctuations at the reception point when waves are propagated in a medium with small random variations in the refractive index. It is shown that the correlation becomes weaker as the receiver is moved further away from the radiator. The paper also examines the problem involved in the autocorrelation of amplitude (or phase) fluctuations at various reception points. It is shown that the autocorrelation of amplitude (or phase) fluctuations extends over a distance which is of the order of the correlation radius of the refractive index in the medium.

A. S. Shein. Hunting Fish by Means of Ultrasonic Waves (All-Union Scientific Research Institute of Ocean Fishing and Oceanography).

The paper examines the problem involved in the application of ultrasonic waves in the fish industry for the purposes of searching out concentrations of commercial fish.

Methods are described for the ultrasonic recording of vertical cross-sections of shoals of fish upon an automatic recorder while depicting the relative dimensions and densities of these shoals.

The paper shows several methods for decoding echograms. It is established that the nature of the echogram picture in recording shoals depends upon the operating frequencies. Using recordings of shoals of various types of commercial fish as examples, the paper demonstrates the possibility of differentiating between the types of fish according to the echogram picture.

A large number of echograms are obtained for commercial shoals of herring, cod, stavriva, khamsa and other fish as detected by ultrasonic instruments, both at a distance away from the ship and under its keel. New problems involved in ultrasonic fish detection are examined.

A. S. Shein. The Excitation of Pulsations in Spherical Vessels by means of Piezoelements (All-Union Scientific-Research Institute of Ocean Fishing and Oceanography).

A method is described for obtaining vibrations of spherical vessels by means of barium titanate piezoelements. Methods are indicated for utilizing this method in order to obtain sonic and ultrasonic pulsating spherical converters.

A method is indicated for using piezoelements to excite cavitation processes in liquids which fill the spherical vessels.

D. S. Shraiber. The Sensitivity Characteristic of Ultrasonic Monitoring Methods.

The paper develops the basic characteristics which determine the sensitivity and precision of the pulse and resonant methods of ultrasonic monitoring, and indicates the paths of rational design for the corresponding equipment.

V. N. Shchepetov. The Application of Ultrasonic Defectoscopy in the Production of Electroceramic Items (State Electroceramic Research Institute). The paper describes an ultrasonic method for detecting the location and dimensions of internal defects (stratifications, cracks, cavities, etc.) in electroceramic articles (made of high-voltage porcelain and steatite); this method can also be used for determining the quality and porosity of glazed glued joints.

The special features of the electrical circuits for ultrasonic instruments that serve these purposes are examined.

In determining the quality of a glazed glued joint, slanted probes which are placed upon the glazed surface of the insulators are utilized (this surface is moistened with soapy water), and the quality of the glued joint is determined on the basis of the relationship between the amplitudes of the control and defect signals.

I. E. El'piner. The Mechanism of the Biological Effect Produced by Ultrasonic Waves (Institute of Biological Physics of the Acad. Sci. USSR).

The paper provides data which shows that ultrasonic waves not only have the ability to destroy cells and cellular structures, but can also cause functional and biochemical shifts in the life processes of cells without destroying them as entities. Data is obtained which makes it evident that the biological effect of ultrasonic waves is due not only to mechanical forces which are genetically associated with cavitation, but by the appreciable role played by chemical reactions which arise as the result of the direct and indirect effects of the ultrasonic waves. An additional proof of the latter fact is provided by data which was obtained on the possibility of controlling the genetics of the chemical processes which take place in an ultrasonic field.

The Conference adopted the following resolution.

The Conference on Acoustics notes with satisfaction the successes attained in the development of both theoretical and applied acoustics and ultrasonics during the period which has transpired since the last conference.

The most important thing which has occurred during this period has been the rapid development of the basic areas of work and trends in acoustics and ultrasonics; this development has led to the successful solution of problems which have great scientific and economic significance. A number of research projects have developed which are devoted to the most diverse application of acoustics and ultrasonics in many varied fields of our technology and national economy.

A great interest is noted in acoustics research on the part of workers in various fields which are close to the field of physics: chemists, biologists, doctors, agronomists.

The acoustic and ultrasonic methods for research and for affecting matter have been firmly introduced into the everyday practice of many industrial laboratories.

An obvious indication of the growing interest in acoustics research is the organization of the Acoustics Institute in the Acad. Sci. USSR, the founding of a special "Journal of Acoustics" of the Acad. Sci. USSR, the formation of special sections in the Acoustics Commission of the Acad. Sci. USSR (sections on ultrasonics, the investigation of speech, physiological acoustics), as well as the participation of staff members from numerous industrial and educational institutes and universities in the work of the Conference.

An expression of the intensified interest in acoustics and of the increased significance of this subject is the establishment of acoustics staffs and the specialization of students in applied and theoretical acoustics in a number of Soviet Universities. In order to guarantee the further rapid development in acoustics and ultrasonics the Conference bids the participants turn their attention to the desirability of a closer coordination of the scientific research which is being carried on in the various institutes of the USSR. This coordination must encompass not only work which is going on in planning scientific research but also in the content of dissertation papers.

It is highly desirable to intensify the coordination between theoretical research and the solution of important practical problems. Here it is necessary to strive for greater results from theoretical research, thus attempting to assure the thorough integration of newly developed and effective methods of research and of new discoveries and inventions into industry, medicine and the national economy.

We therefore recommend the intensification of our contact with foreign science, the invitation of foreign scientists to scientific conferences, and our own participation in international congresses and conferences. From this point of view it is desirable to publish research projects of Soviet scientists in foreign journals in exchange for similar articles from abroad.

The success of our work can be facilitated by establishing a still closer personal contact between Soviet scientists who work in the various cities of the Soviet Union.

The growth in the tempo of housing and industrial construction makes the solution of a series of important problems in architectural acoustics an immediate necessity, and the efforts of all specialists who are in one way or another involved in the problems of acoustics and ultrasonics must be directed toward solving these immediate problems.

It is necessary to increase the number of original and translated books which are devoted to problems of acoustics and ultrasonics.

The plans of the various publishing houses should include the publishing of monographs on theoretical and architectural acoustics, on ultrasonics, on the application of ultrasonics to the investigation of physical and chemical properties of matter and to the processes which go on in matter. In large industrial establishments and in the institutes set up by various fields of industry it is desirable to organize acoustics and ultrasonics laboratories for the purpose of investigating substances and monitoring technological processes.

Here special attention should be paid to the organization of such laboratories in regions where industrial establishments are concentrated. An increase in the number of consultations with the industrial establishments, the reading of lectures at factories and plants, as well as personal visits by leading workers in scientific and educational institutes to large industrial establishments, would be of great help in the whole matter of further developing the fields of acoustics and ultrasonics. The participants of the conference note the difficulties which are associated with acquiring acoustics equipment and instruct the Acoustics Commission to request the Presidium of the Academy of Sciences of the USSR to place before the appropriate bodies the problem of immediately stepping up the production of acoustics and ultrasonics instruments and equipment. It is recommended that the special and educational institutes that are occupied with the problems of acoustics and ultrasonics (Moscow State University, Leningrad Electrical-Engineering Institute, Leningrad State University, etc.) be involved in the preparation of such a report. The Conference considers it desirable to conduct separate conferences devoted to the achievements of acoustics and ultrasonics at regular intervals.

## In the Acoustics Commission of the Acad. Sci. USSR

### The Forthcoming Conference in 1955.

Two conferences will take place in 1955. One of them will be devoted to electroacoustics and to the teaching of acoustics in high schools. It will be called in the summer of 1955 in Kiev. In addition to reports on electroacoustics and on teaching problems, the conference will hear survey reports on certain basic problems of acoustics. The second conference will be devoted to the effects of noise upon the human organism and to methods of combatting noise. In preparation for the second conference the following organizations will participate in addition to the Acoustics Commission: the I. P. Pavlov Institute of Physiology of the Acad. Sci. USSR and the All-Union Scientific-Research Institute of Work Safety of the All-Union Central Committee of Professional Unions. The conference is to be held in November 1955 in Leningrad.

## The Creation of New Scientific Sections

The Commission of Acoustics has organized and activated the following new scientific sections; a section on ultrasonics and a section on the investigation of speech. The primary responsibilities of these sections are to coordinate the scientific work which is being performed in various institutions on closely related subjects and to facilitate the establishment of continuous contact between specialists in various fields who are working on common problems. Research in the field of speech, which has acquired ever growing significance for a number of important technological fields (as well as for medicine, pedagogy and art), is clearly of a complex nature. To insure the successful development of this research it is necessary to guarantee a constant and systematic cooperation between specialists in various sciences: physicists, physiologists, communications engineers, architects, phoneticists, psychologists, teachers, doctors, art teachers, etc.

Many investigations in the field of ultrasonics are also complex in nature. To guarantee the success of these investigations it is also necessary to create the conditions under which there can be constant and systematic exchange in experience and mutual consultation between specialists in various fields (physicists, engineers, technologists, biologists, et. al.).

The newly organized sections are concentrating their main attention precisely upon problems which are in fields where various of the sciences overlap.

The ultrasonics section is headed by Corresponding Member of the Acad. Sci. USSR S. Ia. Sokolov and the section on the investigation of speech is headed by Engineer V. N. Fedorovich.

## The Publishing of Scientific Works

A regular collection of "Transactions of the Acoustics Commission", No. 8 is just off the press. This collection contains the reports made at the expanded conferences of the Acoustics Commission, as well as papers which have been received from Scientific Institutions. Several papers are devoted to electroacoustics (among them are papers on the reciprocity method and on methods of measurement), two papers are devoted to the "Artificial Ear" instrument, three papers are devoted to a new trend in acoustics and optics – acoustical optics. Three papers examine the present pertinent problems in the application of correlation analysis to acoustics. One paper is devoted to the particular problem involved in metrological acoustics – the pumping method – and still another paper is devoted to the old problem of musical acoustics (the striking of a piano hammer upon a string; here the problem is solved by means of new methods). Altogether the collection contains 16 papers. In print at present are the following two publications which have been prepared in the Acoustics Commission: "Problems of Physiological Acoustics", Vol. 3, (a continuation of the series which was published earlier under the same name), and "Scientific Literature on Acoustics during the period 1945-1949".

In Vol. 3 of "Problems of Physiological Acoustics" there will be the papers which were read at the Conference on Physiological Acoustics in 1954; these papers were devoted to auditory biophysics, the methods of objective auditory investigation, and certain other problems in physiological acoustics. The collection was prepared for publishing by the section on physiological acoustics of the Acoustics Commission.

"Scientific Literature on Acoustics During the Period 1945-1949" is a very complete bibliography for these years. It includes the titles of books and of papers in journals on the subject of acoustics (as published in practically all languages) and lists their translations into Russian.

## An Acoustics Colloquium

An acoustics colloquium at which original survey scientific papers are read has been organized and operates regularly under the direction of Academician N. N. Andreev in the Acoustics Institute of the Acad. Sci. USSR. Besides the staff of the Acoustics Institute and members of the Acoustics Commission, participation in the work of the colloquium includes the staffs of the Moscow State University, and of universities and scientific establishments in Moscow and in other cities. The meetings occur twice a month on Thursdays from 4 to 8 pm in the Acoustics Institute Building.

Information on the work of the Acoustics Colloquium can be obtained by writing to the address: Moscow, B-134, p/ia 1578.

The address of the Acoustics Commission is: Moscow, B-134, p/ia 1509.

# BIBLIOGRAPHY

## A New Journal

The first issue of a new acoustical journal titled "Noise Control" has been issued for the American Acoustics Society by the American Institute of Physics.

In the editorial written by the president of this society, L. L. Beranek, it is indicated that the journal is meant for all those who are interested in the efforts to combat noise, be they engineers, industrial executives, architects or otologists.

The journal contains the following articles; A popular scientific article by A. S. Pietrasant titled "Fundamentals of Noise Control" which touches upon sound absorption, sound- and vibration- insulation, and lowering noise generation in ventilation ducts; the article contains a typical example which illustrates the measures that can be taken to combat noise in service establishments. An article by G. Davis, titled "The Meaning of the A. S. A. Communication 'Z24-X2' " discusses the responsibilities of the American Standards Association and the recent article titled "the relationship between hearing loss and the effects of noise."

An article by G. S. Gardy titled "25 years of Investigating Street Noise," reports on the stages of development of these investigations which began in 1929, gives data on street noise and indicates the problems which must be solved in this field.

An article by J. R. Cox, Jr., titled "How Quiet Must it Be While Measuring the Acuteness of Normal Hearing?" gives experimental data on the effect of noise of varying level, height (in octaves) and spectral composition, which is present during audiometric investigations of human hearing, upon the results of audiometric tests on persons with normal hearing.

In an article by R. O. Fear and R. J. Wells, titled "Decreasing the Noise of Mechanisms and Motors", an examination is made of the following items; noise created by magnetic phenomena in transformers and induction motors, and noise of aerodynamic origin. The paper examines compression noise in an air conditioning unit. The same paper indicates the methods for decreasing noise; mounting the equipment in such a way that it is vibration-isolated, sound insulation, vibration damping. Modern technology for metering and analyzing noise is described, and the "noisiness" criterion is examined.

In an article by the English architectural acoustics experts, P. G. Parkin and E. F. Stacy, titled "Lowering Noise in Rooms and Homes", a description is given of the method simultaneously adopted for architectural-acoustic measurements in 1948 in England, Holland, France, Germany and the Scandinavian countries. The paper also provides data on the norms for the sound insulation of walls and coverings, and several typical methods of constructing them.

An article by G. L. Bonvallet and S. N. Potter, titled "Metering Technique for Special Problems" examines the physical properties of a noise field and describes the process of measuring the lowering of the noise in a reactive-motor test booth, the measurement of truck noise, Diesel-motor noise and the measurement of the sound insulation of the walls in a building; the same paper provides data on the calibration of metering equipment which is used for such measurements.

A paper by J. S. Parkinson, titled "Noise Control Inside a Room" sheds light on the development of problems associated with the sound-absorbent treatment of rooms and indicates in which cases it is practical to treat the room in such a manner.

In a long paper by K. N. Stevens, V. A. Rosenblit and R. N. Bolt, titled "Is It Possible to Predict the Reaction of the Population to Noise Which Acts Upon Them?", clarifies the effect of various types of noise upon observers who are listening under various conditions and their reactions to the noisiness; the same paper discusses the possibility of predicting such a reaction and the accuracy of such a prediction.

In the first issue of the journal "Noise Control", the following reports are given; a report on the development of laws governing the campaign against noise in the city of New York, and a chronicle of various new developments and events in the field of noise control; a description is given for a method of lowering the noise of a manual pneumatic drill. The journal also contains a review of the book by L. L. Beranek, titled "Acoustics" and the above-mentioned brochure titled, "The Relationship between Loss in Hearing and the Effect of Noise". Information is given on new sound-absorbent structures which are being produced by industry.

From this brief review it follows that the contents of the first issue of the journal "Noise Control" encompasses a number of problems which are associated with a very important and real problem of our times – the problem of noise control. Since this problem is of general interest, the appearance of the first journal which combines many different kinds of material on noise control and which popularizes the basic knowledge with regard to this problem will be met with satisfaction and interest in the circles of Soviet acoustical scientists, builders and all those who are occupied with the important task of protecting people from noise.

M. M. Efrussi

The first issue of a new scientific journal "Noise Control", [illegible] of the American Acoustical Society [illegible] architects or [illegible]

The journal contains the following articles: A popular scientific article by [illegible] titled "Fundamentals of Noise Control" which touches upon sound absorption, sound- and vibration- insulation, and lowering noise generation in ventilation ducts; the article contains a typical example which illustrates the measures that can be taken to combat noise in service establishments. An article by G. Davis, titled "The Meaning of the A. S. A. Communication 'Z24 -X2' " discusses the responsibilities of the American Standards Association and the recent article titled "The relationship between hearing loss and the effects of noise."

An article by O. S. Gardy titled "25 years of investigating Street Noise," reports on the stages of development of these investigations which began in 1928, gives data on street noise and indicates the problems which must be solved in this field.

An article by J. R. Cox, Jr., titled "How Quiet Must It Be While Measuring the Acuteness of Normal Hearing?" gives experimental data on the effect of noise of varying level, height (in octaves) and spectral composition, which is present during audiometric investigations of human hearing, upon the results of audiometric tests on persons with normal hearing.

In an article by R. O. Fehr and E. I. Wells, titled "Decreasing the Noise of Mechanisms and Motors", an examination is made of the following items: noise created by magnetic phenomena in transformers and induction motors, and noise of aerodynamic origin. The paper examines compression noise in an air conditioning unit. The same paper indicates the methods for decreasing noise: mounting the equipment in such a way that it is vibration isolated, sound insulation, vibration damping. Modern technology for measuring and analyzing noise is described, and the "noisiness" criterion is examined.

In an article by the English architectural acoustics experts, P. H. Parkin and E. F. Stacy, titled "Measuring Noise in Rooms and Homes", a description is given of the method simultaneously adopted for architectural-acoustic measurements in 1948 in England, Holland, France, Germany and the Scandinavian countries. The paper also provides data on the norms for the sound insulation of walls and coverings, and several typical methods of constructing them.

An article by G. L. Bonvallet and [illegible] N. Potter, titled "Metering Technique for Special Problems" examines the physical properties of a noise field and describes the process of measuring the lowering of the noise in a [illegible] test booth, the measurement of truck noise, [illegible] noise and the measurement of the sound insulation of the walls in a building; the same paper provides data on the calibration of metering equipment which is used in such measurements.

A paper by [illegible], titled "Noise Control Inside a Room" sheds light on the development of problems associated with the sound-absorbent treatment of rooms and indicates in which cases it is practical to treat the room in such a manner.

SOVIET PHYSICS – ACOUSTICS VOL. 1, Nos. 1, 2 January-June, 1955

(Published by the American Institute of Physics September, 1957)

## CONTENTS Vol. 1, No. 1

| | Page | Russian Page |
|---|---|---|
| From the Editor. | 1 | 1 |
| Concerning Certain Second-Order Quantities in Acoustics. N. N. Andreev | 2 | 3 |
| Measurement of Non-Linear Distortion in Loudspeakers by Using Infrasonic Modulation. B. G. Belkin | 12 | 12 |
| Concerning One Type of Attenuation of Waves Propagating in Inhomogeneously-Stratified Media. L. M. Brekhovskikh and I. D. Ivanov | 23 | 23 |
| Concerning the General Relationship Between Absorption and Dispersion of Sound Waves. V. L. Ginzberg. | 32 | 31 |
| On the Problem of Axial Oscillations of Polarized Barium Titanate Plates. I. P. Goliamina | 42 | 40 |
| Experimental Investigation of Diffraction of Acoustic Waves by Periodic Structures. A. N. Leporskii | 50 | 48 |
| Scattering of Sound From Plane Inhomogeneous Surfaces with Periodically Varying Acoustic Admittance. Iu. P. Lysanov | 60 | 58 |
| Analysis of Gain of Cylindrical Sound-Focusing Systems. L. D. Rozenberg | 73 | 70 |
| Diffraction of Plane Sound Waves by a Spherical Cavity. D. V. Sivukhin | 82 | 78 |
| Correlation of Amplitude and Phase Fluctuations for Wave Propagation in a Medium with Random Irregularities. L. A. Chernov | 94 | 89 |
| Conference on Physiological Acoustics | 102 | 96 |
| Conference on Physical Acoustics and Ultrasonics. | 103 | 96 |

---

## CONTENTS Vol. 1, No. 2

| | Page | Russian Page |
|---|---|---|
| Survey of Methods Used for the Visualization of Ultrasonic Fields. L. D. Rozenberg | 105 | 99 |
| Measurement of the Acoustic Parameters of Materials at Ultrasonic Frequencies by Means of a Pulse Pipe. N. S. Ageeva | 117 | 110 |
| Investigation of Acoustic Shadow in a Medium Which Has a Vertical Sound Velocity Gradient. A. N. Barkhatov | 128 | 121 |
| Directional Properties of Acoustic Scattering Lenses. L. N. Bondareva and M. I. Karnovskii | 133 | 126 |
| The Effect of the Magnetic Field Distribution at the Recording-Head Gap Upon the Loss of Remanent Induction in the Tape. G. S. Veksler | 141 | 134 |

(continued on following page)

## CONTENTS (continued)

| | Page | Russian Page |
|---|---|---|
| Diffraction of Sound Upon a Thin Bounded Plate in Liquid. L. M. Liamshev | 145 | 138 |
| The Radiation of Sound by the Vibrating Boundaries of an Arbitrary Wedge. Part I. G. D. Maliuzhinets | 152 | 144 |
| Nonlinear Distortion of a Nonperiodic Signal in an Electroacoustic Channel. A. V. Rimskii-Korsakov | 175 | 165 |
| Tonal Method for Determining the Intelligibility of Speech Transmitted by Communications Channels. A. D. Tkachenko | 182 | 171 |
| **CHRONICLE** | | |
| Conference of the Fourth Research Commission of the International Consultative Committee on Telephony (ICCT) | 192 | 181 |

[illegible] of the Academy of Sciences of [illegible] approximately 4,000 Russian pages. Annually [illegible]

[illegible] of the Academy of Sciences of the U.S.S.R. [illegible] Russian pages. Annually, [illegible] domestic, $22.00 [illegible] "Journal of Astronomy" U.S.S.R. will also be published, [illegible] approximately 500 pages, and the subscription price will be [illegible]

[illegible] Section" of the Proceedings of the Academy of [illegible] issues per year, approximately 500 Russian pages. Annually [illegible]

[illegible] of the "Journal of Experimental and Theoretical Physics" of the [illegible] of the U.S.S.R. Twelve issues per year, approximately 7,000 Russian [illegible] domestic, $64.00 foreign. Back issues of Volume 1 and 2 are [illegible] at a special price of $30.00 for both to subscribers to Volume 3.

*Subscriptions should be addressed to the American Institute of Physics, 335 East 45th Street, New York 17, N.Y.*